

6 May 1966

Mem CB 65412

LTV Report No. 2-53420/6R-2279

FINAL ENGINEERING REPORT

**BIAXIAL STRENGTH CHARACTERISTICS OF
SELECTED ALLOYS IN A CRYOGENIC ENVIRONMENT**

Prepared for
NASA Manned Spacecraft Center
General Research Procurement Office
Houston, Texas
under
Contract Number NAS 9-3873

*5966
7
644*

[REDACTED]
[REDACTED]
[REDACTED]

GPO PRICE \$ _____
CFSTI PRICE(S) \$ _____
Hard copy (HC) \$ 5.00
Microfiche (MF) 1.00
853 July 68

FACILITY FORM 802	N66 30085	
	(ACCESSION NUMBER)	(THRU)
	<u>166</u>	<u>1</u>
	(PAGES)	(CODE)
	<u>CR-65412</u>	<u>17</u>
	(NASA CR OR TMX OR AD NUMBER)	(CATEGORY)

FINAL ENGINEERING REPORT FOR
CONTRACT NAS 9-3873

BIAXIAL STRENGTH CHARACTERISTICS OF SELECTED ALLOYS IN A
CRYOGENIC ENVIRONMENT

6 MAY 1966

Prepared for
NASA Manned Spacecraft Center
General Research Procurement Office
Houston, Texas

LTV Report No. 2-53420/6R-2279

Prepared By:

S. W. McClaren

S. W. McClaren
Lead Engineer
Structures Design

Reviewed By:

A. P. Martin

A. P. Martin
Supervisor
Structures Design

Approved By:

G. A. Starr

G. A. Starr
Chief
Applied R&D

C. R. Foreman

C. R. Foreman
Structures Design
Engineer

J. F. Grabinski

J. F. Grabinski
Structures Design
Engineer

LTV Aerospace Corporation

FORWARD

This engineering report was prepared by LTV Aerospace Corporation, Dallas, Texas, for the National Aeronautics and Space Administration's Manned Spacecraft Center, Houston, Texas, under Contract No. NAS 9-3873. This research was accomplished during the period of 6 January 1965 through 6 May 1966.

Mr. H. C. Kavanaugh of the Structural Mechanics Branch acted as NASA-MSC's technical representative while Mr. S. V. Glorioso of the Experimental Mechanics Branch acted as the NASA-MSC's material's representative during the conduct of this research.

Mr. S. W. McClaren was the LTV principal investigator and he was aided in this research by Mr. C. R. Foreman and Mr. J. F. Grabinski. Mr. N. Godbold acted as the LTV test engineer under the direction of Mr. R. J. Calvert, Engineering Test Specialist. Mr. O. H. Cook acted as the program principal metallurgist while Mr. M. Condon was in charge of electron microscope studies.

This research was administered under the direction of Mr. G. A. Starr, Chief of Applied Research and Development who was assisted by Mr. H. Warkentin, R&D Project Engineer. Mr. A. P. Martin, Supervisor of Structures Design, acted as the technical area supervisor.

ABSTRACT

30085

The characteristics and mechanical properties of several metallic sheet materials subjected to uniaxial and biaxial stress fields at cryogenic temperatures were investigated. The test results are compared on a basis of state of stress and on a basis of temperature versus mechanical properties. Standard stress-strain curve data for uniaxial, 1:1 and 2:1 biaxial stress states are presented for tests conducted at room temperature, -105°F , -320°F and -423°F . These data have been compared with the deformation energy theory to illustrate the predictability of results.

Program material ratings were accomplished while using biaxial strength/weight ratios, biaxial ductility, and fracture toughness as the prime rating factors.

This research has generated cryogenic uniaxial and biaxial design data, investigated fracture mechanisms, developed uniaxial and biaxial creep data at -320°F , evaluated the effects of stress states on weldments, compared results to an applicable failure theory, and considered practical design criteria concepts for design of pressurized components at cryogenic temperatures.

TABLE OF CONTENTS

<u>SECTION</u>	<u>PAGE</u>
FORWARD	
ABSTRACT	
I INTRODUCTION	1
II TEST MATERIALS	3
III TEST SPECIMENS	8
IV TEST PROCEDURES	14
V TEST RESULTS	19
VI DATA COMPARISON AND DISCUSSION	33
VII CONCLUSIONS AND RECOMMENDATIONS	72
VIII REFERENCES	75
APPENDICES	76
APPENDIX A - PHOTOELASTICITY ILLUSTRATION OF THE 1:1 BIAXIAL STRESS STATE . .	76
APPENDIX B - TEST EQUIPMENT AND ARRANGEMENTS . .	80
APPENDIX C - LOW TEMPERATURE STRAIN GAGE TECHNIQUES	91
APPENDIX D - CALCULATION OF BIAXIAL STRESS- STRAIN CURVES FROM BIAXIAL LOAD-STRAIN CURVES	93
APPENDIX E - COMPUTER CALCULATION OF PLANE- STRAIN FRACTURE TOUGHNESS PARAMETERS	96
APPENDIX F - COMPUTER CALCULATION OF THE LUDWIK STRAIN HARDENING COEFFICIENT .	102
APPENDIX G - UNIAXIAL STRESS-STRAIN CURVES	106

TABLE OF CONTENTS, CON'T

	<u>PAGE</u>
APPENDIX H - BIAXIAL STRESS-STRAIN CURVES	125
APPENDIX I - DATA COMPILED FROM OTHER SOURCES	130
APPENDIX J - PHOTOFRACTOGRAPHY AND ANALYSIS OF FRACTURE MODES	138

LIST OF ILLUSTRATIONS

<u>Figure No.</u>	<u>Title</u>	<u>Page No.</u>
1	Uniaxial Tensile Specimen	10
2	Uniaxial Fracture Toughness Specimen.	11
3	Biaxial Tensile Specimen (1:1 and 2:1).	12
4	Biaxial Fracture Toughness Specimen	13
5	Comparison of 2219-T87 Aluminum Alloy Properties with Temperature	44
6	Comparison of 2014-T6 Aluminum Alloy Properties with Temperature	45
7	Comparison of 5Al-2.5Sn Titanium Alloy (Annealed) Properties with Temperature.	46
8	Comparison of 6Al-4V Titanium Alloy (Eli, Annealed) Properties with Temperature	47
9	Comparison of Inconel 718 (Heat-Treated) Properties with Temperature	48
10	Comparison of 6Al-4V Titanium Alloy (Sta) Properties with Temperature	49
11	Comparison of 2219-T87 Aluminum Alloy Properties with State of Stress	50
12	Comparison of 2014-T6 Aluminum Alloy Properties with State of Stress	51
13	Comparison of 5Al-2.5Sn Titanium Alloy (Annealed) Properties with State of Stress	52
14	Comparison of 6Al-4V Titanium Alloy (ELI, Annealed) Properties with State of Stress	53
15	Comparison of Inconel 718 (H.T.) Properties with State of Stress	54
16	Comparison of 6Al-4V Titanium Alloy (STA) Properties with State of Stress	55
17	Comparison of 1:1 Biaxial Strength with Two Failure Theories	56

LIST OF ILLUSTRATIONS (CONT)

<u>Figure No.</u>	<u>Title</u>	<u>Page No.</u>
18	Comparison of 2:1 Biaxial Strength with Two Failure Theories	57
19	Comparison of 1:1 Biaxial Weldment Strength with Two Failure Theories	58
20	Comparison of Fracture Toughness as a Function of Temperature for Uniaxial and 1:1 Biaxial Stress States	59
21	5Al-2.5Sn Titanium Alloy (ELI, Annealed) Creep Curves Developed under Uniaxial Stress Field	60
22	6Al-4V Titanium Alloy (ELI, Annealed) Creep Curves Developed under 1:1 Biaxial Stress Field. . .	61
23	5Al-2.5Sn Titanium Alloy (ELI, Annealed) Creep Curves Developed under 1:1 Biaxial Stress Field. . .	62
24	6Al-4V Titanium Alloy (ELI, Annealed) Creep Curves Developed under 1:1 Biaxial Stress Field. . .	64
25	Comparison of Uniaxial Weldment Efficiencies	66
26	Comparison of 1:1 Biaxial Weldment Efficiencies. . .	67
27	Comparative Rating of Program Materials.	68
28	Experimentally Determined Equations for Predication of Strength and Modulus as a Function of Temperature	71
29	Step-By-Step Photo Stress Evaluation of the State of Stress in a 1:1 Biaxial Test Specimen	78
30	Load-Strain Curve for the 1:1 Biaxial Photo Stress Test for the Transverse Grain Direction.	79
31	Uniaxial Cryostat.	81
32	Biaxial Cryostat	81
33	View of Liquid Hydrogen Test Cell with Biaxial Test Machine	81
34	View of Liquid Hydrogen Control Room	81

LIST OF ILLUSTRATIONS (CONT)

<u>Figure No.</u>	<u>Title</u>	<u>Page No.</u>
35	Biaxial Test Machine (Overall View).	82
36	Biaxial Data Recording Equipment and Breadboarded Control Panel.	82
37	Uniaxial Cryostat (Drawing).	83
38	Biaxial Cryostat (Drawing)	84
39	Electrical and Hydraulic Schematic for Uniaxial Tests	85
40	Electrical Schematic for 1:1 and 2:1 Biaxial Tests .	86
41	Hydraulic Schematic for 1:1 and 2:1 Biaxial Stress Test Program	87
42	Uniaxial Creep Test Set-Up	88
43	Biaxial Creep Test Set-Up.	88
44	Illustrations of Various Welding Operations and Facilities	89
45	Illustration of Calculation of 1:1 Biaxial Stress-Strain Values from 1:1 Biaxial Load Strain Curves for 2219-T81 Aluminum Alloy at -100°F.	94
46	Illustration of Calculation of 2:1 Biaxial Stress-Strain Values from 2:1 Biaxial Load Strain Curves for 2219-T81 Aluminum Alloy at -320°F.	95
47	Typical 2219-T87 Aluminum Alloy Uniaxial Stress-Strain Curves.	107
48	Typical 2014-T6 Aluminum Alloy Uniaxial Stress-Strain Curves.	108
49	Typical 5Al-2.5Sn Titanium Alloy (Annealed) Uniaxial Stress-Strain Curves.	109
50	Typical 6Al-4V Titanium Alloy (ELI, Annealed) Uniaxial Stress-Strain Curves.	110

LIST OF ILLUSTRATIONS (CONT)

<u>Figure No.</u>	<u>Title</u>	<u>Page No.</u>
51	Typical Inconel 718 Uniaxial Stress-Strain Curves.	111
52	Typical 6Al-4V Titanium (STA) Uniaxial Stress-Strain Curves	112
53	Typical 2219-T87 Aluminum Alloy Welded Uniaxial Stress-Strain Curves.	113
54	Typical 2014-T6 Aluminum Alloy Welded Uniaxial Stress-Strain Curves.	113
55	Typical 5Al-2.5Sn Titanium Alloy (Annealed) Welded Uniaxial Stress-Strain Curves	113
56	Typical 6Al-4V Titanium Alloy (ELI, Annealed) Welded Uniaxial Stress-Strain Curves.	114
57	Typical Inconel 718 Welded Uniaxial Stress-Strain Curves	114
58	Typical 6Al-4V Titanium Alloy (STA) Welded Uniaxial Stress-Strain Curves	114
59	Typical 2219-T87 Aluminum Alloy 1:1 Biaxial Stress-Strain Curves.	116
60	Typical 2014-T6 Aluminum Alloy 1:1 Biaxial Stress-Strain Curves.	117
61	Typical 5Al-2.5Sn Titanium Alloy (Annealed) 1:1 Biaxial Stress-Strain Curves.	118
62	Typical 6Al-4V Titanium Alloy (ELI, Annealed) 1:1 Biaxial Stress-Strain Curves.	119
63	Typical Inconel 718 (H.T.) 1:1 Biaxial Stress-Strain Curves	120
64	Typical 6Al-4V Titanium Alloy (STA) 1:1 Biaxial Stress-Strain Curves.	121
65	Typical 2219-T87 Aluminum Alloy (As-Welded) 1:1 Biaxial Stress-Strain Curves.	122
66	Typical 2014-T6 Aluminum Alloy (As-Welded) 1:1 Biaxial Stress-Strain Curves.	122

LIST OF ILLUSTRATIONS (CONT)

<u>Figure No.</u>	<u>Title</u>	<u>Page No.</u>
67	Typical 5Al-2.5Sn Titanium Alloy (Annealed) As-Welded 1:1 Biaxial Stress-Strain Curves.	122
68	Typical 6Al-4V Titanium Alloy (Annealed, ELI As Welded) 1:1 Biaxial Stress-Strain Curves	123
69	Typical Inconel 718 (Heat-Treated, As-Welded) 1:1 Biaxial Stress-Strain Curves.	123
70	Typical 6Al-4V Titanium Alloy (STM, As-Welded) 1:1 Biaxial Stress-Strain Curves.	123
71	Typical 2219-T87 Aluminum Alloy 2:1 Biaxial Stress-Strain Curves.	124
72	Typical 2014-T6 Aluminum Alloy 2:1 Biaxial Stress-Strain Curves.	125
73	Typical 5Al-2.5Sn Titanium Alloy (Annealed) 2:1 Biaxial Stress-Strain Curves.	126
74	Typical 6Al-4V Titanium Alloy (ELI, Annealed) 2:1 Biaxial Stress-Strain Curves.	127
75	Typical Inconel 718 (H.T.) 2:1 Biaxial Stress- Strain Curves	128
76	Typical 6Al-4V Titanium Alloy (STM) 2:1 Biaxial Stress-Strain Curves.	129
77	Comparative Electron Microscope Micro-Photographs of Fracture Origins in (Unwelded) 2219-T87 Aluminum Alloy for 1:1 and 2:1 States of Stress.	142
78	Comparative Electron Microscope Micro-Photographs of Fracture Origins in (Unwelded) 6Al-4V Titanium (ELI) Alloy for 1:1 and 2:1 States of Stress.	142
79	Comparative Electron Microscope Micro-Photographs of Fracture Origins in (Unwelded) Inconel 718 Alloy for 1:0, 1:1 and 2:1 States of Stress	143
80	Comparative Electron Microscope Micro-Photographs of Fracture Origins in (Welded) 6Al-4V Titanium (ELI) Alloy for 1:0 and 1:1 States of Stress.	144

LIST OF ILLUSTRATIONS (CONT)

<u>Figure No.</u>	<u>Title</u>	<u>Page No.</u>
81	Comparative Electron Microscope Micro-Photographs of Plane - Strain Fracture Toughness Failure Surfaces in 2219-T87 Aluminum Alloy for 1:0 and 1:1 States of Stress.	144
82	Comparative Electron Microscope Micro-Photographs of Plane-Strain Fracture Toughness Failure Surfaces in Inconel 718 Alloy for 1:0 and 1:1 States of Stress.	145
83	Comparative Electron Microscope Micro-Photographs of Plane - Strain Fracture Toughness Failure Surfaces in 5Al-2.5Sn Aluminum Alloy for 1:0 and 1:1 States of Stress.	145
84	Comparative Electron Microscope Micro-Photographs of Fracture Origins in (Welded) 2219 Aluminum Alloy for 1:0 and 1:1 States of Stress.	146
85	Comparative Electron Microscope Micro-Photographs of Fracture Origins in (Welded) Inconel 718 Alloy for 1:0 and 1:1 States of Stress.	146
86	Comparative Illustration of Fracture Origin and Flaw Zone Area in Typical Uniaxial and Biaxial Partial Through Crack Tests	147
87	Failed Uniaxial Test Specimens.	148
88	Failed Uniaxial and 1:1 Biaxial Fracture Toughness Specimens	149
89	Failed 1:1 Biaxial Test Specimens (Welded and Unwelded Condition)	150
90	Failed 2:1 Biaxial Test Specimens (Unwelded Condition).	151
91	Failed 1:1 Biaxial Creep Test Specimen (-320°F; 90% F _{TY} Stress Level; 172 Hours to Failure)	152-
92	Combined View of Several Failed 5Al-2.5Sn Titanium Alloy (Annealed) Test Specimens at Various Stress States and Temperatures.	153

LIST OF ILLUSTRATIONS (CONT)

<u>Figure No.</u>	<u>Title</u>	<u>Page No.</u>
93	Combined View of Several Failed 2219-T87 Aluminum Alloy Test Specimens at Various Stress States and Temperatures.	154
94	Combined View of Several Failed 2014-T6 Aluminum Alloy Test Specimens at Various Stress States and Temperatures.	155

LIST OF TABLES

<u>TABLE NO.</u>	<u>TITLE</u>	<u>PAGE</u>
1	UNIAXIAL TENSILE PROPERTIES FOR PROGRAM MATERIALS	21
2	BIAXIAL TENSILE PROPERTIES FOR PROGRAM MATERIALS	25
3	PLANE-STRAIN FRACTURE TOUGHNESS PARAMETERS FOR THE PROGRAM MATERIALS	31
4	UNIAXIAL AND 1:1 BIAXIAL CRYOGENIC CREEP PROPERTIES	32
5	RATING PARAMETER DATA FOR EVALUATION OF PROGRAM MATERIALS FOR CRYOGENIC APPLICATIONS	69
6	ADDITIONAL UNIAXIAL DATA	131
7	ADDITIONAL BIAXIAL DATA	134

SYMBOLS AND SUBSCRIPTS

SYMBOLS

B	- biaxial stress ratio of minimum principal stress divided by maximum principal stress, dimensionless
E	- modulus of elasticity, psi
e	- elastic strain, in./in.
P ₁ , P ₂	- loading jack load in principal stress directions in a biaxial tension test, lb.
n	- uniaxial strain-hardening coefficient (Ludwik)
ε	- nominal (engineering) principal plastic strain, in./in.
ν	- Poisson's Ratio (absolute value of lateral strain divided by axial strain); dimensionless
σ, S or F	- nominal (engineering) principal stress, psi
ρ	- density of a material, lb./in. ³
K _{TC}	- fracture toughness parameter (plain-strain), Ksi $\sqrt{\text{in}}$
Φ	- elliptical integral function, dimensionless

SUBSCRIPTS

u	- uniaxial state of stress
b	- biaxial state of stress
L, T	- longitudinal and transverse grain direction
1, 2, 3	- principal stress directions
R ₁	- for 1:1 state of stress
R ₂	- for 2:1 state of stress
R _u	- for uniaxial state of stress
Y ₁	- yield value for 1:1 state of stress (0.2% offset)

- Y_2 - yield value for 2:1 state of stress (0.2% offset)
- Y_u - yield value for uniaxial state of stress (0.2% offset)
- T_u - applicable ultimate strength, psi.
- T_y - applicable yield strength, psi.

SECTION I

INTRODUCTION

The design of future and present aerospace systems require that every advantage of a material be utilized in achieving minimum weight and maximum strength conditions. Some of the advantages that can be utilized with great benefit are (1) use of biaxial strength data along with uniaxial strength data where applicable, (2) use of material property values that reflect improvements due to a low temperature environment, (3) use of the proper special property data such as biaxial and uniaxial stress field effects on weldments, and (4) accurate assessment of cryogenic creep and fracture toughness effects under both uniaxial and biaxial conditions. The use of these basic design advantages will, of course, result in more effective structures with lighter weights and lower cost. However, in order to utilize these advantages with confidence, design test data must be obtained and evaluated. It was the objective of this research to evaluate the uniaxial, 1:1 biaxial and 2:1 biaxial properties of several prospective materials over the temperature range of ambient temperature to minus 423°F. This research generated data, correlated prediction trends and compared these trends with an applicable failure theory. The result was the establishment of analytical techniques for making predictions of design material properties from simple tensile specimens at the appropriate temperature condition.

The data and correlations from this program are applicable for the design of low temperature pressurized components where the tankage walls may or may not be acting as part of the basic structure. In addition the data obtained may be used in the design of life support equipment and systems operating in a low temperature environment. These applications are important because space and aerospace vehicles will continue to utilize tankage for various cryogenic fluids (oxidizers and fuels) in the foreseeable future. Another area of future use will be in the cooling and power systems of nuclear reactors for both ground based and flight operations.

This research evaluated the mechanical properties and characteristics of 2219-T87 aluminum alloy; 2014-T6 aluminum alloy; 5Al-2.5Sn titanium alloy (annealed); 5Al-2.5Sn titanium alloy (ELI, annealed); 6Al-4V titanium alloy (ELI, annealed); 6Al-4V titanium alloy (STA); and

Inconel 718 (Heat-Treated) under 1:0, 1:1 and 2:1 stress states at room temperature, -105°F , -320°F and -423°F . These data and the various resulting comparisons are presented in the following sections of this report.

SECTION II

TEST MATERIALSGeneral

The materials evaluated in this research were:

<u>MATERIAL</u>	<u>CONDITION</u>	<u>SHEET SIZE</u>	<u>DENSITY-LB/IN³</u>
2219 Aluminum Alloy	T-87	48"x120"x.125"	0.10
2014 Aluminum Alloy	T-6	36"x72"x.125"	0.10
5Al-2.5Sn Titanium Alloy	Annealed	36"x120"x.125"	0.162
5Al-2.5Sn Titanium Alloy	ELI, Annealed	36"x96"x.125"	0.162
6Al-4V Titanium Alloy	ELI, Annealed	36"x120"x.125"	0.161
6Al-4V Titanium Alloy	STA	36"x101"x.125"	0.161
Inconel 718	Heat Treated (by LTV)	36"x96"x.125"	0.297

2219-T87 Aluminum

Specification	- MIL-A-8920
Manufacturer	- Reynolds Metals Co.
Supplier	- Glazer Steel Co. New Orleans, La.
Lot	- KC 22670-0
Properties (R.T.)	- Ultimate strength: 68.6 to 69.7 ksi Yield Strength: 53.8 to 54.4 ksi % Elongation (2"): 10.5 to 11.0

2014-T6 Aluminum

Specification - QQ-A250/3 Sta.
 Manufacturer - Reynolds Metal Co.
 Supplier - Glazer Steel Co.
 New Orleans, La.
 Lot - KD-20261-0
 Properties
 (R.T.) - Ultimate Strength: 70.9 to 71.8 ksi
 Yield Strength: 63.2 to 64.2 ksi
 % Elongation (2") 9.5 to 10.0

5Al-2.5Sn (Annealed) Titanium

Specification - MIL-T-9046 (Class 3)
 Manufacturer
 and Supplier - Titanium Metals Corp.
 of America (Toronto)
 New York 7, New York
 Heat Number - D-8634
 Properties
 (R.T.) - Ultimate Strength: 131.1 to 139.8 ksi
 Yield Strength: 120.7 to 130.2 ksi
 % Elongation (2"): 14.0 to 17.0

Chemistry as determined by TMCA

<u>Elements</u>	<u>Percent</u>	<u>Elements</u>	<u>Percent</u>
C	0.023	O ₂	0.17
Fe	0.25	Al	5.0
N	0.010	Sr	2.5
H	0.005	Mn	0.009
		Ti	Balance

5Al-2.5Sn (ELI, Annealed) Titanium

Specification - MIL-T-9046C (ELI)
 Manufacturer
 and Supplier - Titanium Metals Corp.
 of America (Toronto)
 New York 17, New York
 Heat Number - D-4203
 Properties
 (R.T.) - Ultimate Strength: 110.3 to 115.4 ksi
 Yield Strength: 100.0 to 101.3 ksi
 % Elongation: 7.5 to 10.0

Chemistry as determined by TMCA

<u>Elements</u>	<u>Percent</u>	<u>Elements</u>	<u>Percent</u>
C	0.022	N	0.011
Fe	0.14	Sn	2.4
Al	5.0	Mn	0.01
H	0.011	O ₂	0.07
		Ti	Balance

6Al-4V Titanium Alloy (ELI, Annealed)

Specification	- MIL-T-9046 (ELI, Class 3)
Manufacturer and Supplier	- Titanium Metals Corp. of America (Toronto) New York 17, New York
Heat Number	- D-8775
Properties (R.T.)	- Ultimate Strength: 138.0 to 154.0 ksi Yield Strength: 126.0 to 151.0 ksi % Elongation (2"): 12.0 to 15.0

Chemistry as determined by TMCA

<u>Elements</u>	<u>Percent</u>	<u>Elements</u>	<u>Percent</u>
C	0.023	V	3.9
Fe	0.07	H	0.004
N	0.017	O ₂	0.10
Al	5.9	Ti	Balance

6Al-4V Titanium Alloy (STA)

Specification	- MIL-T-9046 (Class 2) STA
Manufacturer and Supplier	- Titanium Metals Corp. (Toronto) New York, 17, New York
Heat Number	- D-8085
Properties (R.T.)	- Ultimate Strength: 167.4 to 178.0 ksi Yield Strength: 152.2 to 166.0 ksi % Elongation (2") 5.5 to 13.0

Chemistry as determined by TMCA

<u>Elements</u>	<u>Percent</u>	<u>Elements</u>	<u>Percent</u>
C	0.026	V	4.0
Fe	0.10	H	0.007
N	0.016	O ₂	0.13
Al	5.8	Ti	Balance

Inconel 718

Specification - SAE-AMS-5596
 Manufacturer and Supplier - Huntington Alloys, International
 Nickel Co., Inc.
 Huntington, W. Virginia
 Heat Number - HT 7951 EV
 Properties (R. T.) - Ultimate Strength: Annealed 122.0 ksi Heat Treated 197.0 ksi
 Yield Strength: 67.0 ksi 137.0 ksi
 % Elongation 47.0 19.0

Chemistry as determined by International Nickel Co.

<u>Elements</u>	<u>Percent</u>	<u>Elements</u>	<u>Percent</u>
C	0.05	Al	0.57
Mn	0.15	Ti	0.97
Fe	18.98	Co	0.06
S	0.007	Mo	3.01
Si	0.26	P	0.10
Cu	0.05	CR	18.54
Ni	52.2		

Heat Treatment Schedule for Inconel 718

- (1) Heat to 1750°F (±25°F) and hold one hour.
- (2) Air cool
- (3) Heat to 1325°F (±15°F) and hold eight hours
- (4) Furnace cool at a rate of 100°F (±15°F) per hour to 1150°F (±15°F)
- (5) Hold at 1150°F (±15°F) for eight hours
- (6) Air cool
- (7) Vapor hone to clean surfaces

Welding Techniques

The uniaxial and 1:1 biaxial weldment specimen blanks were butt-welded using standard MIL-W-8611 procedures by utilizing mechanized TIG processes. Weld wires used for the various program materials were:

<u>Material</u>	<u>Weld Wire</u>
2219 T-87 Aluminum Alloy	2319 Aluminum
2014 T-6 Aluminum Alloy	2014 Aluminum
5Al-2.5Sn Titanium Alloy, Annealed	5Al-2.5Sn Titanium (ELI)
6Al-4V Titanium Alloy, ELI, Annealed	6Al-4V Titanium (ELI)
6Al-4V Titanium Alloy, STA	6Al-4V Titanium (ELI)
Inconel 718	Inconel 718

All materials were tested in the "as-welded" condition after welding operations that were conducted in accordance with the following welding parameters:

	<u>Ti6Al-4V</u> Annealed and STA	<u>Ti5Al-2.5Sn</u>	<u>Inconel</u> 718	<u>2219-T87</u>	<u>2014-T6</u>
Wire Diam. (in.)	0.045	0.045	0.062	0.045	0.045
Wire Feed (IMP)	32	26	22	65	40
Gas Cup Size (in.)	5/8	5/8	5/8	5/8	5/8
Electrode Size (in.) @ 90°	1/8	1/8	1/8	1/8	1/8
Electrode Extension (in.)	0.40	0.45	0.50	0.50	0.50
Torch Gas					
Flow Rate (CFH)	50 He	50 He	50 He	60 He	60 He
Back-up Gas					
Flow Rate (CFH)	50 He	50 He	50 He	40 Ag	40 Ag
Shielding Gas					
Flow Rate (CFH)	20 Ag	20 Ag	None	None	None
Volts	11	10 1/4	11	10 1/4	10 1/2
Amp Pres.	250	250	200	190	195
Welding Speed (INP)	7.2	7.5	8.0	15.75	10.0

Gage Thickness (all alloys): 0.125

Joint Type (all alloys): square butt

Joint Preparation (all alloys): draw filed and hand sanded

Cleaning Method (all alloys): vapor degreased and MEK wiped

Weld Tool (all alloys): air clamp

SECTION III

TEST SPECIMENSUniaxial Tensile Specimens

A uniaxial specimen of the configuration shown in Figure 1 was used to generate uniaxial data for both the longitudinal and transverse grain directions at ambient and cryogenic temperatures.

Uniaxial Fracture Toughness Specimens

The type of specimen used for development of uniaxial fracture toughness data (partial through crack, plane strain) is shown in Figure 2. The partial through crack was generated at room temperature by repeated flexural loads at low stress magnitudes. This specimen was used for all applicable program test temperatures.

Uniaxial Creep Specimens

The same specimen used for the basic uniaxial tensile tests (Figure 1) was used for the -320°F uniaxial creep tests.

Biaxial Tensile Specimens

A biaxial specimen of the configuration shown in Figure 3 was used to generate 1:1 and 2:1 biaxial data at ambient and cryogenic temperatures. Appendix A illustrates previously developed pictorial stress field patterns that were generated by LTV using photostress techniques on the biaxial specimen. This appendix correlates the relationship between visually observed 1:1 biaxial strain field conditions and strain gage measurement values. A pair of doublers were employed on each of the four load application areas (grips) to prevent local load grip failures and utilizes the two shear pin holes shown in Figure 3 as well as the main loading pin.

Biaxial Fracture Toughness Specimen

The type of specimen used for the 1:1 biaxial fracture toughness tests (partial through crack) is shown in Figure 4. The partial through crack was generated at room temperature by repeated axial loads (unidirectional) at low stresses. This specimen was used for all applicable program test

temperatures. The thickness of material in the test area was 0.035" to 0.045" which was chosen for two reasons: (1) to allow generation of a partial through crack conditions, and (2) to allow failure of the specimen through the crack area.

Biaxial Creep Specimen

The same type specimen used for the 1:1 biaxial tensile tests was used in the 1:1 biaxial creep tests at -320°F.

Weldment Specimens

The uniaxial and 1:1 biaxial weldment test specimens were identical to the unwelded specimens of the same types (Figures 1 and 3) except for the weldment which was placed perpendicular to the longitudinal grain direction for all test specimens. Specimens blanks for these types of tests were welded in the 0.125 inch gage thickness using 16 inch by 16 inch blanks and then sized and machined to final specimen configurations.

The various specimen drawings illustrate the location of the weldments. Weldments were made in one pass according to the schedule already shown. All weld beads were machined down during the course of final specimen fabrication. Weld bead width was approximately 3/16 to 1/4 inch.

Appendix B illustrates the various welding facilities employed in this research.

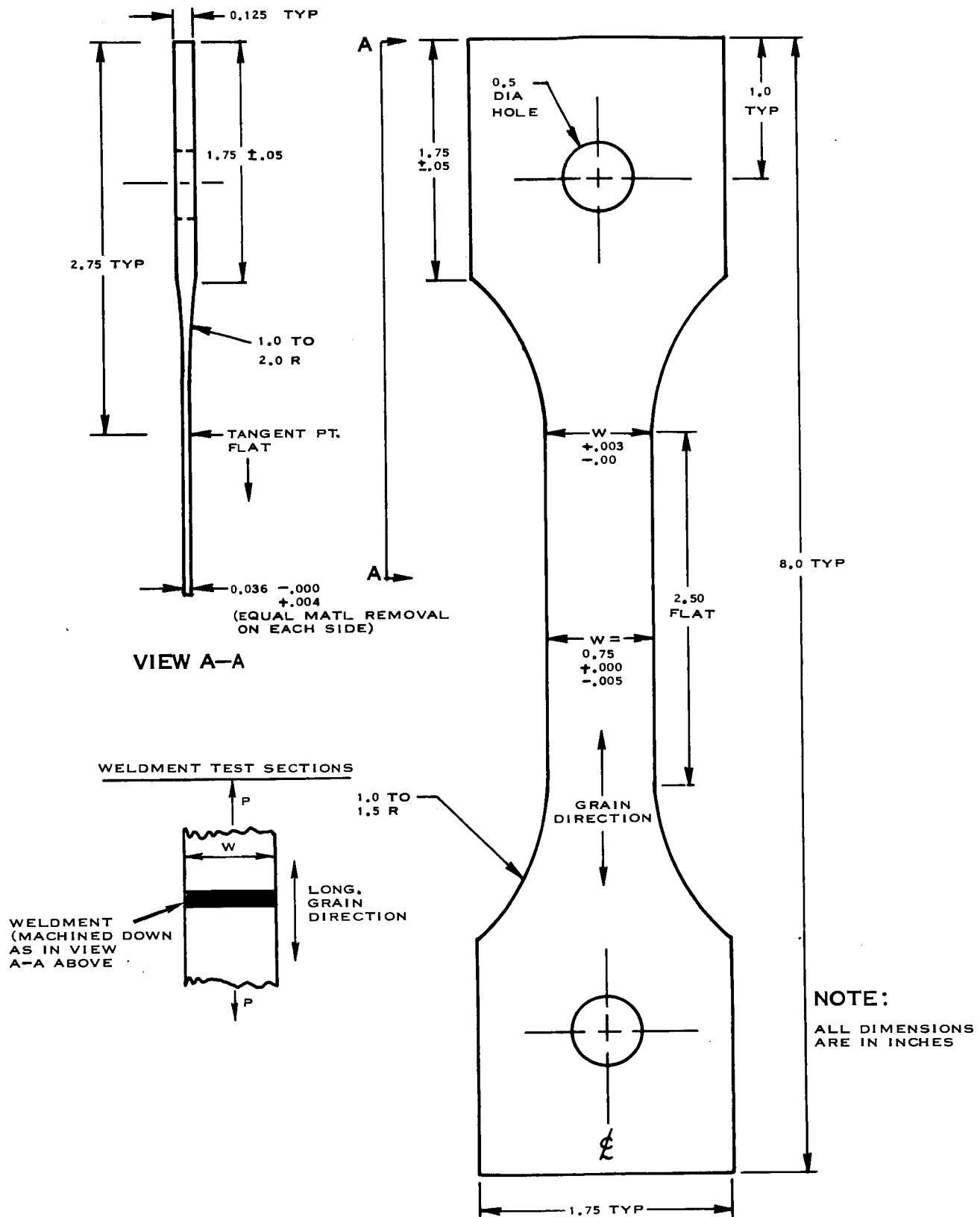
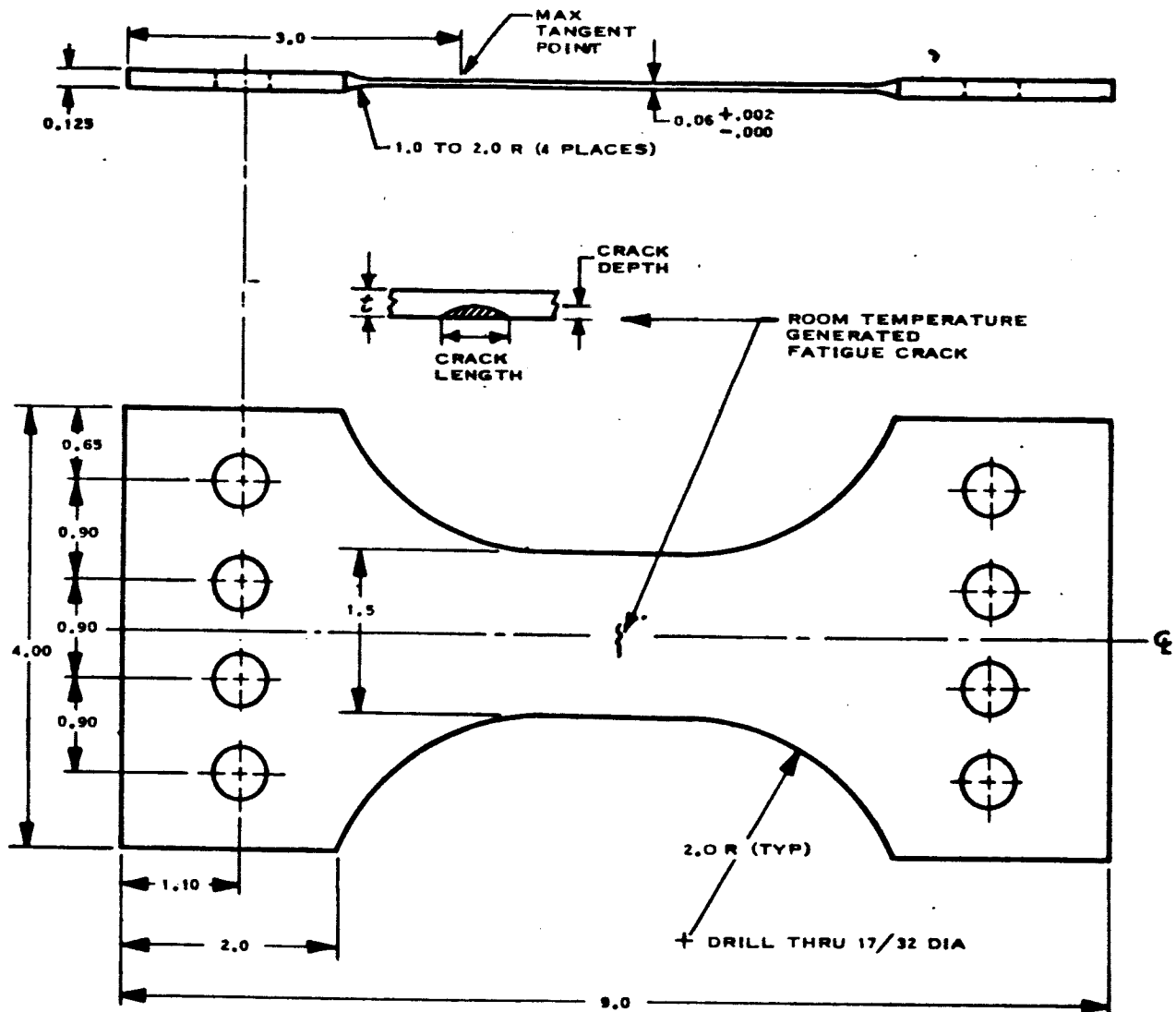


FIGURE 1 - UNIAXIAL TENSILE TEST SPECIMEN



NOTE: (1) ALL DIMENSIONS IN INCHES.
 (2) USING SAME CRACK CONCEPTS AS SHOWN IN FIGURE 7.

FIGURE 2 — UNIAXIAL FRACTURE TOUGHNESS SPECIMEN

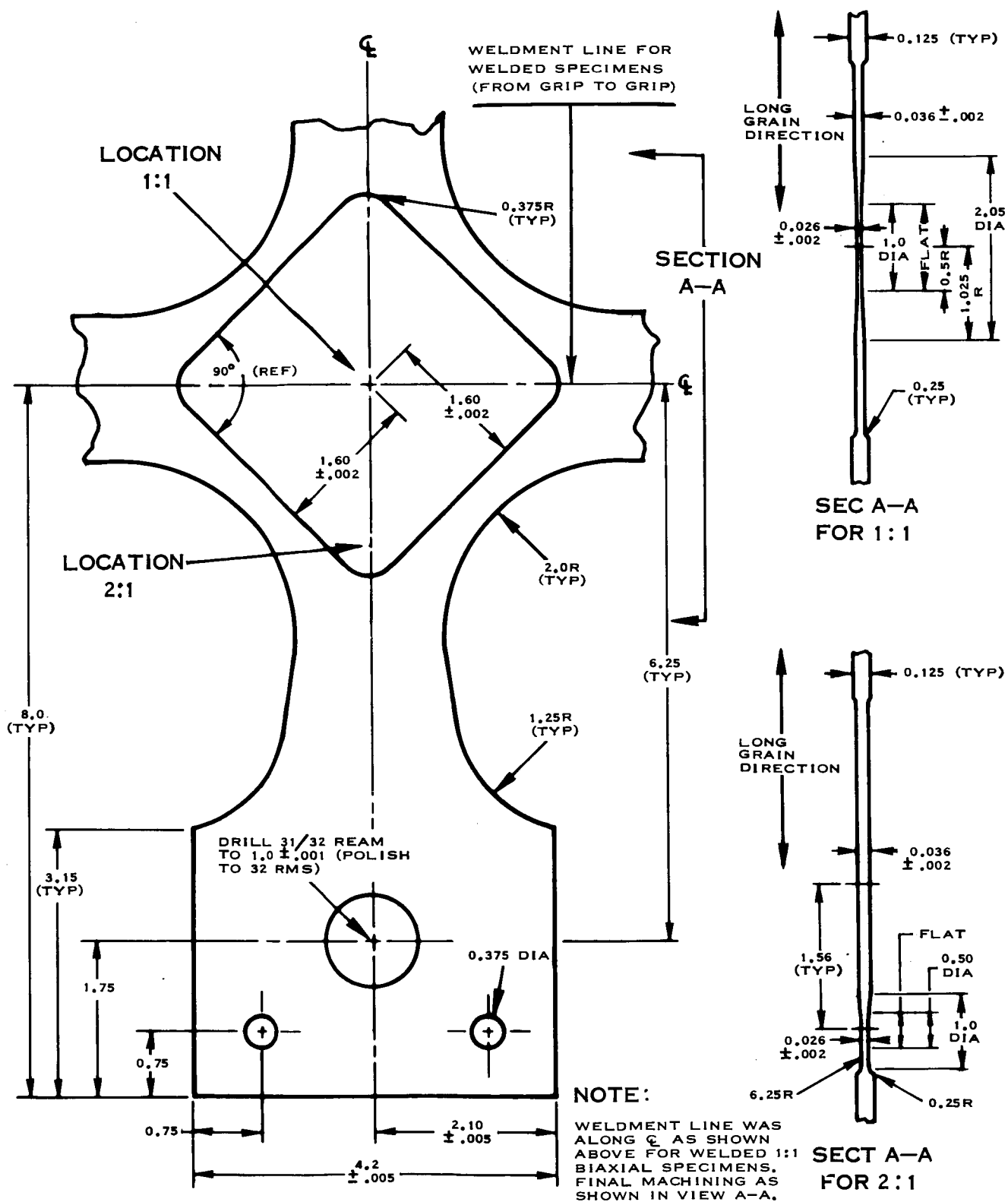


FIGURE 3 - BIAxIAL TEST SPECIMEN



SECTION IV

TEST PROCEDURESGeneral

The development of both unwelded and welded uniaxial, biaxial and fracture toughness data at -105°F, -320°F, and -423°F employed the use of the following test environments (coolants): a dry ice and alcohol solution, liquid nitrogen and liquid hydrogen, respectively. All tests were conducted in permanent type cryostats using a three point carbon-resistor liquid level sensor, thermal measurement and load application equipment. Loads were applied by either a strain paced test machine or by direct strain rate control to maintain the desired 0.005 in/in/min rate to yield while maintaining a strain rate of approximately 0.02 in/in/min from yield to failure. All tests were conducted with the specimens completely submerged in the cooling medium with thermocouples attached to the specimen and load grips. Photographs of the various test apparatus, test set-ups, and drawings of test arrangements are illustrated in Appendix B.

Tests were conducted in a special test cell where maximum protection to personnel and equipment was obtained by use of remote-control mechanisms, proper venting, gas-analysis facilities, and overall minimized safety hazards.

Uniaxial Tests

Full range uniaxial stress-strain curves were developed for each material and test temperature by applying a tensile load through a calibrated load cell while measurement of strain was accomplished by a 1-inch mechanical extensometer, Baldwin SR-4, Class B-2, and 1/2-inch strain gages. The load cell furnished continuous load signals to the three x-y recorders with strain signals being recorded from the extensometer, an axial gage, and a contractional (transverse) gage. Special low-temperature strain gage techniques were employed in order to obtain strain gage data well into the plastic deformation region. Details of use and fabrication of these gages are shown in Appendix C. Strain calibration test to determine the gage factors was accomplished by comparison of strains from the extensometer and strains from the gages as illustrated by the following equation:

$$e_{\text{extensometer}} = \frac{e_{\text{gage}}}{\text{Gage Factor}} = \frac{\text{Resistance}}{\text{Resistance} \times (\text{Gage Factor})} \quad (1)$$

Temperature measurements utilized a series of thermocouples attached to the test specimens and the loading grips inside of the cryostat. In addition temperature compensation effects on gages were balanced-out through a Wheatstone bridge. This compensation allowed the nullification of contractional strain due to lowering the temperature of the specimen.

Biaxial Tests

The biaxial tests were conducted in accordance with the procedures developed and presented in Reference 1 using the same cooling mediums, temperature control and strain compensation-calibration techniques already discussed for uniaxial tests. Loads were applied through two mutually perpendicular calibrated load cells while strains were recorded from 1/2-inch strain gages. Loads and strain were recorded on x-y recorders for each of the two principal stress directions. Appendix B illustrates the biaxial test set-up.

In order to generate full range stress-strain curves, in face of the possibility that the strain gages under these conditions could fail before specimen failure, a set of external gage marks was applied in both stress directions and utilized to determine failing strains. These failing strain values and the failure loads allowed the calculation of the failing stresses and strains and closure of the stress-strain curves; however, this back-up technique was used in very few cases since the low temperature gages performed exceptionally well.

The 1:1 tests at the applicable temperature were conducted in a manner to satisfy the elastic equational requirements of:

$$e_1 = \frac{S_1}{E_1} - \frac{\mu_2 S_2}{E_2} ; e_2 = \frac{S_2}{E_2} - \frac{\mu_1 S_1}{E_1} ; e_3 = -f(\mu, E, S_1, S_2) \quad (2)$$

where $e_1 = e_2$ and $S_1 = S_2$; when $E_1 = E_2$ and $\mu_1 = \mu_2$

Once the material entered the plastic zone, the same load ratios required to cause e_1 to equal e_2 were maintained to failure. These procedures produced and maintained a nominal 1:1 state of stress during the entire test period.

The 2:1 tests at the applicable temperatures were conducted in a manner to satisfy the elastic equational requirement of:

$$e_1 = \frac{S_1}{E_1} - \frac{\mu_2 S_2}{E_2} ; e_2 = \frac{S_2}{E_2} - \frac{\mu_1 S_1}{E_1} ; e_3 = -f(\mu, E, S_1, S_2)$$

where $S_1 = 2S_2$

$$\text{and } e_1 = \frac{S_1}{E_1} - \frac{0.5 \mu_2 S_1}{E_2} ; e_2 = \frac{0.5 S_1}{E_1} - \frac{\mu_1 S_1}{E_2}$$

$$e_3 = -f(\mu, E, S_1, S_2)$$

The ratios of e_1/e_2 at each temperature is the ratio that is required to establish a 2:1 state of stress and is expressed as :

$$\frac{e_1}{e_2} = \frac{E_2 - 0.5 \mu_2 E_1}{0.5 E_1 - \mu_1 E_2} \quad \text{or when } E_1 = E_2 ; \frac{e_1}{e_2} = \frac{1 - 0.5 \mu}{0.5 - \mu}$$

and $\mu_1 = \mu_2$

This ratio was established for each material and each test temperature from uniaxial data (E_1, E_2, μ_1, μ_2) obtained from the same sheets as the biaxial specimens. This strain ratio was then the value required to obtain a 2:1 stress state in the elastic range. Once the material enters the plastic zone, the slope of the load strain curve for the minimum principal stress direction was held constant by a servo system continually monitoring the jack load in this direction. This condition was maintained to failure unless the material went fully plastic and refused to accept load, and therefore an increase in stress in the maximum principal stress direction. When this plasticity condition was attained, the strain in the minimum stress direction was held constant to failure. This means that only enough load was applied in the minimum stress direction to nullify Poisson's effects as a result of fully plastic flow in the maximum stress direction.

Biaxial (effective) modulus values were calculated by the following equation ($\sigma_1/e_1 = E_{\text{biaxial}}$ where σ_1 is a calculated stress (for biaxial case) in the one direction and e_1 was an experimentally determined strain for the given biaxial stress state in the one direction).

Appendix D illustrates the techniques employed to obtain biaxial stress-strain curves from load-strain curves.

Fracture Toughness Tests

The uniaxial and biaxial fracture toughness specimens were fatigue cycled at room temperature to generate partial through cracks (simulated natural flaws) at low stress levels using a unidirectional stress field. Once the cracks or flaws were developed, the cracked uniaxial and 1:1 biaxial specimens were tested in a similar manner as the standard uniaxial and biaxial tensile specimens already discussed. Strain gages mounted over the cracked area along with calibrated load cell values supplied a load versus strain plot. Using the techniques developed and standardized in Reference 2, the applicable "pop-in" (initial crack extension) stress was determined. (Hereafter in this report, the "pop-in" stress is referred to as the gross area stress, S_{\max} .) This was accomplished directly for the uniaxial test by simple load/area calculation for the determined "pop-in" (strain) point. For the 1:1 biaxial stress state test the "pop-in" strain was established and the stress that matched that strain in a standard 1:1 biaxial stress test (uncracked) was used as the 1:1 biaxial "pop-in" stress. The equation used to calculate the fracture toughness parameter, K_{IC} , is the same as the one now in widespread use, originally presented in reference 3, and as shown below:

$$K_{IC} = \sqrt{\frac{1.2 \pi b S_{\max}^2}{\phi^2 - 0.212 \left(\frac{S_{\max}}{S_y} \right)^2}} \quad (6)$$

The respective uniaxial and biaxial yield strength values were used in the S_y term as determined by tests in this research on the applicable material at the given temperature condition. The respective "pop-in" stress values as already discussed were used in the S_{\max} term. The crack depth, a , and half crack length, b , were measured from the fractured specimens after the tests were complete to establish the original (fatigue generated) flaw or crack size. Generated fatigue cracks were perpendicular to the longitudinal grain direction in both the uniaxial and 1:1 biaxial specimens. Appendix E illustrates a computerized technique of evaluating the K_{IC} term from the above noted experimental data.

Creep Tests

The uniaxial and 1:1 biaxial creep specimens were tested in permanent type cryostats shown in Appendix B. The -320°F creep specimens were placed in the cryostat and

the cryostat was then filled with liquid nitrogen to obtain the required -320°F condition. The required load was applied to achieve 90% of the -320°F yield strength (either uniaxial or 1:1 biaxial) stress state condition. Strain was recorded from both mechanical extensometer and strain gages and checked against gage mark extensions at the completion of the tests. This load and temperature was held constant for the applicable time of subjection (minimum of 14 days or until failure) while recording the creep strain.

The 1:1 biaxial creep test conducted at room temperature was conducted in a similar manner except 90% of room temperature yield strength stress condition was used.

The uniaxial creep tests were conducted in an Arcweld, Model G creep machine modified to use the permanent type cryostat. The 1:1 biaxial creep tests were conducted in the biaxial test machine while using a dead-loaded hydraulic actuator as a sourcing pressure system for the two prime load application jacks in the biaxial machine. The carbon-resistor automatic liquid level sensing mechanism and a solenoid system were used to regulate liquid nitrogen flow into the cryostats during the test period and maintain the desired liquid level.

SECTION V

TEST RESULTSUniaxial Tensile Data

The uniaxial tensile data developed at ambient, -105°F , -320°F and -423°F for the program materials are presented in Table 1. The uniaxial properties for these temperature levels that are shown in this table include: ultimate strength, yield strength (0.2% offset), modulus of elasticity, Poisson's ratio, percent elongation and the Ludwik strain hardening coefficient. Appendix F illustrates a computerized program for rapid calculation of the Ludwik strain hardening coefficient.

The tabular data includes data for both the unwelded and welded conditions, as well as, data for both the longitudinal and transverse grain directions. Typical uniaxial stress-strain curves for the various program materials at test temperatures are shown in Appendix G.

Biaxial Tensile Data

The 1:1 and 2:1 biaxial tensile data developed at ambient, -105°F , -320°F and -423°F for the program materials are presented in Table 2. The biaxial properties for these temperature levels shown in this table are: biaxial ultimate strength, biaxial yield strength, biaxial (effective) modulus and percent elongations. This tabular data includes 1:1 and 2:1 biaxial data in the unwelded condition, as well as, 1:1 biaxial data in the welded condition. Typical biaxial stress-strain curves for the various program materials at test temperatures are shown in Appendix H.

Fracture Toughness Data

Fracture toughness data of the partial through crack (flaw) type were developed on three of the program materials. These alloys were chosen to develop trends as to the effects of stress state on the K_{IC} plane strain fracture toughness. The uniaxial and 1:1 biaxial stress state fracture toughness data is presented in Table 3. This table includes the crack (flaw) size dimensions, flaw half length/depth ratio, gross section stress at "pop-in", applicable yield strength (uniaxial or 1:1 biaxial) and the calculated K_{IC} fracture toughness parameter.

Cryogenic Creep Data

Uniaxial and 1:1 biaxial creep data (strains and times) are presented in Table 4. These data were generated at -320°F on the 5Al-2.5Sn titanium alloy (ELI) and the 6Al-4V titanium alloy (ELI) under uniaxial and 1:1 biaxial stress levels of 90% of -320°F yield for a minimum period of 14 days or until failure. One test at room temperature on a 5Al-2.5Sn (ELI) titanium specimen (1:1 biaxial) at 90% room temperature yield is also included.

Data Compiled from Other Sources

Appendix I presents a compilation of data from other sources, as well as other research efforts conducted by LTV. These data include both uniaxial and biaxial stress states and are presented in a series of tables in this appendix.

TABLE 1
UNIAXIAL TENSILE PROPERTIES OF PROGRAM MATERIALS

MATERIAL	SPEC. NO.	GRAIN DIRECTION	TEST TEMP. °F	ULTIMATE STRENGTH KSI	YIELD STRENGTH KSI	ELASTIC MODULUS PSI $\times 10^6$	POISSON'S RATIO	PERCENT ELONGATION (2" GAGE LENGTH)	LUDWIK STRAIN HARDENING COEFFICIENT "n"
2219-T87 Aluminum Alloy	ALL1	Long.	75	66.4	53.9	10.2	.25	6.0	.145
	ALT1	Trans.	75	65.5	51.7	10.3	.27	7.0	.151
	ALL2	Long.	-105	70.9	55.0	11.0	.24	6.5	.130
	ALL3	Long.	-105	71.4	56.1	10.1	.30	6.0	.137
	ALT2	Trans.	-105	70.1	54.4	12.0	.30	6.5	.121
	ALT3	Trans.	-105	70.8	54.3	11.7	-	7.0	.139
	ALL4	Long.	-320	84.0	61.0	13.1	.34	7.0	.133
	ALL8	Long.	-320	81.5	63.3	12.3	.28	7.5	.125
	ALT4	Trans.	-320	82.8	62.7	13.2	.24	6.0	.134
	ALT5	Trans.	-320	83.6	63.9	13.9	.28	7.5	.114
	ALL6	Long.	-423	98.6	68.0	14.6	.28	11.0	.167
	ALL7	Long.	-423	100.8	79.6	13.4	.26	8.5	.170
	ALT6	Trans.	-423	101.4	69.9	12.9	.26	8.5	.175
	ALT7	Trans.	-423	94.0	68.2	13.5	.27	7.5	.142
2014-T6 Aluminum Alloy	A2L1	Long.	75	71.9	67.8	10.1	.29	6.5	.181
	A2T1	Trans.	75	71.8	63.9	11.1	.27	6.5	.105
	A2L2	Long.	-105	74.6	69.2	11.2	.32	5.5	.072
	A2L3	Long.	-105	74.4	69.9	11.3	.32	6.5	.067
	A2T2	Trans.	-105	76.6	68.3	12.3	.31	6.5	.115
	A2T3	Trans.	-105	75.8	66.1	11.2	.32	7.0	.113
	A2L4	Long.	-320	87.4	79.6	12.6	.24	7.5	.075
	A2L5	Long.	-320	86.4	77.5	12.0	.26	7.0	.095
	A2T4	Trans.	-320	86.7	74.4	12.3	.25	4.5	.125
	A2T5	Trans.	-320	86.6	76.6	12.8	.26	5.0	.120
	A2L6	Long.	-423	97.6	87.5	12.9	.26	10.0	.083
	A2L7	Long.	-423	93.9	86.2	12.2	.23	8.0	.075
	A2T6	Trans.	-423	99.3	87.4	12.8	.22	8.5	.135
	A2T7	Trans.	-423	100.3	82.6	11.9	.24	7.5	.119

TABLE 1 - CONT.
UNIAXIAL TENSILE PROPERTIES OF PROGRAM MATERIALS

MATERIAL	SPEC. NO.	GRAIN DIRECTION	TEST TEMP. °F	ULTIMATE STRENGTH KSI	YIELD STRENGTH KSI	ELASTIC MODULUS $\text{PSI} \times 10^6$	POISSON'S RATIO	PERCENT ELONGATION (2" GAGE LENGTH)	LUDWIK STRAIN HARDENING COEFFICIENT "n"
5AL-2.5SN Titanium Alloy (Annealed)	T3L1	Long.	75	136.0	127.6	16.0	.28	14.0	.065
	T3T1	Trans.	75	146.4	138.0	16.7	.29	13.5	.047
	T3L2	Long.	-105	166.0	-	16.9	.25	9.5	.061
	T3L3	Long.	-105	167.0	154.0	18.0	.35	13.0	.066
	T3T2	Trans.	-105	169.0	162.0	17.6	.34	12.5	.066
	T3T3	Trans.	-105	173.5	162.0	19.6	.35	12.0	.056
	T3L4	Long.	-320	218.0	212.0	17.4	.25	12.0	.082
	T3L5	Long.	-320	216.0	199.0	17.7	.26	9.5	.135
	T3T4	Trans.	-320	216.0	210.0	19.3	.27	10.0	.100
	T3T5	Trans.	-320	214.0	206.0	19.5	.29	11.5	.110
	T3L6	Long.	-423	246.0	241.0	18.5	.24	1.7	.222
	T3L7	Long.	-423	249.0	240.0	17.5	.21	2.0	.294
	T3T6	Trans.	-423	240.0	231.0	20.0	.21	1.7	.170
	T3T7	Trans.	-423	241.1	239.0	19.7	.22	2.5	.189
6AL-4V Titanium Alloy (ELI, Annealed)	T4L8	Long.	75	130.0	122.0	16.7	.21	7.0	.070
	T4T1	Trans.	75	155.0	150.0	16.7	.27	10.0	.051
	T4L2	Long.	-105	168.0	160.0	16.5	.23	6.5	.062
	T4L3	Long.	-105	160.5	152.8	16.3	.25	8.0	.055
	T4T2	Trans.	-105	173.5	167.0	16.6	.28	12.0	.045
	T4T3	Trans.	-105	189.0	184.0	17.6	.22	10.5	.057
	T4L4	Long.	-320	220.0	216.0	17.3	.18	7.5	.050
	T4L5	Long.	-320	218.0	216.0	18.6	.22	2.0	.149
	T4T4	Trans.	-320	225.0	223.0	21.5	.25	12.0	.055
	T4T5	Trans.	-320	229.0	222.0	19.0	.23	5.0	.070
	T4L6	Long.	-423	264.0	254.0	18.6	.18	2.1	.349
	T4L7	Long.	-423	258.0	254.0	17.2	.18	1.7	.244
	T4T6	Trans.	-423	249.0	241.0	20.1	.22	2.1	.156
	T4T7	Trans.	-423	232.0	230.0	19.7	.18	1.5	.190

TABLE 1 - CONT.
UNIAXIAL TENSILE PROPERTIES OF PROGRAM MATERIALS

MATERIAL	SPEC. NO.	GRAIN DIRECTION	TEST TEMP. °F	ULTIMATE STRENGTH KSI	YIELD STRENGTH KSI	ELASTIC MODULUS $\text{PSI} \times 10^6$	POISSON'S RATIO	PERCENT ELONGATION (2" GAGE LENGTH)	LUDWIK STRAIN HARDENING COEFFICIENT "n"
Inconel 718 (Heat-Treated) (See Section II for Heat Treatment Schedule)	I5L1	Long.	75	193.0	161.0	29.9	.28	16.0	.142
	I5T1	Trans.	75	193.0	170.0	28.8	.29	16.0	.111
	I5L2	Long.	-105	207.0	154.0	31.0	.32	14.0	.117
	I5L3	Long.	-105	208.0	162.0	32.5	.35	22.5	.094
	I5T2	Trans.	-105	209.0	175.0	31.8	.28	6.5	.110
	I5T3	Trans.	-105	199.0	156.6	29.8	.27	4.0	.169
	I5L4	Long.	-320	242.0	193.0	32.5	.26	16.0	.126
	I5L5	Long.	-320	254.0	199.0	32.5	.24	9.5	.079
	I5T4	Trans.	-320	234.0	186.0	33.6	.26	11.5	.110
	I5T5	Trans.	-320	236.0	194.0	33.4	.24	8.5	.081
	I5L6	Long.	-423	240.0	181.5	33.6	.28	8.2	.174
	I5L7	Long.	-423	236.0	185.0	31.7	.20	9.0	.175
	I5T6	Trans.	-423	246.0	208.0	35.7	.26	5.0	.135
	I5T8	Trans.	-423	230.0	192.6	33.7	.33	4.6	.128
6AL-4V Titanium Alloy (STA)	T6L1	Long.	75	165.0	152.0	16.2	.25	6.3	.083
	T6T1	Trans.	75	178.0	166.0	17.6	.28	9.1	.076
	T6L2	Long.	-105	190.0	178.0	16.9	.25	5.5	.089
	T6L3	Long.	-105	193.0	180.0	16.8	.26	5.0	.090
	T6T2	Trans.	-105	204.0	194.0	19.2	.28	5.5	.082
	T6T3	Trans.	-105	206.0	197.0	19.0	.28	5.5	.079
	T6L4	Long.	-320	252.0	245.0	19.3	.21	3.2	.094
	T6L5	Long.	-320	254.0	244.0	18.1	.22	3.7	.093
	T6T4	Trans.	-320	254.0	250.0	20.8	.26	2.3	.072
	T6T5	Trans.	-320	258.0	-	20.5	.22	2.0	.093

TABLE 1 - CONT.
UNIAXIAL TENSILE PROPERTIES OF PROGRAM MATERIALS

MATERIAL	SPEC. NO.	GRAIN DIRECTION	TEST TEMP. °F	ULTIMATE STRENGTH KSI	YIELD STRENGTH KSI	ELASTIC MODULUS $\text{PSI} \times 10^6$	POISSON'S RATIO	PERCENT ELONGATION (2" GAGE LENGTH)	LUDWIK STRAIN HARDENING COEFFICIENT "n"
2219-T87 Aluminum Alloy (As-Welded)	A1W1	Long.	75	41.2	34.8	10.7	.20	1.3	.308
	A1W2	Long.	-320	69.3	50.3	13.6	.25	2.2	.311
	A1W3	Long.	-423	64.0	-	14.8	.27	.5	-
2014-T6 Aluminum Alloy (As-Welded)	A2W1	Long.	75	42.0	34.0	10.8	.31	1.2	.343
	A2W2	Long.	-320	47.9	34.8	12.2	.31	1.0	.394
	A2W3	Long.	-423	45.6	31.6	14.0	-	1.0	.308
5AL-2.5SN Titanium Alloy (Annealed) (As-Welded)	T3W1	Long.	75	136.0	123.0	16.2	.31	14.5	.100
	T3W2	Long.	-320	216.0	203.0	17.6	.27	4.0	.122
	T3W3	Long.	-423	234.0	222.0	19.5	.29	1.5	-
6AL-4V Titanium Alloy (ELI, Annealed) (As-Welded)	T4W1	Long.	75	131.0	123.0	16.2	.28	5.2	.091
	T4W2	Long.	-320	222.0	211.0	19.2	.22	4.0	.087
	T4W3	Long.	-423	233.0	-	20.0	.25	1.5	-
Inconel 718 (As-Welded)	I5W1	Long.	75	113.0	80.0	29.2	.25	4.0	.213
	I5W2	Long.	-320	152.0	117.0	30.6	.23	3.2	.212
	I5W3	Long.	-423	126.0	71.5	28.2	.34	4.1	.264
6AL-4V Titanium Alloy (STA) (As-Welded)	T6W1	Long.	75	154.0	145.0	16.8	.28	4.5	.143
	T6W2	Long.	-320	248.0	241.0	18.5	.24	3.5	.121

NOTES: (1) All weldment failures were in the weld area.
(2) Poisson's ratio values obtained in welded specimens were obtained using a 1/2-inch gage length and include effects of the weld area and the heat affected zone.

TABLE 2
BIAXIAL TENSILE PROPERTIES OF PROGRAM MATERIALS

MATERIAL	SPEC. NO.	GRAIN DIRECTION	TEST TEMP °F	STATE OF STRESS	BIAXIAL ULTIMATE STRENGTH KSI	BIAXIAL YIELD STRENGTH KSI	BIAXIAL MODULUS $\text{PSI} \times 10^6$ *	% ELONGATION (1/2" GAGE) (LONG. GRAIN DIRECTION)	% ELONGATION (1/2" GAGE) (TRAN. GRAIN DIRECTION)
2219-T87 Aluminum Alloy	BAL-4	Long.	75	1:1	65.6	51.4	13.7	4.1	3.0
	BAL-5	Long.	-105	1:1	69.4	55.0	14.6	3.8	3.1
	BAL-6	Long.	-105	1:1	67.2	53.6	14.5	3.6	3.2
	BAL-7	Long.	-105	1:1	69.0	54.6	14.9	3.8	3.7
	BAL-8	Long.	-320	1:1	85.5	69.5	18.0	3.5	2.5
	BAL-9	Long.	-320	1:1	87.5	69.0	18.1	5.4	5.5
	BAL-10	Long.	-320	1:1	89.0	70.1	18.1	3.7	3.5
	BAL-11	Long.	-423	1:1	104.0	82.5	18.5	5.0	4.5
	BAL-12	Long.	-423	1:1	99.5	78.5	18.6	7.0	6.7
	BAL-13	Long.	-423	1:1	103.5	83.0	18.5	4.0	6.0
	BAL-14	Long.	75	2:1	74.6	58.3	11.6	5.9	-
	BAL-15	Long.	-105	2:1	81.5	62.0	12.0	6.5	-
	BAL-16	Long.	-105	2:1	79.5	60.8	12.1	6.2	-
	BAL-17	Long.	-105	2:1	82.0	61.0	12.0	7.0	-
	BAL-18	Long.	-320	2:1	94.0	65.0	14.3	4.0	-
	BAL-19	Long.	-320	2:1	97.0	73.3	13.9	7.0	-
	BAL-20	Long.	-320	2:1	94.0	69.5	14.3	6.5	-
	BAL-11	Long.	-423	2:1	119.5	90.0	15.6	9.0	-
	BAL-12	Long.	-423	2:1	119.2	87.5	15.6	8.0	-
	BAL-13	Long.	-423	2:1	118.0	91.5	15.6	5.0	-
2014-T6 Aluminum Alloy	BA2-4	Long.	75	1:1	69.9	62.0	13.8	2.5	-
	BA2-5	Long.	-105	1:1	74.5	65.0	15.7	3.7	3.7
	BA2-6	Long.	-105	1:1	75.0	64.3	16.1	2.0	4.0
	BA2-7	Long.	-105	1:1	74.2	67.0	16.0	3.7	3.4
	BA2-8	Long.	-320	1:1	86.0	70.5	16.6	4.4	3.8
	BA2-9	Long.	-320	1:1	88.9	76.8	16.6	6.0	4.4
	BA2-10	Long.	-320	1:1	86.5	75.4	16.7	4.0	3.5
	BA2-11	Long.	-423	1:1	93.6	82.0	17.2	9.0	7.5

TABLE 2 - CONT.
 BIAxIAL TENSILE PROPERTIES OF PROGRAM MATERIALS

MATERIAL	SPEC. NO.	GRAIN DIRECTION	TEST TEMP of	STATE OF STRESS	BIAxIAL ULTIMATE STRENGTH KSI	BIAxIAL YIELD STRENGTH KSI	BIAxIAL MODULUS $\text{PSI} \times 10^6$ *	% ELONGATION (1/2" GAGE) (LONG. GRAIN DIRECTION)	% ELONGATION (1/2" GAGE) (TRAN. GRAIN DIRECTION)
2014-T6 Aluminum Alloy	BA2-2	Long.	-423	1:1	98.0	83.0	17.1	7.0	7.0
	BA2-3	Long.	-423	1:1	96.0	83.5	17.2	5.0	5.0
	BA2-14	Long.	75	2:1	79.0	68.5	11.6	3.4	-
	BA2-15	Long.	-105	2:1	86.0	73.5	13.3	5.6	-
	BA2-16	Long.	-105	2:1	86.5	71.5	13.3	6.1	-
	BA2-17	Long.	-105	2:1	83.5	69.4	13.4	5.7	-
	BA2-18	Long.	-320	2:1	100.4	85.0	14.0	-	-
	BA2-19	Long.	-320	2:1	99.8	78.5	14.0	-	-
	BA2-20	Long.	-320	2:1	100.2	89.1	13.9	4.5	-
	BA2-11	Long.	-423	2:1	120.0	100.5	14.6	6.0	-
	BA2-12	Long.	-423	2:1	117.5	93.7	13.9	5.5	-
	BA2-13	Long.	-423	2:1	118.2	95.4	13.9	4.0	-
5AL-2.5SN Titanium Alloy (Annealed)	BT3-4	Long.	75	1:1	136.1	106.0	22.4	2.9	4.2
	BT3-5	Long.	-105	1:1	166.5	154.5	24.0	6.4	3.9
	BT3-6	Long.	-105	1:1	171.0	157.0	24.0	5.6	4.0
	BT3-7	Long.	-105	1:1	161.8	152.2	24.0	5.5	5.1
	BT3-8	Long.	-320	1:1	220.2	215.0	24.9	3.8	3.0
	BT3-9	Long.	-320	1:1	218.5	214.0	24.4	4.7	3.2
	BT3-10	Long.	-320	1:1	216.0	206.0	24.4	3.0	2.5
	BT3-11	Long.	-423	1:1	233.0	230.0	25.2	1.3	1.2
	BT3-12	Long.	-423	1:1	231.5	230.5	25.2	1.1	1.2
	BT3-13	Long.	-423	1:1	234.5	231.0	25.2	1.3	1.1
	BT3-14	Long.	75	2:1	153.0	131.0	18.5	9.0	-
	BT3-15	Long.	-105	2:1	188.5	170.4	20.2	5.7	-
	BT3-16	Long.	-105	2:1	189.6	163.8	20.1	5.6	-
	BT3-17	Long.	-105	2:1	193.0	170.0	20.3	6.9	-
	BT3-18	Long.	-320	2:1	249.4	223.5	20.1	4.7	-
	BT3-19	Long.	-320	2:1	250.6	211.5	20.1	8.0	-

TABLE 2-CON'T
 BIAxIAL TENSILE PROPERTIES OF PROGRAM MATERIALS

MATERIAL	SPEC. NO.	GRAIN DIRECTION	TEST TEMP °F	STATE OF STRESS	BIAxIAL ULTIMATE STRENGTH KSI	BIAxIAL YIELD STRENGTH KSI	BIAxIAL MODULUS PSI x 10 ⁶ *	% ELONGATION (1/2" GAGE) (LONG. GRAIN DIRECTION)	% ELONGATION (1/2" GAGE) (TRAN. GRAIN DIRECTION)
5AL-2.5SN Titanium Alloy (Annealed)	BT3-20	Long.	-320	2:1	238.0	204.0	20.0	8.0	-
	BT3-11	Long.	-423	2:1	263.5	254.0	20.9	1.6	-
	BT3-12	Long.	-423	2:1	260.5	253.0	20.8	1.5	-
	BT3-13	Long.	-423	2:1	266.5	248.5	20.8	1.7	-
6AL-4V Titanium Alloy (ELI, Annealed)	BT4-4	Long.	75	1:1	156.5	146.5	23.0	4.2	1.6
	BT4-5	Long.	-105	1:1	166.3	155.5	21.8	2.6	1.1
	BT4-6	Long.	-105	1:1	172.5	161.0	21.7	5.3	1.7
	BT4-7	Long.	-105	1:1	159.0	151.7	22.1	1.7	1.2
	BT4-8	Long.	-320	1:1	222.0	217.3	22.5	3.0	2.5
	BT4-9	Long.	-320	1:1	206.5	195.0	22.5	3.2	2.2
	BT4-10	Long.	-320	1:1	213.0	208.5	23.5	3.1	2.2
	BT4-1	Long.	-423	1:1	260.0	258.0	22.8	1.4	1.5
	BT4-2	Long.	-423	1:1	258.5	256.0	22.6	1.4	1.4
	BT4-3	Long.	-423	1:1	261.5	257.5	22.2	1.2	1.3
	BT4-14	Long.	75	2:1	162.4	141.5	17.9	5.6	-
	BT4-15	Long.	-105	2:1	185.4	155.0	18.8	4.6	-
	BT4-16	Long.	-105	2:1	180.5	157.2	18.7	5.3	-
	BT4-17	Long.	-105	2:1	188.7	161.5	18.7	6.0	-
	BT4-18	Long.	-320	2:1	229.5	187.3	17.4	4.0	-
	BT4-19	Long.	-320	2:1	235.5	189.0	17.1	4.5	-
	BT4-20	Long.	-320	2:1	239.8	198.0	17.1	8.0	-
	BT4-11	Long.	-423	2:1	265.4	261.0	19.7	1.6	-
	BT4-12	Long.	-423	2:1	258.2	250.8	19.9	1.7	-
	BT4-13	Long.	-423	2:1	266.5	264.0	20.0	1.6	-

TABLE 2-CONT.
BIAXIAL TENSILE PROPERTIES OF PROGRAM MATERIALS

MATERIAL	SPEC. NO.	GRAIN DIRECTION	TEST TEMP °F	STATE OF STRESS	BIAXIAL ULTIMATE STRENGTH KSI	BIAXIAL YIELD STRENGTH KSI	BIAXIAL MODULUS $\text{PSI} \times 10^6$ *	% ELONGATION (1/2" GAGE) (LONG. GRAIN DIRECTION)	% ELONGATION (1/2" GAGE) (TRAN. GRAIN DIRECTION)
Inconel 718 (Heat-Treated) (See Section II for Heat Treatment Schedule)	BI5-4	Long.	75	1:1	191.5	170.5	41.5	4.7	5.2
	BI5-5	Long.	-105	1:1	212.0	186.4	43.6	6.5	4.0
	BI5-6	Long.	-105	1:1	208.2	185.3	43.7	4.0	3.2
	BI5-7	Long.	-105	1:1	210.5	181.5	43.7	5.8	4.5
	BI5-8	Long.	-320	1:1	248.5	217.5	43.5	4.2	4.0
	BI5-9	Long.	-320	1:1	246.8	218.3	44.7	4.0	4.0
	BI5-10	Long.	-320	1:1	247.2	219.5	44.5	4.0	5.0
	BI5-11	Long.	-423	1:1	239.0	197.0	43.0	3.7	4.0
	BI5-12	Long.	-423	1:1	236.5	193.5	42.8	5.5	6.5
	BI5-13	Long.	-423	1:1	237.5	205.0	42.9	4.0	4.1
	BI5-14	Long.	75	2:1	208.2	168.2	30.5	6.0	-
	BI5-15	Long.	-105	2:1	228.5	196.5	32.2	11.0	-
	BI5-16	Long.	-105	2:1	231.2	182.0	33.8	6.0	-
	BI5-17	Long.	-105	2:1	222.0	194.2	31.8	8.0	-
	BI5-18	Long.	-320	2:1	281.0	217.0	35.3	14.0	-
	BI5-19	Long.	-320	2:1	269.5	216.2	33.6	10.0	-
	BI5-20	Long.	-320	2:1	264.5	214.5	37.1	8.0	-
	BI5-11	Long.	-423	2:1	256.5	194.0	36.0	5.5	-
	BI5-12	Long.	-423	2:1	268.5	197.5	34.6	5.8	-
	BI5-13	Long.	-423	2:1	262.2	203.8	36.9	5.4	-
6AL-4V Titanium Alloy (STA)	BT6-1	Long.	75	1:1	167.0	147.5	23.7	2.6	1.7
	BT6-2	Long.	-105	1:1	193.5	180.5	22.6	2.7	2.0
	BT6-3	Long.	-105	1:1	188.0	176.5	22.6	2.0	1.6
	BT6-4	Long.	-105	1:1	191.5	181.5	22.5	2.1	1.1
	BT6-5	Long.	-320	1:1	248.2	236.2	24.0	1.8	1.5
	BT6-6	Long.	-320	1:1	253.0	242.0	24.0	2.2	1.7
	BT6-7	Long.	-320	1:1	249.8	236.0	23.9	2.4	1.6
	BT6-11	Long.	75	2:1	172.5	153.5	17.6	4.8	-
	BT6-12	Long.	-105	2:1	210.5	183.0	19.3	4.5	-
	BT6-13	Long.	-105	2:1	221.0	197.0	19.2	3.5	-

TABLE 2-CONT.
 BIAxIAL TENSILE PROPERTIES OF PROGRAM MATERIALS

MATERIAL	SPEC. NO.	GRAIN DIRECTION	TEST TEMP °F	STATE OF STRESS	BIAxIAL ULTIMATE STRENGTH KSI	BIAxIAL YIELD STRENGTH KSI	BIAxIAL MODULUS $\text{PSI} \times 10^6$ *	% ELONGATION (1/2" GAGE) (LONG. GRAIN DIRECTION)	% ELONGATION (1/2" GAGE) (TRAN. GRAIN DIRECTION)
6AL-4V Titanium Alloy (STA)	BT6-14	Long.	-105	2:1	216.0	187.2	19.3	4.2	-
	BT6-15	Long.	-320	2:1	269.0	226.0	18.2	5.0	-
	BT6-16	Long.	-320	2:1	272.5	232.0	19.5	4.0	-
	BT6-17	Long.	-320	2:1	268.5	236.0	18.7	4.6	-

* Biaxial (effective) modulus was calculated by techniques shown in Section IV.

TABLE 2-CONT.
BIAXIAL TENSILE PROPERTIES OF PROGRAM MATERIALS

MATERIAL	SPEC. NO.	GRAIN DIRECTION	TEST TEMP OF	STATE OF STRESS	BIAXIAL ULTIMATE STRENGTH KSI	BIAXIAL YIELD STRENGTH KSI	BIAXIAL MODULUS $\text{PSI} \times 10^6$ *	% ELONGATION (1/2" GAGE) (LONG. GRAIN DIRECTION)	% ELONGATION (1/2" GAGE) (TRAN. GRAIN DIRECTION)
2219-T87 Aluminum Alloy (As-Welded)	BAL-W1	Long.	75	1:1	35.0	19.0	13.3	2.4	2.0
	BAL-W2	Long.	-320	1:1	65.5	29.0	18.1	9.0	4.0
	BAL-W3	Long.	-423	1:1	64.0	35.4	20.1	3.2	1.0
2014-T6 Aluminum Alloy (As-Welded)	BA2-W4	Long.	75	1:1	45.7	31.0	15.7	1.1	.25
	BA2-W2	Long.	-320	1:1	47.2	29.7	17.6	1.9	.5
	BA2-W3	Long.	-423	1:1	44.1	29.4	14.0	1.2	1.2
5AL-2,5SN Titanium Alloy (Annealed) (As-Welded)	BT3-W1	Long.	75	1:1	143.0	128.5	23.5	2.1	2.0
	BT3-W2	Long.	-320	1:1	179.5	127.5	24.2	4.0	2.0
	BT3-W3	Long.	-423	1:1	221.5	209.0	27.4	2.0	2.0
6AL-4V Titanium Alloy (ELI, Annealed) (As-Welded)	BT4-W1	Long.	75	1:1	124.5	117.5	21.2	1.9	1.2
	BT4-W2	Long.	-320	1:1	214.0	179.4	24.6	3.5	.7
	BT4-W3	Long.	-423	1:1	204.0	204.0	26.6	.9	1.5
Inconel 718 (Heat-Treated) (As-Welded)	BI5-W1	Long.	75	1:1	131.0	79.8	38.9	5.0	3.0
	BI5-W2	Long.	-320	1:1	155.5	148.0	39.9	1.4	.45
	BI5-W3	Long.	-423	1:1	176.0	-	42.6	.5	.55
6AL-4V Titanium Alloy (STA) (As-Welded)	BT6-W1	Long.	75	1:1	161.5	138.5	23.3	2.0	1.2
	BT6-W2	Long.	-320	1:1	218.0	218.0	25.3	1.1	1.0

NOTE: All biaxially stressed weldments failed in the weld area

TABLE 3
PLANE-STRAIN FRACTURE TOUGHNESS PARAMETERS FOR THE
PROGRAM MATERIALS

MATERIAL	SPEC. NO.	TEST TEMP °F	STATE OF STRESS	CRACK HALF LENGTH b, IN.	CRACK DEPTH a, IN	a/b	GROSS STRESS AT POP-IN KSI	YIELD STRENGTH KSI (UNIAXIAL OR BIAXIAL)	K _{IC} KSI $\sqrt{\text{IN.}}$
2219-T87 Aluminum Alloy	UCR1-1	-105	1:0	.100	.030	.300	52.0	48.7	31.7
	UCR1-2	-320	1:0	.090	.035	.389	56.3	50.4	32.1
	UCR1-3	-423	1:0	.165	.040	.242	56.0	73.8	43.7
Inconel 718 (Heat-Treated)	UCR5-1	-105	1:0	.070	.035	.500	172.6	160.2	80.3
	UCR5-2	-320	1:0	.085	.038	.447	186.0	172.1	98.6
	UCR5-3	-423	1:0	.230	.050	.218	95.8	183.2	86.6
5AL-2.5SN Titanium Alloy (ELI, Annealed)	UCR7-1	-105	1:0	.090	.035	.389	138.0	126.7	78.7
	UCR7-4	-105	1:0	.075	.030	.400	121.6	120.4	61.2
	UCR7-2	-320	1:0	.035	.030	.857	168.5	159.0	44.5
	UCR7-3	-423	1:0	.040	.025	.625	197.0	199.5	63.2
2219-T87 Aluminum Alloy	BCR1-1	-320	1:1	.050	.017	.340	60.0	69.5	24.9
	BCR1-2	-423	1:1	.035	.018	.515	53.0	81.3	16.3
Inconel 718 (Heat-Treated)	BCR5-4	-105	1:1	.040	.033	.825	152.0	184.4	42.6
	BCR5-2	-320	1:1	.045	.026	.578	182.0	218.4	62.4
	BCR5-3	-423	1:1	.055	.028	.509	164.3	198.5	64.7
5AL-2.5SN Titanium Alloy (ELI, Annealed)	BCR7-4	-320	1:1	.055	.024	.436	150.0	165.3	62.4
	BCR7-3	-423	1:1	.065	.032	.492	185.0	205.1	80.9

TABLE 4
UNIAXIAL AND 1:1 BIAXIAL CRYOGENIC CREEP PROPERTIES

MATERIAL	SPEC. NO.	TEST TEMP °F	GRAIN DIRECTION	STRESS STATE	STRESS LEVEL KSI (% of Yield)	SPECIMEN FAILURE		DURATION OF TEST HOURS	TOTAL STRAIN %	CREEP STRAIN %
						YES	NO			
6Al-4V Titanium Alloy (ELI, Annealed)	UCP4-2	-320	Long.	1:0	194.5 (90)		X	336	2.82	1.60
	UCP4-3	-320	Trans.	1:0	200.2 (90)		X	336	1.05	.025
	BCP4-2	-320	-	1:1	186.0 (90)	X		172	1.34(L) 1.12(T)	.64(L) .32(T)
	BCP4-3	-320	-	1:1	200.3 (97)	X		8.2	1.97(L) 1.97(T)	1.02(L) .97(T)
	BCP4-4	-320	-	1:1	186.0 (90)		X	345	1.84(L) 1.58(T)	.94(L) .68(T)
5Al-2.5Sn Titanium Alloy (ELI, Annealed)	UCP7-1	-320	Long.	1:0	162.0 (90)		X	276	1.14	.26
	UCP7-2	-320	Long.	1:0	162.0 (90)		X	527	1.09	.18
	BCP7-1	-320	-	1:1	149.0 (90)		X	429	1.08(L) 1.40(T)	.34(L) .65(T)
	BCP7-2	-320	-	1:1	149.0 (90)	X		68.5	2.60(L) 2.50(T)	1.90(L) 1.80(T)
	BCP7-3	75	-	1:1	91.2 (90)		X	430	1.15(L) 1.44(T)	.65(L) .86(T)

SECTION VI

DATA COMPARISON AND DISCUSSIONGeneral

The test data already presented in tabular form have been presented in this section in a comparison format that allows a more direct evaluation of results. These comparisons are:

- a) properties versus temperature for various stress states
- b) properties versus stress state for various temperatures
- c) biaxial/uniaxial strength ratio versus strain hardening coefficient as compared to the deformation energy theory
- d) fracture toughness parameter, K_{IC} , versus temperature for various stress states
- e) uniaxial and biaxial cryogenic creep curves (strain versus time)
- f) uniaxial and biaxial weldment efficiency versus temperature

Figures 5 through 26 illustrate these various comparisons in the sequence as they are listed above. Table 5 and Figure 27 illustrate comparative rating parameter data that evaluate the relative ability of each program material to be used in a cryogenic environment under biaxial stress states.

Post fracture evaluations of the fracture modes, metallurgical condition and flaw origin studies are presented in Appendix J.

LTV AEROSPACE CORPORATION

Properties versus Temperature

Figures 5 through 10 compare the program materials by illustrating the effect of temperature on mechanical properties for the uniaxial and 1:1 and 2:1 biaxial stress states. The properties compared are ultimate strength, yield strength (0.2% offset), modulus of elasticity, percent elongation, and Poisson's ratio. The curves presented in these figures are fitted to average data values at each of the test temperatures.

2219-T87 Aluminum Alloy

Plots of material properties versus temperature for 2219-T87 aluminum alloy are shown in Figure 5. The ultimate and yield strengths for this material have similar characteristics, increasing in value with lower temperatures. The modulus of elasticity values also exhibited this pattern, reaching a maximum at -423°F . The percent elongation remained relatively constant at the higher temperatures, but increased slightly at -423°F . Poisson's ratio also remained nearly constant for all test temperatures except -320°F , where a higher value was obtained.

2014-T6 Aluminum Alloy

Temperature versus material property curves for 2014-T6 aluminum alloy are shown in Figure 6. Ultimate and yield strengths for this alloy showed the same trend as the other aluminum alloy, having minimum values at room temperature and successively higher values at the lower temperatures. This was also true of the modulus of elasticity properties. In general, the elongation values for this aluminum remained fairly constant except at -320°F and -423°F temperatures, where higher values were obtained. The only exception to this trend was in the 2:1 biaxial stress state, where a maximum value was obtained at -105°F . Poisson's ratio was highest at the higher temperatures, and decreased slightly at -320°F and -423°F .

5Al-2.5Sn Titanium Alloy (Annealed)

Comparison curves of 5Al-2.5Sn titanium alloy (annealed) properties versus temperature are shown in Figure 7. Both the ultimate and yield strengths for this material increase linearly from room temperature to -423°F . This increase is very large, with the -423°F strength values being nearly 100% greater than those at room temperature. The modulus of elasticity was nearly constant at all temperature levels, except at room temperature, where a lesser value was found. The highest elongations were attained at room temperature, with lower values at the middle

LTV AEROSPACE CORPORATION

temperatures, and very low values at -423°F . The maximum Poisson's ratio value was at the -105°F temperature.

6Al-4V Titanium Alloy (ELI, Annealed)

Plots of material properties versus temperature for 6Al-4V titanium alloy (ELI, Annealed) are presented in Figure 8. As with the other titanium alloy, the ultimate and yield strengths increased considerably from room temperature to -423°F . There was no general trend in the modulus of elasticity values, as they were relatively constant for all test temperatures, with only slight variations. The elongation properties were again highest at room temperature, and with successively lower values at lower temperatures. The maximum Poisson's ratio was found to be at -105°F , just as with the other titanium alloy.

Inconel 718 (Heat-treated)

Figure 9 is a comparison of Inconel 718 (Heat-treated) material properties with temperature. Generally, the ultimate and yield strength values increased for lower temperatures, except that maximum values were measured at -320°F , with slightly lower properties at -423°F . The modulus of elasticity was practically the same for all temperature levels, with only a slight increase at the lower temperatures. The percent elongation curves varied with each of the three stress states. For the uniaxial and 1:1 biaxial stress states, the elongation values decreased with lower temperatures. In the 2:1 biaxial stress state, the elongation values increased with lower temperatures to a maximum at -320°F . The Poisson's ratio curve is very similar to those of the titanium alloys, having the largest value at the -105°F temperature.

6Al-4V Titanium Alloy (STA)

Curves illustrating the effects on material properties with variation in temperature for 6Al-4V titanium alloy (STA) are shown in Figure 10. It should be noted that no tests were performed at -423°F for this material. The ultimate and yield strength values increased considerably from room temperature to -320°F . In general, the modulus of elasticity remained nearly constant at all temperatures, with only small variances. The elongation of this titanium tended to decrease slightly with lower temperatures. Again, as with the other titaniums, the maximum Poisson's ratio value was obtained at -105°F .

Properties versus State of Stress

Figures 11 through 16 compare the program materials by illustrating the effect of the state of stress on material properties for the temperature range from 75°F to -423°F. The properties that were compared are the ultimate strength, yield strength (0.2% offset), modulus of elasticity, and the percent elongation to failure. The curves that are presented are fitted through average data values at each of three stress states.

2219-T87 Aluminum Alloy

The material property comparison curves for 2219-T87 aluminum alloy are presented in Figure 11. The ultimate and yield strengths for this alloy exhibit highest values in the 2:1 biaxial stress state, with lower values in uniaxial and 1:1 biaxial stress states. The modulus of elasticity values are greatest in the 1:1 stress state, with successively lower values in the 2:1 and uniaxial states. The elongation curves are converse to those of the modulus of elasticity, having lowest values in the 1:1 stress state and higher values in the 2:1 and uniaxial stress states.

2014-T6 Aluminum Alloy

Figure 12 presents the material property values for 2014-T6 aluminum alloy in the various stress states. The ultimate and yield strength curves are similar to those of the other aluminum alloy, having a maximum in the 2:1 stress state and lower values for the uniaxial and 1:1 states of stress. Also, the modulus of elasticity properties were highest in the 1:1 stress state and were lower for the 2:1 and uniaxial states. Maximum elongations were obtained in the uniaxial stress state, with lesser values in the 2:1 and 1:1 biaxial stress states.

5Al-2.5Sn Titanium Alloy (Annealed)

Material properties for 5Al-2.5Sn titanium alloy for the various stress states are shown in Figure 13. Maximum ultimate and yield strengths were obtained in the 2:1 biaxial stress state, with slightly lower values in the uniaxial and 1:1 biaxial stress states. Modulus of elasticity values were highest for the 1:1 biaxial stress state and decreased for the 2:1 and uniaxial states. Generally, the elongation values increased in order from the 1:1, 2:1, up to the uniaxial state. Elongations at -423°F were very low for all stress states.

6Al-4V Titanium Alloy (ELI, Annealed)

The 6Al-4V titanium material properties for the various stress states are illustrated in Figure 14. The ultimate and yield strengths for this material remained nearly constant for all stress states, particularly for the lower temperatures. The room temperature strengths decreased slightly for the uniaxial stress state. Highest values for modulus of elasticity were obtained in the 1:1 stress state, with correspondingly lower values for the 2:1 and uniaxial stress states. The only exception was at -423°F , where the uniaxial modulus was higher than that of the 2:1 stress state. Elongation values increased gradually from the 1:1 state through the 2:1 and uniaxial stress states.

Inconel 718 (Heat-treated)

The Inconel material property comparisons at different stress states are shown in Figure 15. The maximum ultimate strengths were obtained at the 2:1 stress state. The yield strengths were about the same for both of the biaxial stress states, but less for the uniaxial state. The modulus of elasticity values were typical, with the highest values at the 1:1 state and the lowest at the uniaxial state. The elongations increased from the 1:1 stress state through the 2:1 state up to the uniaxial state. This increase was not as marked for the lower temperatures.

6Al-4V Titanium Alloy (STA)

Figure 16 illustrates the 6Al-4V titanium alloy material properties at the different stress states. Again, the ultimate strengths were higher for the 2:1 stress state than the other two stress states, although the difference was not significant. This was also true of the yield strengths except at -320°F , where the 2:1 stress state produced the lowest value. The modulus of elasticity values were similar to those of the other titaniums, being highest for the 1:1 state and lowest for the uniaxial state. The elongation properties gradually increased from the 1:1 stress state up to a maximum in the uniaxial state.

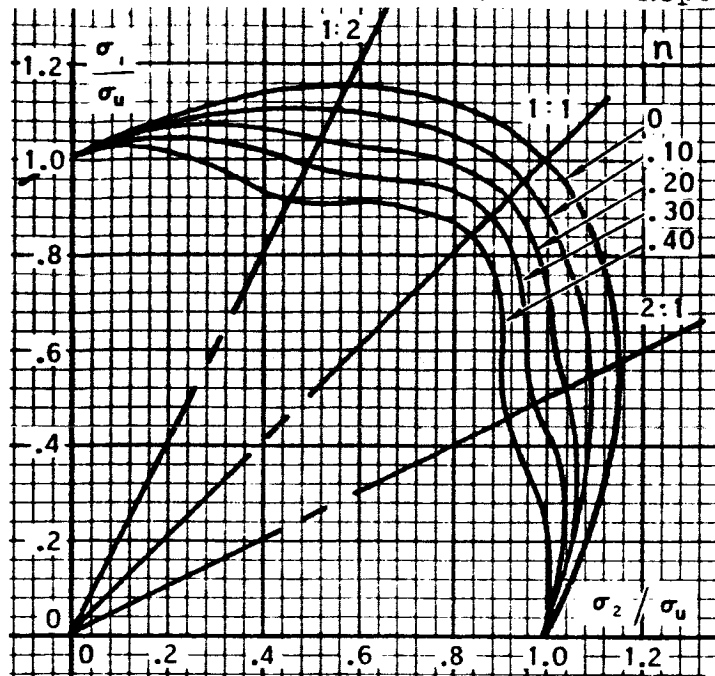
Comparison of Test Results with the Deformation Energy Theory

Figures 17, 18 and 19 illustrate a comparison of test results (biaxial/uniaxial strength ratio) versus the Ludwick strain hardening coefficient while being compared with the theoretical curve of the deformation energy and the Hencky-Von Mises failure theories. The above mentioned figures include the 1:1 and 2:1 biaxial stress state data of the unwelded program materials, as well as, the 1:1 biaxial stress state data of the program materials in the welded condition. Individual (average value) test points at the applicable test temperature are shown in these comparisons.

In comparing the 1:1 biaxial strengths obtained by testing with those predicted by the two theories, it is seen that the deformation energy theory predictions are more conservative than the Hencky-Von Mises theory predictions. This point is illustrated by the fact that no test points (1:1 biaxial unwelded condition) fell below the deformation energy theory curve while most test points form an average about the Hencky-Von Mises theory curve. Of the test materials the three titanium alloys seem to correlate more closely to the deformation energy theory.

The test values for the 2:1 biaxial strength show about the same trends when compared to the two failure theories. In summary the deformation energy theory is again more conservative than the Hencky-Von Mises theory with only a few points falling below the deformation energy curve. The majority of the test points (2:1 biaxial-unwelded condition) fell on or below the Hencky-Von Mises theory curve. The 2:1 biaxial strengths of the two aluminum alloys, 2219-T87 and 2014-T6, exhibit the least amount of correlation with the deformation energy theory curve, with test values being consistently higher than predicted values. Of the titanium alloys 5Al-2.5Sn has the least correlation with the deformation energy theory values, since they were higher than the predicted values. The other two titanium alloys, 6Al-4V(ELI) and 6Al-4V(STA), along with Inconel 718, have very good correlation between test values and predicted values of the deformation energy theory.

The 1:1 biaxial welded strength values generally do not correspond well with the values predicted by either of the two failure theories. With the exception of one material, the test points have no consistent relationship to the theory curves, which would be expected because of the effects of weldment efficiency and greater sensitivity to stress field-fracture origins in the local weldments. The difference between uniaxial and 1:1 biaxial weldment efficiencies is also shown in Figures 25 and 26. The 6Al-4V(ELI) titanium alloy was the only material which showed good correlation to the theory (deformation energy).



FAILURE THEORIES FOR TENSION-TENSION QUADRANT

- (1) Deformation energy-curves with "n" equal zero to 0.40.
- (2) Hencky-Von Mises-Curve where "n" equals zero.
- (3) Maximum distortion energy-same as Hencky-Von Mises.

σ_1 and σ_2 = biaxial strength
 σ_u = Uniaxial strength

Fracture Toughness versus Temperature

Figure 20 illustrates a comparison of uniaxial and 1:1 biaxial fracture toughness resistance (K_{IC}) as a function of temperature for three of the program materials. Only single data points were generated in this research at -105°F , -320°F and -423°F and the data presented in Figure 20 should be viewed as relative trends for resistance to critical crack growth.

The 5Al-2.5Sn titanium alloy shows better fracture toughness in the 1:1 biaxial state of stress than in the uniaxial state at the test temperatures investigated. The highest fracture uniaxial toughness values in this alloy were obtained at the -105°F and -423°F temperatures, with a lesser value at -320°F . For the 2219-T87 aluminum alloy, the fracture toughness remained about the same for both states of stress at all temperature levels, except at -423°F where the uniaxial value increases and the biaxial value decreases. The K_{IC} values for Inconel 718 in the uniaxial stress state are considerably higher than the biaxial values. For both stress states, minimum values were obtained at -105°F and higher values at -320°F and -423°F .

In comparing the three materials, it is seen that Inconel 718 has better fracture toughness properties than 5Al-2.5Sn titanium in the uniaxial stress state, while for the 1:1 biaxial stress state the reverse is true. In both stress states and all temperatures, the 2219-T87 aluminum alloy exhibited lower fracture toughness values than either the 5Al-2.5Sn titanium alloy or Inconel 718.

Creep Strain versus Time

Figures 21 through 24 illustrate relative comparisons of the effect of uniaxial and 1:1 biaxial stress states on two of the program materials (6Al-4V Titanium(ELI), and 5Al-2.5Sn Titanium(ELI)) at 90% of the uniaxial and 1:1 biaxial yield strength at -320°F. One 1:1 biaxial creep test at room temperature was conducted at a 90% of R.T. yields stress condition to probe temperature effects. Figures 21 and 22 show the effects of the uniaxial stress state while Figures 23 and 24 show the effects of the 1:1 biaxial stress state. These comparison curves illustrate creep strain versus time, with statements indicating whether the specimen did or did not fail during the test period.

Creep curves for two 5Al-2.5Sn Titanium alloy (ELI, annealed) uniaxial specimens are presented in Figure 21. The first specimen (UCP7-1) accumulated 0.26% creep strain at 276 hours with no failure. At this point, the -320°F temperature environment could not be maintained and the specimen failed due to the increase in temperature and resulting loss in strength. Specimen UCP7-2, also with longitudinal grain direction, was tested to 527.1 hours without failure. The creep strain was 0.18% at the completion of the test. The two creep curves are very similar in shape and magnitude, indicating that they probably represent typical values for this program material.

Two creep curves for 6Al-4V Titanium alloy (ELI, annealed) are shown in Figure 22; one each for the longitudinal and transverse grain direction. The first test was conducted using the longitudinal specimen. A significant amount of creep occurred during the 336 hours duration of the test, but the specimen did not fail. The initial strain was approximately 1.2%. Fifty percent of the creep strain occurred during the first 60 hours, after which the creep rate decreased considerably. Total strain at the end of the test was 2.8%, and the total creep strain was 1.6%.

A transverse grain direction specimen was used in the second 6Al-4V titanium creep test to determine whether this material would experience the same relatively large magnitude of creep in the transverse grain direction as it did in the longitudinal direction. As shown in Figure 22, this specimen incurred similar initial strain (1.025%) as the longitudinal specimen, but practically no creep strain.

Creep curves for the 1:1 biaxial stress state for 5Al-2.5Sn titanium alloy (ELI, annealed) are shown in Figure 23. The first specimen (BCP7-1) had accumulated

0.34% creep strain in the longitudinal grain direction and 0.65% in the transverse grain direction when the test was stopped at 429 hours. Approximately two-thirds of the creep strain occurred during the first 40 hours of the test, and the remainder during the last 210 hours. The second specimen (BCP7-2) accumulated about 1.9% creep strain in the longitudinal grain direction and about 1.5% creep strain in the transverse direction before failure which took place in 68.5 hours. While a significant difference in results is illustrated in these two tests (one failed in a short period and one did not in a much longer period) it is important to note that the shape of the two test curves are very similar during the first few hours of the test period. As time at test conditions continued it can be observed that one specimen continued to strain while the other stabilized at a constant strain level and then began to creep at an increased rate later in the test period. The third specimen was tested at 90% of R.T. yield at room temperature and did not fail in a 430 hour test period. However, significant creep strains of 0.65% and 0.86% in the longitudinal and transverse grain directions were experienced.

Creep curves for the 1:1 biaxial stress state for 6Al-4V titanium alloy (ELI annealed) are shown in Figure 24. The first specimen (BCP4-2) accumulated about 0.6% creep strain in the longitudinal grain direction and 0.35% creep strain in the transverse grain direction before failure occurred at the end of 172 hours of test. The second specimen was overloaded during the initial load application (to 97% F_{ty} instead of 90% F_{ty}) and it accumulated about an equal amount of creep strain (1.0%) in both grain directions in only 8.2 hours. These two tests illustrate the effect of what a 7% increase in stress level will do to the creep life. The third specimen (a retest of the second specimen—90% of -320°F yield) did not produce a failure in a 345 hour test period. However, creep strain of 0.94% and 0.68% in the longitudinal and transverse grain directions were experienced.

These creep tests illustrate: (1) the increased severity of the 1:1 biaxial stress state over that of the uniaxial stress state in the area of cryogenic creep in the (ELI) titanium alloys, (2) the effect of increased stress level on creep life under the 1:1 stress state (97% compared to 90%), and (3) that the creep problem with these alloys also exists at room temperature, as well as, at -320°F under the 1:1 stress state.

Weldment Efficiency versus Temperature

Figures 25 and 26 illustrate the relative comparison of the program materials with regard to weldment efficiency (uniaxial and 1:1 biaxial weldment strengths/uniaxial and 1:1 biaxial parent material strengths) as a function of temperature. Figure 25 illustrates the uniaxial comparisons while Figure 26 illustrates the 1:1 biaxial comparisons.

The weldment efficiency comparison shows how the strengths of the program materials are affected by welding. The weldment efficiency is defined as the ratio of the welded joint strength to the parent material (unwelded) strength.

For the uniaxial weldment efficiencies, it is seen that two of the titanium alloys, 5Al-2.5Sn and 6Al-4V(ELI), retain their basic strength when welded for all test temperatures, except at -423°F where the efficiency drops off to about 90%. The other titanium alloy, 6Al-4V(STA), has an efficiency of 94% at room temperature and increases to 98% at -320°F. The aluminum alloy 2219-T87 has an efficiency of 62% at room temperature, reaches a maximum efficiency in the -320°F range and then decreases at -423°F. The Inconel 718 alloy retains an efficiency of about 60% for all temperatures down to -320°F, where the efficiency decreases at -423°F. The 2014-T6 aluminum alloy efficiency gradually decreases from about 60% at room temperature down to 47% at -423°F.

The 1:1 biaxial weldment efficiencies vary considerably from the uniaxial efficiencies. The 6Al-4V (ELI) alloy has an efficiency of 80% at room temperature, increases to 100% at -320°F, then decreases to 80% at -423°F. The other two titanium alloys, 5Al-2.5Sn and 6Al-4V (STA), have efficiencies of 100% at room temperature and reach a minimum of about 85% at -320°F. The efficiency of the 5Al-2.5Sn alloy then increases to 96% at -423°F. No tests were conducted for the 6Al-4V (STA) alloy at -423°F. The 2219-T87 aluminum alloy has a low efficiency at room temperature (53%), but increases to 76% at -320°F, then decreases to 63% at -423°F. Inconel 718 has an efficiency of about 65% for the temperature range from 75°F to -320°F, then abruptly increases to 74% at -423°F. The 2014-T6 efficiency curve decreases gradually from a maximum value of 66% at room temperature down to 46% at -423°F.

In conclusion, it is apparent that all three titanium alloys are very acceptable for welding purposes, retaining nearly 100% of their basic strength for all temperature levels. For biaxial welds, the 6Al-4V(STA) and 5Al-2.5Sn weld efficiencies fall to 85% and the 6Al-4V(ELI) alloy decreases

to 80% at room temperature, but these efficiencies are still high when compared to the other materials. Inconel 718 has a fairly constant weld efficiency (uniaxial and biaxial) for most temperature levels, ranging between 60% and 65%, which is relatively low for a high strength alloy. Of the two aluminum alloys, 2219-T87 is better suited for welding, particularly in cryogenic environments. The weld efficiency of the 2219-T87 alloy reaches a maximum of about 80% at cryogenic temperatures, compared to about 55% for the 2014-T6 alloy.

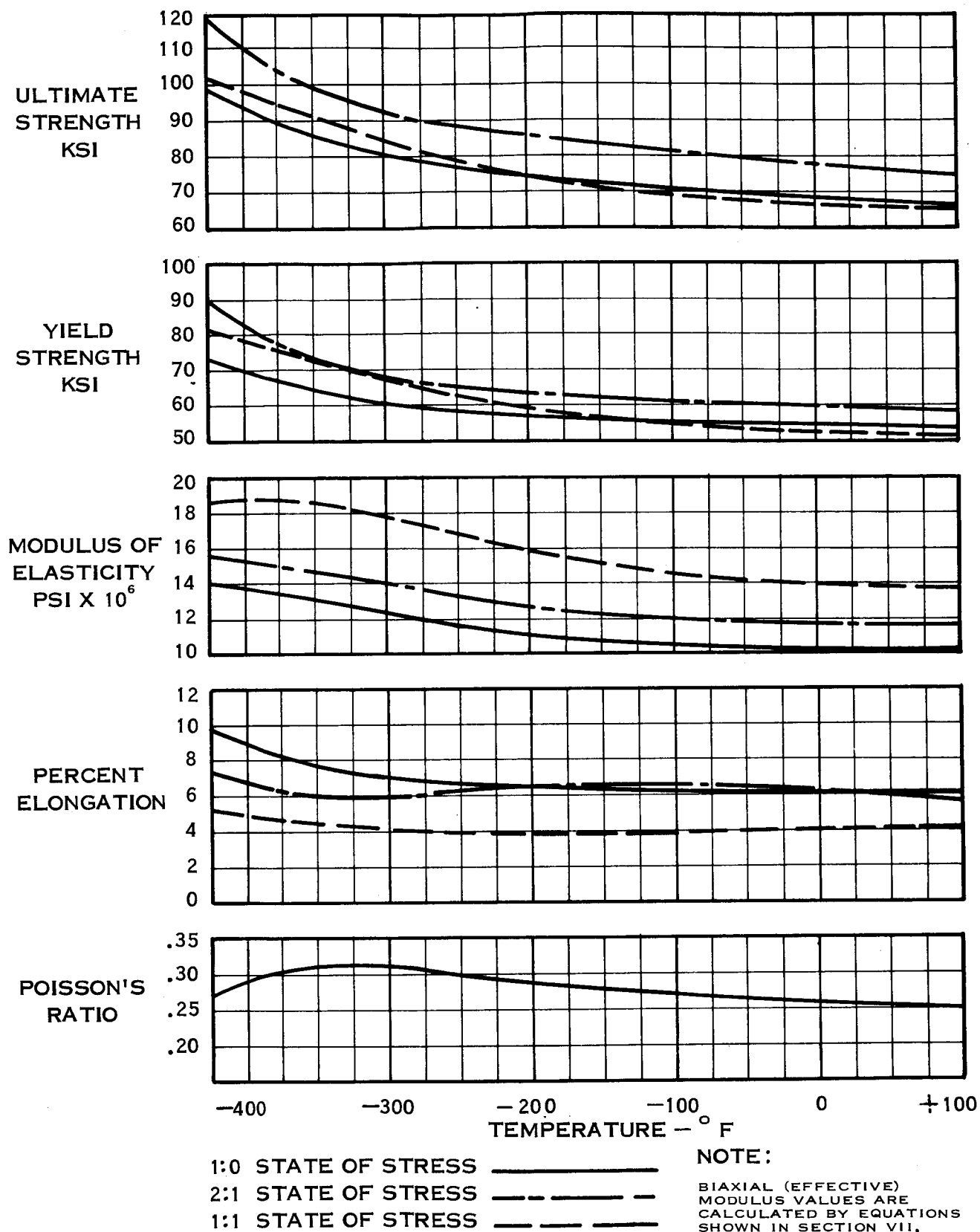
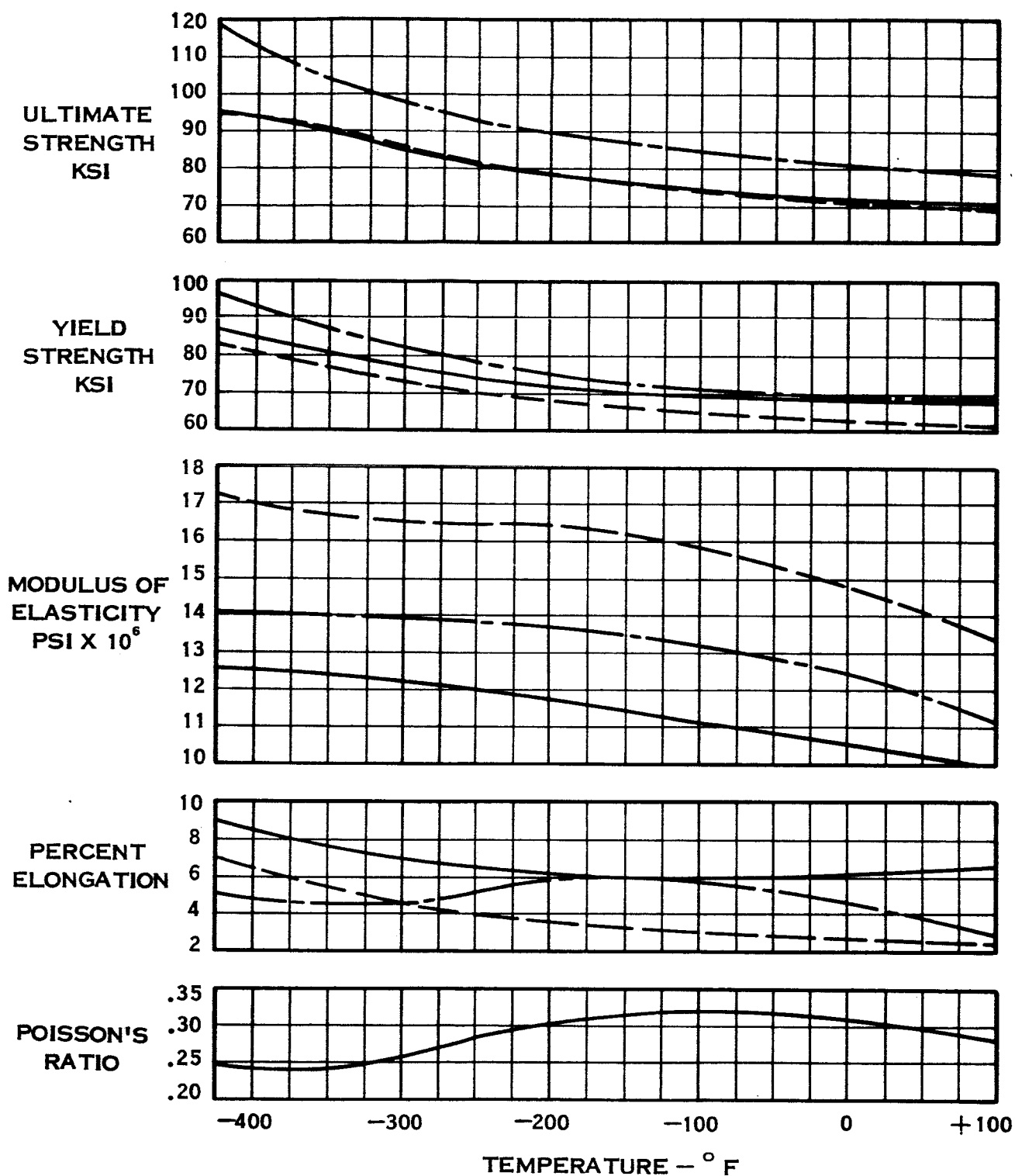


FIGURE 5 - COMPARISON OF 2219-T87 ALUMINUM ALLOY PROPERTIES WITH TEMPERATURE



1:0 STATE OF STRESS _____
 2:1 STATE OF STRESS - - - - -
 1:1 STATE OF STRESS — · — · —

NOTE:

BIAXIAL (EFFECTIVE)
 MODULUS VALUES ARE
 CALCULATED BY EQUATIONS
 SHOWN IN SECTION VII.

**FIGURE 6 - COMPARISON OF 2014-T6 ALUMINUM ALLOY PROPERTIES
 WITH TEMPERATURE**

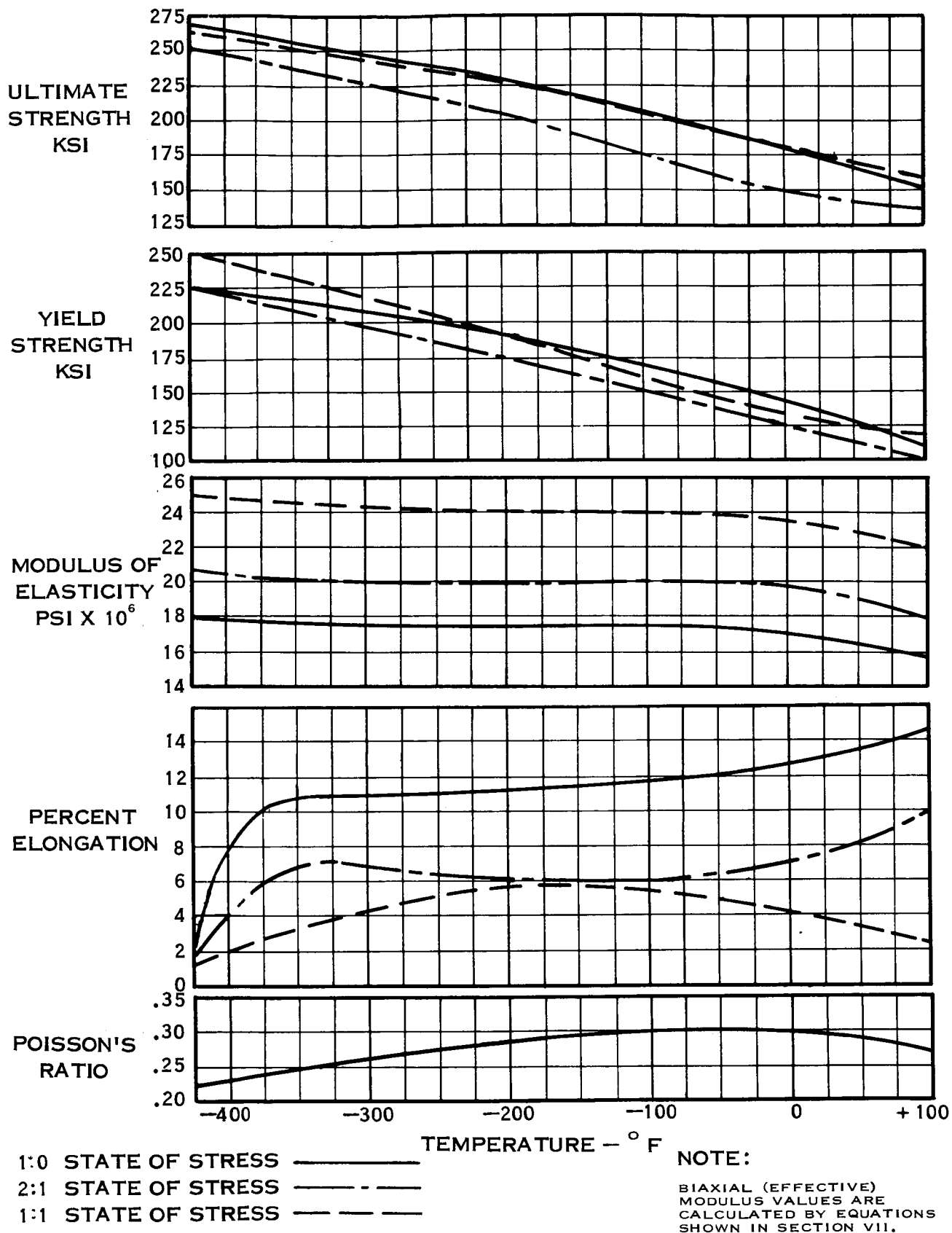


FIGURE 7 — COMPARISON OF 5 Al — 2.5 Sn TITANIUM ALLOY
 (ANNEALED) PROPERTIES WITH TEMPERATURE

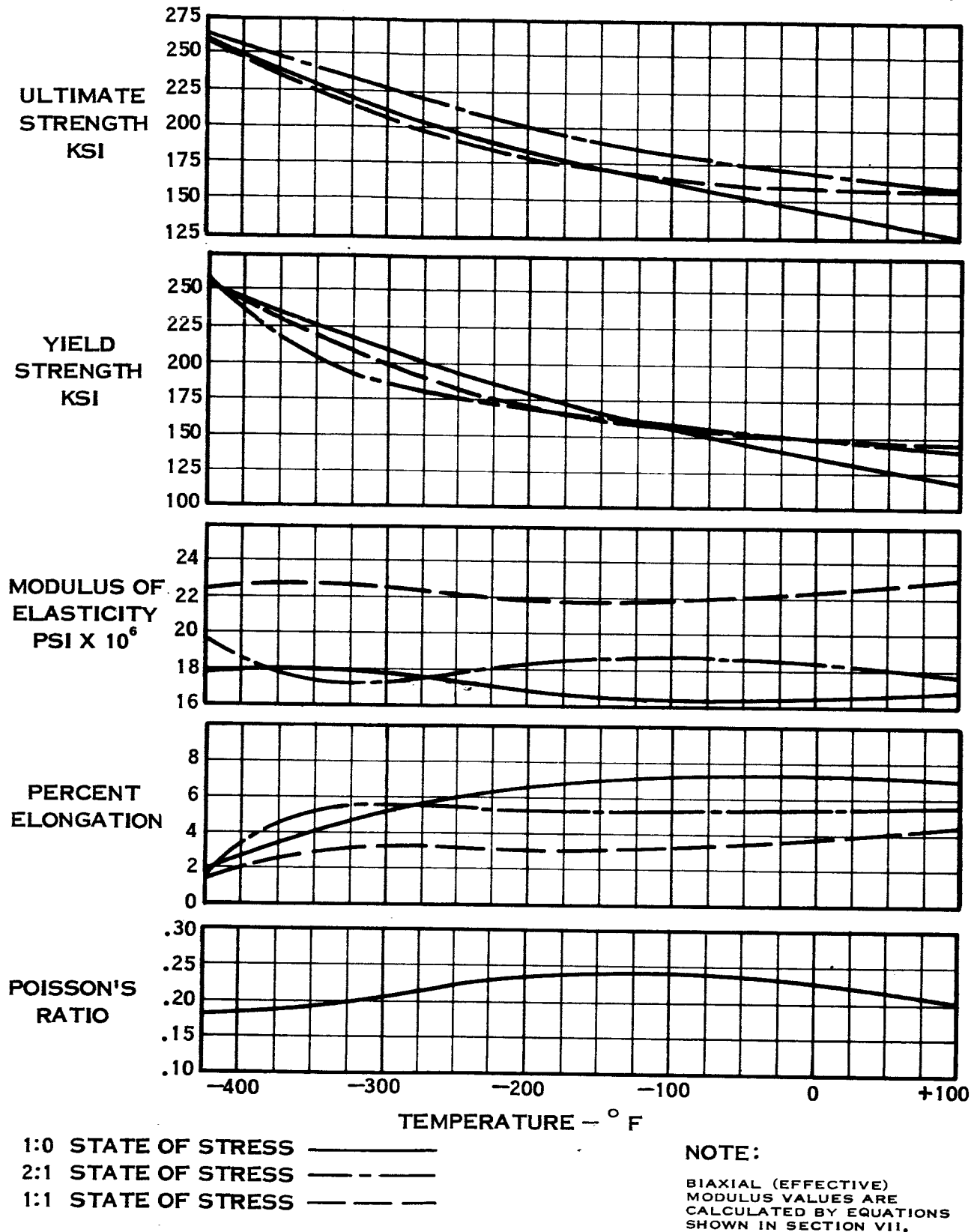


FIGURE 8 — COMPARISON OF 6 AL — 4V TITANIUM ALLOY (ELI, ANNEALED) PROPERTIES WITH TEMPERATURE

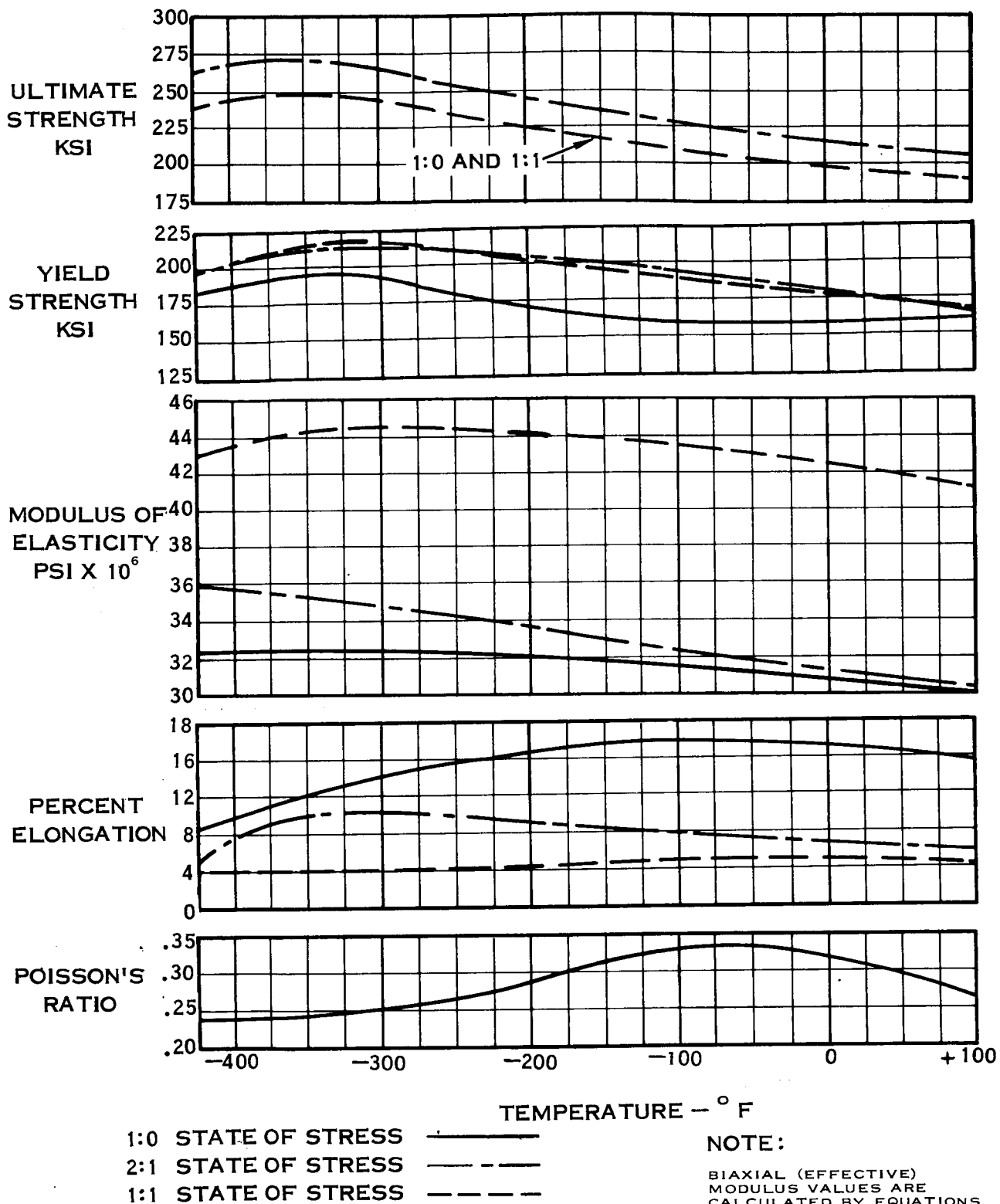


FIGURE 9 — COMPARISON OF INCONEL 718 (HEAT-TREATED)
 PROPERTIES WITH TEMPERATURE

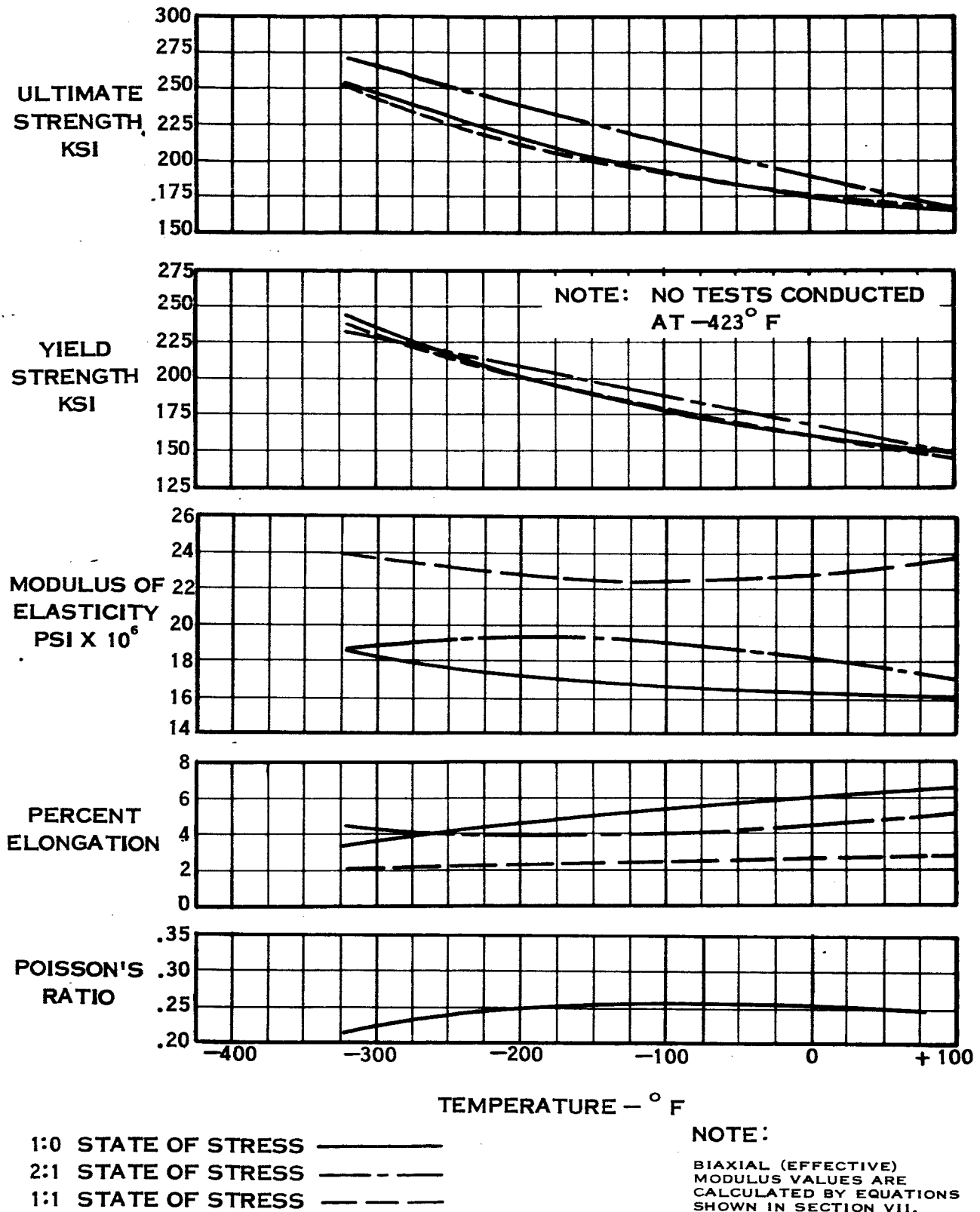
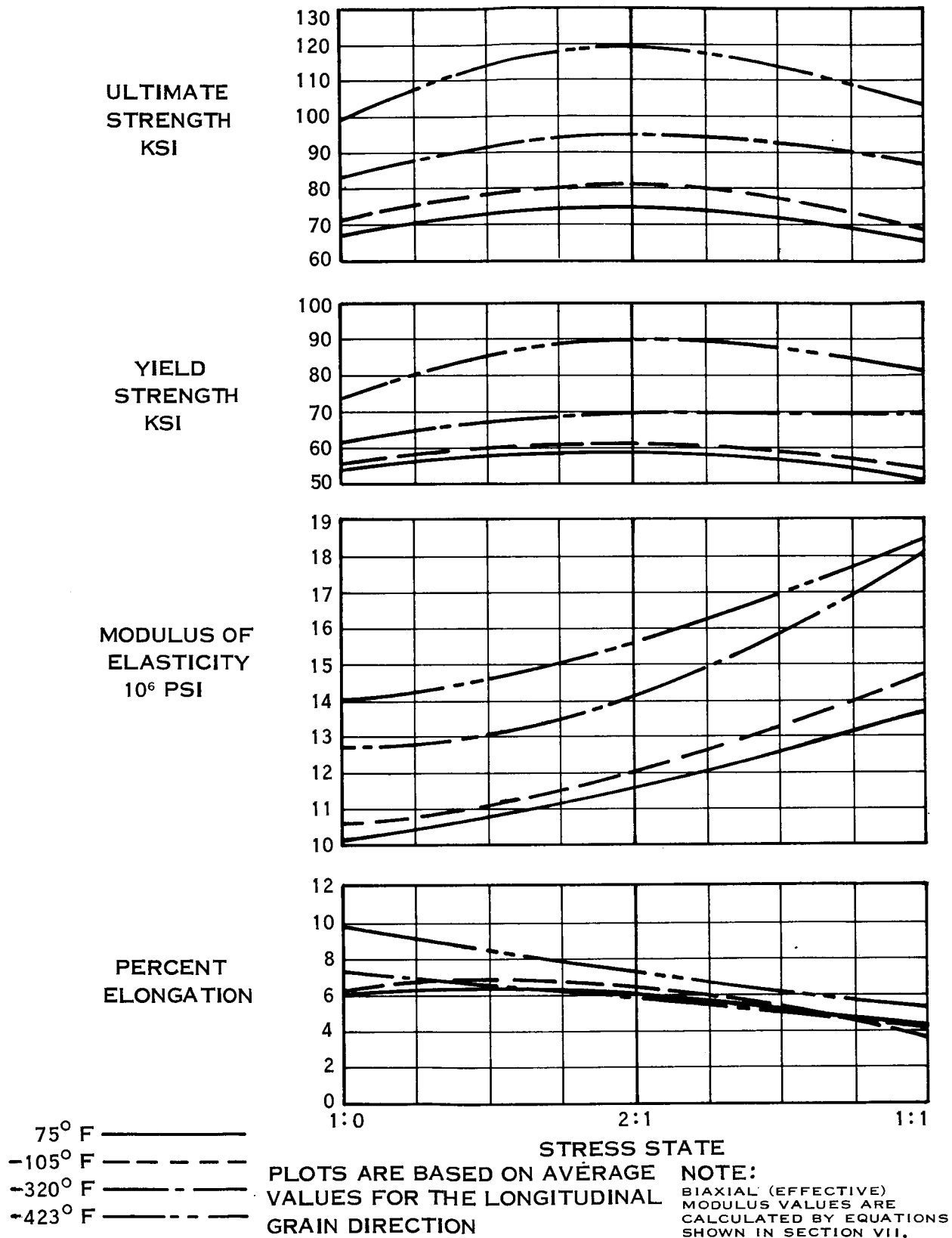


FIGURE 10 — COMPARISON OF 6Al-4V TITANIUM ALLOY (STA) PROPERTIES WITH TEMPERATURE



**FIGURE 11 —COMPARISON OF 2219-T87 ALUMINUM ALLOY
 PROPERTIES WITH STATE OF STRESS**

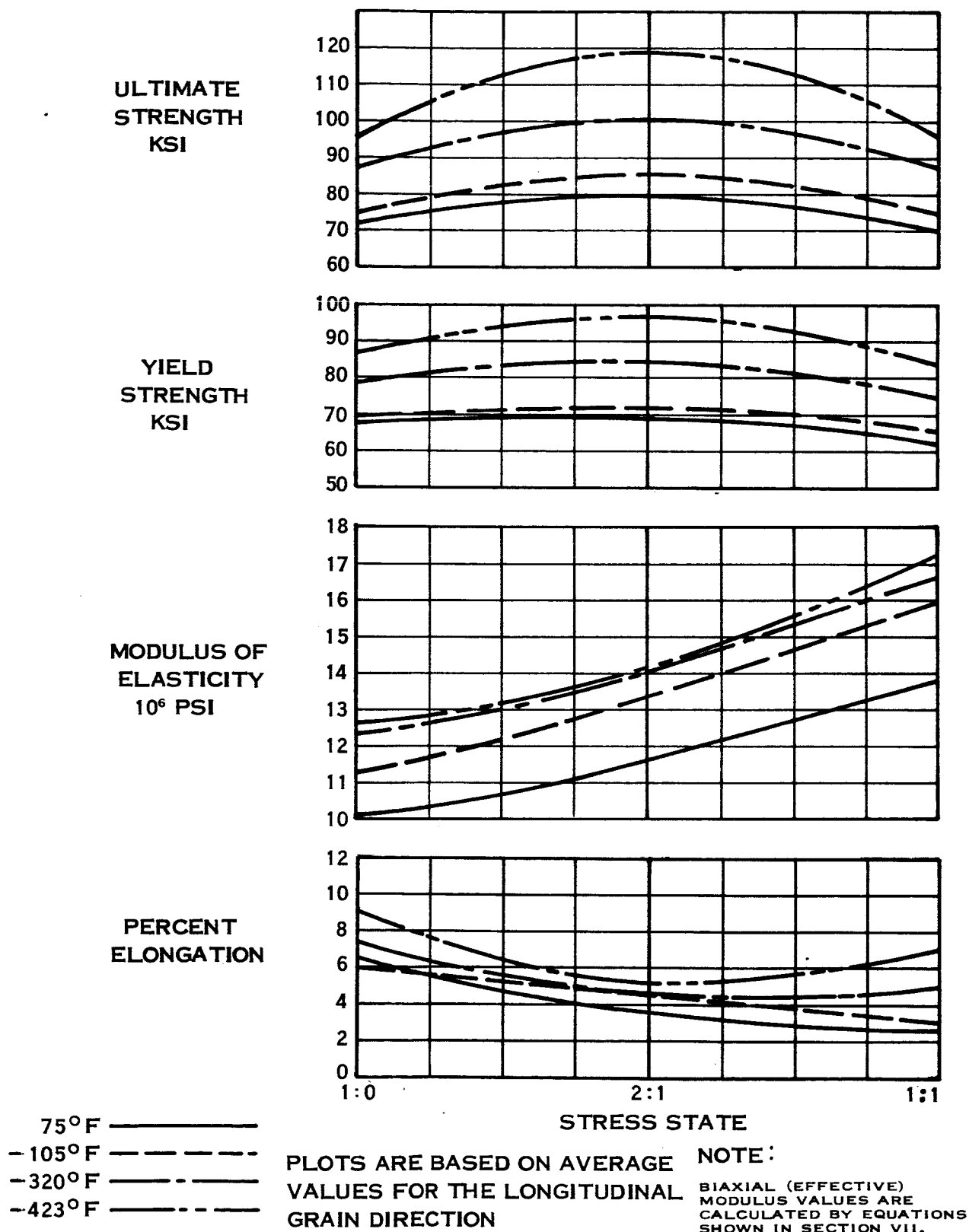


FIGURE 12 —COMPARISON OF 2014-T6 ALUMINUM ALLOY PROPERTIES WITH STATE OF STRESS

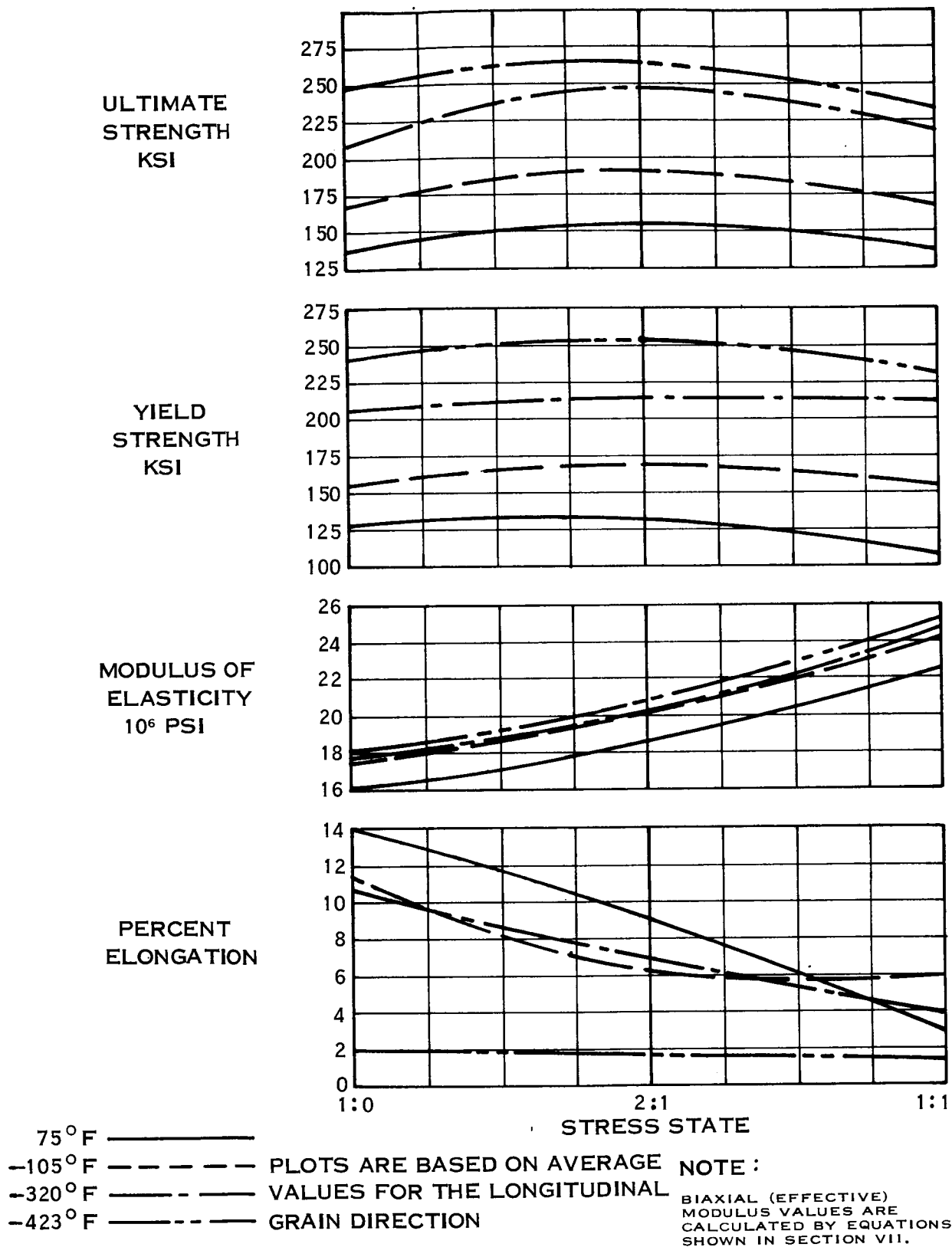


FIGURE 13 — COMPARISON OF 5Al-2.5 Sn ALLOY (ANNEALED)
 PROPERTIES WITH STATE OF STRESS

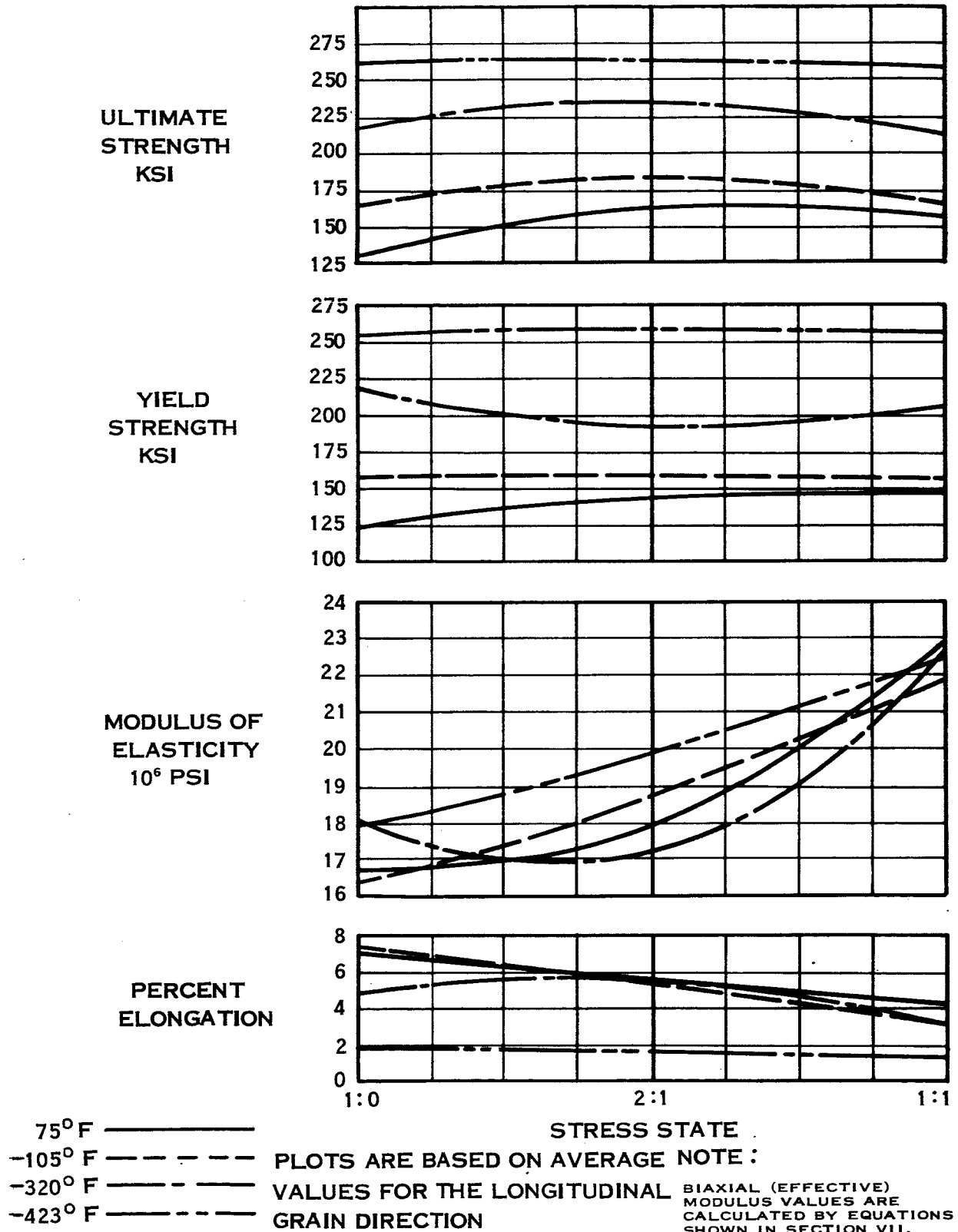


FIGURE 14 — COMPARISON OF 6Al-4V TITANIUM ALLOY (ELI, ANNEALED) PROPERTIES WITH STATE OF STRESS

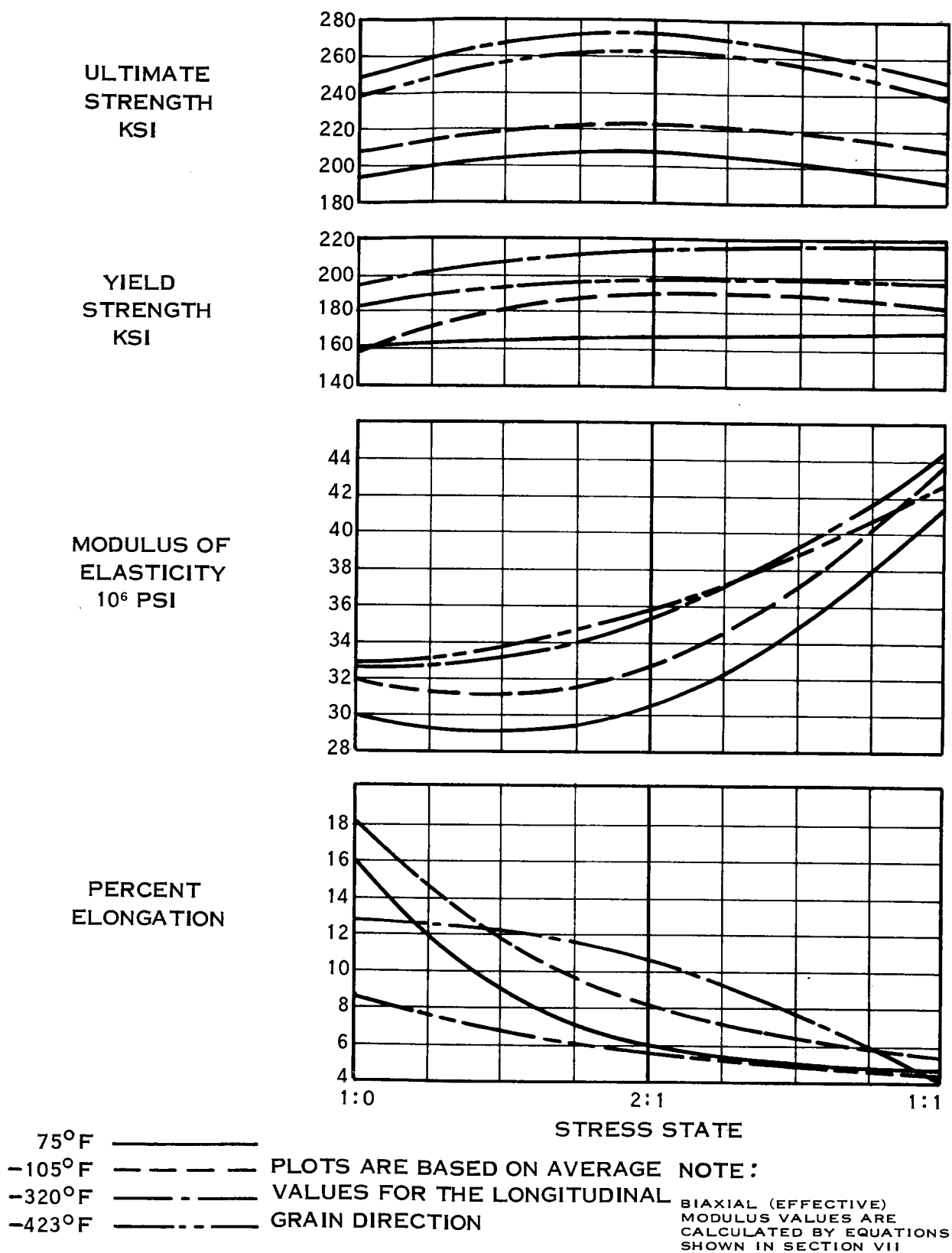
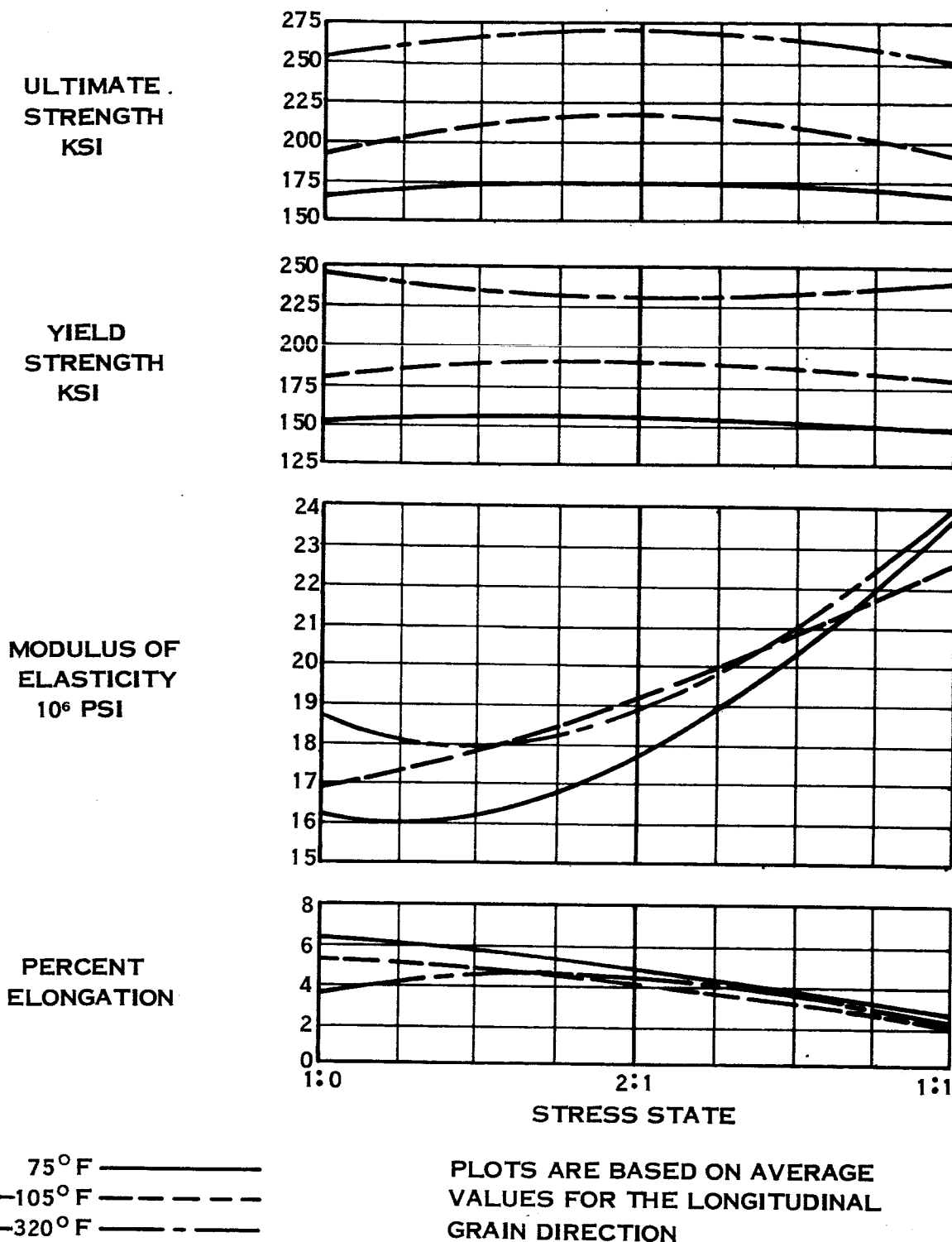


FIGURE 15 — COMPARISON OF INCONEL 718 (HEAT TREATED)
 PROPERTIES WITH STATE OF STRESS



NOTE :

BIAXIAL (EFFECTIVE)
MODULUS VALUES ARE
CALCULATED BY EQUATIONS
SHOWN IN SECTION VII.

FIGURE 16 —COMPARISON OF 6Al-4V TITANIUM ALLOY (STA)
PROPERTIES WITH STATE OF STRESS

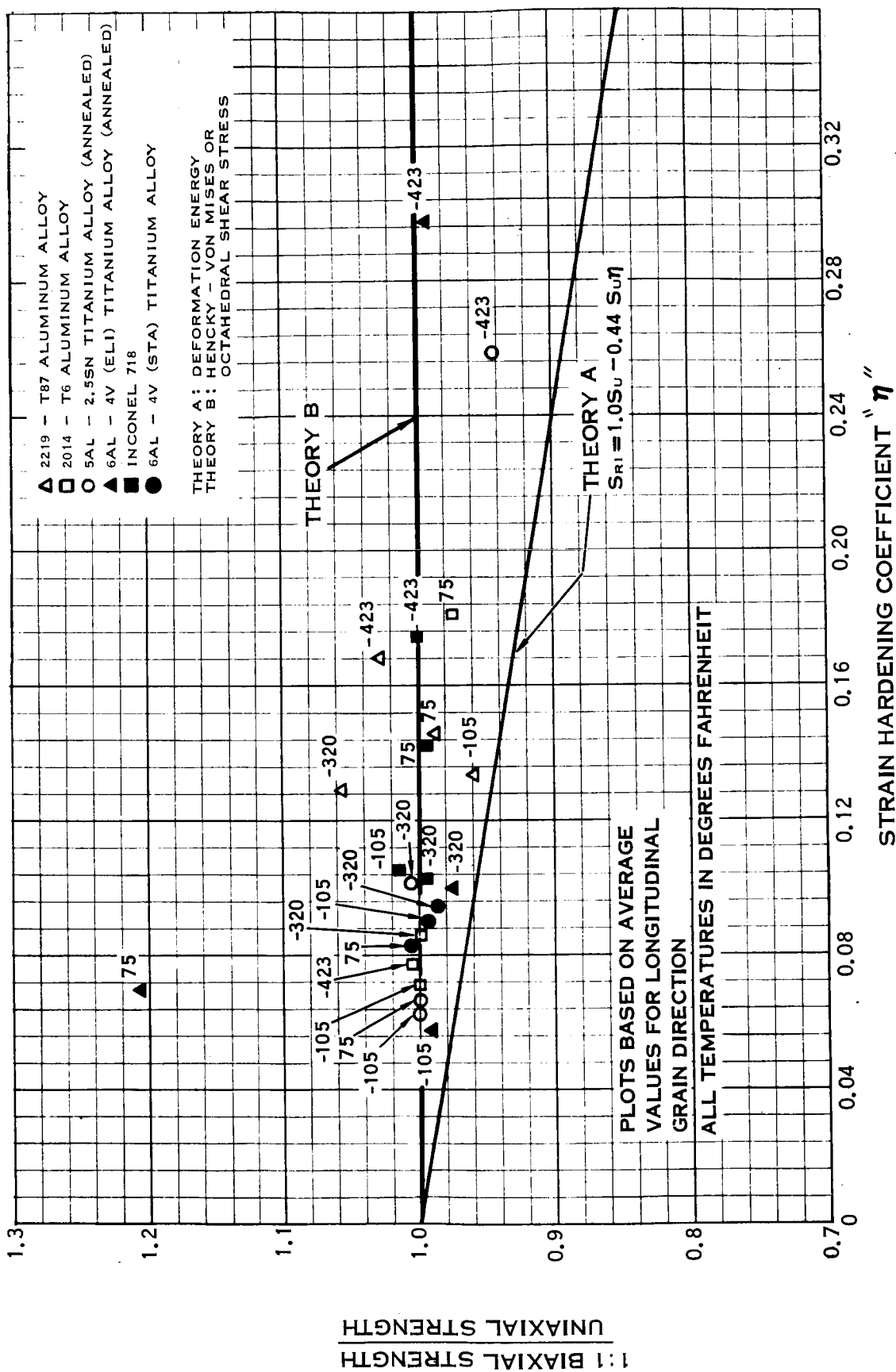


FIGURE 17 - COMPARISON OF 1:1 BIAxIAL STRENGTH WITH TWO FAILURE THEORIES



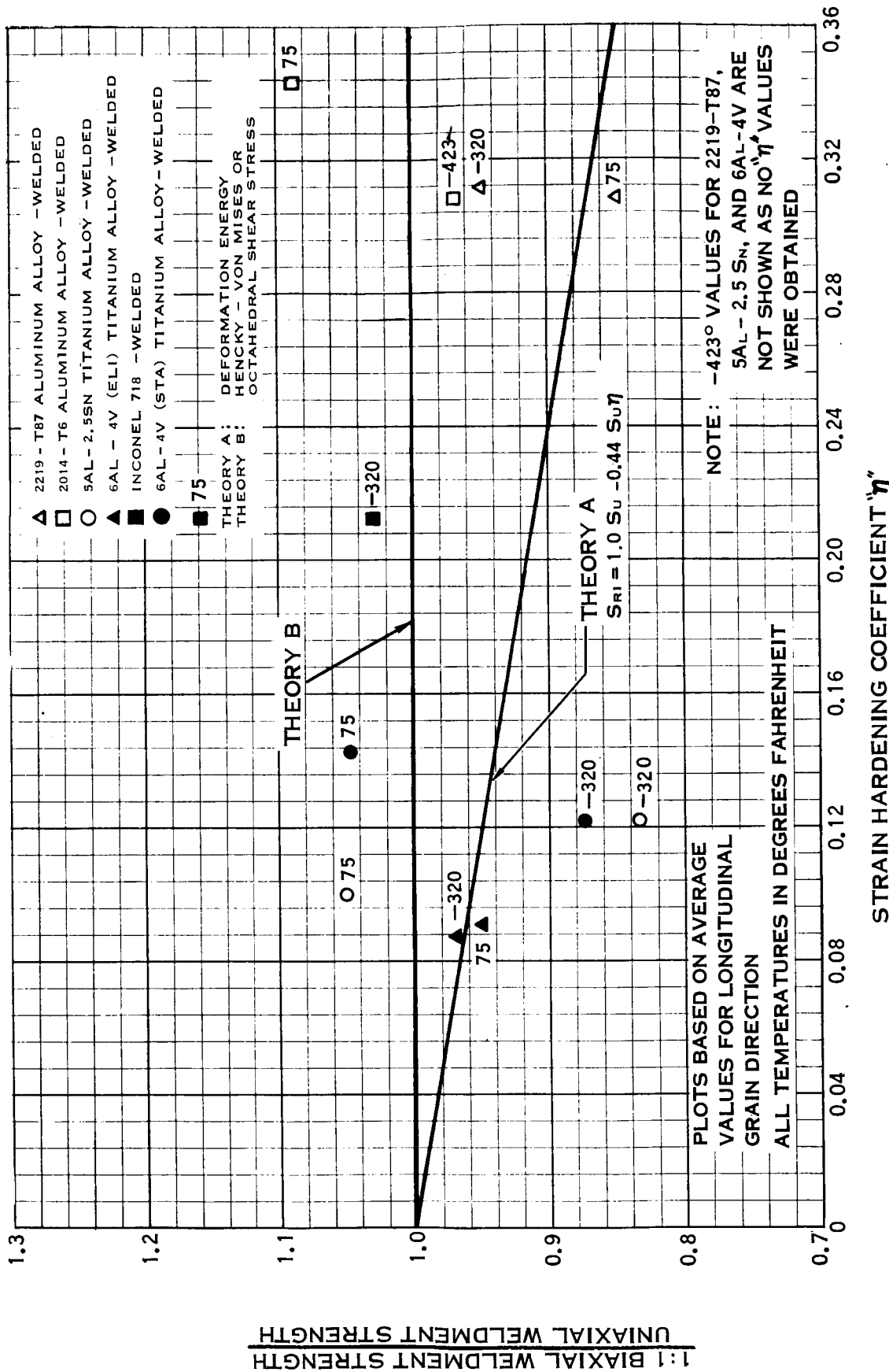


FIGURE 19 - COMPARISON OF 1:1 BIAXIAL WELDMENT STRENGTH WITH TWO FAILURE THEORIES

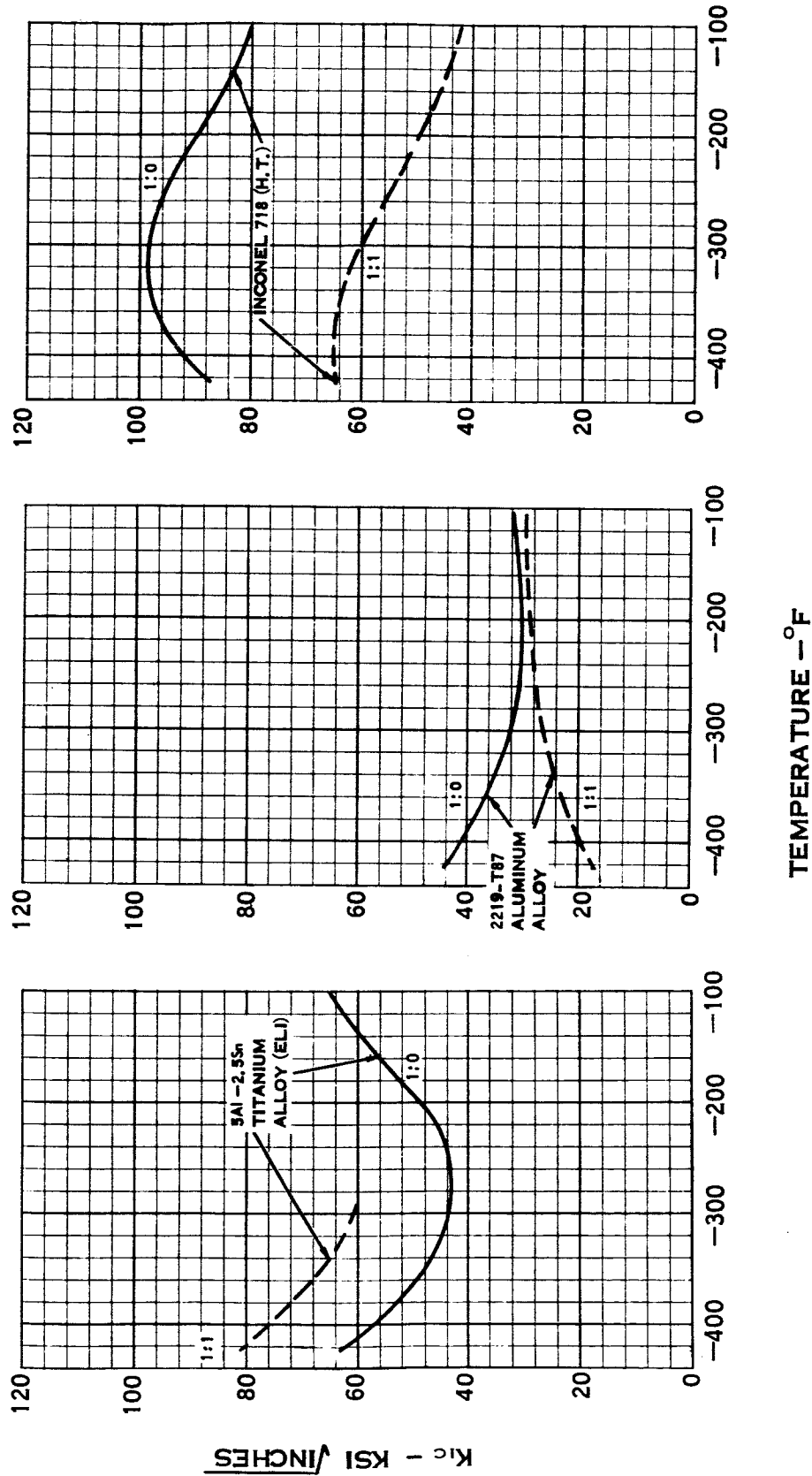


FIGURE 20—COMPARISON OF FRACTURE TOUGHNESS AS A FUNCTION OF TEMPERATURE FOR UNIAXIAL AND 1:1 BIAxIAL STRESS STATES

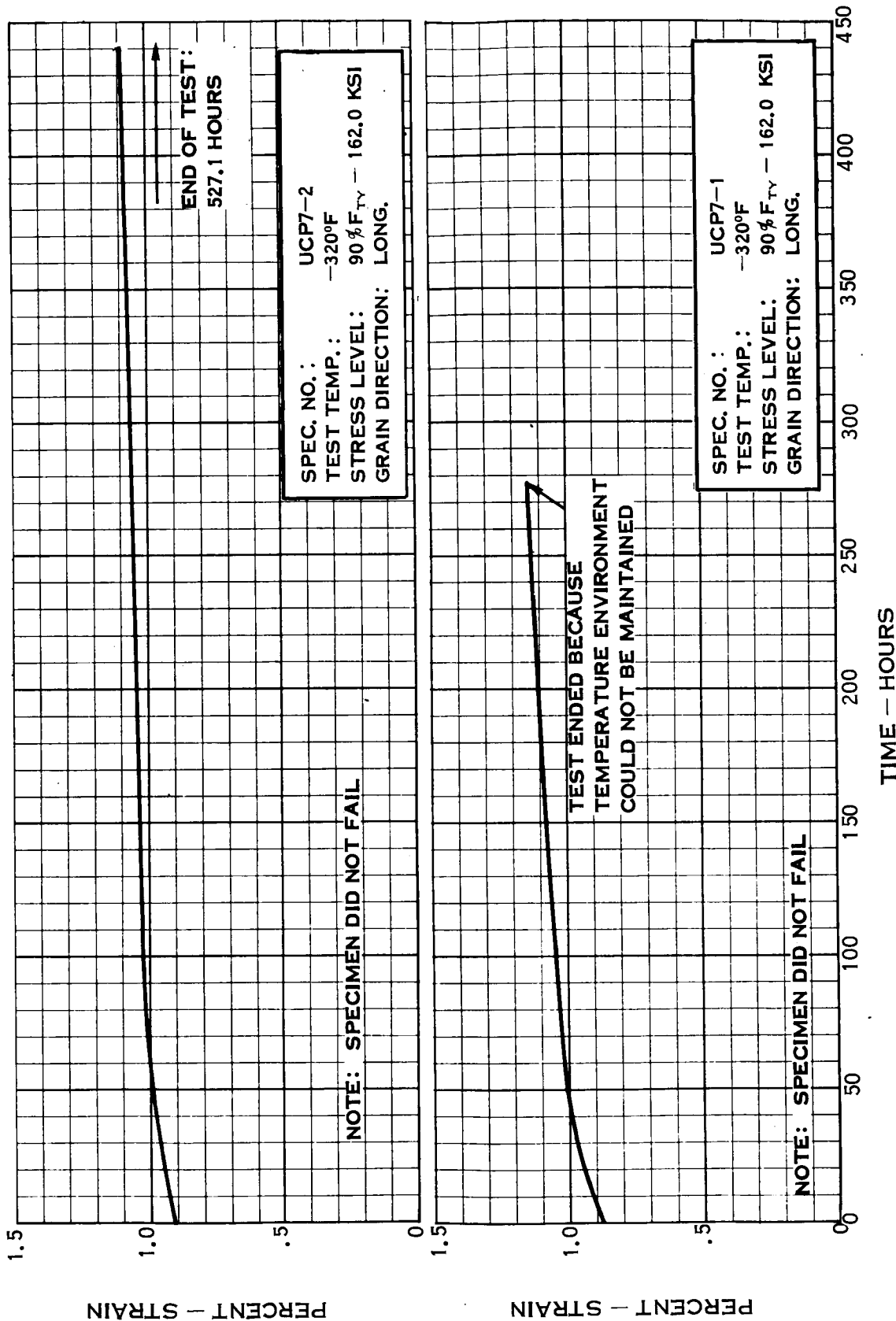


FIGURE 21 — 5 AL — 2.5 SN TITANIUM ALLOY (ELI, ANNEALED) CREEP CURVES DEVELOPED UNDER UNIAXIAL STRESS FIELD

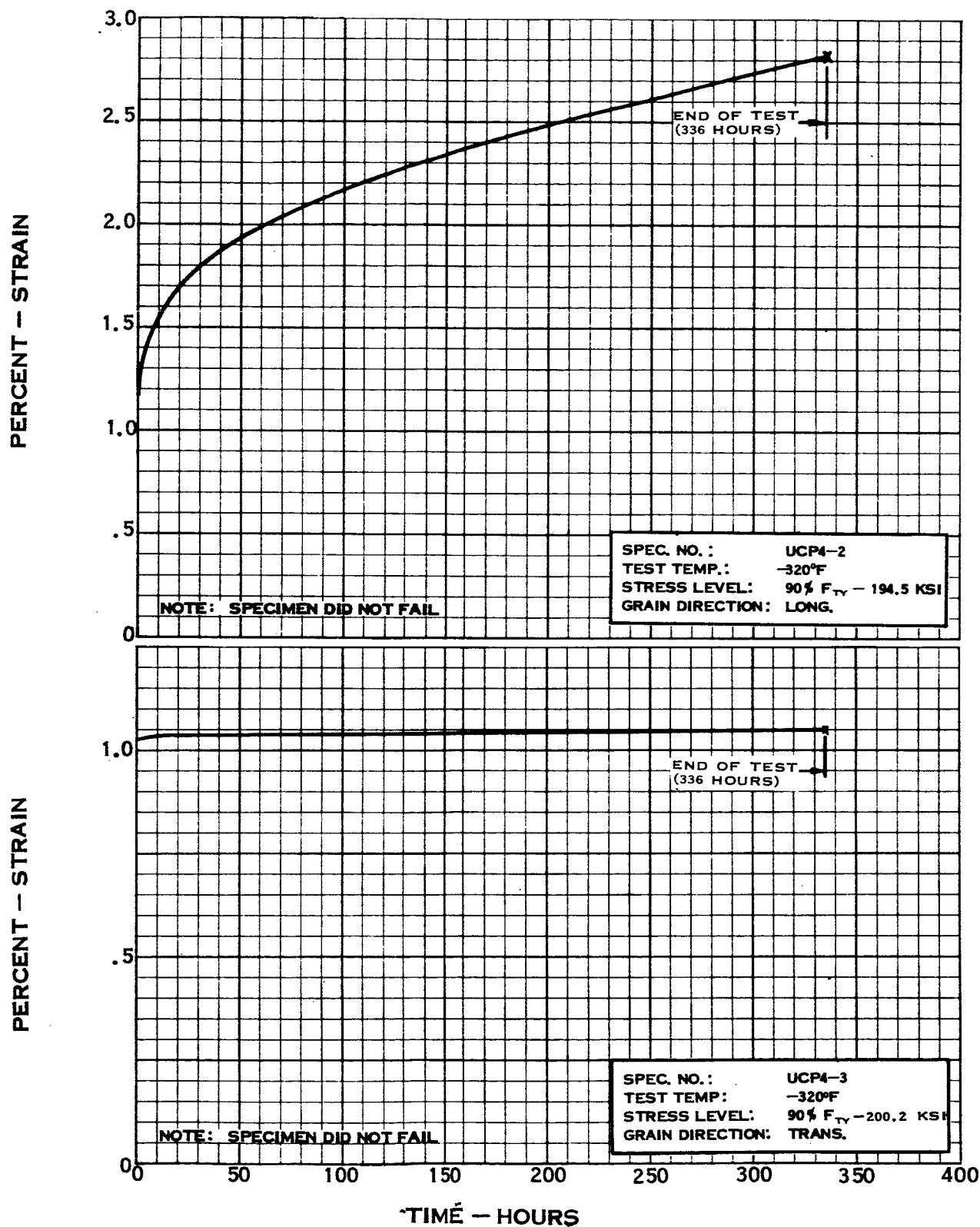


FIGURE 22 - 6 Al - 4V TITANIUM ALLOY (ELI, ANNEALED) CREEP CURVES DEVELOPED UNDER UNIAXIAL STRESS FIELD

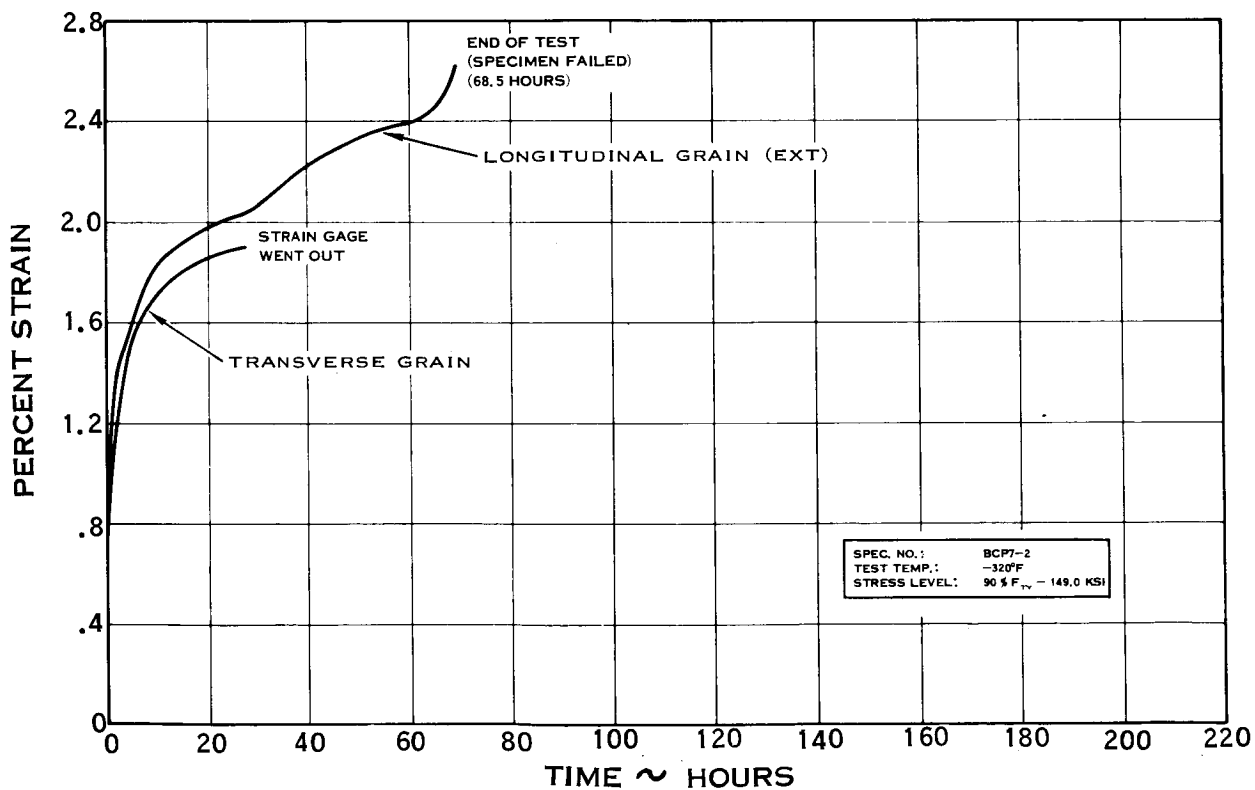
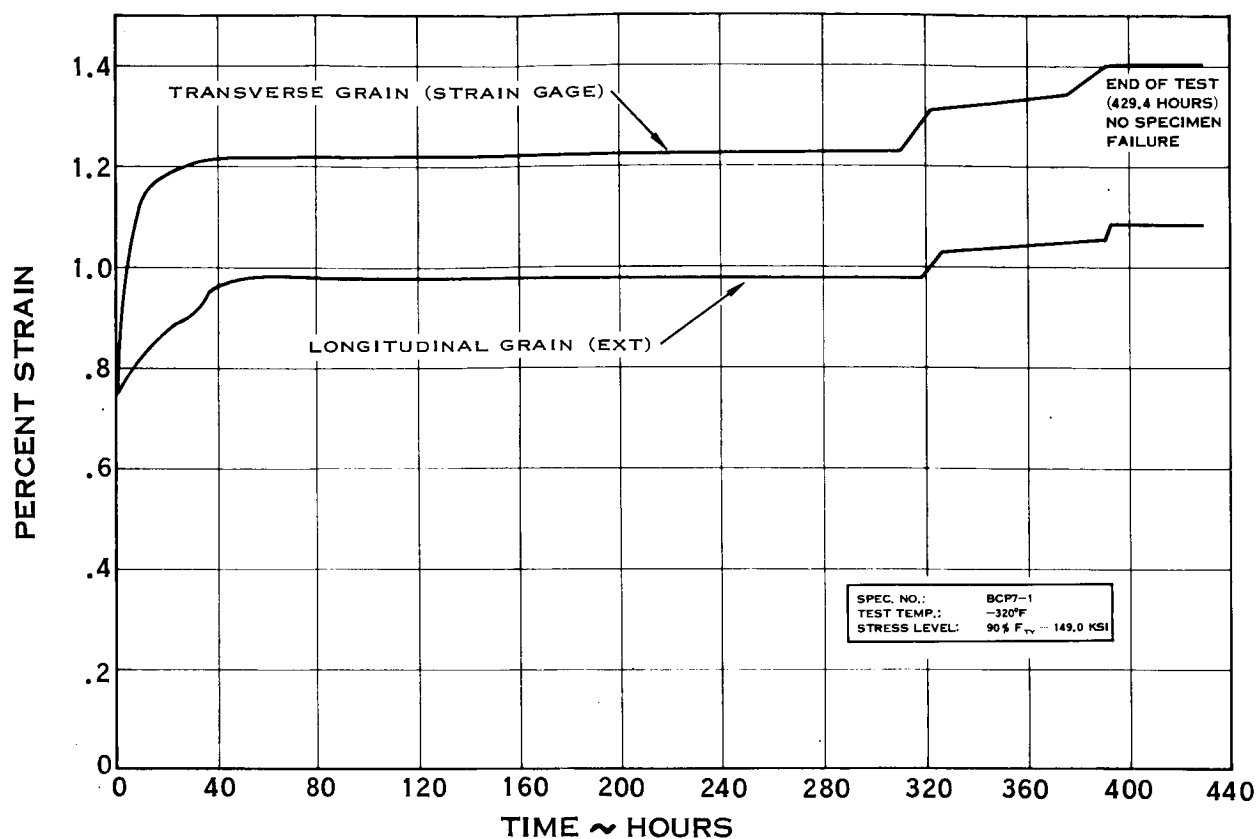


FIGURE 23 — 5AL-2.5 SN TITANIUM ALLOY (ELI, ANNEALED) CREEP CURVES DEVELOPED UNDER 1:1 BIAxIAL STRESS FIELD

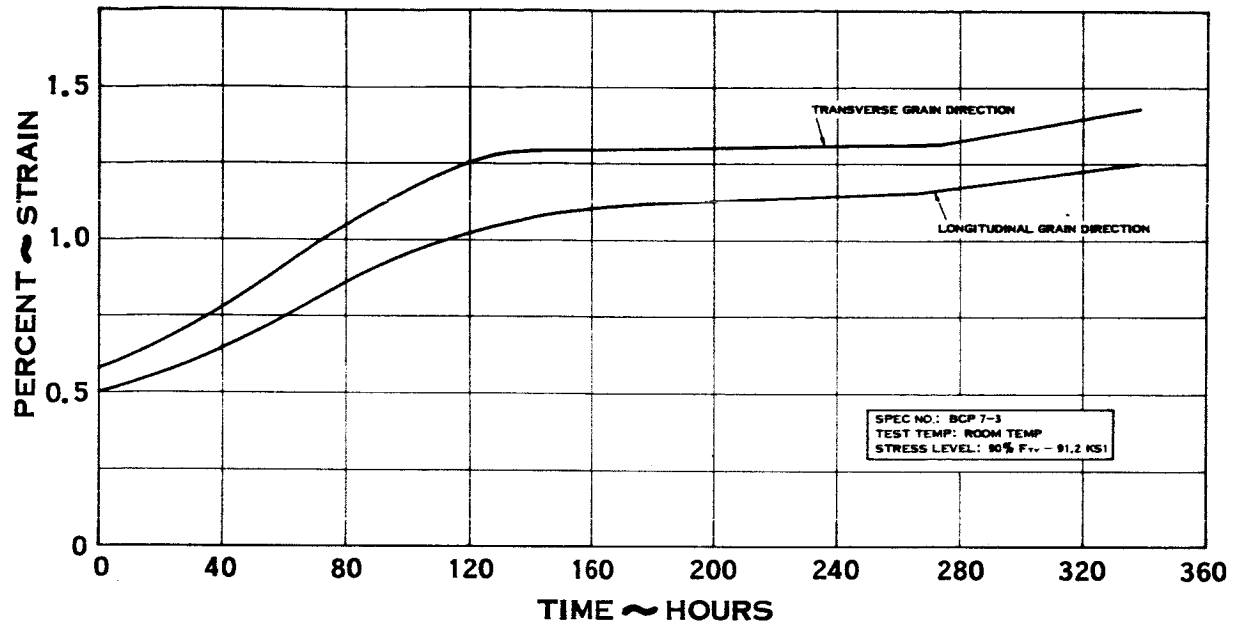


FIGURE 23 - 5A_L - 2.5 S_N TITANIUM ALLOY (ELI, ANNEALED) CREEP CURVES DEVELOPED UNDER 1:1 BIAXIAL STRESS FIELD (CONT)

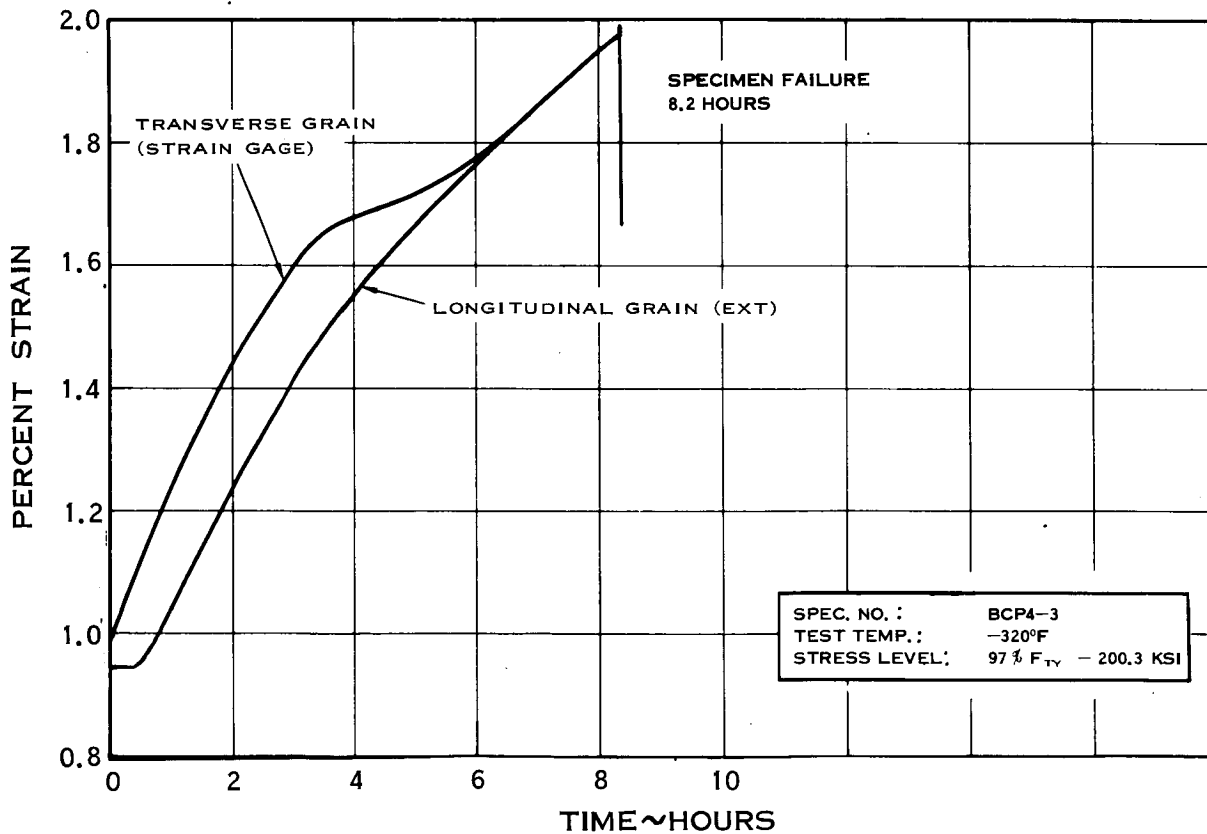
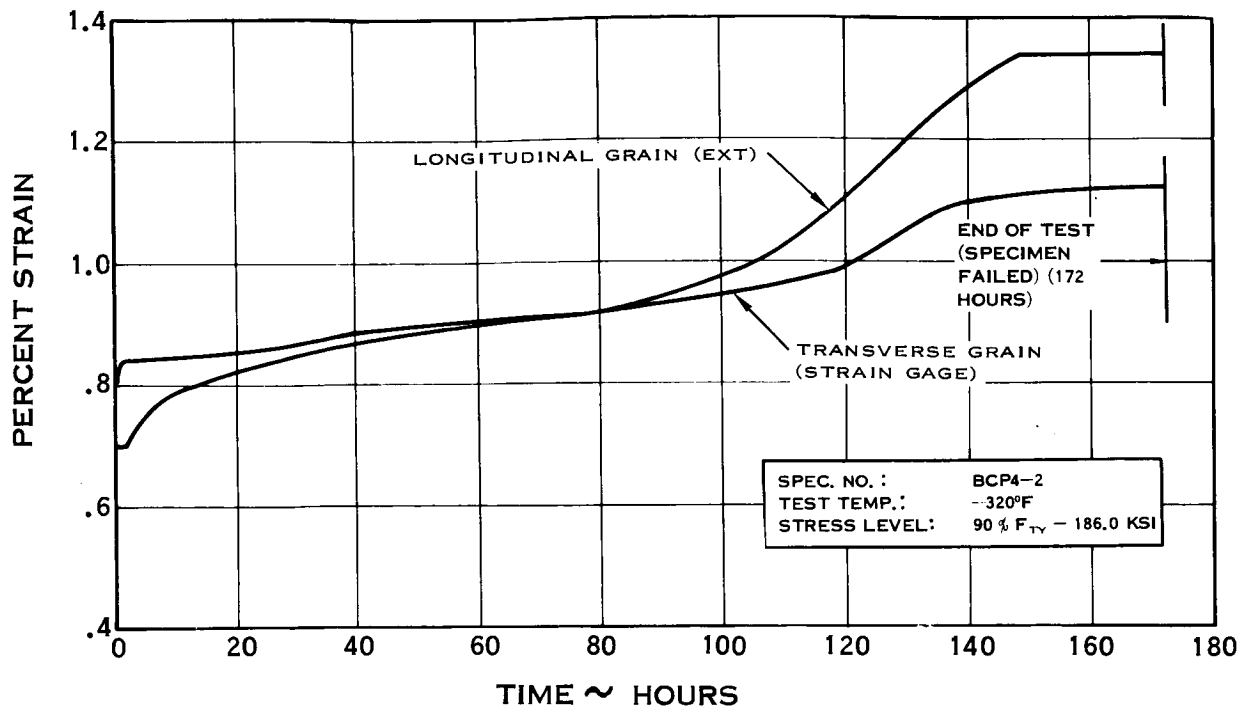


FIGURE 24 - 6AL - 4V TITANIUM ALLOY (ELI, ANNEALED) CREEP CURVES DEVELOPED UNDER 1:1 BIAxIAL STRESS FIELD

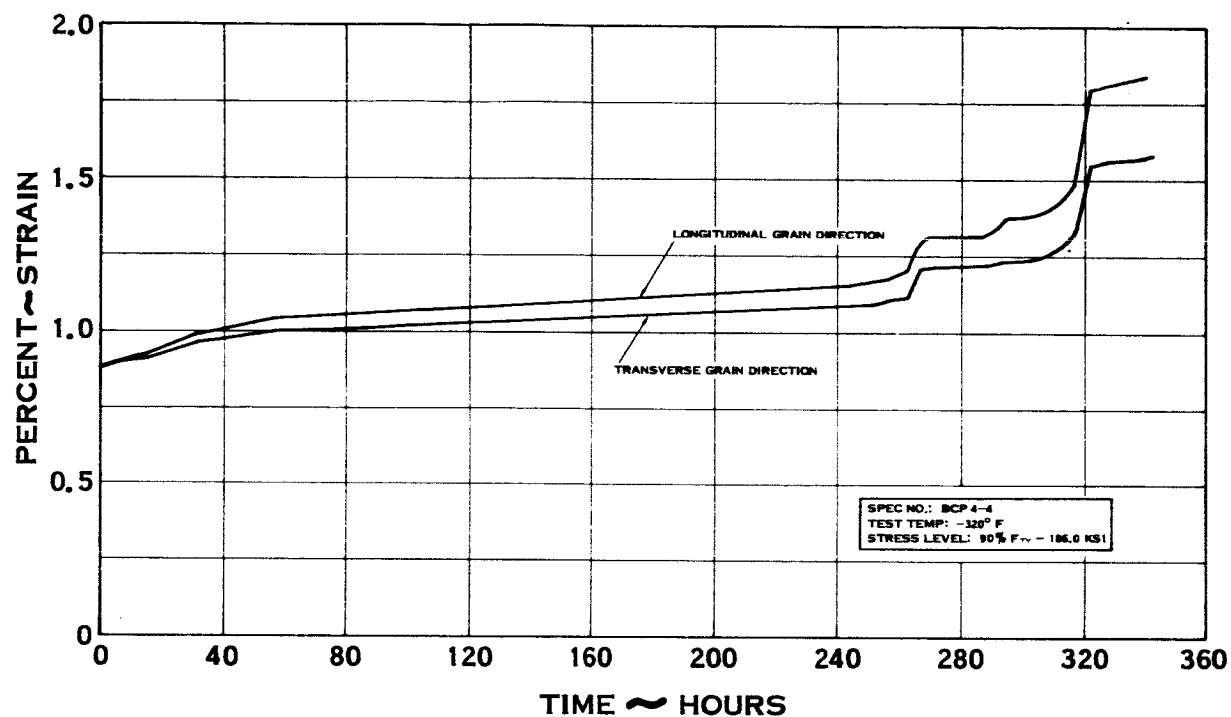


FIGURE 24 — 6AL — 4V TITANIUM ALLOY (ELI, ANNEALED) CREEP CURVES DEVELOPED UNDER 1:1 BIAxIAL STRESS FIELD (CONT)

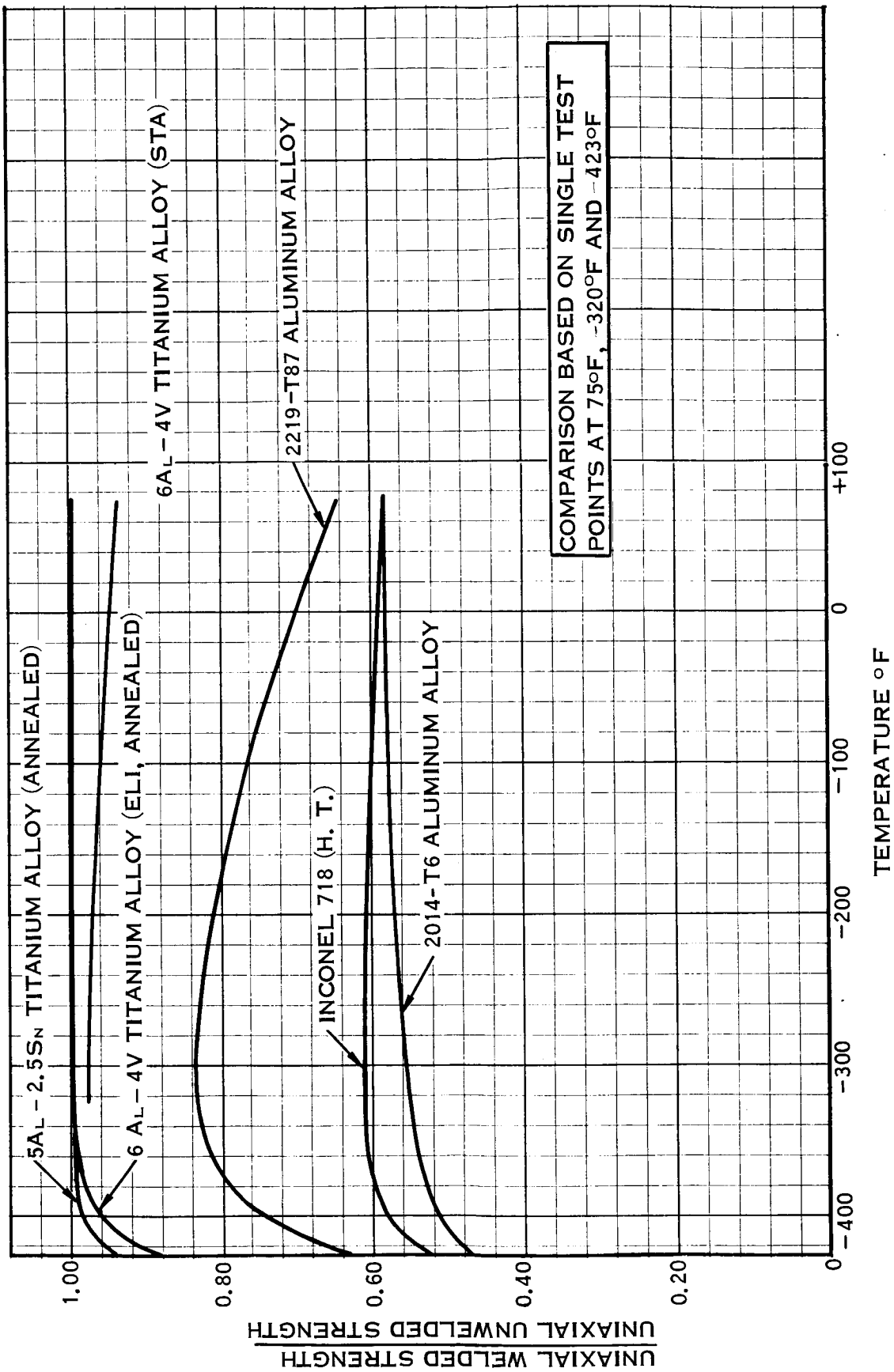


FIGURE 25 — COMPARISON OF UNIAxIAL WELDMENT EFFICIENCIES

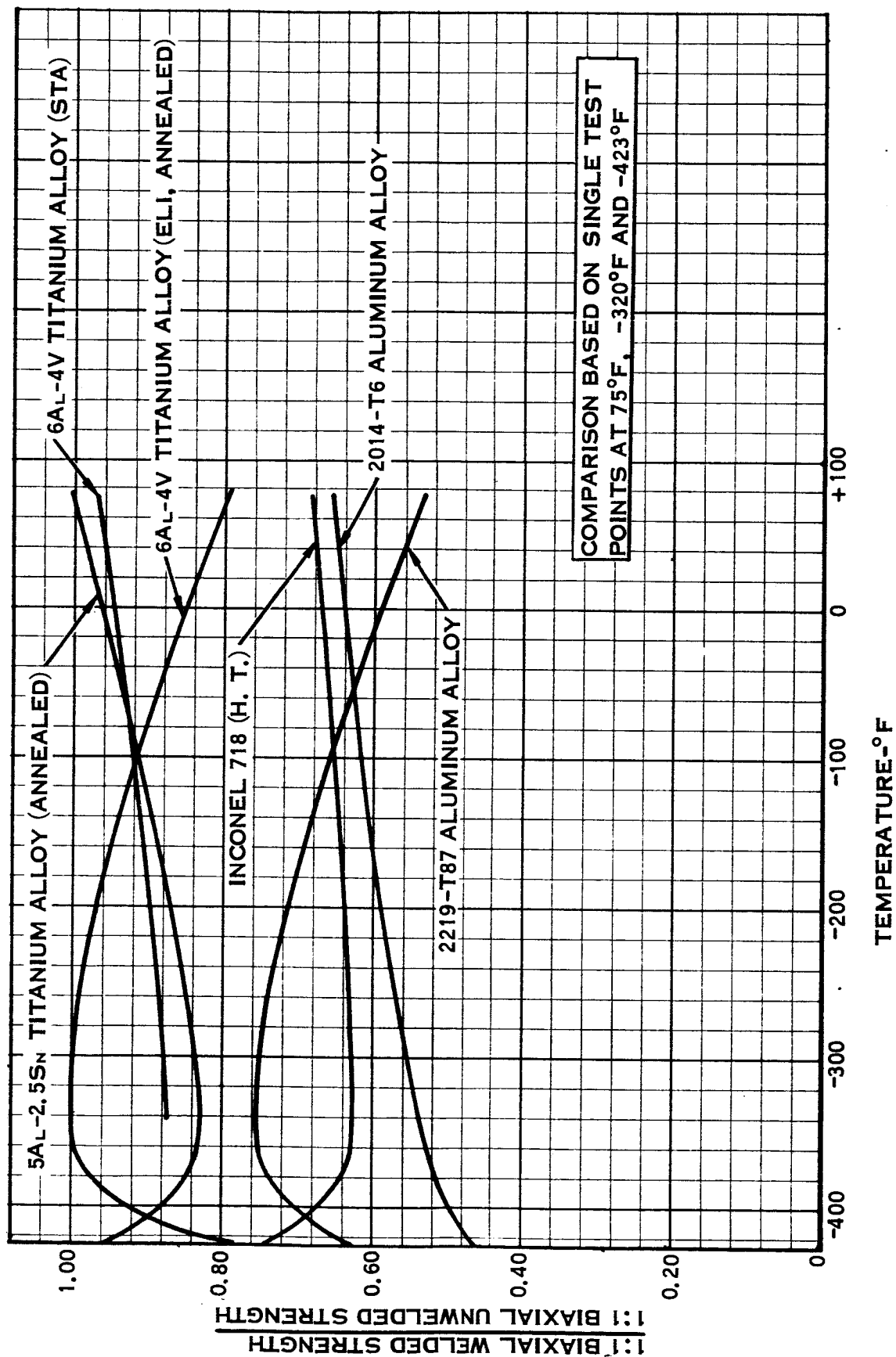


FIGURE 26 —COMPARISON OF 1:1 BIAxIAL WELDMENT EFFICIENCIES

MATERIAL	STRENGTH/DENSITY RATIO RATING						BIAXIAL/UNIAXIAL DUCTILITY RATIO RATING	
	1:0 UNIAXIAL	1:1 BIAXIAL	2:1 BIAXIAL	1:0 UNIAXIAL (WELDED)	1:1 BIAXIAL (WELDED)	2:1 BIAXIAL	1:1 BIAXIAL	2:1 BIAXIAL
2219-T87 AL 2014-T6 AL TITANIUM 6 AL - 4V (ELI) TITANIUM 5 AL - 2.5 Sn INCONEL 718 TITANIUM 6 AL - 4V (STA)	5 4 3 2 6 1	6 4 2 3 5 1	5 4 2 3 6 1	5 4 3 2 6 1	6 4 3 2 5 1	1 4 2 6 5 3	1 4 2 6 5 3	1 5 2 4 6 3
2219-T87 AL 2014-T6 AL TITANIUM 6 AL - 4V (ELI) TITANIUM 5 AL - 2.5 Sn INCONEL 718 TITANIUM 6 AL - 4V (STA)	6 4 3 2 5 1	6 4 3 2 5 1	5 4 3 2 6 1	— — — — — —	— — — — — —	1 2 4 3 6 5	1 2 4 3 6 5	1 2 4 5 6 3
2219-T87 AL 2014-T6 AL TITANIUM 6 AL - 4V (ELI) TITANIUM 5 AL - 2.5 Sn INCONEL 718 TITANIUM 6 AL - 4V (STA)	6 4 2 3 5 1	4 5 3 2 6 1	5 4 2 3 6 1	4 6 2 3 5 1	4 6 2 3 5 1	3 1 4 5 6 2	3 1 4 5 6 2	3 6 4 5 2 1
2219-T87 AL 2014-T6 AL TITANIUM 6 AL - 4V (ELI) TITANIUM 5 AL - 2.5 Sn INCONEL 718 TITANIUM 6 AL - 4V (STA)	3 4 1 2 5 —	3 4 1 2 5 —	3 4 2 1 5 —	3 4 2 1 5 —	3 5 2 1 4 —	4 1 2 3 5 —	4 1 2 3 5 —	3 5 2 1 4 —

NOTE:

- SEE TABLE 5 FOR DETAIL VALUES
- MATERIAL RATING VALUES OF 1, 2, 3 ETC. INDICATE BEST TO POOREST PERFORMANCE

FIGURE 27 — ILLUSTRATIVE CRYOGENIC MATERIAL RATING DATA

Material	Temp	1:0 Uniaxial		1:1 Biaxial		2:1 Biaxial	
		$\frac{\text{Strength}}{\text{Density}} \times 10^{-6}$	Rated Value	$\frac{\text{Strength}}{\text{Density}} \times 10^{-6}$	Rated Value	$\frac{\text{Strength}}{\text{Density}} \times 10^{-6}$	Rated Value
2219-T87 Aluminum Alloy	75 -105 -320 -423	.651 .697 .811 .977	5 6 6 3	.642 .671 .865 1.003	6 6 4 3	.731 .793 .931 1.167	
2014-T6 Aluminum Alloy	75 -105 -320 -423	.712 .747 .861 .948	4 4 4 4	.692 .738 .862 .949	4 4 5 4	.782 .843 .992 1.173	
5A1-2.5Sn Titanium Alloy (Annealed)	75 -105 -320 -423	.844 1.033 1.348 1.537	2 2 3 2	.845 1.034 1.355 1.446	3 2 2 2	.951 1.183 1.528 1.636	
6Al-4V (ELI) Titanium Alloy (Annealed)	75 -105 -320 -423	.808 1.020 1.361 1.622	3 3 2 1	.972 1.030 1.326 1.615	2 3 3 1	1.008 1.148 1.459 1.636	
Inconel 718 (Heat Treated)	75 -105 -320 -423	.650 .698 .836 .803	6 5 5 5	.644 .708 .833 .917	5 5 6 5	.701 .764 .914 .884	
6Al-4V(STA) Titanium Alloy	75 -105 -320	1.024 1.188 1.572	1 1 1	1.037 1.186 1.555	1 1 1	1.071 1.340 1.677	

NOTE: 1. Strength/Density values based on ultimate strengths.

2. Rated Value show relative ratings of materials for a given parameter at each temperature. Number 1 is best; number 2 is next, etc.

ILE 5

EVALUATION OF THE PROGRAM
CRYOGENIC APPLICATIONS

ed ue	1:0 Uniaxial (Welded)		1:1 Biaxial (Welded)		1:1 Biaxial		2:1 Biaxial	
	Strength Density $\times 10^{-6}$	Rated Value	Strength Density $\times 10^{-6}$	Rated Value	Biaxial Duct Uniaxial Duct	Rated Value	Biaxial Duct Uniaxial Duct	Rated Value
	.404	5	.343	6	.683	1	.983	1
	-	-	-	-	.597	1	1.055	1
	.680	4	.642	4	.579	3	.800	3
	.627	3	.627	3	.543	4	.752	3
	.416	4	.453	4	.385	4	.523	5
	-	-	-	-	.522	2	.967	2
	.474	6	.468	6	.662	1	.621	6
	.451	4	.446	5	.778	1	.575	5
	.845	2	.888	2	.207	6	.642	4
	-	-	-	-	.518	3	.540	5
	1.342	3	1.115	3	.356	5	.642	5
	1.454	1	1.375	1	.665	3	.863	1
	.813	3	.773	3	.600	2	.800	2
	-	-	-	-	.441	4	.732	4
	1.378	2	1.329	2	.413	4	.733	4
	1.447	2	1.267	2	.700	2	.860	2
	.381	6	.441	5	.293	5	.375	6
	-	-	-	-	.297	6	.457	6
	.512	5	.524	5	.319	6	.872	2
	.424	5	.593	4	.512	5	.652	4
	.957	1	1.003	1	.412	3	.762	3
	-	-	-	-	.433	5	.777	3
	1.540	1	1.353	1	.617	2	1.342	1

st temperature.

LTV AEROSPACE CORPORATION

STATE OF STRESS	MATERIAL	S_u ULTIMATE STRENGTH (KSI)	S_y YIELD STRENGTH (KSI)	E MODULUS OF ELASTICITY $\times 10^6$ PSI
1:0 UNIAXIAL	2219-T87 ALUMINUM	$S_u = 67.32 - .0073T + (1.495 \times 10^{-4})T^2$	$S_yu = 53.46 - .0044T + (1.145 \times 10^{-4})T^2$	$E_u = 10.12 - .0015T + (1.847 \times 10^{-5})T^2$
	2014-T6 ALUMINUM	$S_u = 71.97 - .0143T + (1.008 \times 10^{-4})T^2$	$S_yu = 67.52 - .0058T + (.938 \times 10^{-4})T^2$	$E_u = 10.60 - .0064T - (.392 \times 10^{-5})T^2$
	5A1-2.58n TITANIUM	$S_u = 147.29 - .1629T + (1.742 \times 10^{-4})T^2$	$S_yu = 136.43 - .1348T + (2.607 \times 10^{-4})T^2$	$E_u = 16.66 - .0071T - (1.015 \times 10^{-5})T^2$
	6A1-4V(ELI) TITANIUM	$S_u = 141.93 - .1680T + (2.586 \times 10^{-4})T^2$	$S_yu = 134.33 - .1803T + (2.404 \times 10^{-4})T^2$	$E_u = 16.57 - .0003T + (.792 \times 10^{-5})T^2$
	INCONEL 718 ALLOY	$S_u = 201.51 - .1426T - (.999 \times 10^{-4})T^2$	$S_yu = 161.56 - .0548T + (.322 \times 10^{-4})T^2$	$E_u = 30.73 - .0099T - (1.261 \times 10^{-5})T^2$
	6A1-4V(STA) TITANIUM	$S_u = 176.16 - .1806T + (1.183 \times 10^{-4})T^2$	$S_yu = 164.23 - .2000T + (.678 \times 10^{-4})T^2$	$E_u = 16.48 - .0051T + (.259 \times 10^{-5})T^2$
1:1 BIAXIAL	2219-T87 ALUMINUM	$S_{r1} = 65.62 - .0142T + (1.697 \times 10^{-4})T^2$	$S_{y1} = 51.81 - .0123T + (1.351 \times 10^{-4})T^2$	$E_{r1} = 14.17 - .0078T + (.834 \times 10^{-5})T^2$
	2014-T6 ALUMINUM	$S_{r1} = 71.20 - .0249T + (.768 \times 10^{-4})T^2$	$S_{y1} = 62.24 - .0141T + (.811 \times 10^{-4})T^2$	$E_{r1} = 14.68 - .0102T - (1.064 \times 10^{-5})T^2$
	5A1-2.58n TITANIUM	$S_{r1} = 149.21 - .1922T + (.278 \times 10^{-4})T^2$	$S_{y1} = 127.32 - .2853T - (.908 \times 10^{-4})T^2$	$E_{r1} = 23.09 - .0073T - (.748 \times 10^{-5})T^2$
	6A1-4V(ELI) TITANIUM	$S_{r1} = 154.72 - .0124T + (5.541 \times 10^{-4})T^2$	$S_{y1} = 145.55 - .0197T + (5.681 \times 10^{-4})T^2$	$E_{r1} = 22.53 + .0040T + (1.066 \times 10^{-5})T^2$
	INCONEL 718 ALLOY	$S_{r1} = 201.93 - .1598T - (1.490 \times 10^{-4})T^2$	$S_{y1} = 179.65 - .1496T - (2.132 \times 10^{-4})T^2$	$E_{r1} = 42.70 - .0143T - (3.205 \times 10^{-5})T^2$
	6A1-4V(STA) TITANIUM	$S_{r1} = 176.63 - .1601T + (1.611 \times 10^{-4})T^2$	$S_{y1} = 161.84 - .2146T + (.063 \times 10^{-4})T^2$	$E_{r1} = 23.08 + .0056T + (2.498 \times 10^{-5})T^2$
2:1 BIAXIAL	2219-T87 ALUMINUM	$S_{r2} = 75.86 - .0009T + (2.261 \times 10^{-4})T^2$	$S_{y2} = 57.43 + .0118T + (1.960 \times 10^{-4})T^2$	$E_{r2} = 11.75 - .0022T + (1.719 \times 10^{-5})T^2$
	2014-T6 ALUMINUM	$S_{r2} = 79.77 - .0154T + (1.729 \times 10^{-4})T^2$	$S_{y2} = 68.99 - .0064T + (1.381 \times 10^{-4})T^2$	$E_{r2} = 12.29 - .0092T - (1.199 \times 10^{-5})T^2$
	5A1-2.58n TITANIUM	$S_{r2} = 168.82 - .2255T + (.086 \times 10^{-4})T^2$	$S_{y2} = 144.34 - .1747T + (1.728 \times 10^{-4})T^2$	$E_{r2} = 19.22 - .0073T - (.982 \times 10^{-5})T^2$
	6A1-4V(ELI) TITANIUM	$S_{r2} = 170.15 - .1246T + (2.298 \times 10^{-4})T^2$	$S_{y2} = 141.52 - .0024T + (6.090 \times 10^{-4})T^2$	$E_{r2} = 17.93 + .0027T + (1.354 \times 10^{-5})T^2$
	INCONEL 718 ALLOY	$S_{r2} = 218.80 - .1693T - (1.228 \times 10^{-4})T^2$	$S_{y2} = 181.30 - .1793T - (3.030 \times 10^{-4})T^2$	$E_{r2} = 31.46 - .0132T - (.618 \times 10^{-5})T^2$
	6A1-4V(STA) TITANIUM	$S_{r2} = 192.95 - .2798T - (1.840 \times 10^{-4})T^2$	$S_{y2} = 169.73 - .2188T - (1.146 \times 10^{-4})T^2$	$E_{r2} = 18.43 - .0087T - (2.089 \times 10^{-5})T^2$

NOTES:

(1) Temperature Range: +75°F to -423°F

(2) Substitute Temperature (T) in degrees Fahrenheit (for example: -300°F, +30°F, 0°F)

FIGURE 28 — EXPERIMENTALLY DETERMINED EQUATIONS FOR PREDICTION OF STRENGTH AND MODULUS PROPERTIES AS A FUNCTION OF TEMPERATURE

SECTION VII

CONCLUSIONS AND RECOMMENDATIONS

As a result of the research summarized in this report the following conclusions and recommendations have been formulated.

CONCLUSIONSMATERIALS AND DATA:

1. Basic material data (figure 27 and table 5) illustrate that each of the program materials can be considered as a prime prospect for use in various uniaxially and biaxially stressed components at cryogenic temperatures. The above noted figure and table illustrates which alloy would serve best in a given environment under various stress conditions. With the exception of a few special situations (creep, fracture toughness, costs, etc.) the program materials may be generally rated in three groups as:

FIRST: PROGRAM TITANIUM ALLOYS
SECOND: PROGRAM ALUMINUM ALLOYS
THIRD: PROGRAM NICKEL ALLOY
2. Biaxial strength characteristics of the program alloys are different from uniaxial strength values. Biaxial strength values obtained from the 1:1 stress state are generally equal to or slightly less than the uniaxial stress state. Biaxial strength values obtained from the 2:1 stress state are equal to or greater (5 to 15%) than the uniaxial stress state. The following conclusion items discuss individual property affects.
3. Ultimate strength, yield strength, and modulus properties for the program materials increased as the thermal environment was lowered.
4. Elongation values followed less predictable trends as this property either increased or decreased as the temperature was lowered depending on the particular alloy and the stress state involved.
5. Results indicate that at cryogenic temperatures, as at room temperature, the most severe stress state was the 1:1 biaxial stress state. This observation was illustrated by the reduced elongation values under this stress state as compared with the 1:0 and 2:1 stress state.

6. In the "as welded" condition the three titanium alloys in this research illustrated significantly better weldment efficiency values than was obtained from the Inconel and aluminum alloys. This was true for the entire program temperature range and for both the 1:0 and 1:1 stress states.
7. The 1:1 biaxial stress state proved to be much more severe than the 1:0 (uniaxial) stress state under cryogenic creep conditions in both of the program ELI titanium alloys.
8. The comparison of fracture toughness for the 1:0 and the 1:1 stress states indicated that the 1:1 stress state is not necessarily the most severe condition. Relative severity is involved with the given alloy, stress state, temperature and the materials ability to deformed under a balanced shear-tension mode. (See Appendix J for discussion)

THEORY:

1. Test results compared with the deformation energy theory indicate that the theory curve forms a lower bound or minimum predicted value for the 1:1 biaxial stress state condition. In the case of the 2:1 biaxial stress state the test results form more of a mean (average) value about the deformation energy theory curve.
2. Modulus (effective) of elasticity values for the 2:1 and 1:1 stress state can be predicted by the use of the standard equations of elasticity ($E_{1:1} = E_u/1 - \mu$ and $E_{2:1} = E_u/1 - 0.5\mu$)

RECOMMENDATIONS

1. Immediate efforts should be undertaken to evaluate the detail effects of 1:1 and 2:1 biaxial creep effects on various titanium alloys of the ELI types. These evaluations efforts should include effects of temperature (R.T.; -320°F; etc.) and effects of biaxial stress state compared with the uniaxial stress state. The prime point to be evaluated should be that of determining the critical (threshold) stress level at which cryogenic creep begins under uniaxial and biaxial stresses and at what stress level failure will occur in a prescribed time period. This program has only touched

on these aspects in that it has established that a problem exists and has shown that feasible evaluation and testing techniques are available.

SECTION VIII

REFERENCES

1. AFML-TR-65-140, Cryogenic Design Data for Materials Subjected to Uniaxial and Multiaxial Stress Field, S. W. McClaren and C. R. Foreman, LTV Aerospace Corporation, May 1965.
2. AFML-TR-65-213, Development of Standardized Test Methods to Determine Plane Strain Fracture Toughness, G. L. Hanna and E. A. Stelgerwald, TRW Inc., September 1965.
3. Journal of Applied Mechanics, "Crack-Extension Force for a Part-Through Crack In A Plate," G. R. Irwin, NRL, December 1962, pp. 651-654.
4. ASD-TDR-62-401, Biaxial Stress and Strain Data on High Strength Alloys for Design of Pressurized Components, E. L. Terry and S. W. McClaren, Chance Vought Corporation, May 1962.

APPENDIX A

PHOTOELASTICITY ILLUSTRATIONS OF THE 1:1
BIAXIAL STRESS STATEGeneral

In order to illustrate the use of the biaxial cross-shaped specimen as an effective instrument for developing biaxial states of stress and for testing materials under biaxial stress states, the following test was included. This test was conducted as a part of the "in-house" R&D effort and utilized a 1:1 biaxial specimen of 7075-T6 aluminum alloy at room temperature. A specimen without a second depression was used to have a constant photostress coating condition; otherwise observed fringe patterns would not illustrate comparative stress values. In addition strain gages on the opposite side of the specimen were used to obtain the desired strain (stress) state.

1:1 Biaxial Photostress Data

The test of a 1:1 biaxial specimen was conducted in a standard test manner with the only exceptions being those noted above concerning constant thickness and strain gage locations (2) on the same side of the specimen. As the specimen was loaded a series of photoelastic photographs was made at periodic intervals. These comparative and continuous photographs are shown in Figure 29. In addition, the tabular data, also shown in Figure 29, illustrates strain gage measured strains at individual points and key-in important remarks of occurrences during the test. This data illustrates the development and maintenance of the nominal 1:1 stress state in the test section (Black area; isotropic point; $\sigma_1 = \sigma_2$; $\tau_{\max} = 0$) from the first recorded load position "B", point of low elastic strain, to position "F", point of yielding definitely occurring (see Figures 29 and 30). At position "G", top of the first unload loop, the effects of anisotropic materials properties are occurring as the material in the longitudinal grain direction is yielding a little faster than the material in the transverse grain direction. The result is a loss of the "pure" isotropic condition ($\sigma_1 = \sigma_2$) as also observed in the recorded strain gage values in the tabulated data (Figure 29). The difference shown by the photostress fringe pattern is about 0.18 of one fringe (graying area). The calibrated photostress material has a 0.00186 in./in./fringe value; therefore the longitudinal stress is approximately 2500 psi lower than the transverse stress at position "G". This delta difference is further verified by the observed

strain delta strain value of 0.03% at this point. (Compare: 0.03% with $(0.00186 \times 0.18) = 0.033\%$). At position "H", bottom of the first unload loop -0.026% strain, the anisotropic effects vanish almost completely while a basic isotropic point is again observed. The specimen was then reloaded (1:1) up the generated line, "H-G," and the test continued until position "I" was reached where similar conditions are reached as noted at position "G" above; that is, the longitudinal strain is leading the transverse strain by about 0.03%. Finally, a position a little further out on the stress-strain curve was desired; but the photostress plastic failed as observed in position "J". These results illustrate rather dramatically the usefulness of the 1:1 biaxial specimen in simulating the 1:1 stress state as it occurs in spherical pressure vessels. For in a spherical pressure vessel a basic 1:1 stress state is developed due to configuration and pressure and remains 1:1 until a material's anisotropic property condition causes yielding in one or other of the principal stress directions. At this point in a spherical pressure vessel the two stresses (S_1 and S_2) are both still increasing with pressure (load); but the direction that is yielding most will have a slightly lower stress than the other direction. This is due to a flattening out of the vessel radius in one direction while the other dimensions are still basically constant. In this test the longitudinal grain direction sustained the greatest strain (normally the case) so the stress in the transverse grain direction is slightly higher. The limiting condition that can be experienced in such cases is the formation of a cylindrical strip (hoop) and the final observance of a 2:1 stress state. Obviously, this limit is not experienced in actual spherical pressure vessel tests. Therefore, the situation experienced in a spherical pressure vessel (1:1) in the elastic and the plastic range is directly analogous to the conditions experienced in the 1:1 biaxial specimen as illustrated by Figure 29 and 30 (up to the yield condition) and by the strain gage plots (out in the plastic range to failure).

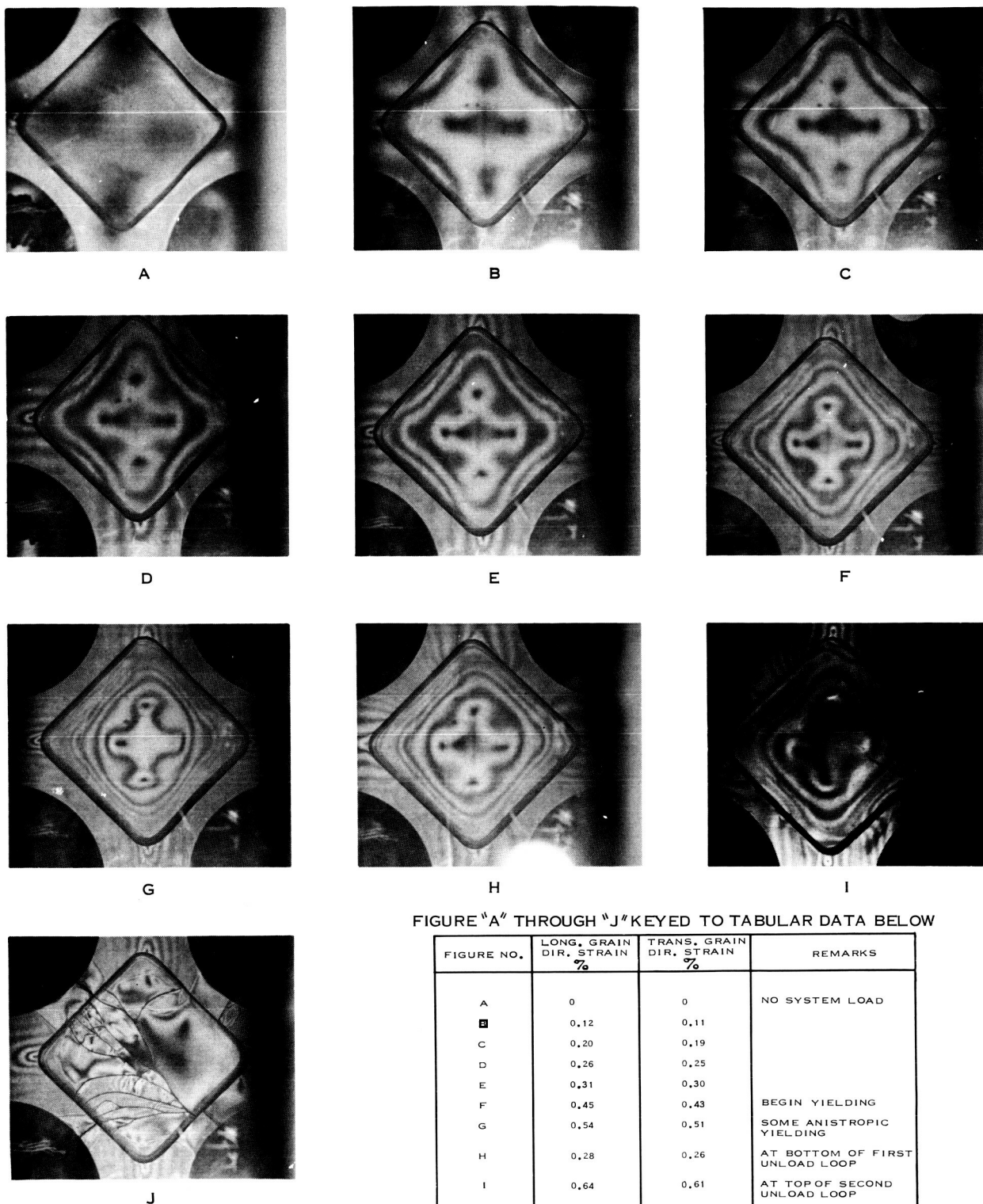


FIGURE 29. — STEP-BY-STEP PHOTO STRESS EVALUATION OF THE STATE OF STRESS IN A 1:1 BIAxIAL TEST SPECIMEN (MATERIAL 7075-T6 ALUMINUM ALLOY)

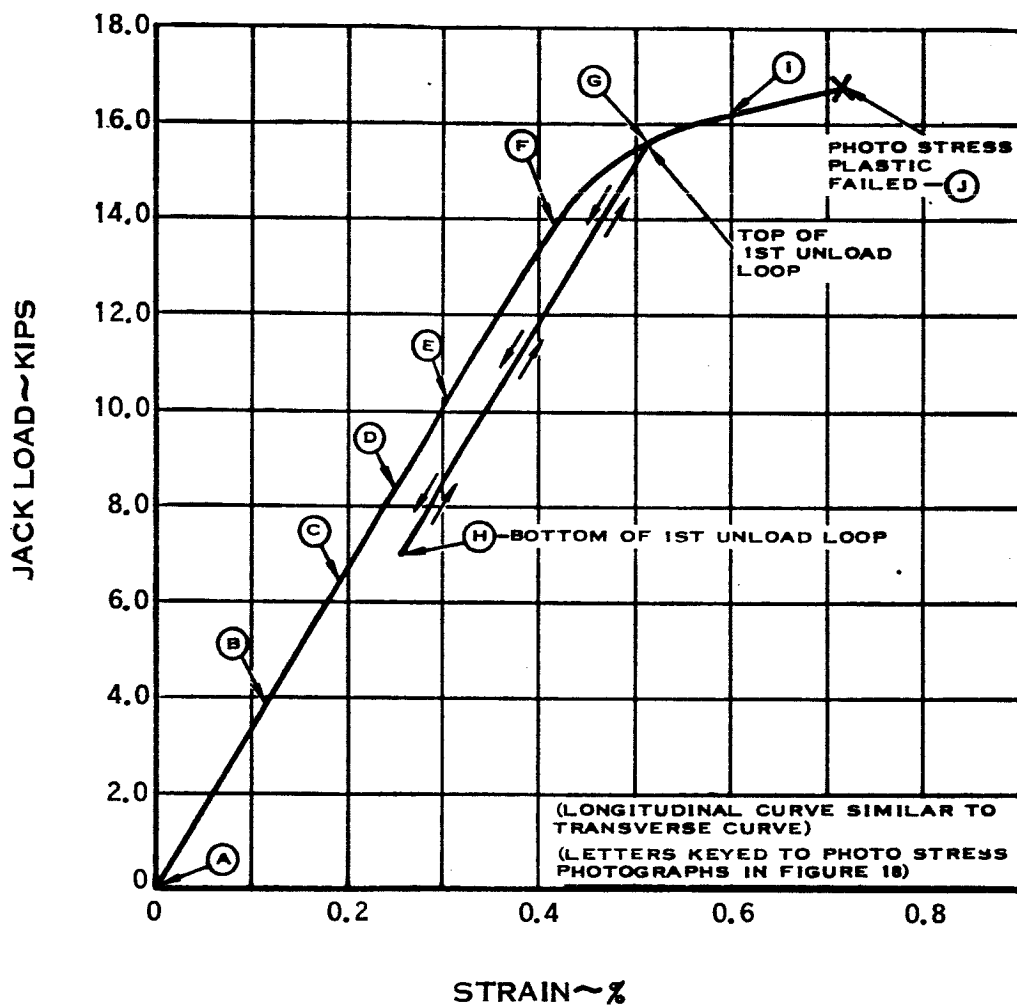


FIGURE 30 — LOAD-STRAIN CURVE FOR 1:1 BIAxIAL PHOTO STRESS TEST FOR THE TRANSVERSE GRAIN DIRECTION

APPENDIX B

TEST EQUIPMENT AND ARRANGEMENTS

Figures 31 through 44 illustrate the various program test arrangements, pieces of test equipment, facilities and test set-ups that were utilized in the conduct of this research.

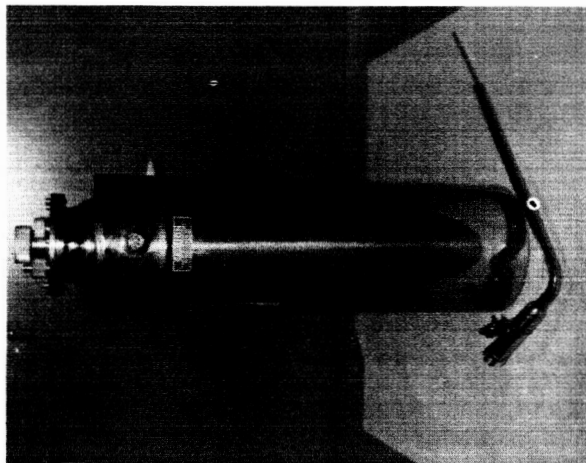


FIGURE 31 — UNIAXIAL
CRYOSTAT

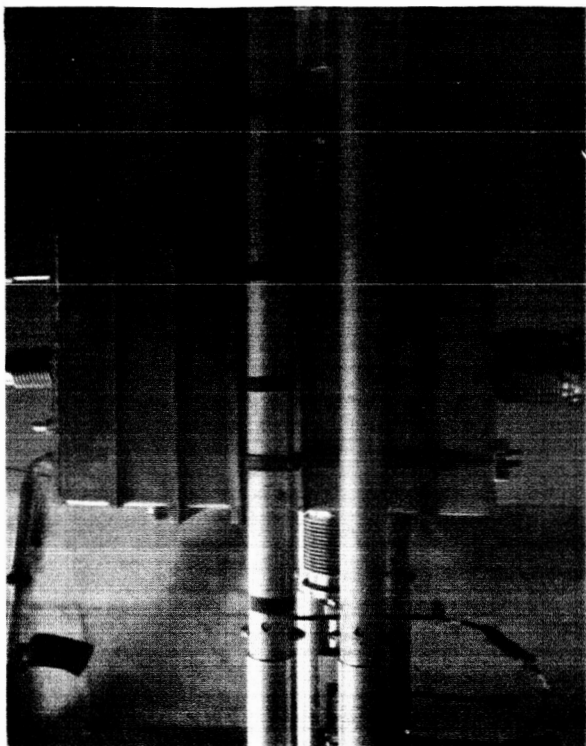


FIGURE 32 — BIAXIAL CRYOSTAT

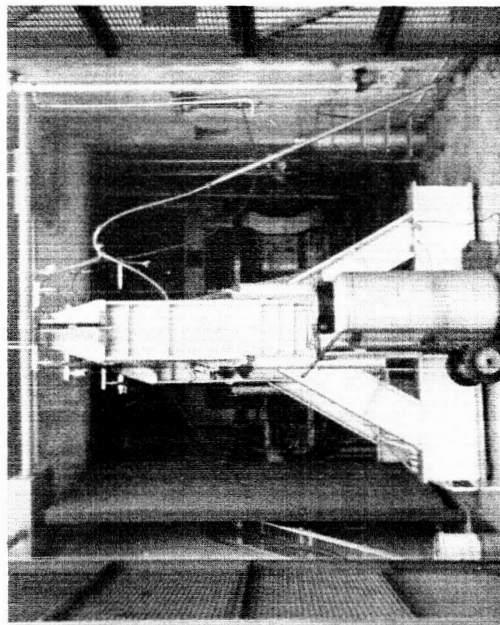


FIGURE 33 — VIEW OF LIQUID HYDROGEN
TEST CELL WITH BIAXIAL
TEST MACHINE (-423°F)

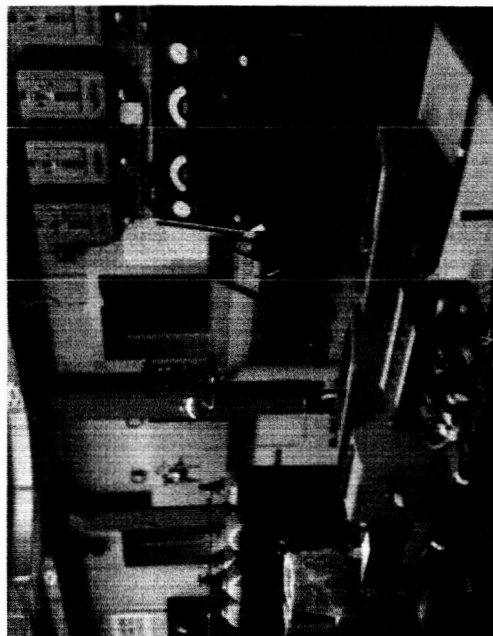
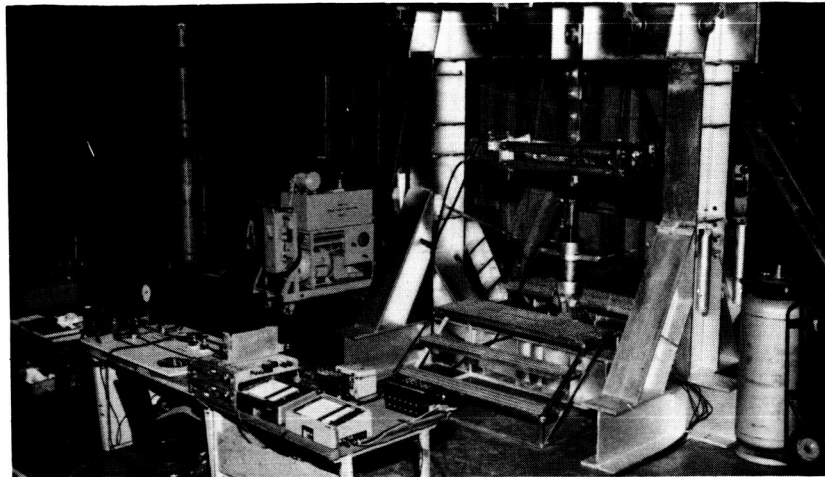
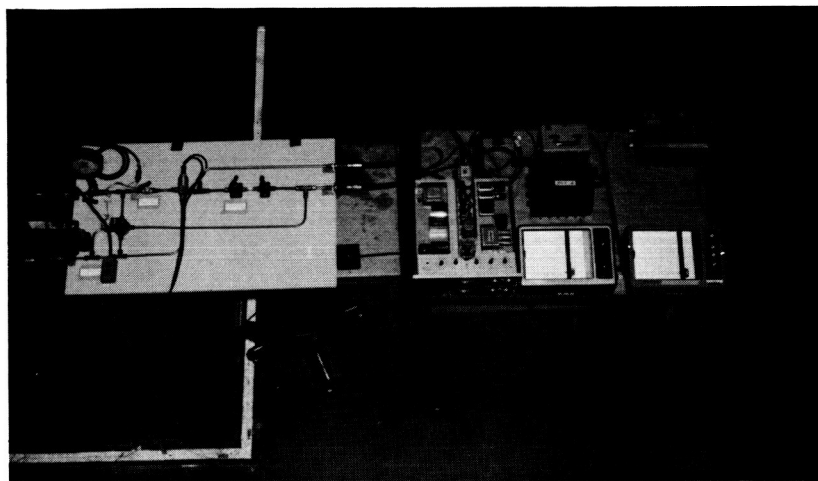


FIGURE 34 — VIEW OF LIQUID HYDROGEN
CONTROL ROOM (-423°F)



**FIGURE 35 — BIAXIAL TEST MACHINE
(OVERALL VIEW)**



**FIGURE 36 — BIAXIAL DATA RECORDING EQUIPMENT
AND BREAD-BOARDED CONTROL PANEL**

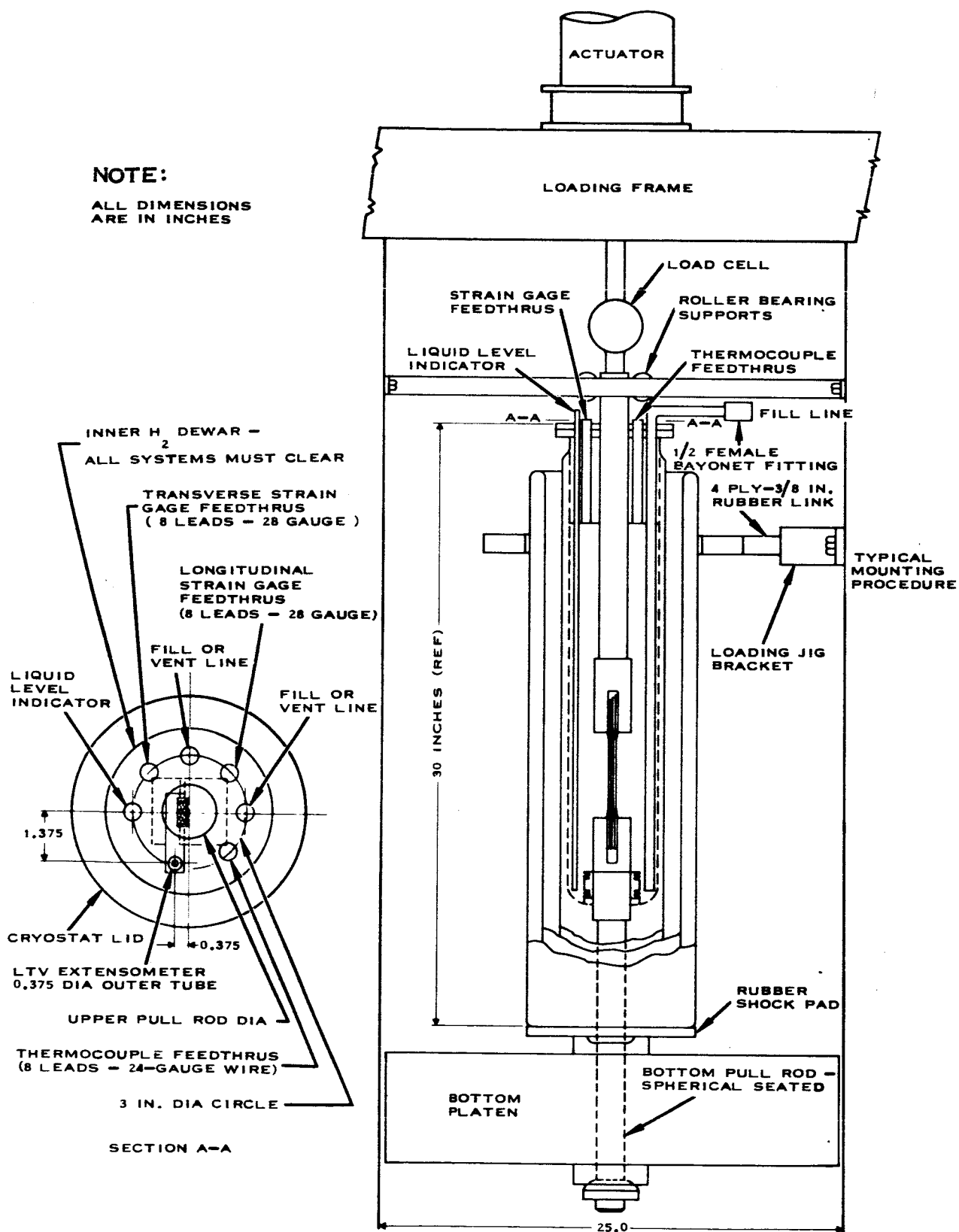


FIGURE 37 - UNIAXIAL CRYOSTAT

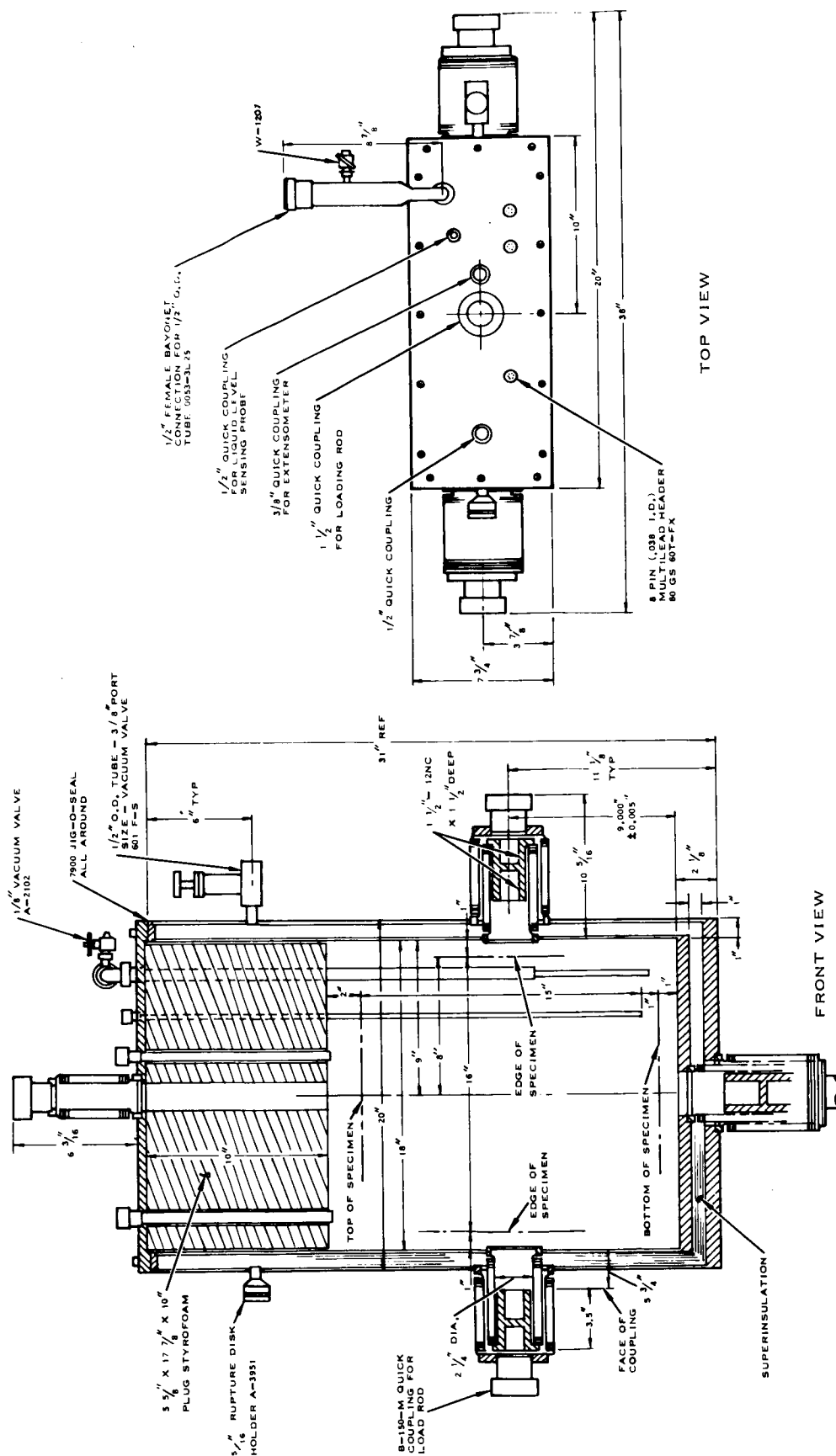


FIGURE 38 -BIAXIAL CRYOSTAT

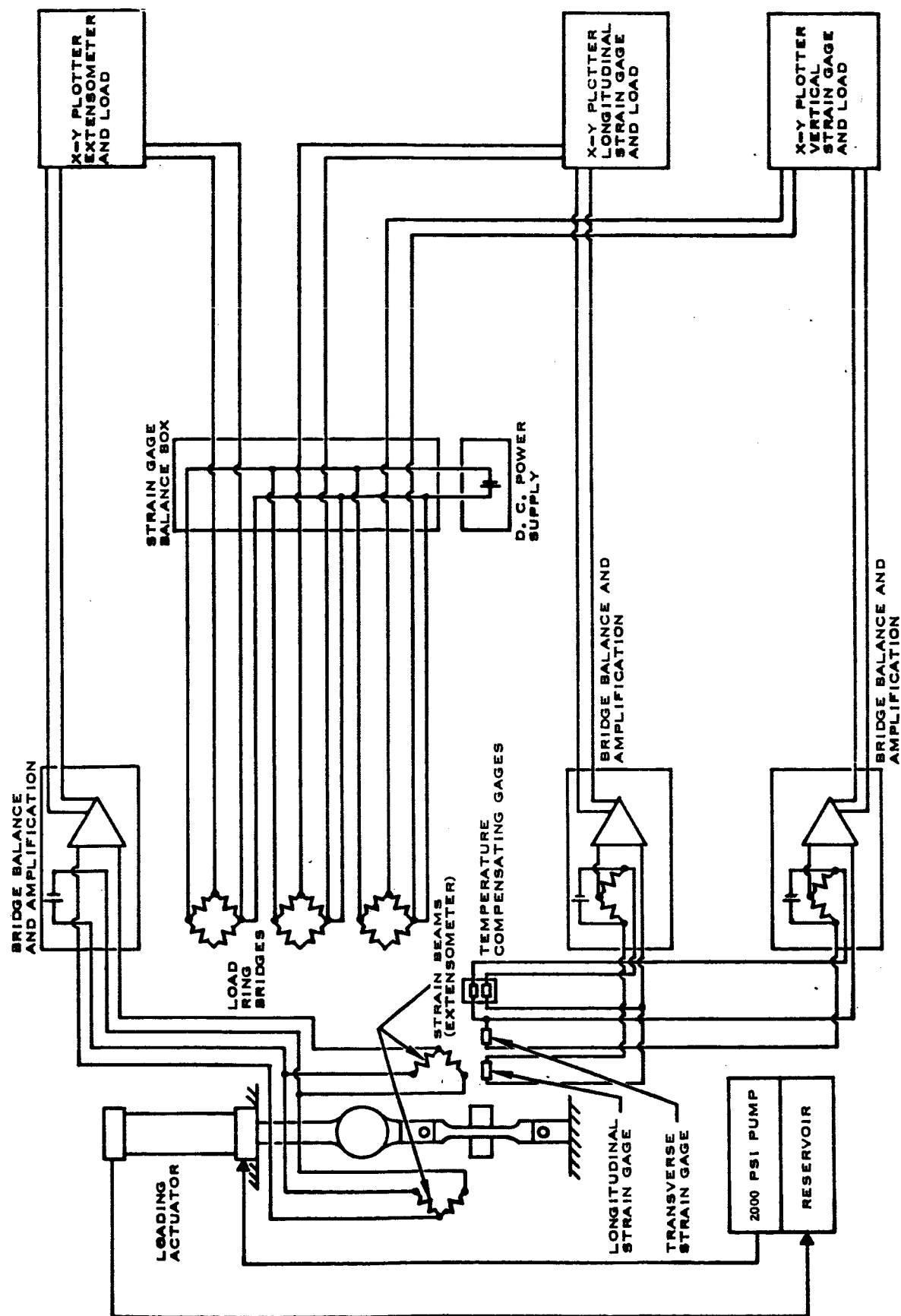


FIGURE 39 — ELECTRICAL AND HYDRAULIC SCHEMATIC FOR UNIAXIAL TESTS

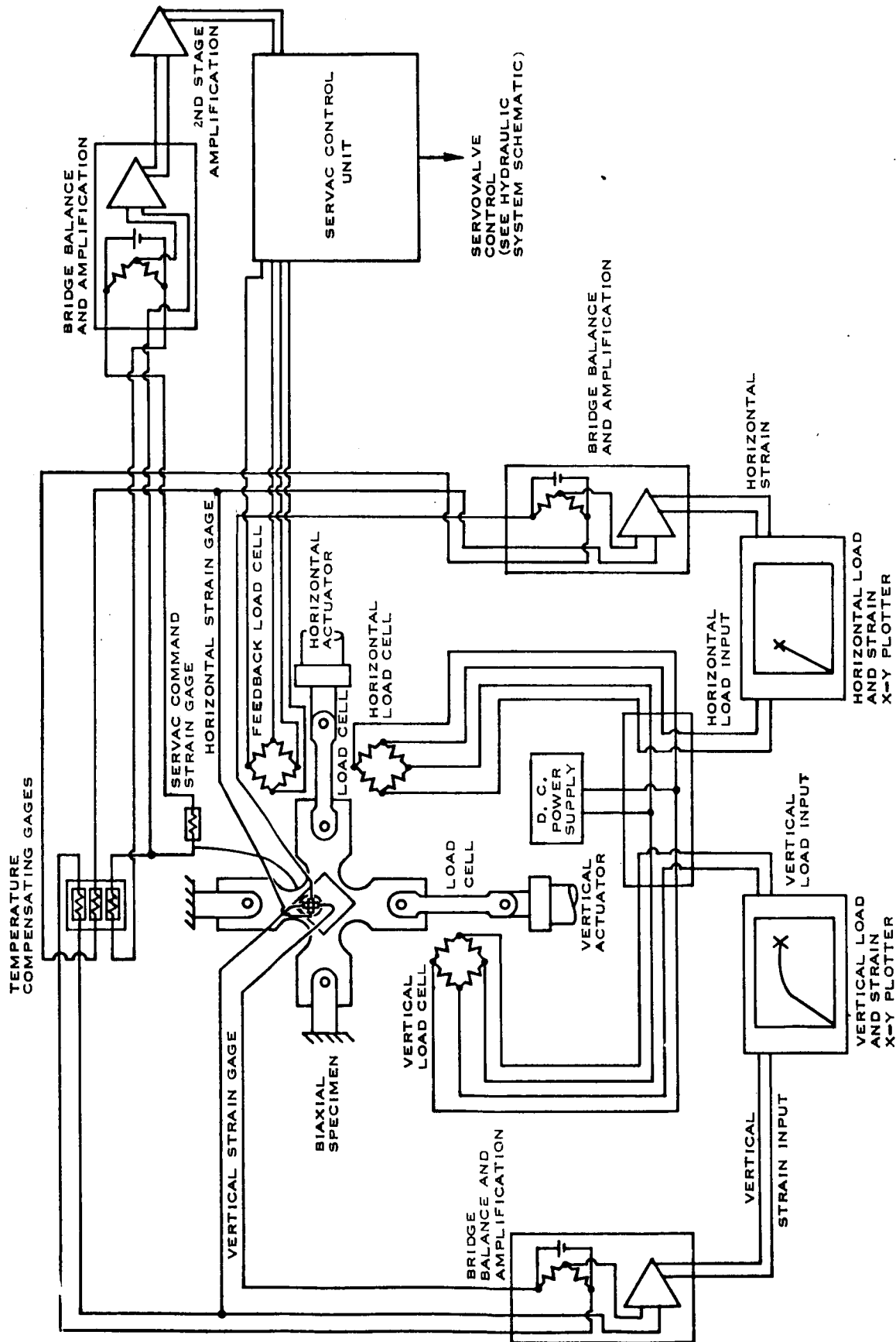


FIGURE 40 — ELECTRICAL SCHEMATIC FOR 1:1 AND 2:1 BIAxIAL TESTS

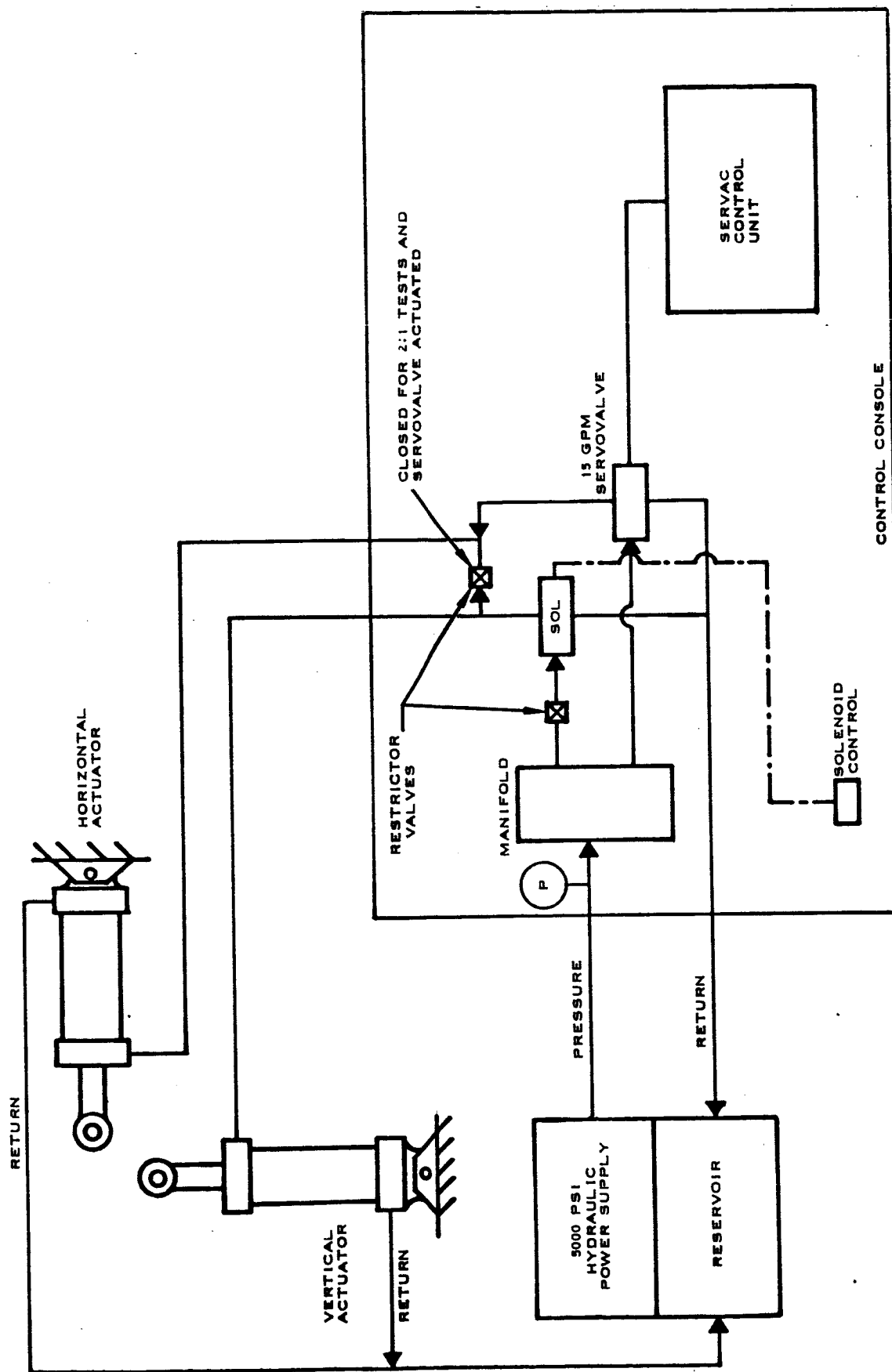


FIGURE 41 - HYDRAULIC SCHEMATIC FOR 1:1 AND 2:1 BIAxIAL STRESS TESTS PROGRAM

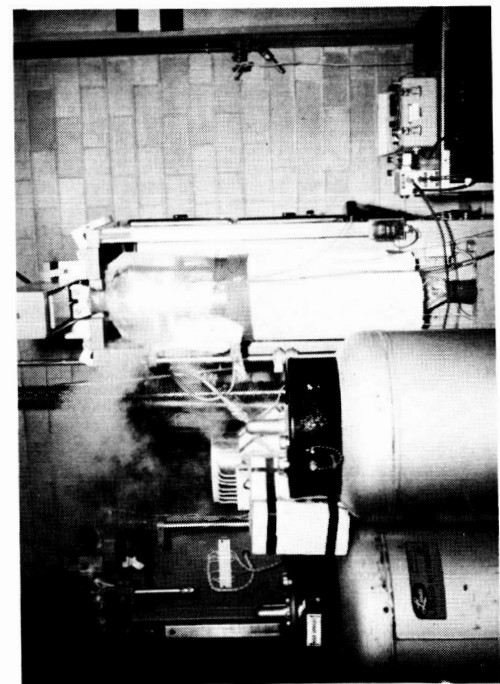


FIGURE 42 — UNIAXIAL CREEP TEST SET-UP

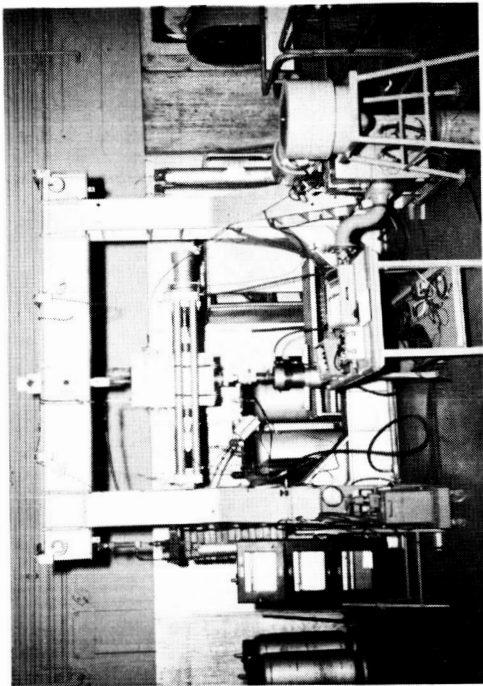


FIGURE 43 — BIAXIAL CREEP TEST SET-UP

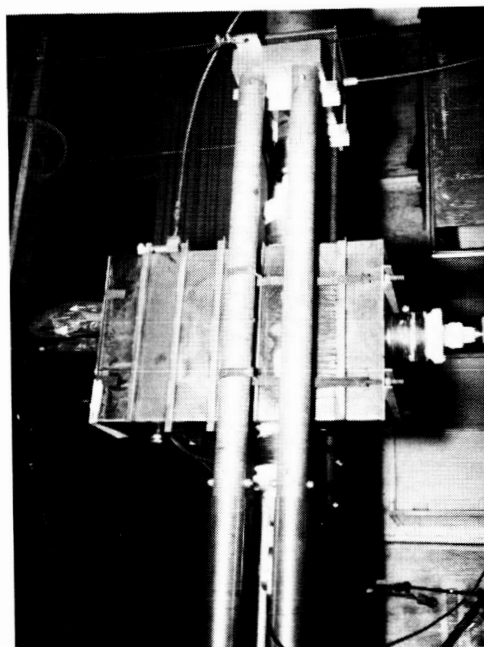
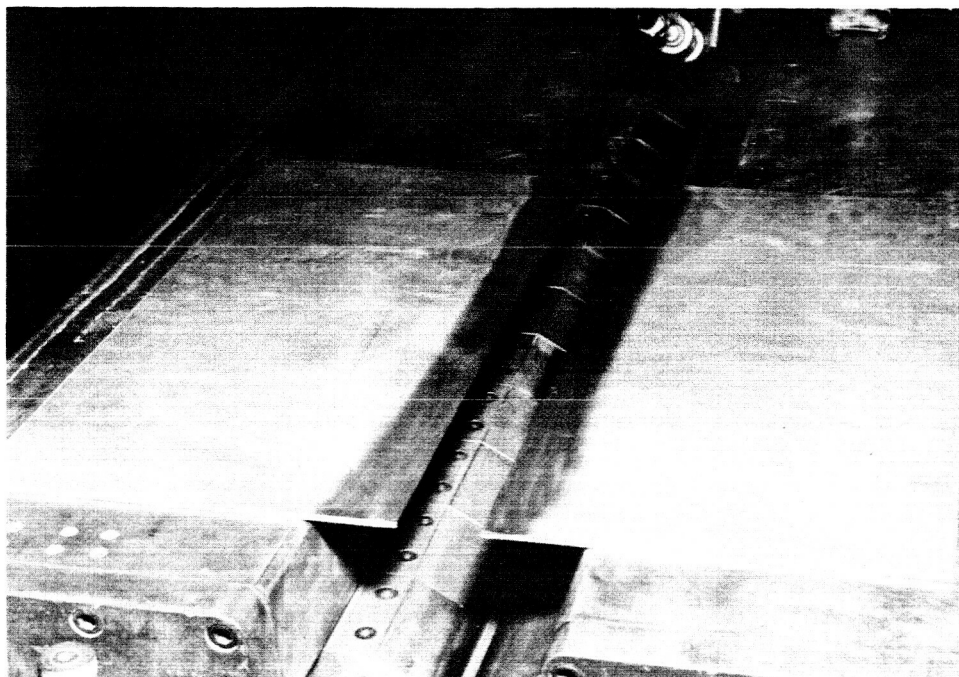
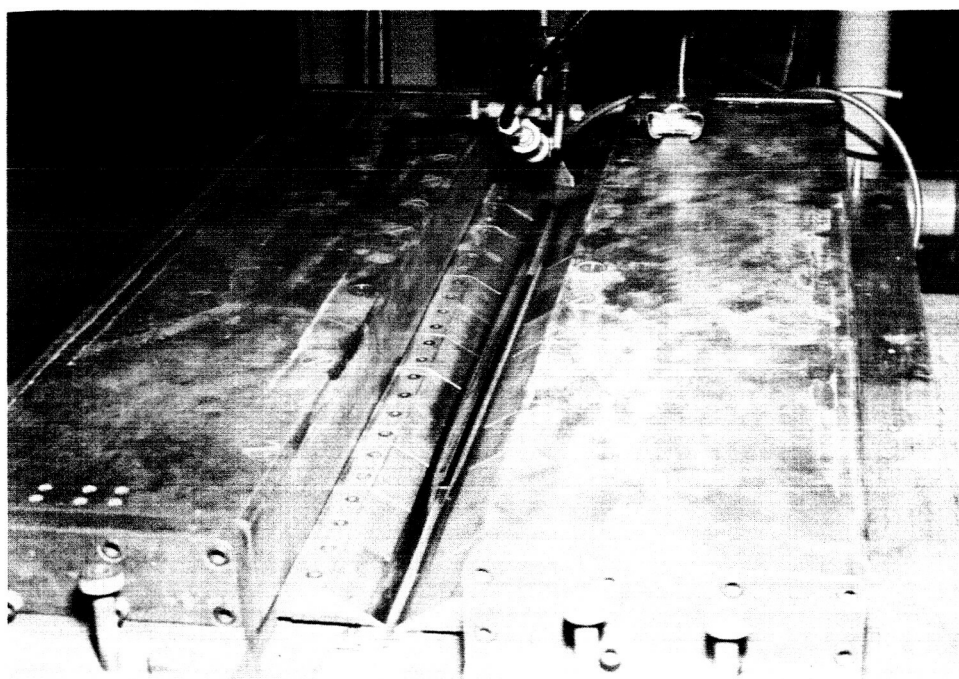


FIGURE 43 — BIAXIAL CRYOSTAT IN USE DURING A CREEP TEST (CONT)

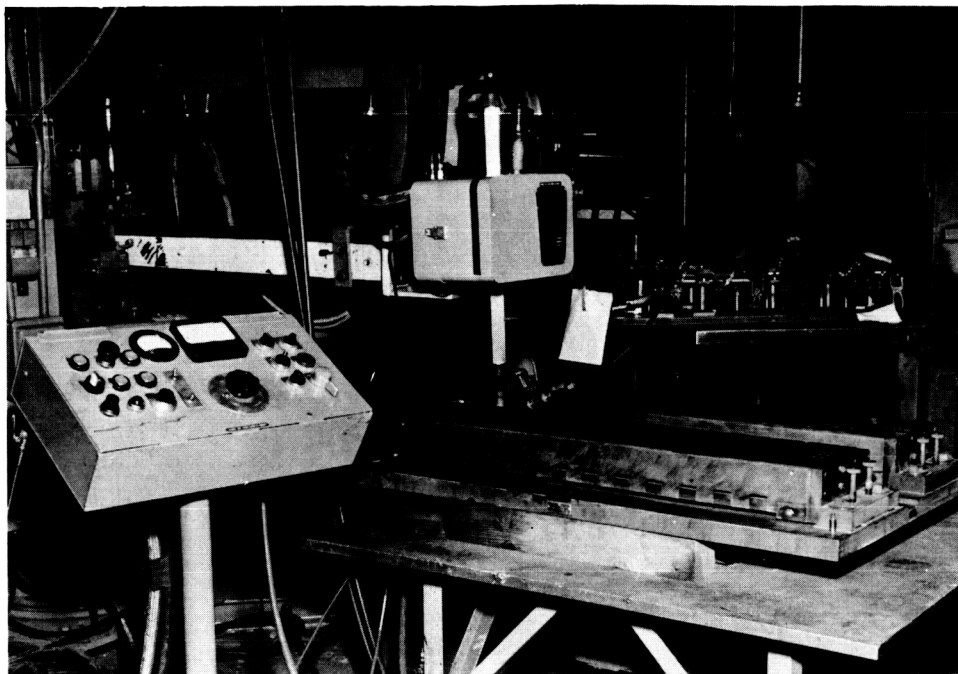


(A) PREPARED WELD BLANK

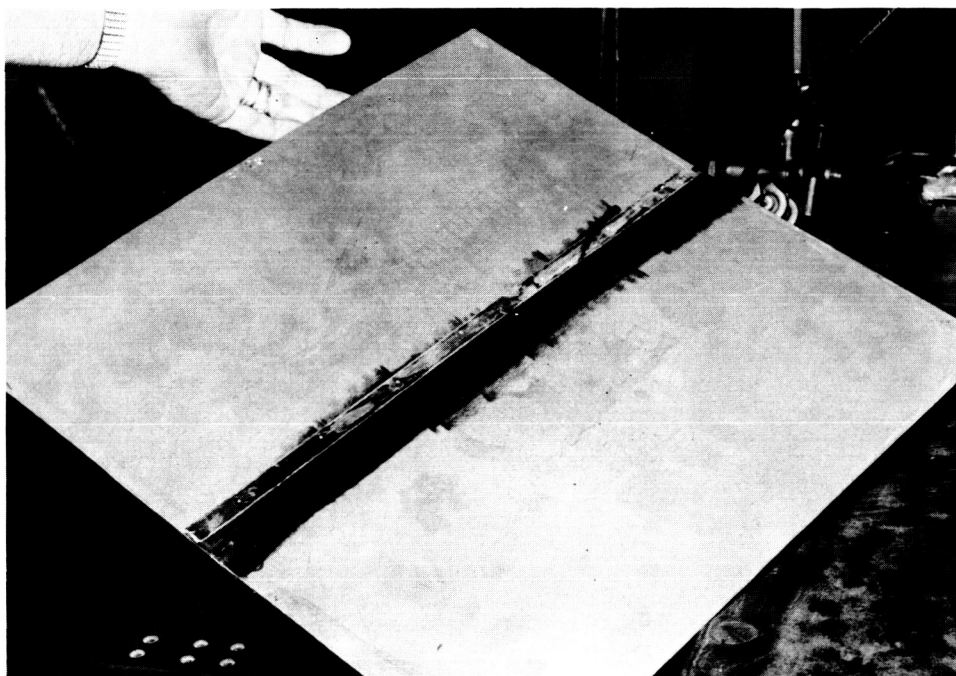


(B) BLANK IN CLAMP JIG

FIGURE 44 — ILLUSTRATIONS OF VARIOUS WELDING
OPERATIONS AND FACILITIES



(C) OVERALL FACILITIES



(D) COMPLETED WELD SPECIMEN

FIGURE 44 — ILLUSTRATIONS OF VARIOUS WELDING
OPERATIONS AND FACILITIES (CONT)

APPENDIX C

LOW TEMPERATURE STRAIN GAGE TECHNIQUES

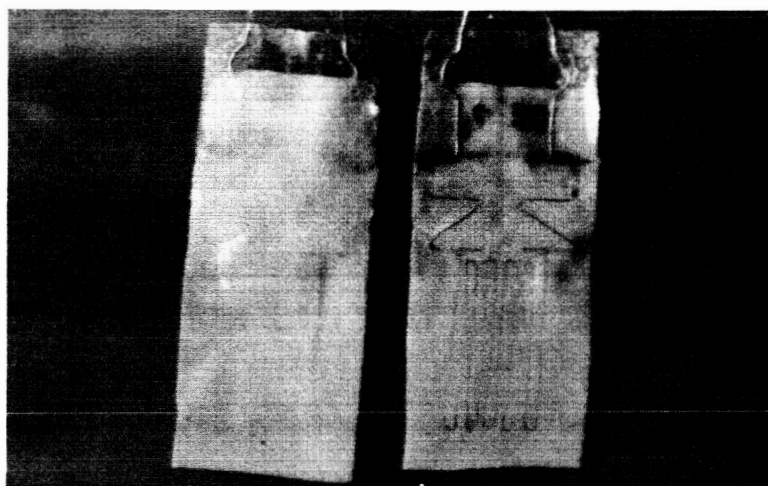
LTV Vought Aeronautics Division, developed techniques for the installation and use of commercial strain gages capable of measuring large strains at cryogenic temperatures. Strains in the order of 12%, 5% and 3% at -105°F, -320°F and -423°F respectively, have been measured on sheet type specimens.

These techniques involved use of a silicone rubber composition, developed curing cycles, special gage handling procedures and applicable bonding methods.

The shear strengths attained in the adhesive increased significantly at -100°F and formed a very satisfactory strain transmitting bond. These techniques were calibrated by direct comparison with mechanical extensometer data with an appropriate adjustment in gage factor being recorded.

An extremely low percentage of gage failures occurred using these techniques and it appears that these gages are even more satisfactory on biaxial specimens than on uniaxial specimens. This is due to the reduction of the transverse strain field state in biaxial tests.

A front and back view of a typically prepared wire gage is shown in the following photograph.



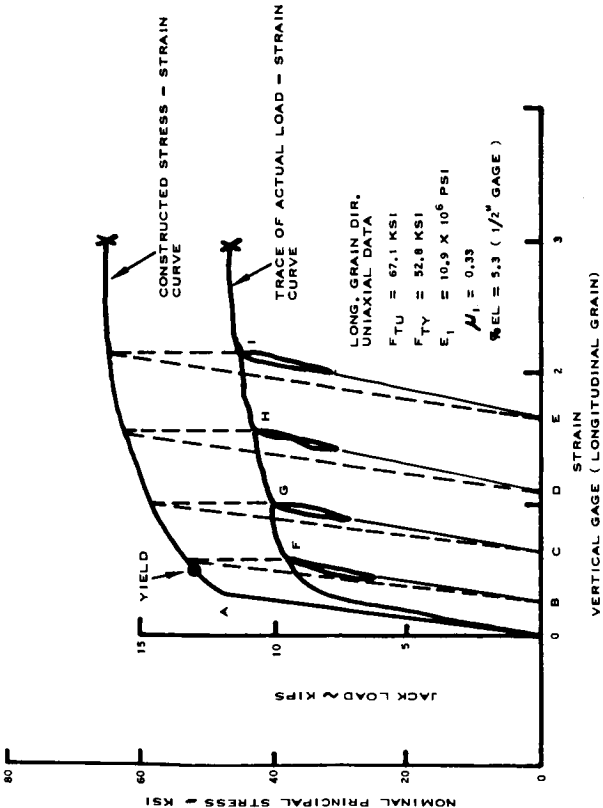
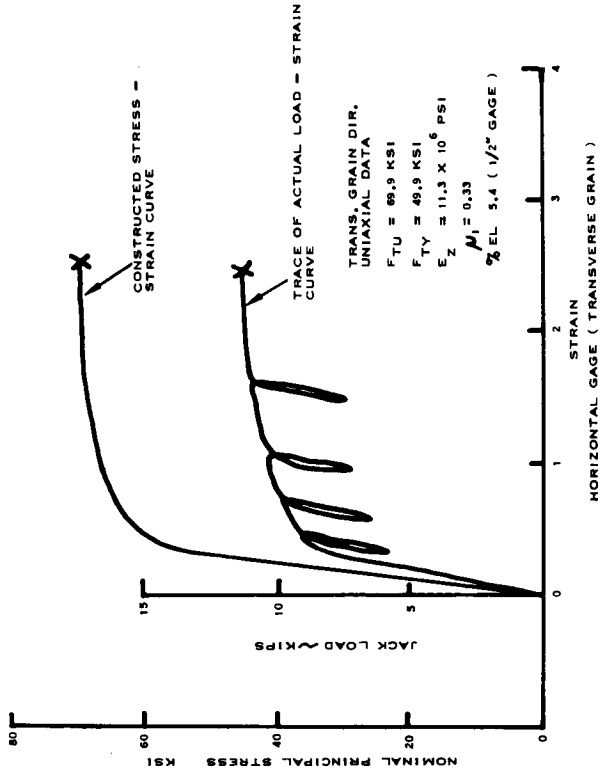
The basic steps in use of these types of gages at cryogenic temperatures are summarized below:

- (1) begin with a standard (wire) strain gage
- (2) remove the backing by use of solvent
- (3) clean and dry the gage filaments
- (4) apply a silicone rubber backing
- (5) cure the backing material
- (6) mount gages on the test specimen with silicone rubber adhesive
- (7) cure the applied adhesive
- (8) test the specimen at applicable cryogenic temperature (-100°F to -423°F)

APPENDIX D

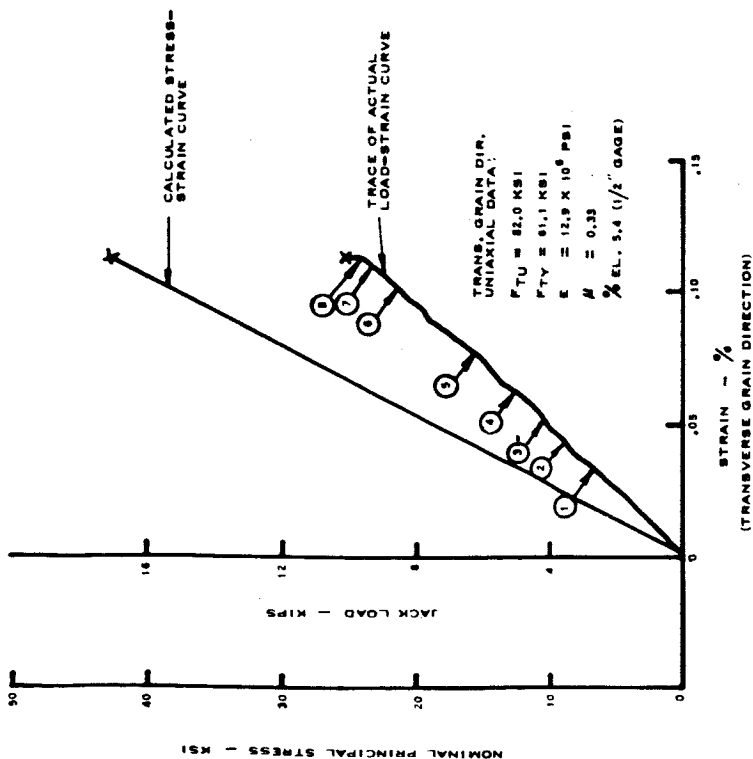
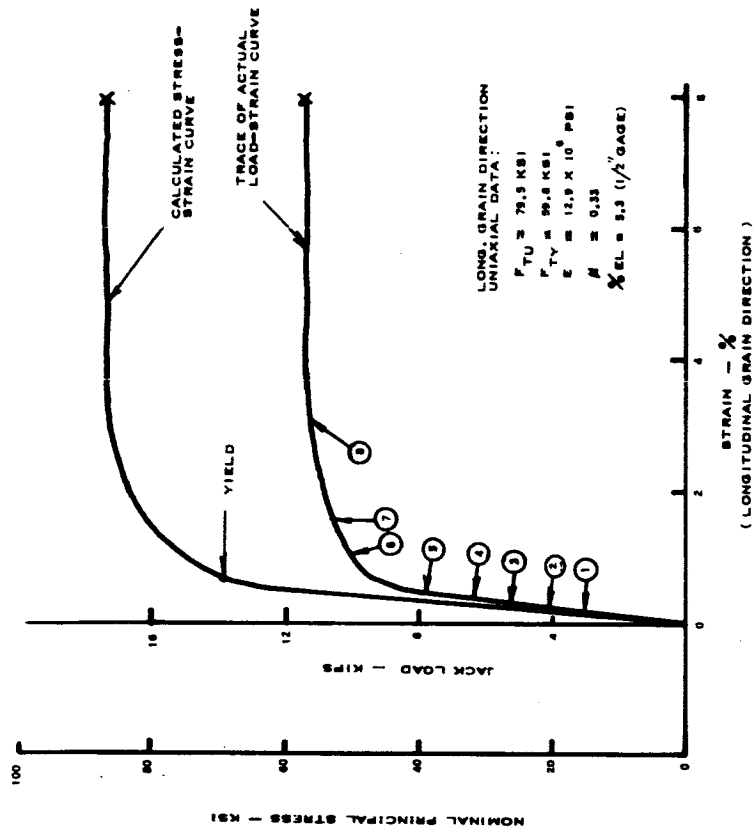
CALCULATION OF BIAXIAL STRESS-STRAIN CURVES
FROM BIAXIAL LOAD-STRAIN CURVES

Figures 45 and 46 illustrate the graphical and analytical techniques for development of a complete 2:1 and 1:1 biaxial stress-strain curve from applied biaxial load-strain curves. These techniques are illustrated in a sequential method showing how the specimen is loaded, what the resulting load-strain looks like and how to obtain the end result, the biaxial stress-strain curve. Typical uniaxial material properties are shown to compare with the obtained biaxial properties.



- PROCEDURE: (SAME FOR BOTH DIRECTIONS - ONLY LONGITUDINAL CURVE SHOWN IN DETAIL)
- STEP (1): $\sigma_1 = \frac{F}{A_0}$ USE THIS EQUATION TO CALCULATE STRESSES IN THE ELASTIC RANGE AND FROM THESE STRESS VALUES SET UP A STRESS SCALE).
- STEP (2): FROM THE GENERATED UNLOAD LOOPS - EXTEND THESE TO ZERO STRESS CONDITION (PERMANENT SET IF CARRIED TO ZERO STRESS).
- STEP (3): FROM POINTS B, C, D, E - CONSTRUCT A STRESS - STRAIN CURVE PARALLEL TO THE ORIGINAL ELASTIC MODULUS - ESTABLISHED USING EQUATION IN STEP (1) ABOVE AND STRAIN OBTAINED FROM LOAD-STRAIN CURVE)
- STEP (4): FROM POINTS F, G, H, I - CONSTRUCT A TOTAL STRAIN LINE UP OR DOWN TO INTERSECT THE POINT ON THE LONGITUDINAL STRESS-STRAIN CURVE IN THE PLASTIC RANGE)
- NOTE: STRAIN VALUES WERE OBTAINED BY USING THE LTV LONGITUDINAL STRAIN GAGE TECHNIQUES (GAGES IN THIS TEST AT -100°F WENT TO FAILURE OF THE SPECIMEN)
- STEP (5): THE INTERSECTION OF THE TWO LINES IS THE STRESS AT POINT F (IN THIS EXAMPLE, STRESS AT POINT F IS 54.0 KSI).
- STEP (6): COMPLETE CURVE BY CONNECTING ELASTIC AND PLASTIC PARTS OF THESE CURVES.
- STEP (7): DETERMINE YIELD STRENGTH (0.2% OFFSET) SHOWN BY BLACK DOT (●).
- DATA: LONGITUDINAL GRAIN DIRECTION DATA UNDER A 1:1 BIAxIAL STRESS STATE ARE:
- | | | | |
|----------------|--------|----------------------------|-----------------------|
| FTU = 65.0 KSI | E: 1:1 | 15.3 x 10 ⁶ PSI | %EL (FRACTURE) = 3.0% |
| FTY = 52.0 KSI | | %EL (MAX LOAD) = 2.1% | |

FIGURE 45 -ILLUSTRATION OF CALCULATION OF 1:1 BIAxIAL STRESS-STRAIN VALUES FROM 1:1 BIAxIAL LOAD STRAIN CURVES FOR 2219 T-81 ALUMINUM ALLOY AT -100°F



PROCEDURE:

- STEP (1) $\sigma_2 = \frac{\sigma_1 + \sigma_3}{2}$ (USE THIS EQUATION TO CALCULATE STRESSES AT THE VARIOUS TICK-MARK LOCATIONS IN THE MINIMUM STRESS DIRECTION (σ_2))
- STEP (2) $\sigma_1 = \frac{\sigma_2 + \sigma_3}{2}$ (USE THIS EQUATION TO CALCULATE STRESSES AT THE VARIOUS TICK-MARK LOCATIONS IN THE MAXIMUM STRESS DIRECTION (σ_1)). THE EQUATION FOR THE CALCULATION OF THE STRESS VALUES OF THE MINIMUM STRESS DIRECTION IS THAT REQUIRED TO OBTAIN A 2:1 STRESS STATE)
- STEP (3) FROM CALCULATIONS MADE IN STEPS (1) AND (2) - PLOT THE STRESSES OBTAINED AGAINST STRAIN FOR THE PARTICULAR DIRECTION INVOLVED.
- STEP (4) NOTE THAT AT THE MARKS THE INCREASE IN STRESS IN THE MAXIMUM PRINCIPAL STRESS DIRECTION IS APPROXIMATELY ZERO - SO FROM THE MARKS IN THE MINIMUM STRESS DIRECTION, THE INCREASE IN STRESS MAINTAINED (1100 MICRO-INCHES OR 0.0113 IN/IN) IS MAINTAINED TO FAILURE. FURTHERMORE, IT MAY BE NOTED THAT AS THIS STRAIN VALUE IS MAINTAINED AN INCREASE IN JACK LOAD IS REQUIRED TO MAINTAIN IT AS THE MATERIAL LOWS PLASTICALLY TO FAILURE IN THE (σ_1) DIRECTION
- STEP (5) COMPLETE STRESS-STRAIN CURVE PLOT

DATA: BIAxIAL DATA - MINIMUM STRESS DIRECTION $F_{TU} = 49.0 \text{ KSI}$ $E' = 38.0 \times 10^6 \text{ PSI}$ $\%EL = 0.113 \%$ $F_{TY} = N/A$

BIAxIAL DATA - MAXIMUM STRESS DIRECTION $F_{TU} = 86.0 \text{ KSI}$ $E' = 13.1 \times 10^6 \text{ PSI}$ $F_{TY} = 70.0 \text{ KSI}$ $\%EL = 5.0 \%$

NOTES: STRESS VALUES WERE OBTAINED BY USING THE LTV DEVELOPED LOW TEMPERATURE-STRAIN GAGE TECHNIQUES IN THIS TEST AT -320°F WENT TO FAILURE OF THE SPECIMEN IN 9 MIN MAXIMUM STRESS DIRECTION) E' = EFFECTIVE MODULUS (STRESS/STRAIN) FOR THE APPLICABLE DIRECTION

FIGURE 46 - ILLUSTRATION OF CALCULATION OF 2:1 BIAxIAL STRESS-STRAIN VALUES FROM 2:1 BIAxIAL LOAD STRAIN CURVES FOR 2219 T-81 ALUMINUM ALLOY AT -320°F

APPENDIX E
COMPUTER CALCULATION OF
PLANE-STRAIN FRACTURE TOUGHNESS PARAMETERS

The computations required to obtain the plane-strain fracture toughness parameter, K_{IC} , are tedious in nature and involve the evaluation of an elliptic integral; although the actual number of calculations per parameter is not large. The task of obtaining K_{IC} values for a large number of specimens is quite laborious, and introduces many chances for computational errors. A computer program has been written to eliminate most of the hand computation and reduce the possibilities for error.

The computer program solves the following equations:

$$\phi = \int_0^{\pi/2} \sqrt{1 - \left(\frac{b^2 - a^2}{b^2}\right) \sin^2 \theta} d\theta \quad (1)$$

$$K_{IC} = \sqrt{\frac{1.2 \pi (\sigma_{MAX.})^2 b}{\phi^2 - 0.212 \left(\frac{\sigma_{MAX.}}{\sigma_y}\right)^2}} \quad (2)$$

Where: $\sigma_{MAX.}$ = Gross Section Stress at pop-in, $\frac{LB}{IN^2}$

σ_y = Yield Stress, $\frac{LB}{IN^2}$

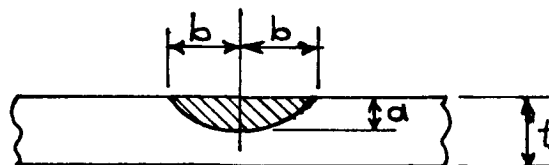
a = Crack Depth, IN.

b = One-Half Crack Length, IN.

ϕ = An Elliptic Integral Function
(Dependent on "a" and "b")

K_{IC} = A fracture toughness parameter or stress intensity factor (plane strain conditions) which characterizes the stress environment at the crack tip at the instant of crack instability that provides a means of assessing relative material behavior and component performances.

The crack geometry is:



SPECIMEN CROSS-SECTION

To solve equation (1), use the standard elliptic integral form listed in most math handbooks:

$$E = \int_0^{\pi/2} \sqrt{1 - K^2 \sin^2 x} dx \quad (3)$$

Let $K^2 = \left(\frac{b^2 - a^2}{b^2}\right)$. Then, values of $E(\phi)$ may be obtained for different values of "K" from the elliptic integral table.

The computer Fortran program listed on page 98 performs all of the above operations. Two data tape inputs are required. Data Tape 1 contains the required elliptic integral table data, and is shown on page 99 as it should be input to the computer (for all problems). Data Tape 2 input for four sample K_{IC} calculations is shown on Page 100 as it should be input to the computer.

The computer output for the sample problems, including the desired K_{IC} values, is shown on Page 101.

K_{IC} FRACTURE TOUGHNESS PARAMETER
FORTRAN PROGRAM

```
6 format (//42ha;is;the;crack;depth.;b;is;the;crack;width)
1 format (10f7.0)
2 format (i3)
3 format (2f10.0,2f6.0)
4 format (f5.3,f6.3,f8.2,f9.4,f9.0)
5 format (3x,1ha,5x,1hb,4x,5htheta,5x,3hphi,6x,1hk)
dimension e(80)
read 1, (e(k), K=26,80)
pause 1111
read 2,n
punch 5
do 20 j=1,n
read 3,syld,smax,a,b
ak=sqrtf(1.-a'a/(b'b))
xcos=a/b
tang=ak/xcos
theta=atanf(tang)
theta=theta'57.3
ithet=theta
athet=ithet
e1=e(ithet)
e2=e(ithet+1)
ee=e1-(theta-athet)'(e1-e2)
rat=smax/syld
const=sqrtf(3.77'smax'smax'b/(ee'ee-.212'rat'rat))
punch 4,a,b,theta,ee,const
20 continue
punch 6
end
end
```

K_{IC} - ELLIPTIC INTEGRAL DATA
DATA TAPE 1

1.4924/1.4864/1.4803/1.4740/1.4675/1.4608/1.4539/1.4469/1.4397/1.4323/
1.4248/1.4171/1.4092/1.4013/1.3931/1.3849/1.3765/1.3680/1.3594/1.3506/
1.3418/1.3329/1.3238/1.3147/1.3055/1.2963/1.2870/1.2776/1.2681/1.2587/
1.2492/1.2397/1.2301/1.2206/1.2111/1.2015/1.1920/1.1826/1.1732/1.1638/
1.1545/1.1453/1.1362/1.1272/1.1184/1.1096/1.1011/1.0927/1.0844/1.0764/
1.0686/1.0611/1.0538/1.0468/1.0401/

K_{IC} INPUT DATA
DATA TAPE 2

4/ ← (NO. OF SPECIMEN CALCULATIONS)

50400./56300./	.035/	.09/	UCR1-2
160200./172600./	.035/	.07/	UCR5-1
172100./186000./	.038/	.085/	UCR5-2
159000./168500./	.03/	.035/	UCR7-2

↑
F_{Ty}
OR
σ_y

↑
F_{Tmax.}
OR
σ_{max.}

↑
CRACK
DEPTH

↑
1/2 CRACK
LENGTH

K_{IC} OUTPUT DATA

$K_{IC} - \text{PSI} \sqrt{\text{IN.}}$

a	b	theta	phi	k	
.035	.090	67.11	1.1442	32085.	UCR1-2
.035	.070	60.00	1.2110	80256.	UCR5-1
.038	.085	63.44	1.1783	98573.	UCR5-2
.030	.035	31.00	1.4607	44454.	UCR7-2

a is the crack depth. b is the crack width ($\frac{1}{2}$ CRACK LENGTH)

APPENDIX F
COMPUTER CALCULATION OF THE
LUDWIK STRAIN HARDENING COEFFICIENT

A computer program has been written that calculates Ludwik strain hardening coefficients, n , directly from given material stress-strain curves. This eliminates the tedious hand calculations and considerably minimizes the chances for error.

The Fortran program is shown on page 103 as it should be input to the computer. This program performs the following operations:

- (1) Calculates true stress and true strain values for four points on the nominal, or engineering, stress-strain diagram for a particular material, using the equations below:

$$\sigma_T = \sigma_N (1 + \epsilon_N)$$

$$\epsilon_T = \ln (1 + \epsilon_N)$$

Where:

σ_T = true stress, psi

ϵ_T = true strain, in/in

σ_N = nominal stress, psi

ϵ_N = nominal strain, in/in

- (2) "Plots" (in effect) the four true stress and true strain points using a logarithm ordinate and abscissa. A "best-fit" straight line is drawn through these points, using the method of least squares.
- (3) Determines the geometric slope of the straight line, which is Ludwik's strain hardening coefficient, n .

The required computer input data for four sample calculations, Data Tape 1, is shown (in the proper input form) on Page 104. The computer output for the sample problems, including the Ludwik coefficients, n , is shown on Page 105.

" n " = Ludwik strain hardening coefficient as used in the equation true stress is a function of plastic strain raised to the " n " power. The " n " coefficient expresses the shape or is the power exponent of the above equation that relates true stress to true strain in the plastic zone. A large value of " n " indicates that a material has significant ability to resist deformation by strain hardening as load is increased.

LUDWIK STRAIN-HARDENING COEFFICIENT
FORTRAN PROGRAM

```
1 format(2i5)
2 format(2f10.0)
4 format(46h;specimen;;;;stress;;;;strain;;;;hard.;coeff.;;)
5 format(i5)
6 format(9x,f10.0,f10.5)
7 format(32x,f8.5)
  dimension x(4), y(4), sts(4), stn(4)
  punch 4
  read 1,j,k
  do 50 i=j,k
  punch 5,i
  read 2,xload,area
  do 20 m=1,4
  read 2,x(m),y(m)
  sts(m)=(1.+x(m))*y(m)*xload/area
  stn(m)=logf(1.+x(m))
  punch 6, sts(m),stn(m)
  sts(m)=logf(sts(m))
  stn(m)=logf(stn(m))
20 continue
  acoe=stn(1)+stn(2)+stn(3)+stn(4)
  bcoe=stn(1)*stn(1)+stn(2)*stn(2)+stn(3)*stn(3)+stn(4)*stn(4)
  suma=sts(1)+sts(2)+sts(3)+sts(4)
  sumb=sts(1)*stn(1)+sts(2)*stn(2)+sts(3)*stn(3)+sts(4)*stn(4)
  ccoe=acoe
  fact=-4./ccoe
  ccoe=fact*ccoe
  bcoe=fact*bcoe
  sumb=fact*sumb
  b=(suma+sumb)/(acoe+bcoe)
  punch 7,b
50 continue
end
end
```

INPUT DATA
DATA TAPE 1

1/4/ FIRST SPECIMEN NUMBER
8000./0305/ LAST SPECIMEN NUMBER
LOAD SCALE RANGE OF LOAD-STRAIN CURVE
SPECIMEN CROSS SECTIONAL AREA - IN.²
PER CENT OF SCALE RANGE (LOAD)

STRAIN .0105/.66/
.0130/.683/
.0190/.706/
.0290/.71/
8000./0302/
.0103/.67/
.0140/.694/
.0195/.711/
.030/.724/
8000./0296/
.0105/.705/
.0135/.723/
.0195/.742/
.0315/.756/
8000./0294/
.0104/.70/
.0134/.731/
.0204/.751/
.0404/.761/

OUTPUT DATA

specimen	stress	strain	hard. coeff.
1	174932.	.01044	
	181476.	.01291	
	188698.	.01882	
	191630.	.02858	
			.08865
2	179311.	.01024	
	186414.	.01390	
	192017.	.01931	
	197541.	.02955	
			.09020
3	192541.	.01044	
	198043.	.01340	
	204451.	.01931	
	210760.	.03101	
			.08211
4	192457.	.01034	
	201576.	.01331	
	208522.	.02019	
	215440.	.03960	
			.07878

APPENDIX G

UNIAXIAL STRESS-STRAIN CURVES

Figures 47 through 58 illustrate typical uniaxial stress-strain curves for the program materials. Individual figures illustrate the effects of test temperature and grain direction on strength, modulus and percent elongation. The curves in this appendix include both welded and unwelded material conditions.

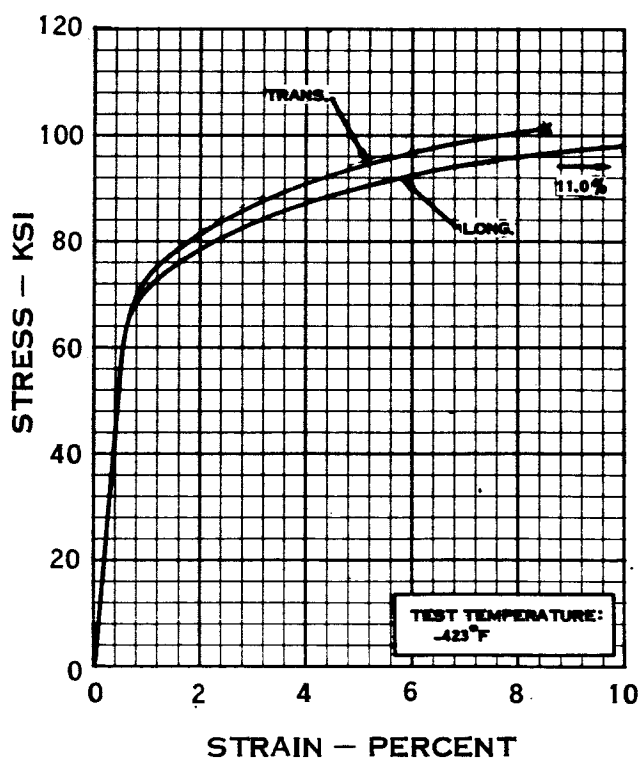
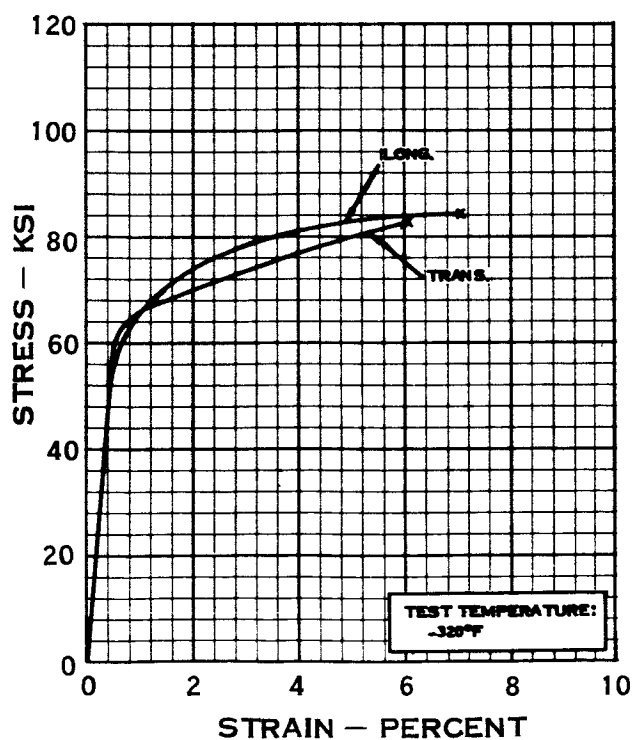
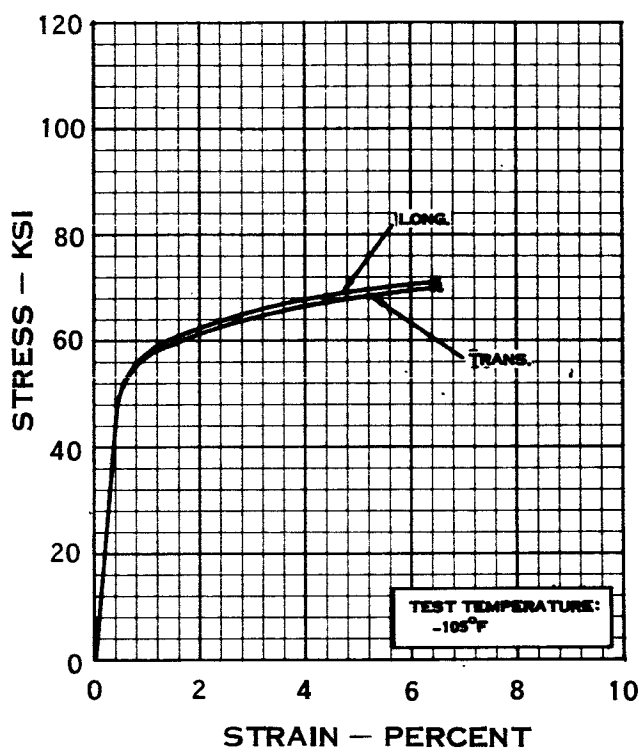
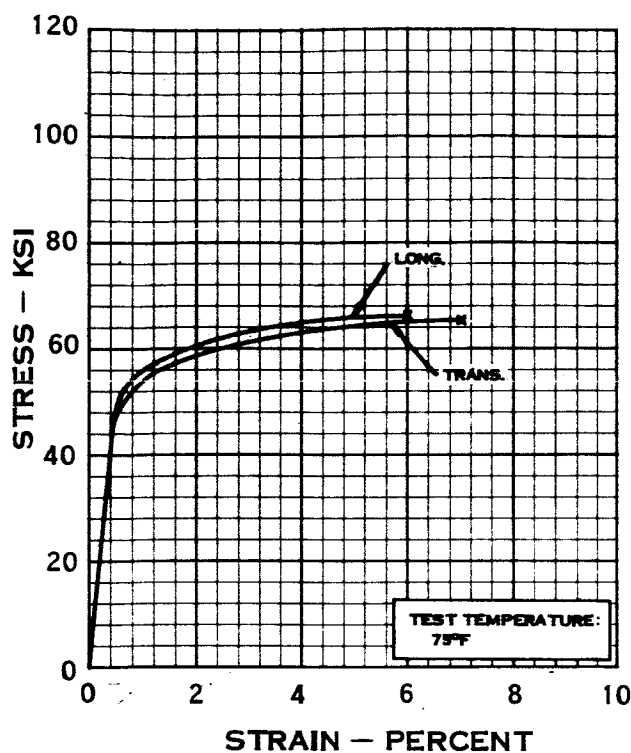


FIGURE 47 — TYPICAL 2219-T87 ALUMINUM ALLOY UNIAXIAL STRESS-STRAIN CURVES

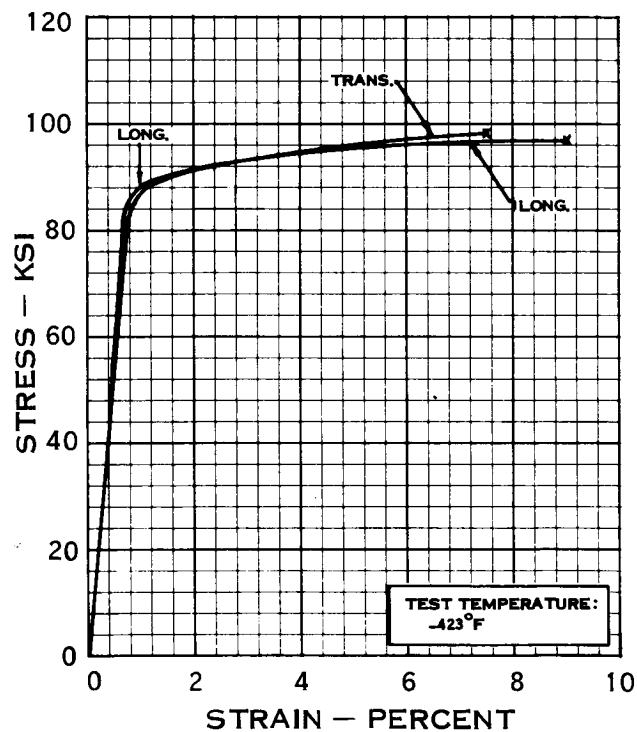
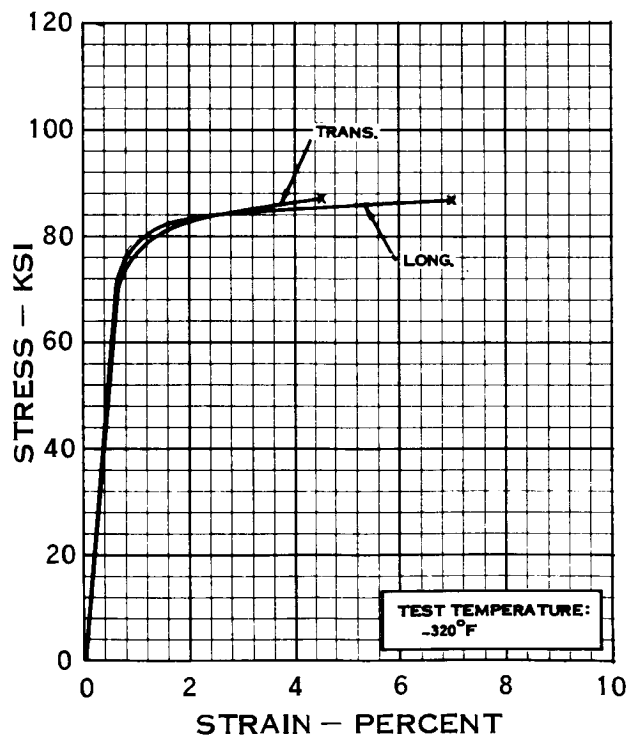
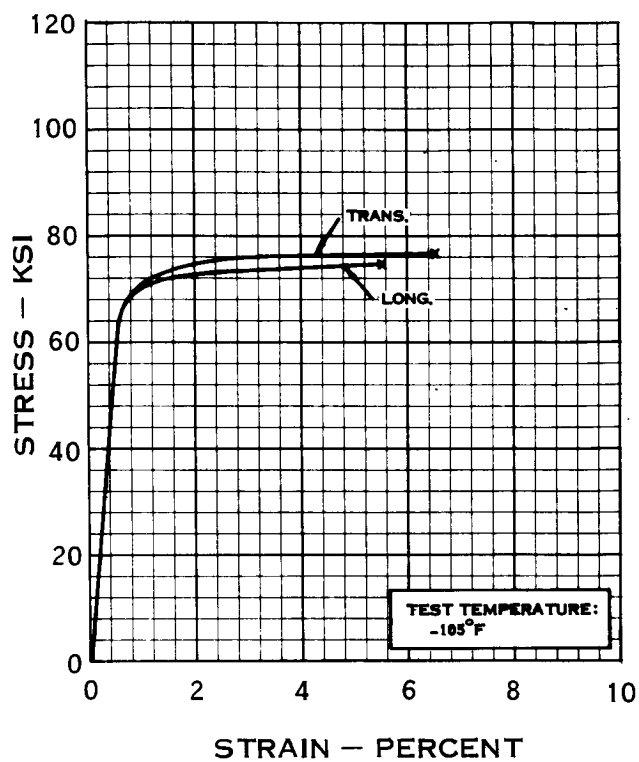
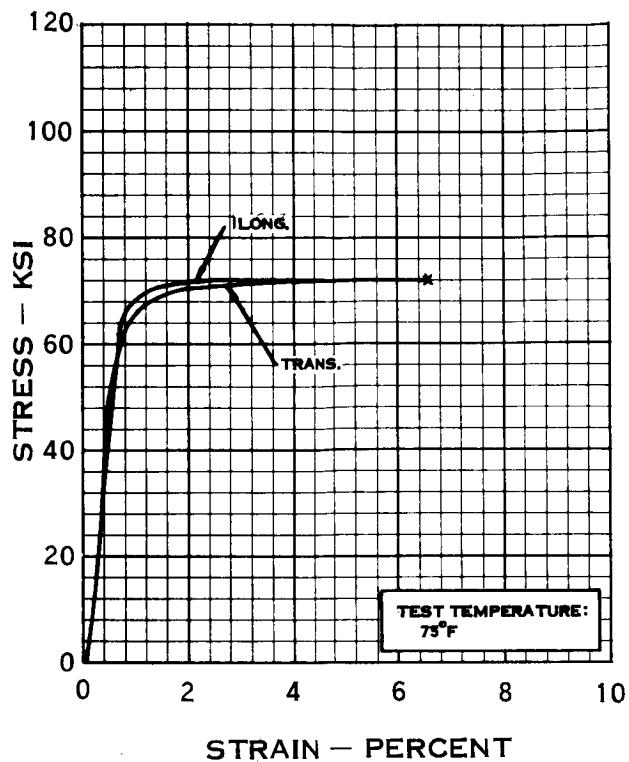


FIGURE 48 - TYPICAL 2014-T6 ALUMINUM ALLOY UNIAXIAL STRESS - STRAIN CURVES

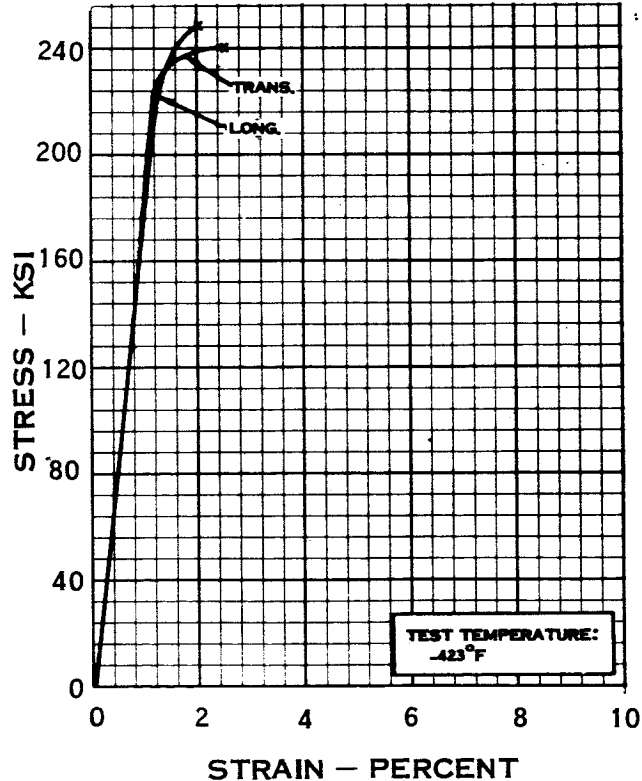
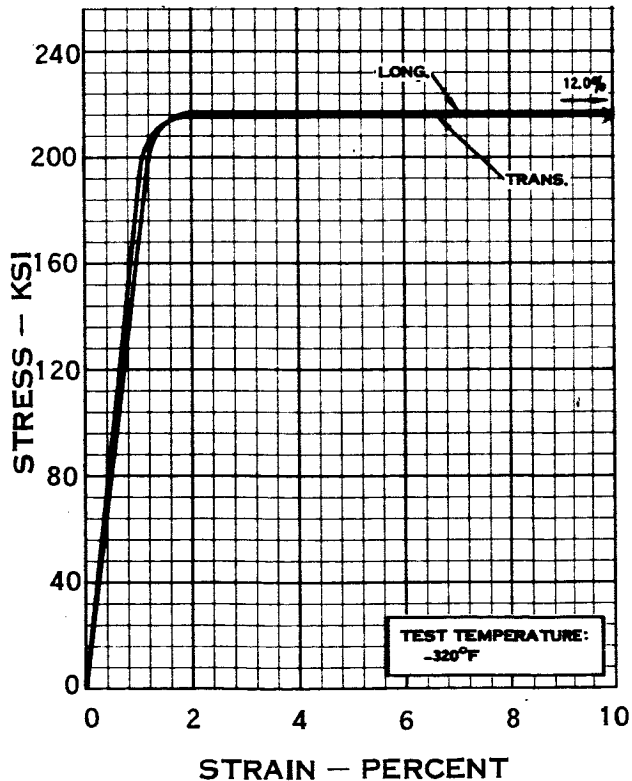
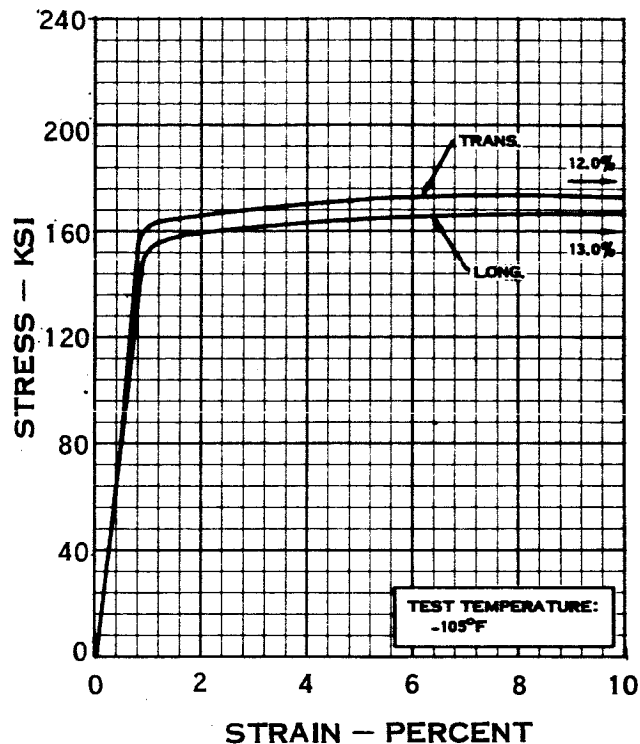
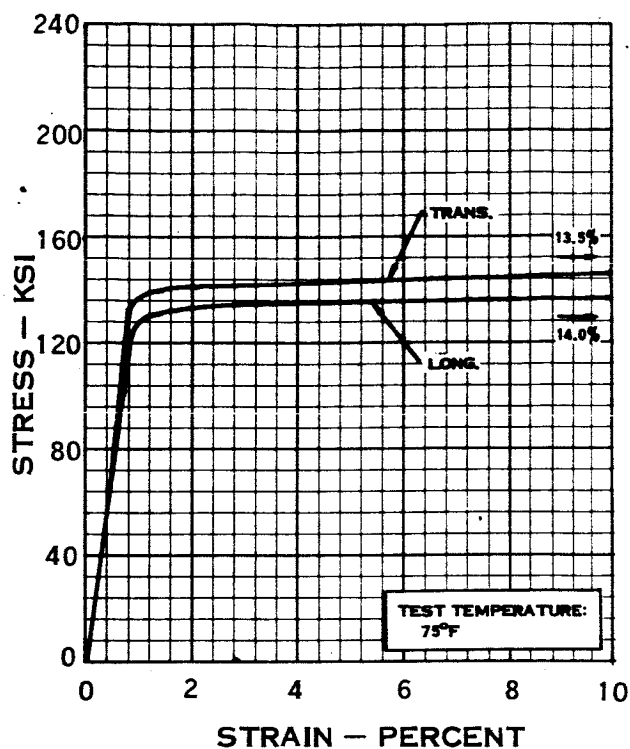


FIGURE 49 - TYPICAL 5Al-2.5Sn TITANIUM ALLOY (ANNEALED)
UNIAXIAL STRESS - STRAIN CURVES

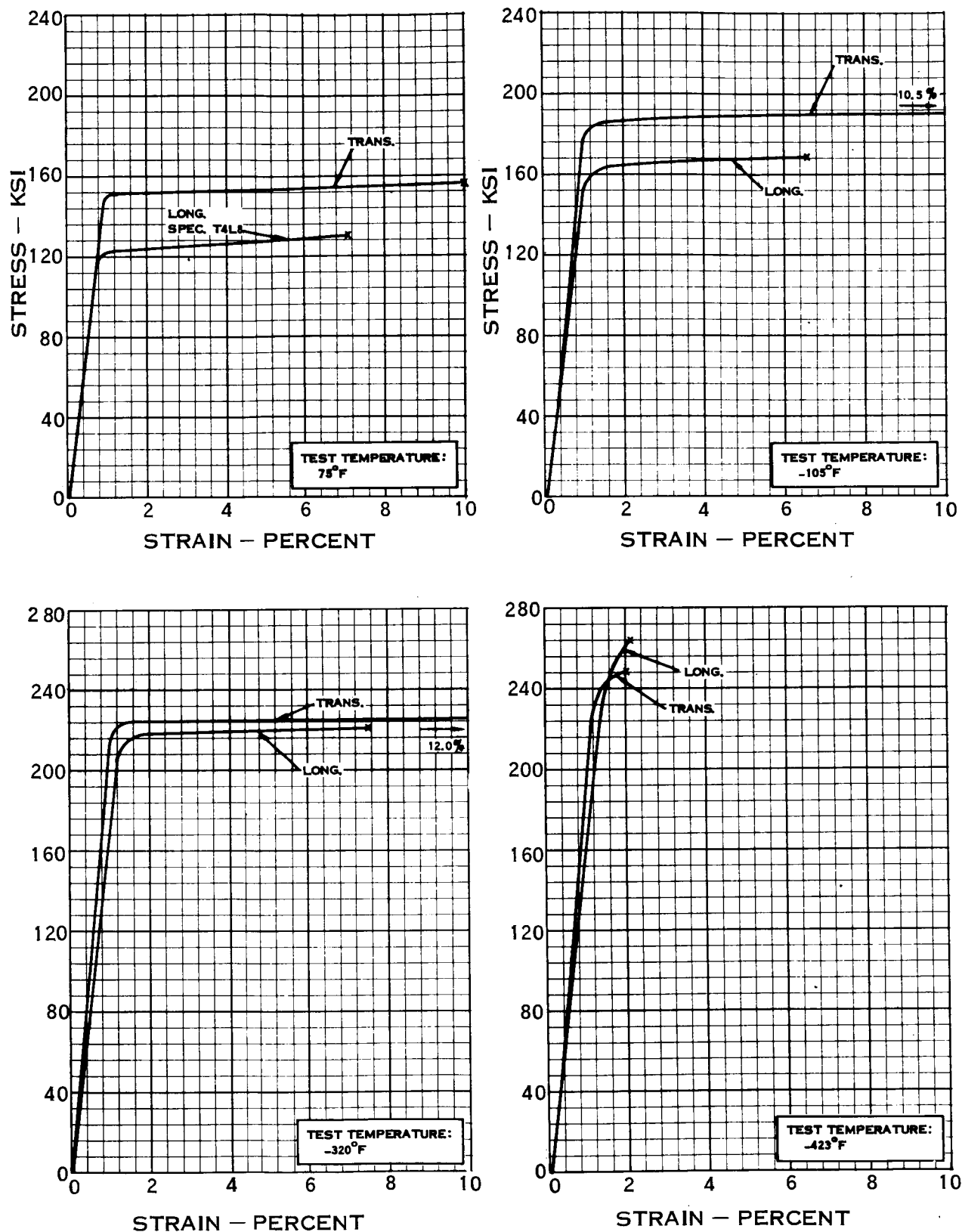


FIGURE 50 - TYPICAL 6Al-4V TITANIUM ALLOY (ELI, ANNEALED)
UNIAXIAL STRESS - STRAIN CURVES

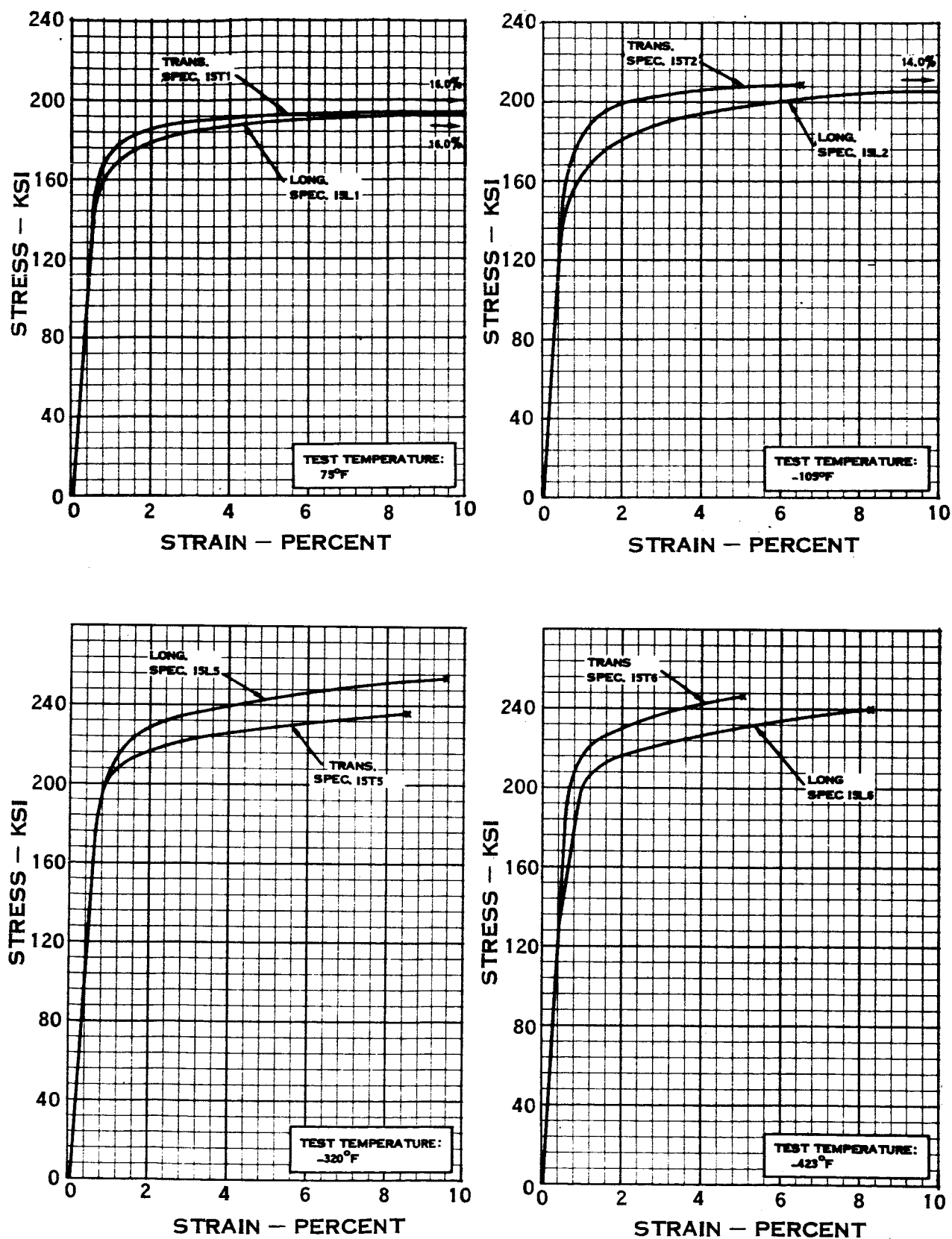


FIGURE 51 - TYPICAL INCONEL 718 UNIAXIAL STRESS - STRAIN CURVES

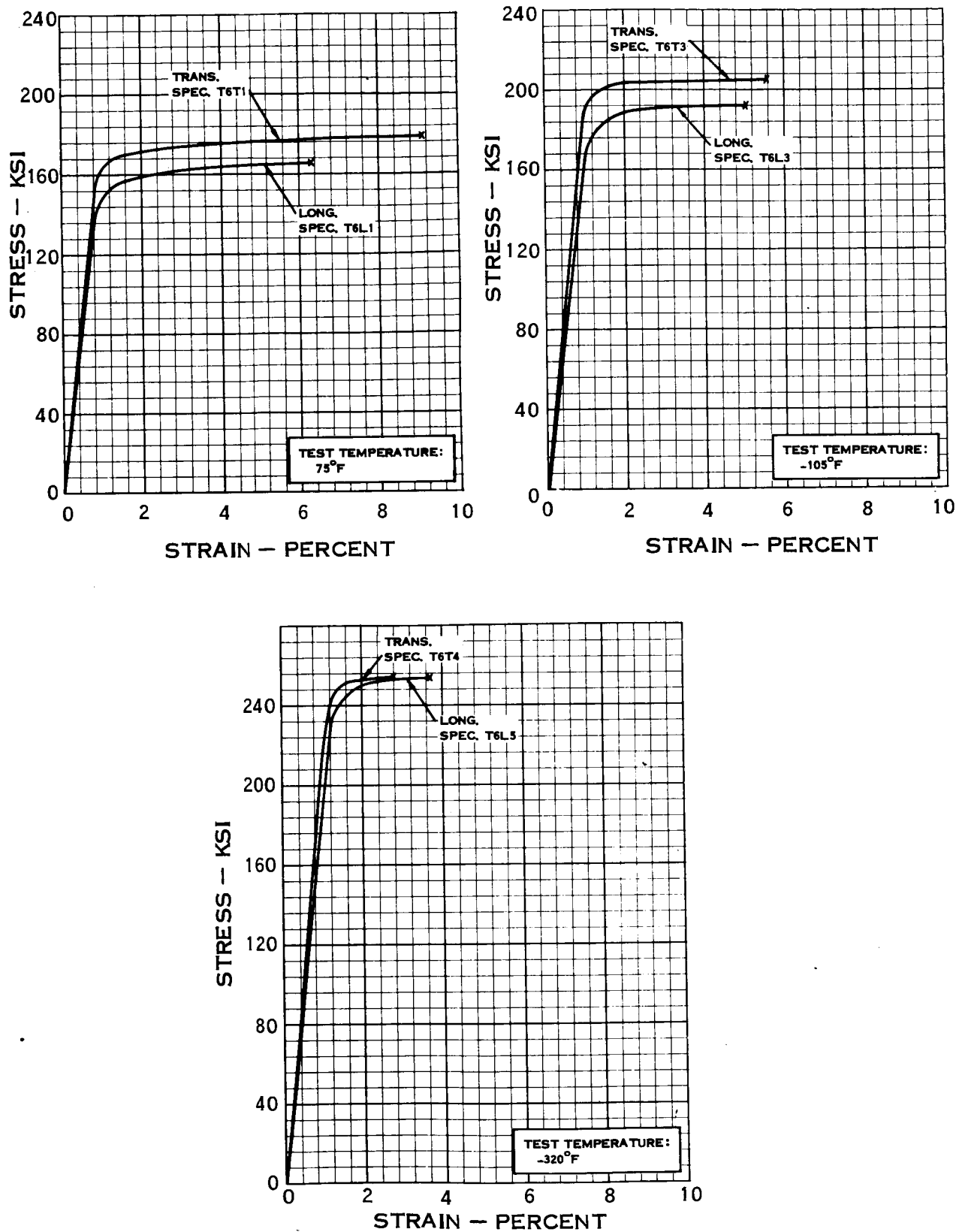


FIGURE 52 — 6Al-4V TITANIUM ALLOY (STA) UNIAXIAL STRESS — STRAIN CURVES

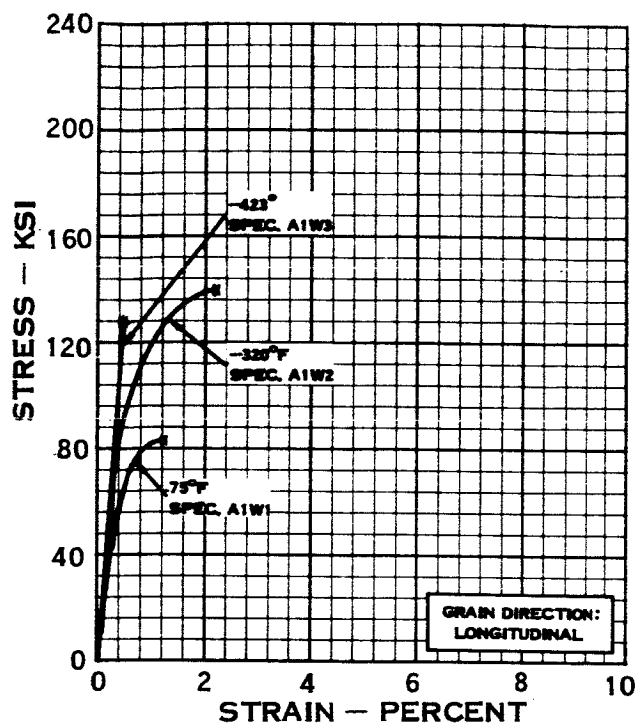


FIGURE 53 TYPICAL 2219-T87
ALUMINUM ALLOY WELDED
UNIAXIAL STRESS-STRAIN
CURVES

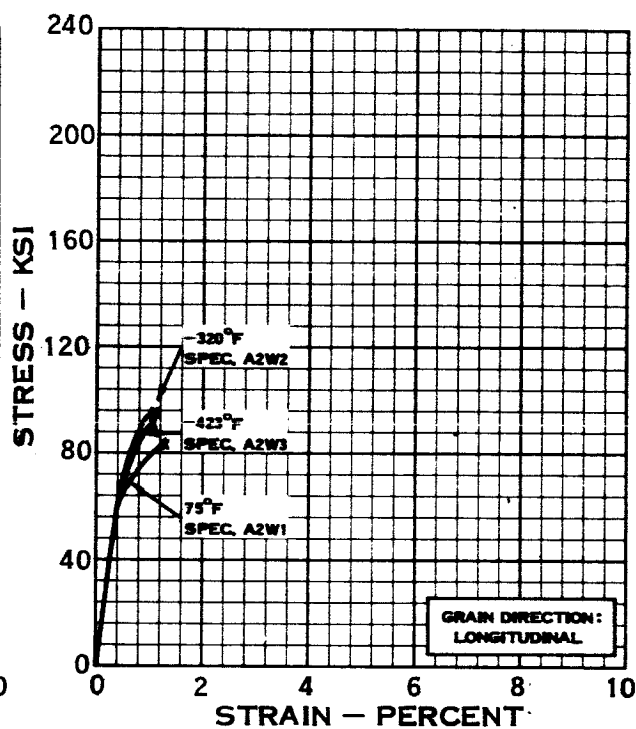


FIGURE 54 TYPICAL 2014-T6
ALUMINUM ALLOY WELDED
UNIAXIAL STRESS-STRAIN
CURVES

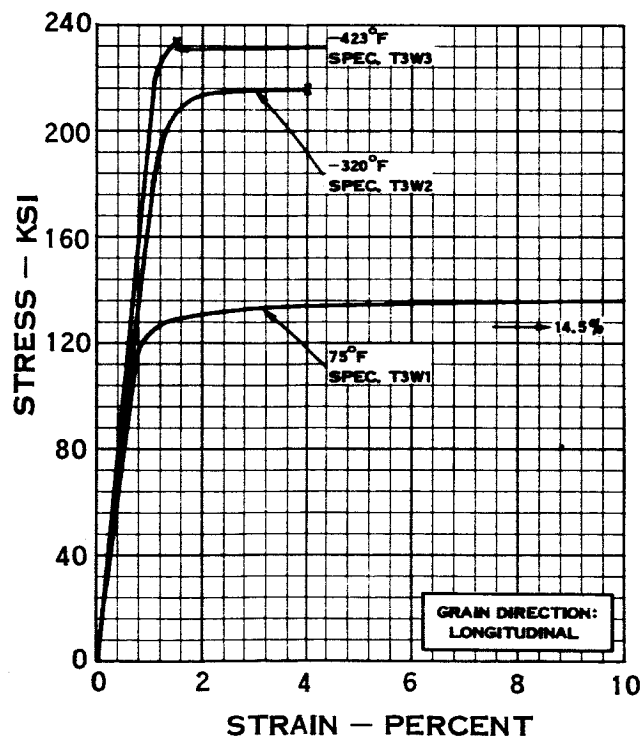


FIGURE 55 -TYPICAL 5 Al-2.5Sn TITANIUM ALLOY (ANNEALED) WELDED
UNIAXIAL STRESS-STRAIN CURVES

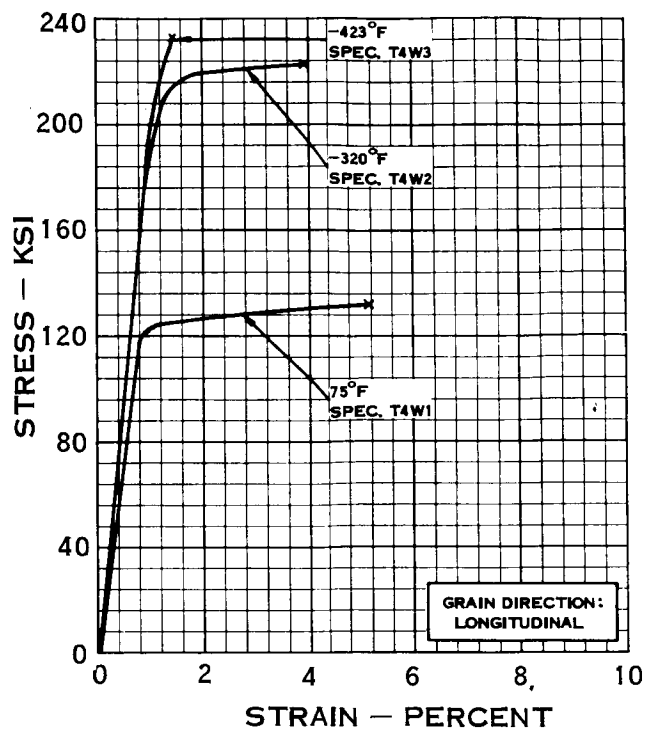


FIGURE 56 TYPICAL 6 AL-4V
TITANIUM ALLOY (ELI, ANNEALED)
WELDED UNIAXIAL STRESS-
STRAIN CURVE

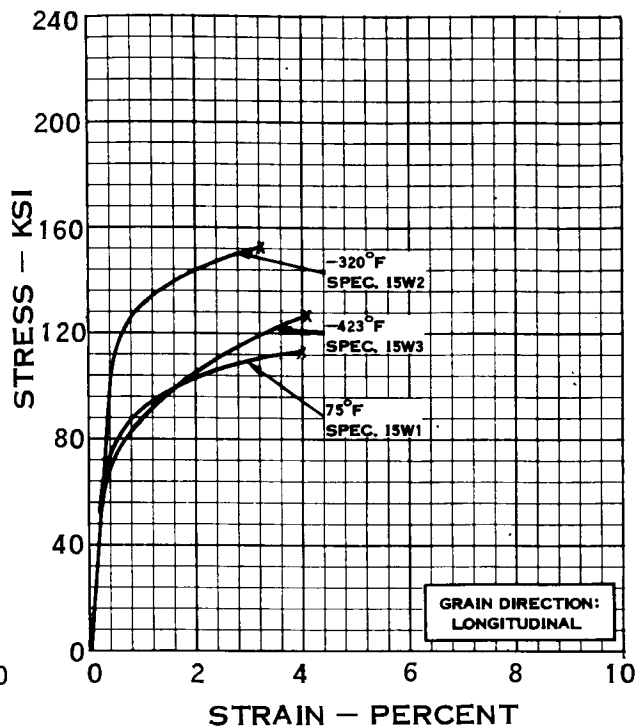


FIGURE 57 TYPICAL INCONEL 718
WELDED UNIAXIAL STRESS-
STRAIN CURVES

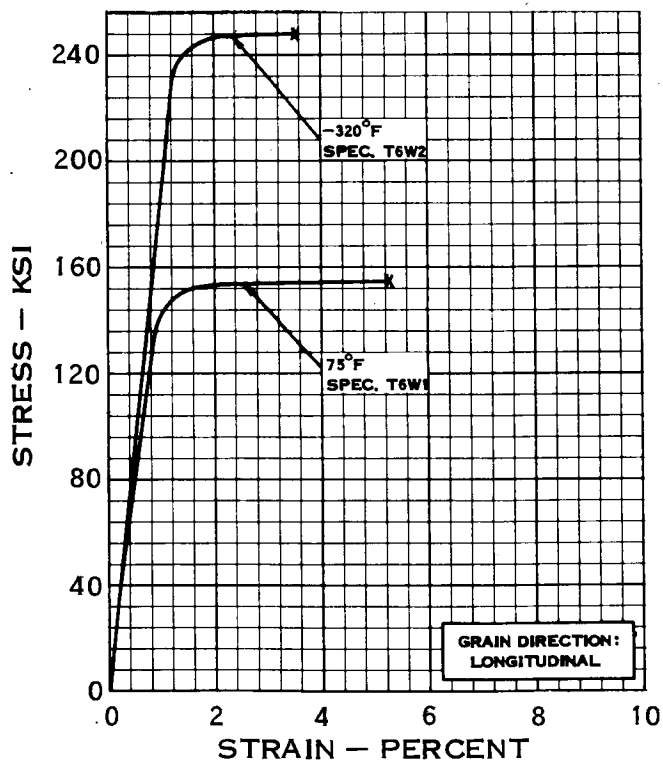


FIGURE 58 TYPICAL 6 AL-4V TITANIUM ALLOY (STA) WELDED
UNIAXIAL STRESS-STRAIN CURVES

APPENDIX H

BIAXIAL STRESS-STRAIN CURVES

Figures 59 through 76 illustrate typical 1:1 and 2:1 biaxial stress-strain curves for the program materials. Individual figures show the effects of test temperatures on five material properties in both the unwelded and welded conditions.

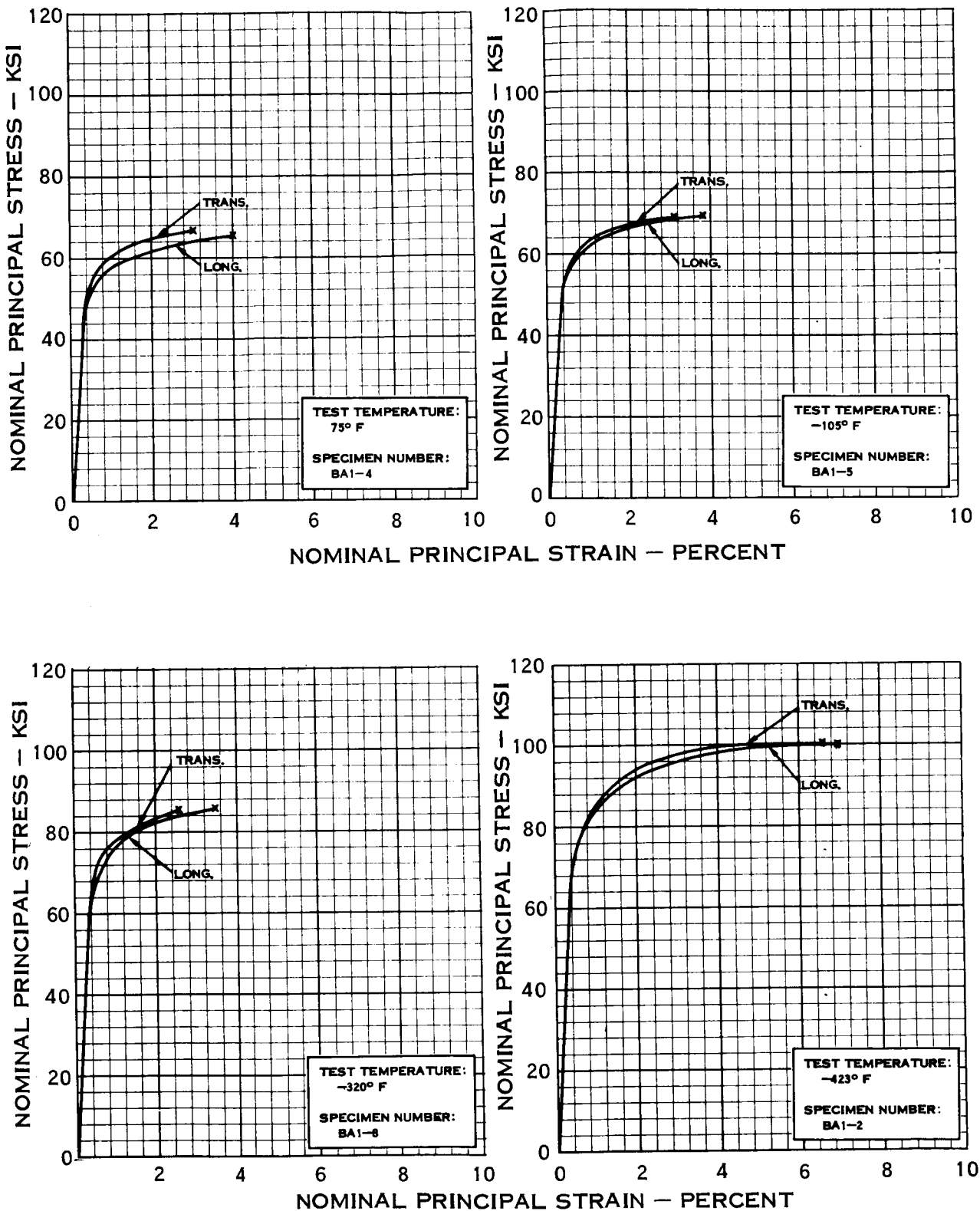


FIGURE 59 — TYPICAL 2219-T87 ALUMINUM ALLOY 1:1 BIAxIAL STRESS — STRAIN CURVES

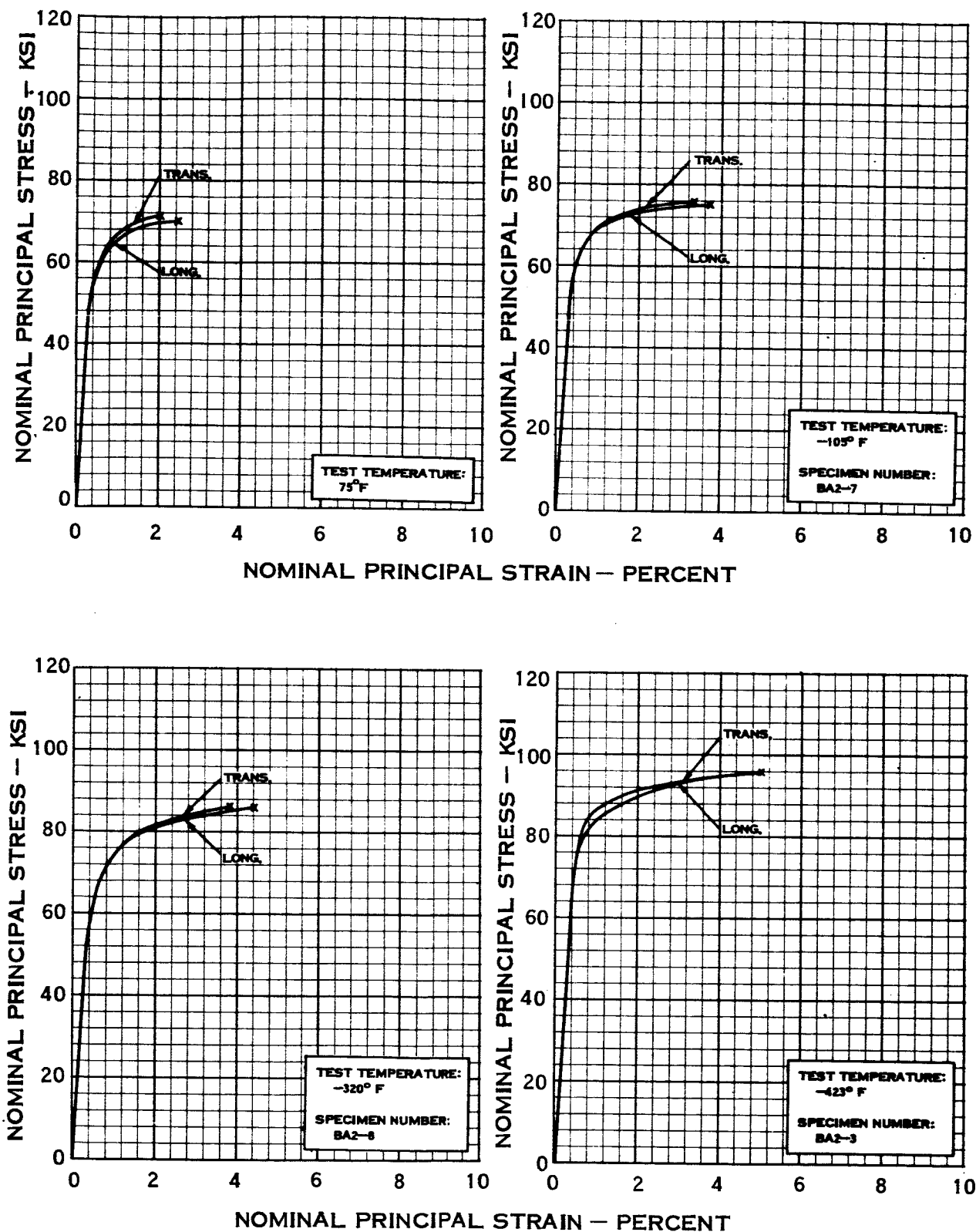


FIGURE 60 —TYPICAL 2014-T6 ALUMINUM ALLOY 1:1 BIAxIAL STRESS-STRAIN CURVES

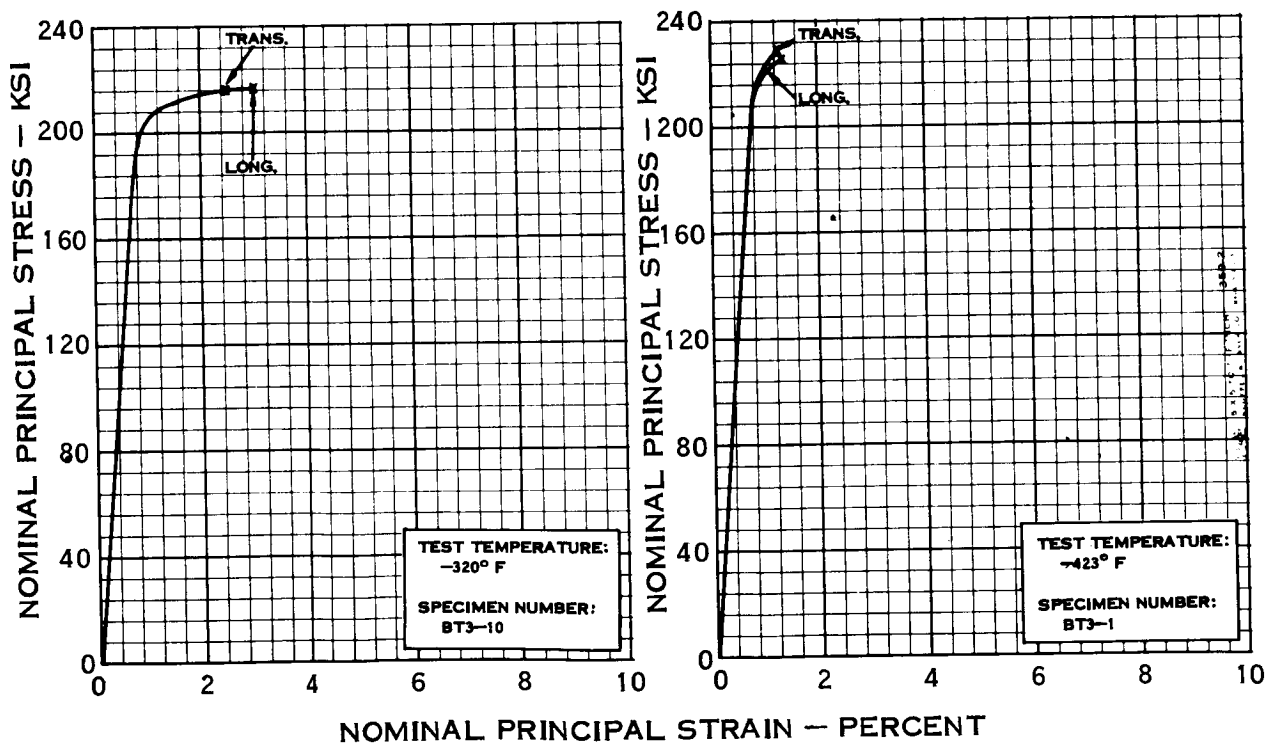
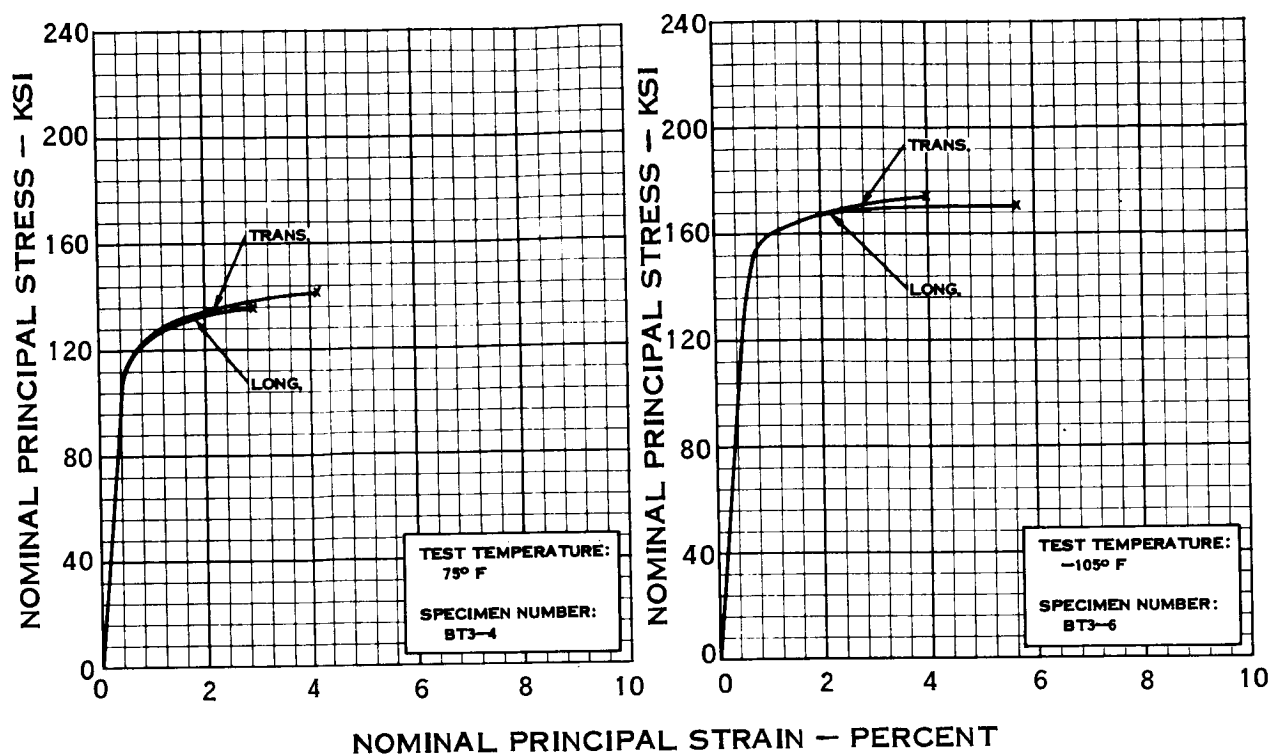


FIGURE 61 —TYPICAL 5 Al — 2.5 Sn TITANIUM ALLOY (ANNEALED)
1:1 BIAxIAL STRESS-STRAIN CURVES

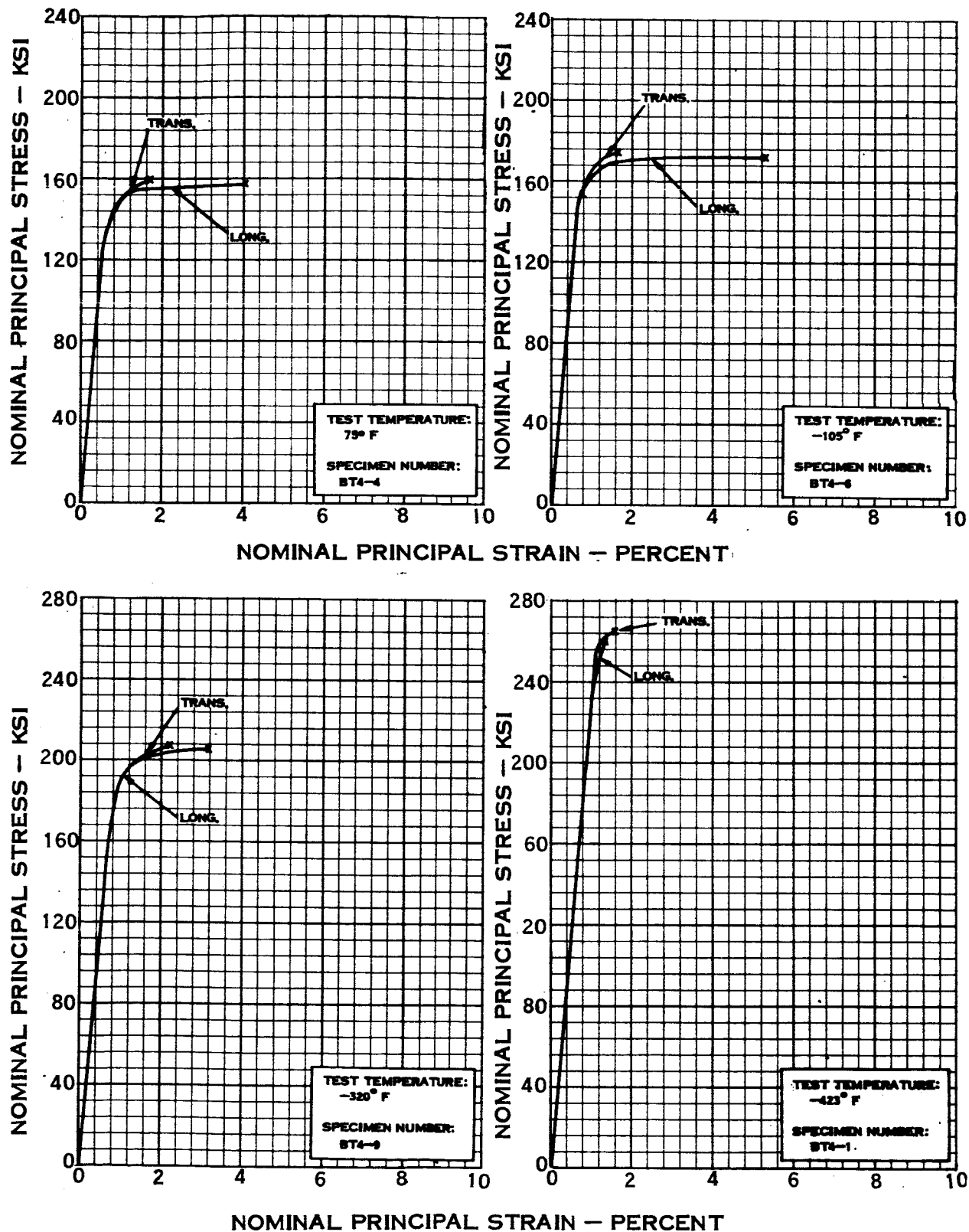


FIGURE 62 —TYPICAL 6 AL — 4 V TITANIUM ALLOY (ELI, ANNEALED)
1:1 BIAXIAL STRESS-STRAIN CURVES

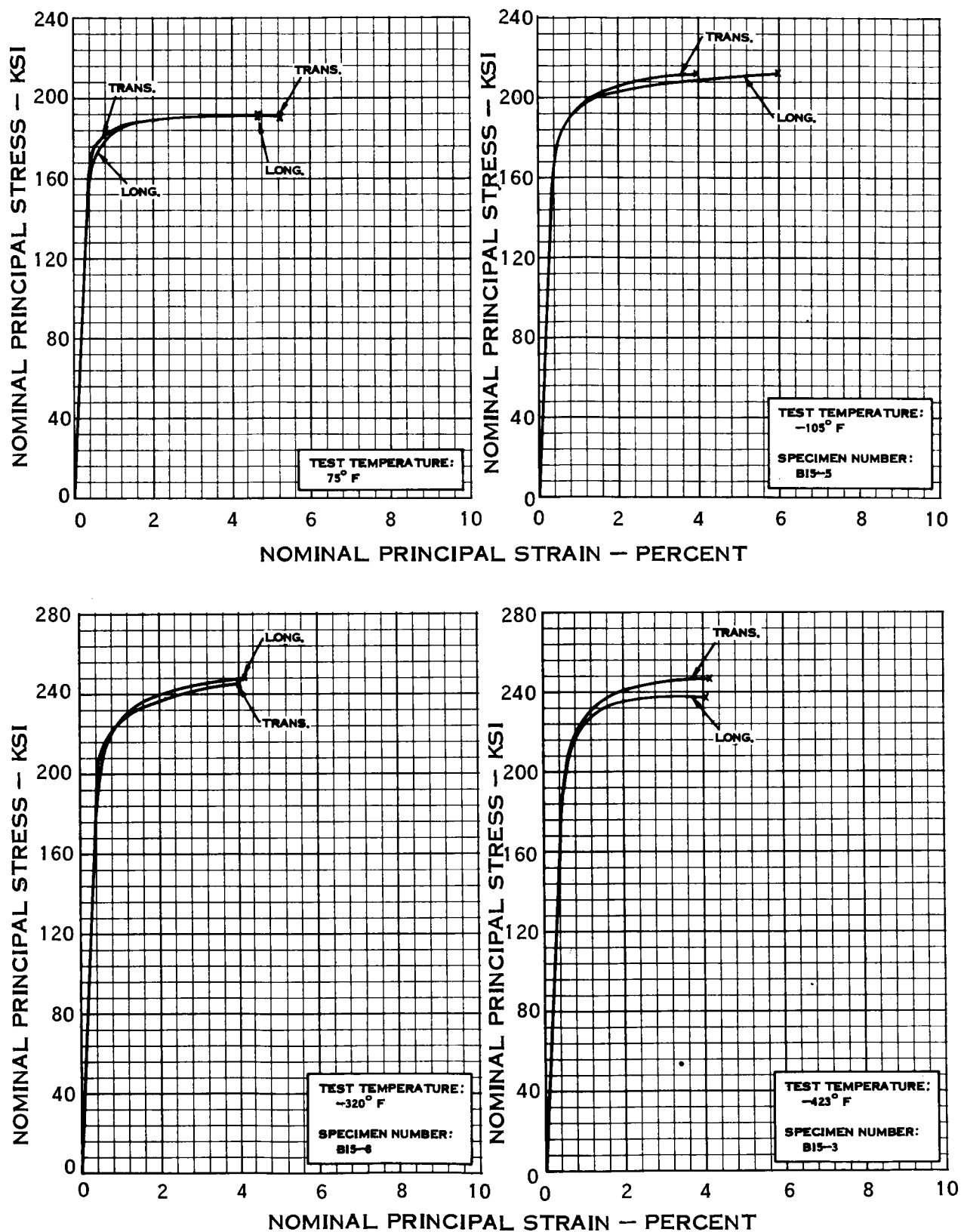


FIGURE 63 -TYPICAL INCONEL 718 (H.T.) 1:1 BIAxIAL STRESS-STRAIN CURVES

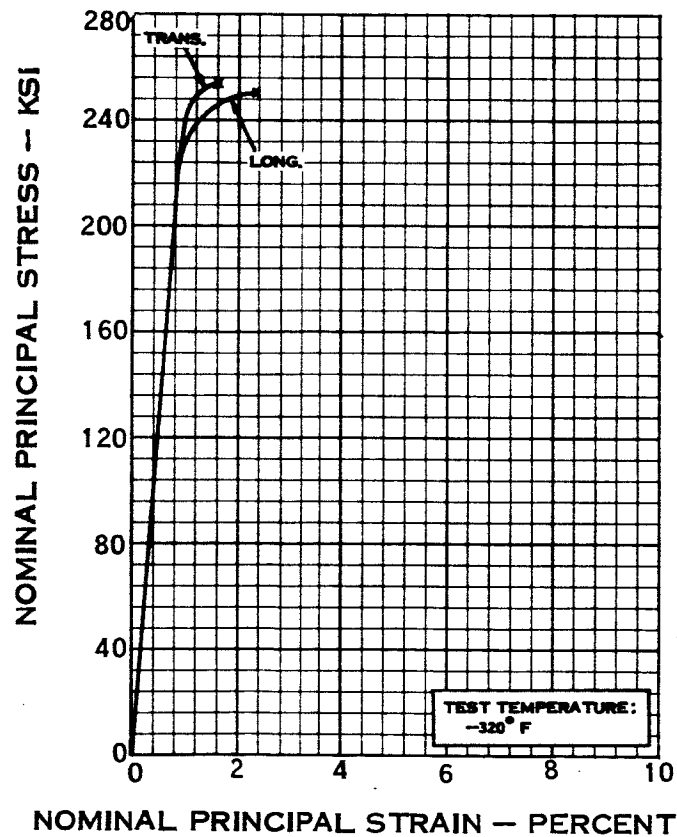
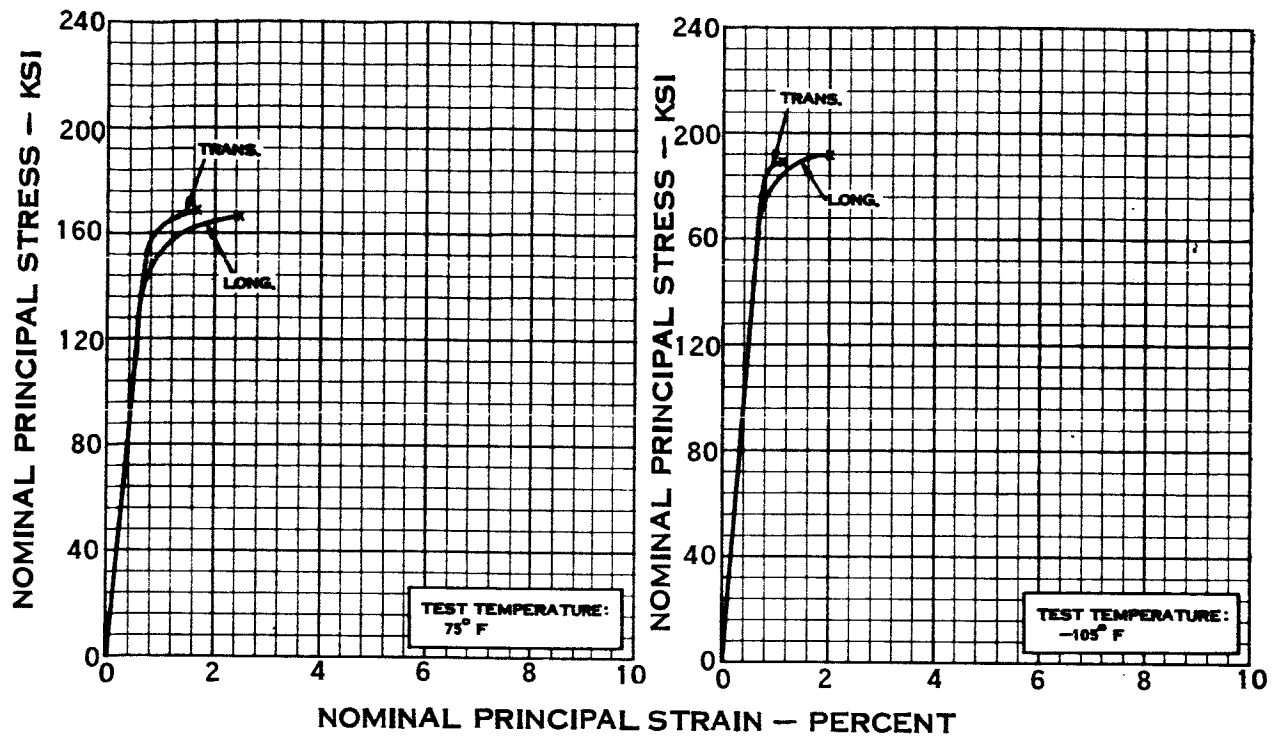


FIGURE 64 —TYPICAL 6 AL — 4 V TITANIUM ALLOY (STA) 1:1 BIAXIAL STRESS-STRAIN CURVES

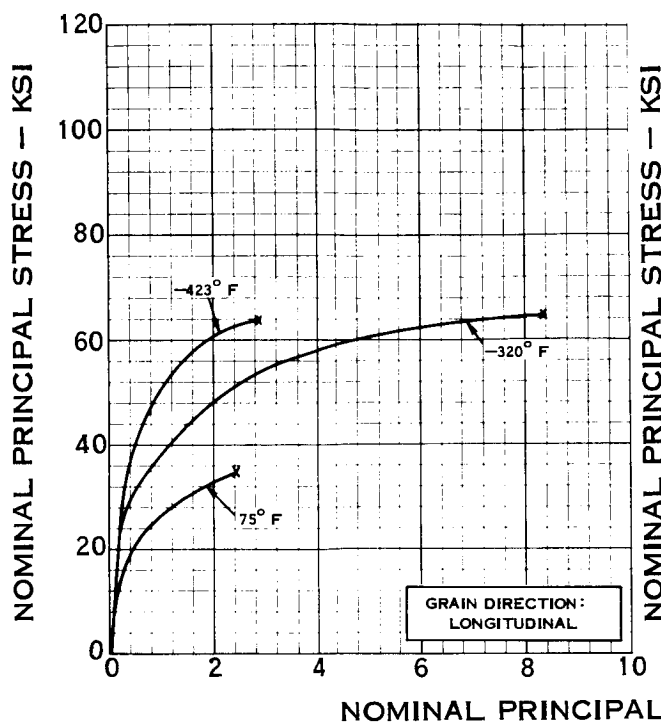


FIGURE 65 TYPICAL 2219 - T87
ALUMINUM ALLOY (AS-WELDED)
1:1 BIAxIAL STRESS-STRAIN
CURVES

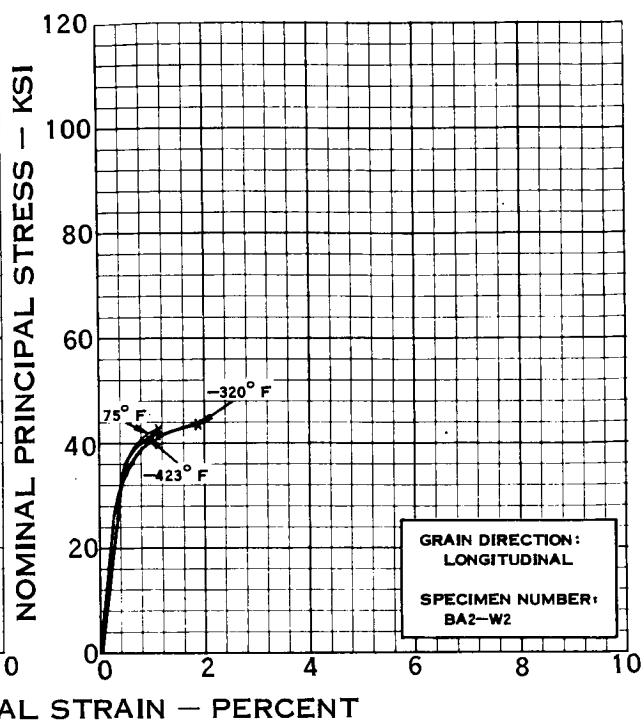


FIGURE 66 TYPICAL 2014 - T6
ALUMINUM ALLOY (AS-WELDED)
1:1 BIAxIAL STRESS-STRAIN
CURVES

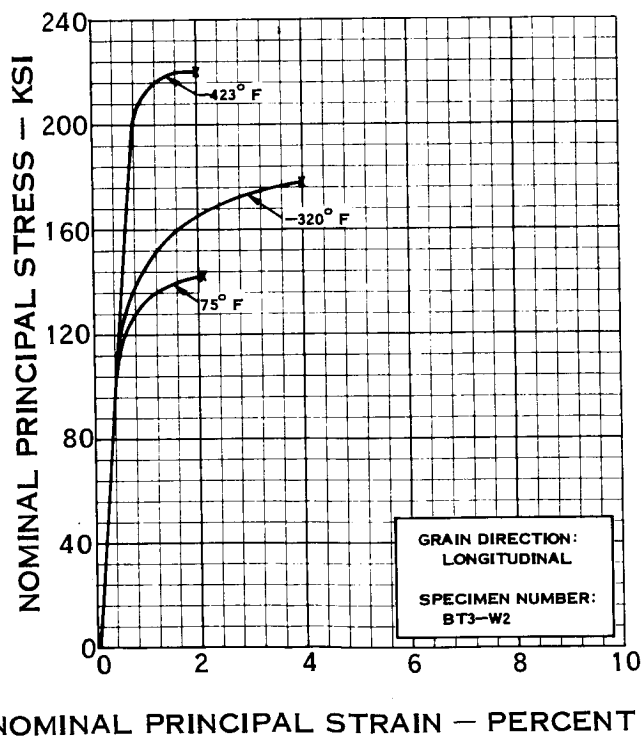


FIGURE 67 -TYPICAL 5 Al -2.5Sn TITANIUM ALLOY (ANNEALED, AS-
WELDED) 1:1 BIAxIAL STRESS-STRAIN CURVES

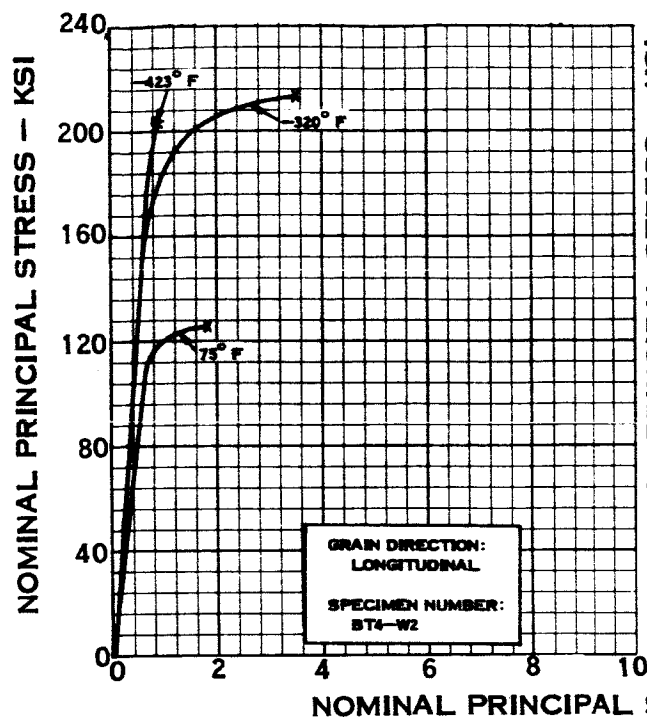


FIGURE 68 TYPICAL 6 AL-4V
TITANIUM ALLOY (ANNEALED,
ELI, AS-WELDED) 1:1 BIAxIAL
STRESS-STRAIN CURVES

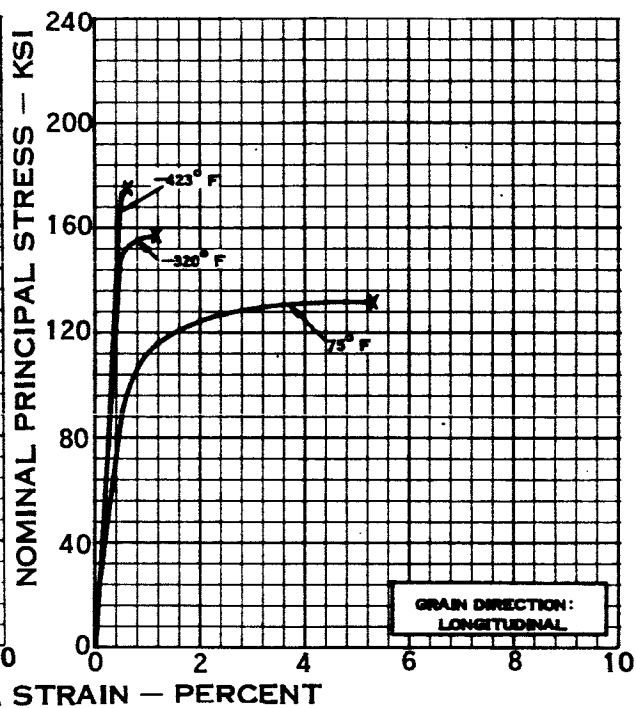


FIGURE 69 TYPICAL INCONEL 718
(HEAT TREATED, AS-WELDED)
1:1 BIAxIAL STRESS-STRAIN
CURVES

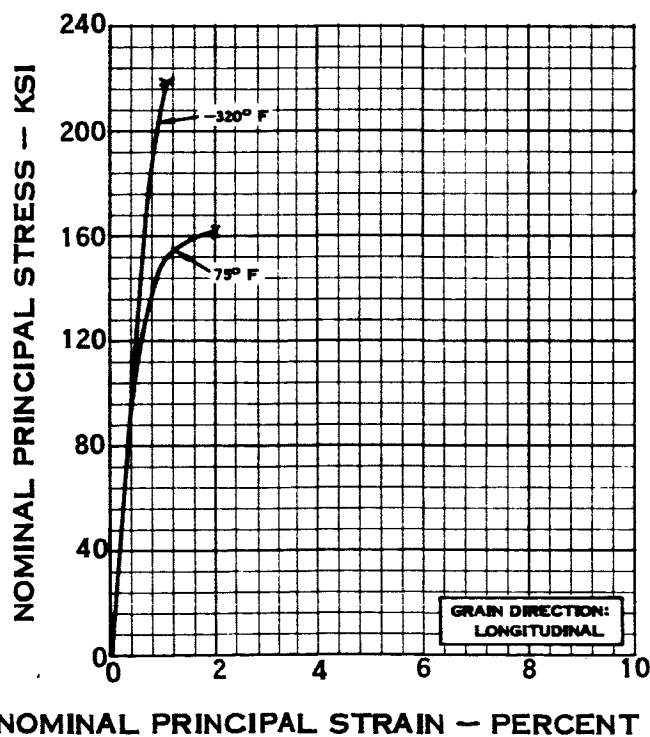


FIGURE 70-TYPICAL 6 AL-4V TITANIUM ALLOY (STA, AS-WELDED) 1:1
BIAxIAL STRESS-STRAIN CURVES

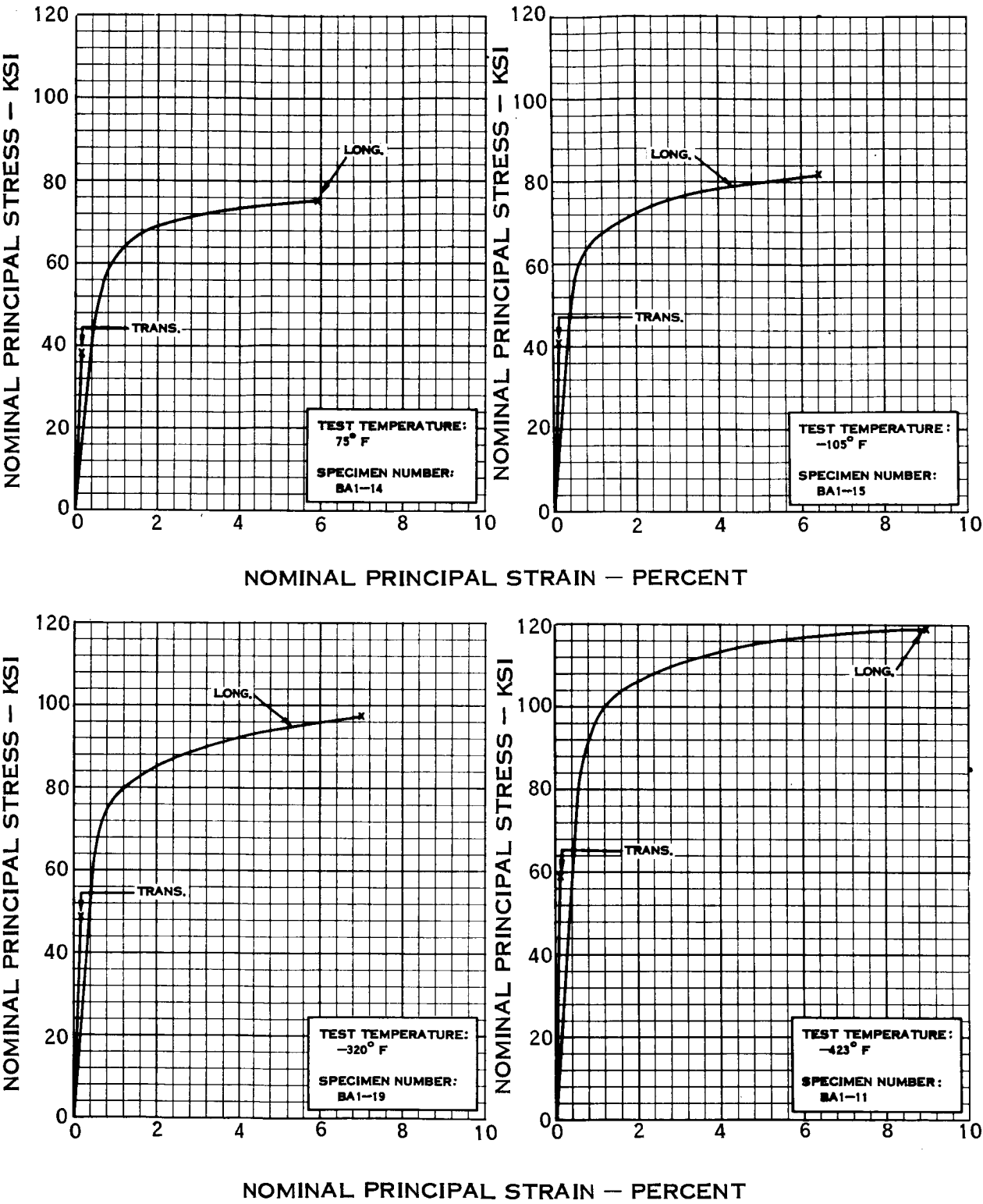


FIGURE 71 -TYPICAL 2219-T87 ALUMINUM ALLOY
2:1 BIAXIAL STRESS-STRAIN CURVES

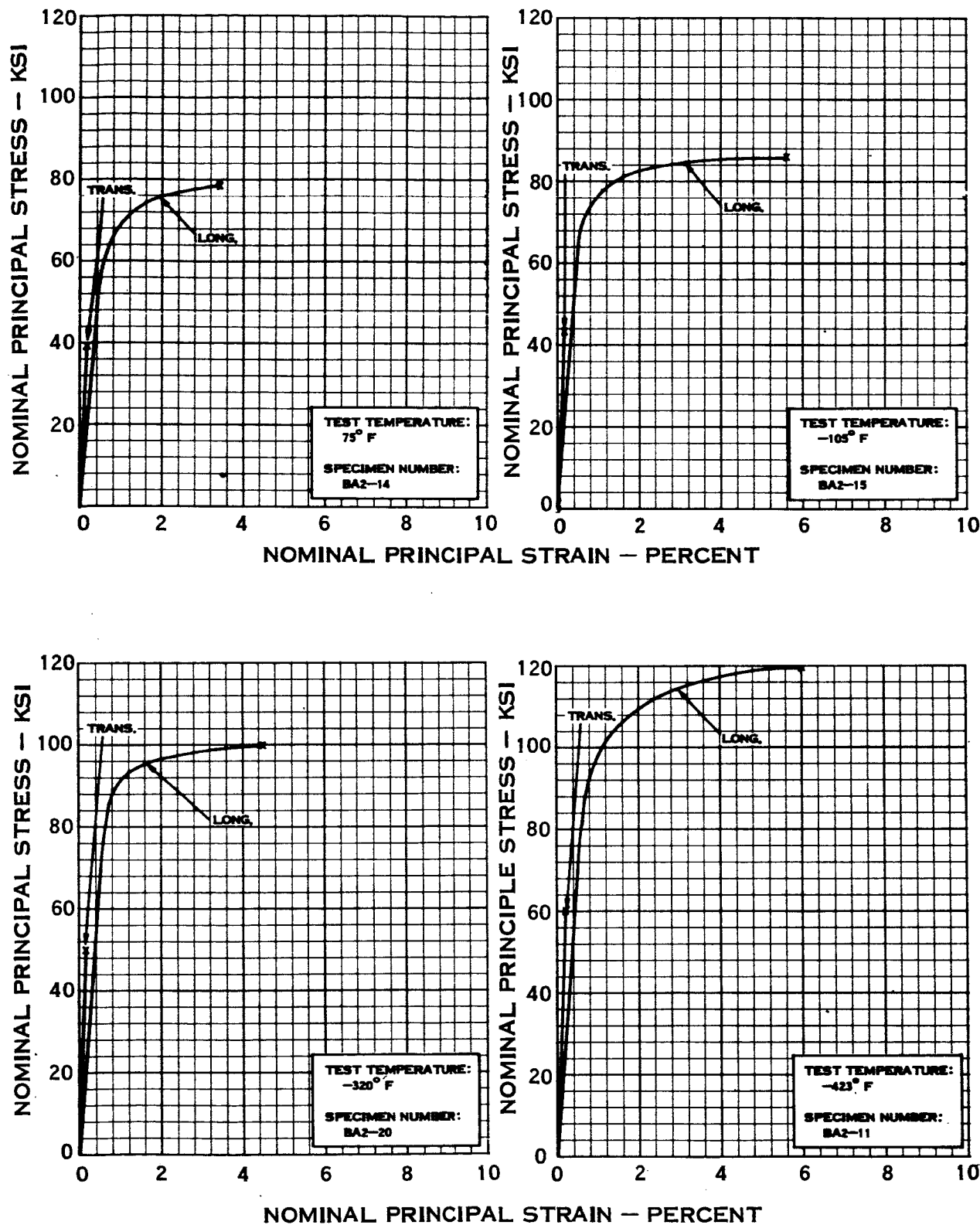


FIGURE 72 -TYPICAL 2014-T6 ALUMINUM ALLOY 2:1 BIAxIAL STRESS-STRAIN CURVES

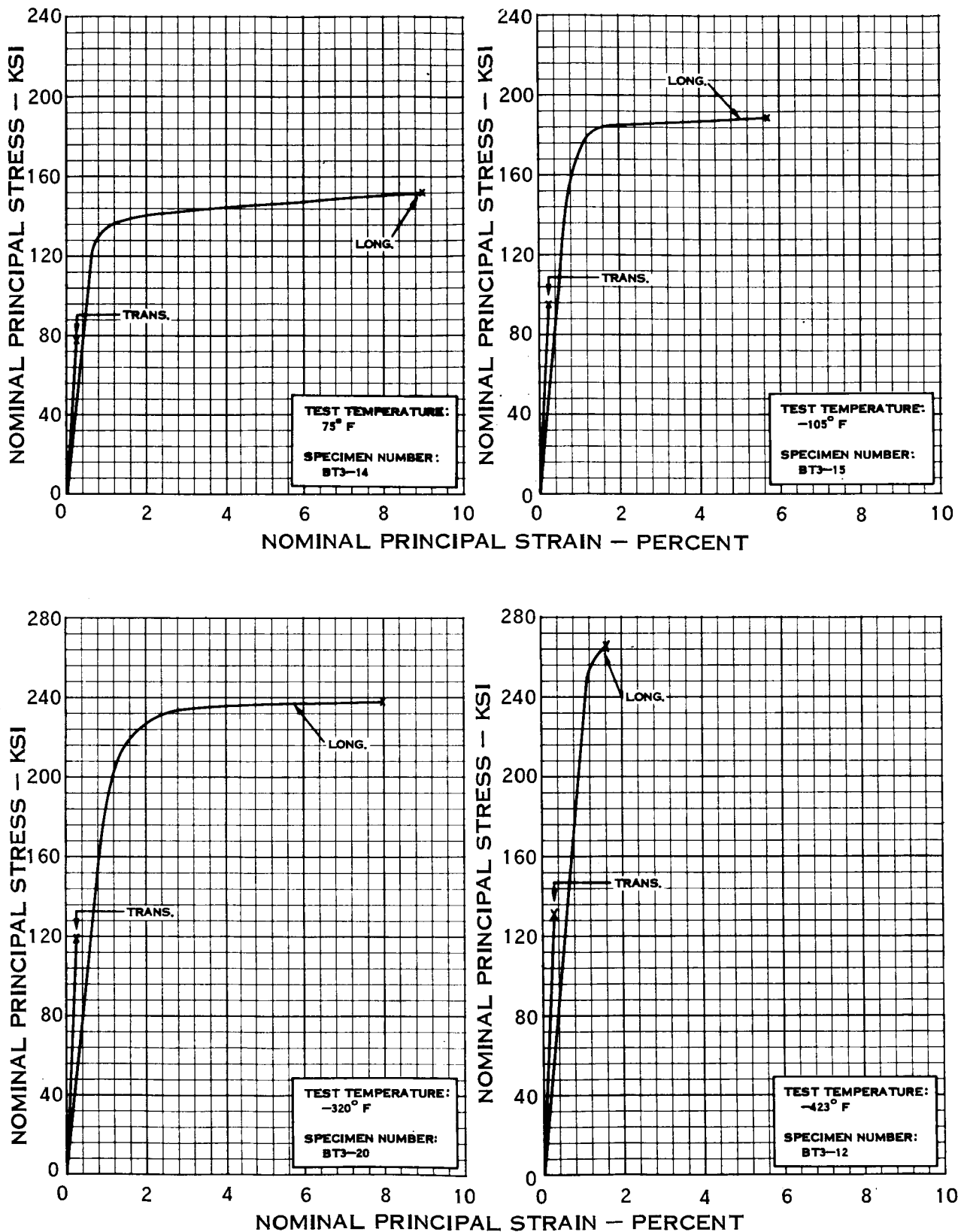


FIGURE 73 —TYPICAL 5 Al — 2.5 Sn TITANIUM ALLOY (ANNEALED)
2:1 BIAxIAL STRESS-STRAIN CURVES

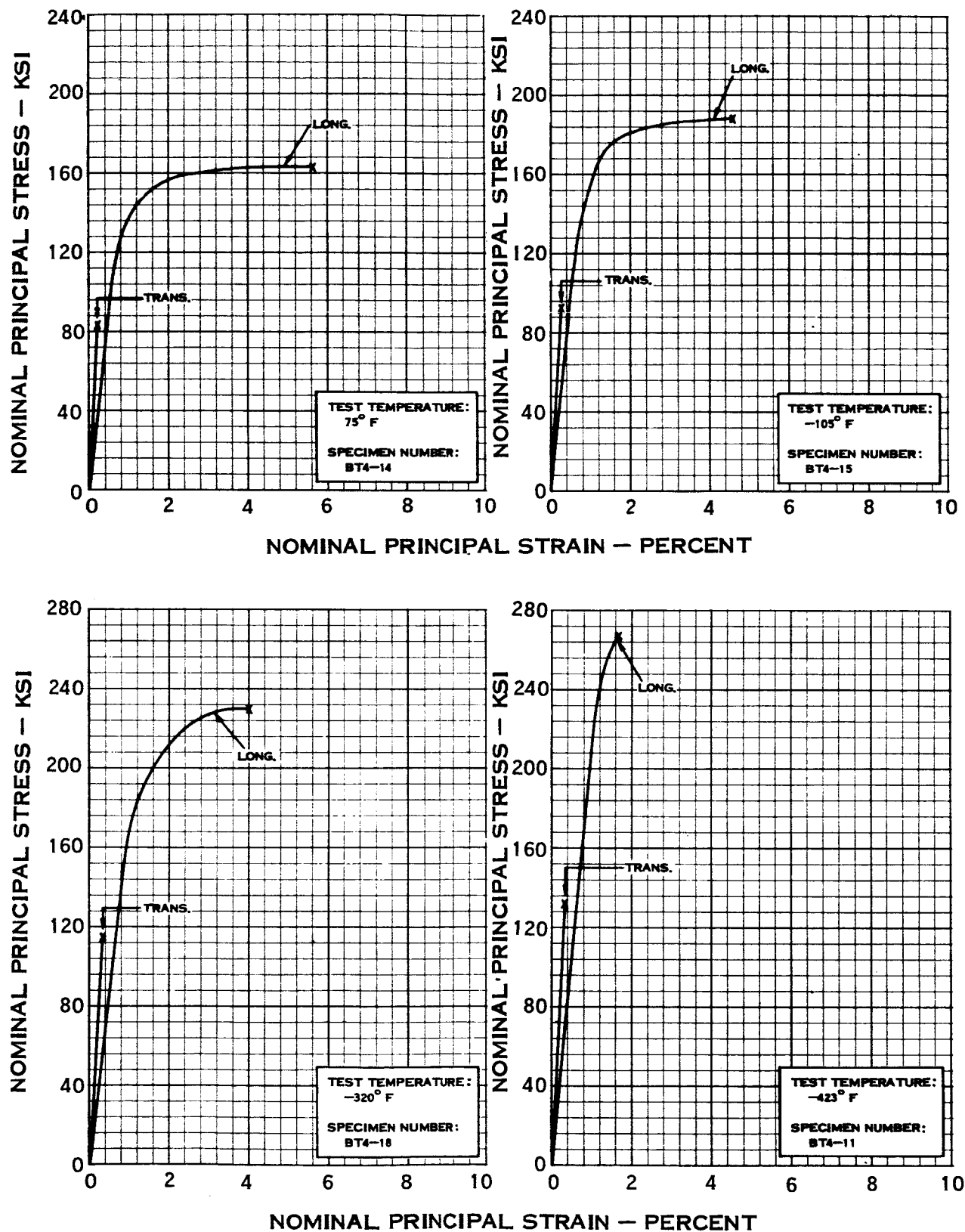


FIGURE 74 -TYPICAL 6 AL -4 V TITANIUM ALLOY (ELI, ANNEALED)
2:1 BIAxIAL STRESS-STRAIN CURVES

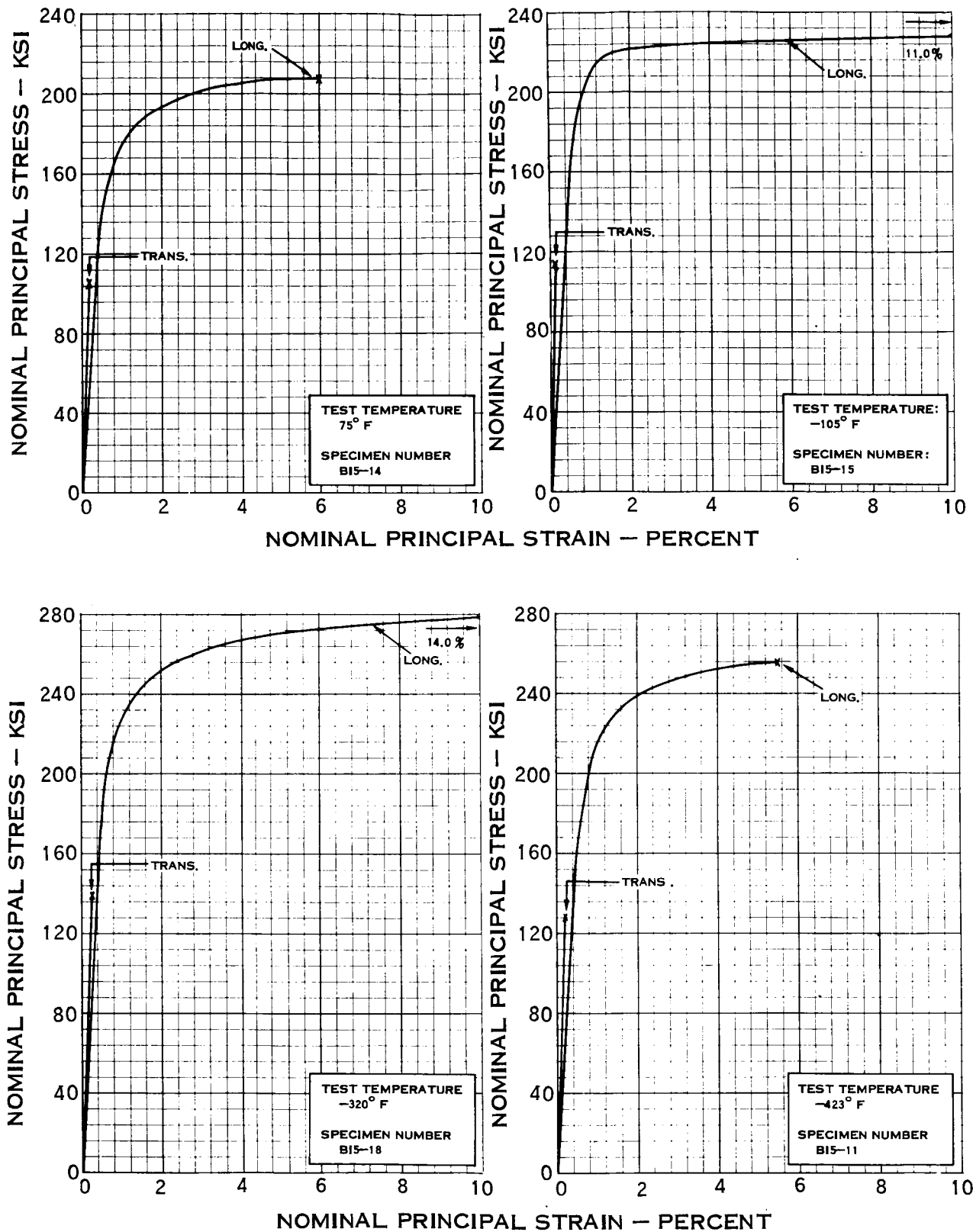


FIGURE 75 -TYPICAL INCONEL 718 (HEAT-TREATED) 2:1 BIAxIAL STRESS-STRAIN CURVES

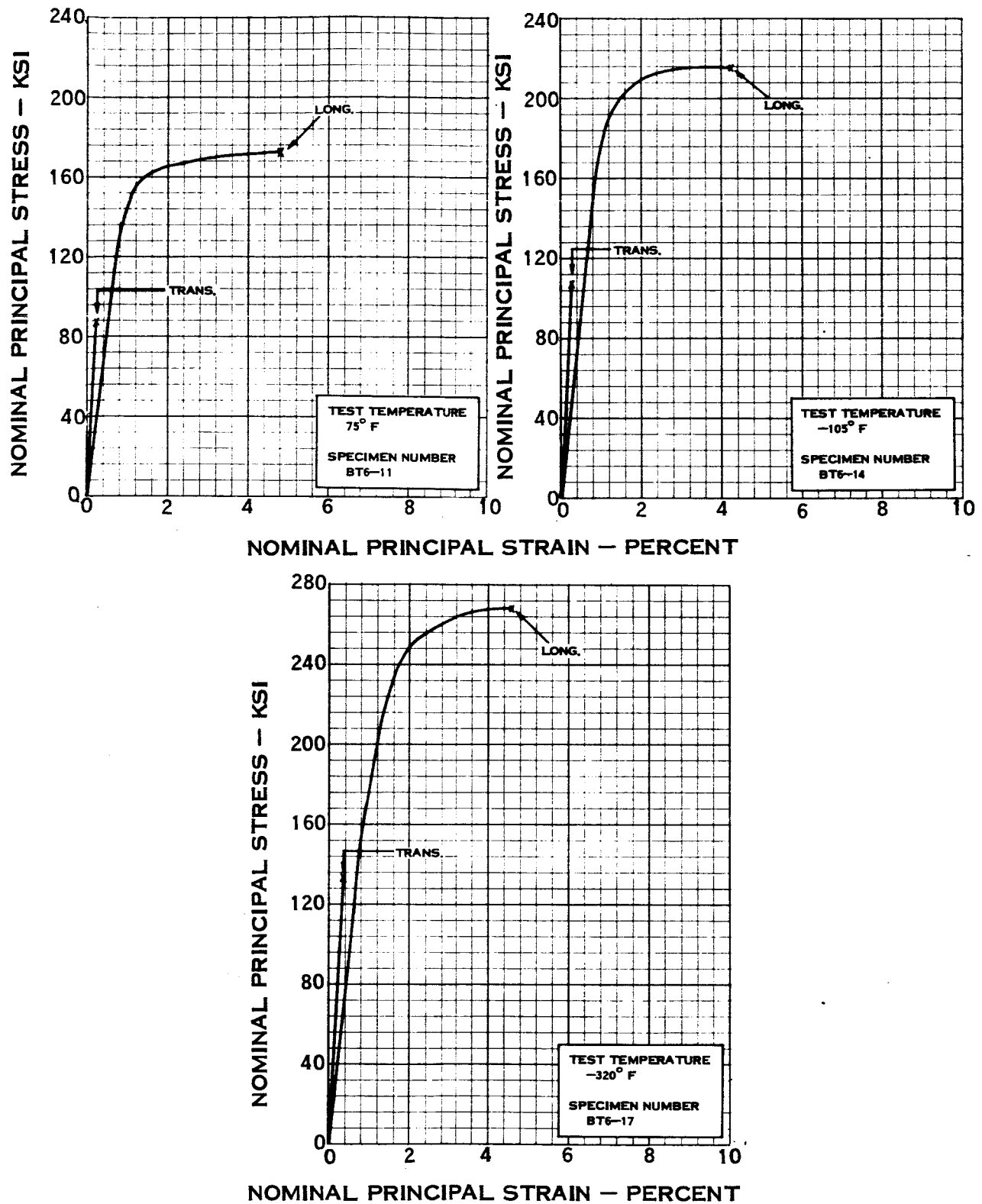


FIGURE 76 -TYPICAL 6 Al - 4 V TITANIUM ALLOY (STA) 2:1 BIAxIAL STRESS-STRAIN CURVES

APPENDIX I

DATA COMPILED FROM OTHER SOURCES

The data compiled in Table I-1 from results of other research efforts is presented as additional data that has been generated by LTV in the environmental range of room temperature down to -423°F.

TABLE 6 - ADDITIONAL UNIAXIAL DATA

Material	Spec No.	Test Temp °F	Grain Direction	Ultimate Strength ksi	Yield Strength ksi	Elastic Modulus x10 ⁶ psi	Poisson's Ratio	Percent Extension meter 1-inch	Elongation Gage Marks 2-inch	Ludwik Coefficient "n"
2219-T81 Aluminum Alloy	UAL-1	75	Long.	63.7	50.8	10.9	0.34	4.5	6.0	0.17
	UAL-2	75	Long.	63.6	49.2	10.2	0.33	4.2	4.3	0.18
	UAL-3	75	Long.	65.1	49.3	10.1	0.31	6.9	7.5	0.13
	UAT-1	75	Tran.	63.2	46.7	10.7	0.32	5.7	9.5	0.14
	UAT-2	75	Tran.	64.6	48.2	10.3		7.3	7.3	0.18
	UAT-3	75	Tran.	64.8	47.3	10.4	0.33	8.9	9.3	0.14
	UAL-4	-105	Long.	67.6	52.5	10.9	0.33	6.1	7.0	0.14
	UAL-5	-105	Long.	66.8	53.2	10.9	0.34	5.7	6.5	0.11
	UAT-4	-105	Tran.	70.0	47.9	11.3	0.33	11.2	8.0	0.15
	UAT-5	-105	Tran.	69.8	51.9	11.2	0.32	7.1	8.5	0.12
	UAT-6	-320	Tran.	82.7	62.1	12.7	0.32	6.0	9.8	0.15
	UAT-7	-320	Tran.	81.9	61.3	12.9	0.35	13.5	8.8	0.13
	UAL-6	-320	Long.	79.0	57.0	12.9	0.32	7.0	7.1	0.14
	UAL-7	-320	Long.	79.9	61.8	12.7	0.35	6.5	7.0	0.15
	UAL-9	-423	Long.	87.0	74.0	13.0	0.33	5.0	7.0	0.060
	UAT-9	-423	Tran.	90.7	70.0	14.1	0.34	-	6.0	0.068
310 Stainless Steel	UST-1	75	Tran.	176.1	146.9	30.4	0.30	2.1	2.1	0.11
	UST-2	75	Tran.	179.4	143.2	30.7	0.29	2.6	5.5	0.10
	USL-2	75	Long.	163.0	142.0	30.6	0.29	1.5	2.8	0.08
	USL-4	75	Long.	163.9	155.0	30.6	0.29	1.8	3.5	0.08
	UST-3	-105	Tran.	194.7	145.0	31.0	0.30	4.2	4.0	0.09
	UST-4	-105	Tran.	198.5	162.1	31.0	0.29	5.5	7.0	0.10
	USL-1	-105	Long.	182.5	169.5	31.3	0.29	7.1	7.3	0.07
	USL-3	-105	Long.	185.0	161.2	31.7	0.30	7.0	7.0	0.06
	UST-6	-320	Tran.	238.5	201.5	32.1	0.30	6.0	6.5	0.08
	UST-5	-320	Tran.	236.0	200.0	32.5	0.29	7.5	11.7	0.06

TABLE 6 - ADDITIONAL UNIAxIAL DATA (CONT)

Material	Spec No.	Test Temp °F	Grain Direction	Ultimate Strength ksi	Yield Strength ksi	Elastic Modulus x10 ⁶ psi	Poisson's Ratio	Percent Elongation 1-inch	Elongation Gage Marks 2-inch	Ludwik Coef- ficient "n"
310 Stainless Steel (con't)	USL-5	-320	Long.	232.5	208.0	32.9	0.29	8.0	13.0	0.07
	USL-6	-320	Long.	237.0	211.0	31.8	0.29	8.2	12.5	0.06
	USL-7	-423	Long.	247.0	230.0	33.5	0.29	1.7	2.0	0.040
	USL-8	-423	Long.	242.0	220.0	33.3	0.29	-	2.0	0.043
	UST-10	-423	Tran.	258.0	228.5	31.0	0.31	-	2.5	0.043
	UST-9	-423	Tran.	257.0	234.0	31.3	0.29	-	2.5	0.046
	UTT-3	75	Tran.	110.3	101.8	16.5	0.29	5.25	7.5	0.055
	UTT-4	75	Tran.	115.4	112.0	15.9	0.32	5.5	6.5	0.036
	ULT-3	75	Long.	110.0	101.3	16.2	0.29	6.0	6.5	0.069
5A1-2.5Sn Titanium Alloy (ELI, Annealed)	ULT-4	75	Long.	113.0	101.2	16.3	0.28	7.0	8.5	0.052
	UTT-5	-105	Tran.	132.0	130.1	18.4	0.31	5.0	5.5	0.082
	UTT-6	-105	Tran.	135.9	130.0	18.4	0.30	5.0	4.0	0.039
	ULT-5	-105	Long.	132.5	128.2	18.0	0.28	7.3	5.5	0.061
	ULT-6	-105	Long.	134.0	118.5	18.1	0.29	7.5	13.5	0.057
	UTT-7	-320	Tran.	193.0	189.0	19.2	0.28	1.5	1.5	0.039
	UTT-8	-320	Tran.	185.2	174.7	17.5	0.27	7.0	4.0	-
	ULT-7	-320	Long.	190.2	176.0	19.2	0.26	2.6	3.0	-
	ULT-8	-320	Long.	191.5	184.8	20.0	0.30	5.0	3.5	0.047
	UTL-1	-423	Long.	208.0	198.0	19.9	0.29	-	1.5	0.064
	UTL-2	-423	Long.	208.0	201.0	20.0	0.30	1.2	2.5	-
	UTT-1	-423	Tran.	207.5	207.0	20.6	0.31	-	2.0	-
	UTT-2	-423	Tran.	210.0	206.0	19.6	0.32	-	1.5	0.060
	UAW-1	75	Long.	35.0	24.7	12.2	0.35	4.2	3.0	0.123
	UAW-2	75	Long.	37.2	25.1	11.7	0.33	4.1	3.0	0.177
	UAW-5	-105	Long.	36.2	26.3	13.3	0.34	2.5	2.5	0.122

TABLE 6 - ADDITIONAL UNIAXIAL DATA (CONT)

Material	Spec No.	Test Temp °F	Grain Direction	Ultimate Strength ksi	Yield Strength ksi	Elastic Modulus x10 ⁶ psi	Poisson's Ratio	Percent Elongation 1-inch	Elongation Gage Marks 2-inch	Ludwik Coefficient "n"
2219-T81 Aluminum (Welded) Con't	UAW-6	-105	Long.	38.2	27.3	11.5	0.34	3.6	3.1	0.102
	UAW-3	-320	Long.	55.2	38.8	12.3	0.33	3.6	3.5	0.125
	UAW-4	-320	Long.	52.2	37.7	13.0	0.31	3.8	3.5	0.152
310 Stainless Steel (Cold-Rolled, Welded)	USW-1	75	Long.	79.0	57.6	26.4	0.30	12.8*	4.0	0.141
	USW-2	75	Long.	74.6	52.5	26.0	0.34	10.4*	4.5	0.163
	USW-5	-105	Long.	105.0	76.8	27.4	0.32	6.4*	4.0	0.115
	USW-6	-105	Long.	103.5	75.0	26.7	0.34	3.3	3.5	0.135
	USW-3	-320	Long.	150.0	109.0	29.4	0.29	7.0	4.0	0.159
	USW-4	-320	Long.	147.5	109.0	28.1	0.28	7.2*	4.0	0.155
5A1-2.5Sn Titanium Alloy (ELI, Annealed WELDED)	UTW-1	75	Long.	114.8	102.8	18.0	0.31	6.2	9.2	0.071
	UTW-2	75	Long.	115.6	98.9	18.2	0.29	6.1	7.0	0.105
	UTW-5	-105	Long.	143.7	135.5	18.2	0.29	5.2	5.4	0.038
	UTW-6	-105	Long.	141.5	133.8	20.3	0.31	4.3	4.0	0.047
	UTW-3	-320	Long.	190.0	186.5	22.0	0.29	2.0	3.0	--
	UTW-4	-320	Long.	190.0	180.0	21.0	0.24	2.7	3.0	0.022

* Some slippage of the mechanical extensometer was observed.

TABLE 7 - ADDITIONAL BIAxIAL DATA

Material	Spec No.	Test Temp °F	Grain Direction	State of Stress	Biaxial Modulus Ex10 ⁶ psi *	Biaxial Ultimate ksi	Biaxial Yield ksi	%Elongation (1/2 in. gage) (Long. Grain Direction)	% Elongation (1/2 in. gage) (Tran. Grain Direction)
2219 T-81 Aluminum Alloy	BA1	75	-	1:1	14.8	68.0	56.1	3.4	2.8
	BA3	75	-	1:1	14.6	64.1	56.5	3.3	3.5
	BA2	75	Long.	2:1	11.6	72.9	62.0	2.2	-
	BA6	75	Long.	2:1	11.9	74.1	62.3	5.5	-
	BA11	-105	-	1:1	15.3	66.5	57.5	3.3	3.6
	BA5	-105	-	1:1	15.9	65.5	55.2	3.1	2.5
	BA8	-105	Long.	2:1	11.6	78.2	67.2	4.9	-
	BA14	-105	Long.	2:1	12.3	71.2	54.7	4.6	-
	BA7	-320	-	1:1	18.3	79.8	75.0	0.7	4.3
	BA9	-320	-	1:1	18.0	76.0	71.0	2.0	1.9
	BA10	-320	Long.	2:1	13.8	91.9	79.5	4.8	-
	BA12	-320	Long.	2:1	13.5	91.8	75.6	8.0	-
	BA21	-423	-	1:1	19.8	88.0	70.5	2.5	2.5
	BA15	-423	-	1:1	19.9	92.0	75.0	3.0	2.9
	BA18	-423	-	1:1	20.0	94.1	81.0	2.3	2.0
	BA20	-423	Long.	2:1	16.0	108.0	76.0	6.0	-
	BA17	-423	Long.	2:1	16.0	105.0	75.8	4.5	-
	BA18	-423	Long.	2:1	15.9	104.0	75.8	4.0	-
310 Stainless Steel	BS26	75	-	1:1	41.2	164.0	154.4	1.1	0.9
	BS13	75	-	1:1	41.0	168.4	163.2	0.9	0.9
	BS27	75	Long.	2:1	30.9	189.5	170.4	2.3	-
	BS7	75	Long.	2:1	30.8	188.0	168.0	2.6	-
	BS8	-105	-	1:1	43.6	192.0	176.0	2.0	1.7
	BS18	-105	-	1:1	44.0	188.1	162.2	2.7	1.4
	BS10	-105	Long.	2:1	31.8	212.0	169.0	2.8	-
	BS12	-105	Long.	2:1	32.0	216.0	184.0	3.6	-

TABLE 7 - ADDITIONAL BIAxIAL DATA (CONT)

Material	Spec	Test Temp °F	Grain Direction	State of Stress	Biaxial Modulus Ex10 ⁶ psi	Biaxial Ultimate ksi	Biaxial Yield ksi	% Elongation (1/2 in. gage) (Long. Grain Direction)	% Elongation (1/2 in. gage) (Tran. Grain Direction)
310 Stainless Steel Con't	BS14	-320	-	1:1	44.6	232.0	202.2	2.3	2.3
	BS15	-320	-	1:1	46.0	222.8	172.0	2.6	1.8
	BS20	-320	-	1:1	45.0	233.5	213.0	3.0	3.3
	BS19	-320	Long.	2:1	33.1	226.0	158.0	2.4	-
	BS21	-320	Long.	2:1	33.0	243.5	180.0	3.7	-
	BS32	-320	Long.	2:1	32.2	238.0	173.0	3.8	-
	BS24	-423	-	1:1	42.5	248.0	230.0	1.4	1.0
	BS30	-423	-	1:1	42.6	242.5	230.5	1.9	1.25
	BS29	-423	-	1:1	43.0	246.0	233.5	1.7	1.0
	BS22	-423	Long.	2:1	32.2	264.0	182.0	2.9	-
	BS31	-423	Long.	2:1	33.0	268.0	193.0	2.4	-
	BS28	-423	Long.	2:1	32.8	268.5	204.0	2.6	-
	BT7	75	-	1:1	22.5	106.0	96.0	4.3	4.9
	BT8	75	-	1:1	23.2	106.0	95.0	4.0	4.1
5Al-2.5Sn Titanium Alloy (Annealed) (ETI)	BT9	75	Long.	2:1	16.9	212.8	109.0	3.6	-
	BT12	75	Long.	2:1	17.1	113.0	94.0	3.0	-
	BT2	-105	-	1:1	24.6	129.6	124.0	1.9	2.4
	BT5	-105	-	1:1	25.0	124.5	120.5	2.4	1.1
	BT4	-105	Long.	2:1	19.2	133.0	119.0	6.0	-
	BT10	-105	Long.	2:1	18.9	132.0	94.0	6.0	-
	BT14	-320	-	1:1	27.0	174.0	160.2	1.8	5.2
	BT26	-320	-	1:1	28.3	-	-	-	(Grip failure)
	BT24	-320	-	1:1	27.4	-	-	-	(Grip failure)
	BT1	-320	-	1:1	28.0	178.2	170.5	4.3	-
	BT13	-320	Long.	2:1	18.7	168.0	150.0	3.4	-
	BT20	-320	Long.	2:1	19.9	193.0	178.0	6.9	-

TABLE 7 - ADDITIONAL BIAxIAL DATA (CONT)

Material	Spec No.	Test Temp °F	Grain Direction	State of Stress	Biaxial Modulus Ex10 ⁶ psi *	Biaxial Ultimate ksi	Biaxial Yield ksi	% Elongation (1/2 in. gage) (Long. Grain Direction)	% Elongation (1/2 in. gage) (Tran. Grain Direction)
5A1-2.5Sn Titanium Alloy (Annealed) (ELI) Con't	BT25	-320	Long.	2:1	19.2	166.5	114.0	6.6	-
	BT23	-423	-	1:1	28.1	210.0	205.5	1.3	1.7
	BT15	-423	-	1:1	28.6	213.0	208.5	1.75	1.60
	BT2	-423	-	1:1	28.7	207.0	201.5	1.80	1.80
	BT19	-423	Long.	2:1	21.0	213.0	190.0	1.8	-
	BT26	-423	Long.	2:1	21.5	222.0	190.5	2.0	-
	BT18	-423	Long.	2:1	21.6	221.5	191.0	3.0	-
2219 T-81 Aluminum Alloy (Welded)	BAW7	75		1:1	16.0	39.5	31.0	3.9	0.3
	BAW26	75		1:1	15.4	38.6	31.0	2.2	0.3
	BAW3	-105		1:1	17.1	39.0	26.5	2.7	0.3
	BAW2	-105		1:1	17.5	37.0	24.5	2.1	0.3
	BAW14	-320		1:1	18.3	55.0	40.5	1.0	0.3
	BAW5	-320		1:1	18.1	57.0	35.0	6.0	0.8
310 Stainless Steel (Cold-Rolled) (Welded)	BSW1	75		1:1	34.5	80.5	53.0	3.6	0.4
	BSW2	75		1:1	36.0	81.0	46.0	2.9	0.4
	BSW6	-105		1:1	38.0	97.0	86.0	1.4	0.3
	BSW5	-105		1:1	37.4	96.5	77.8	1.5	0.3
	BSW3	-320		1:1	39.5	144.5	82.0	4.7	1.5
	BSW4	-320		1:1	38.0	152.0	110.0	4.4	0.5
5A1-2.5Sn Titanium Alloy (Annealed) (ELI)	BTW1	75		1:1	25.2	114.0	99.4	3.5	4.9
	BTW2	75		1:1	26.0	118.0	95.0	4.4	3.9
	BTW6	-105		1:1	27.2	140.0	120.0	3.0	1.6
	BTW4	-105		1:1	27.5	140.5	126.5	2.3	1.7
	BTW3	-320		1:1	29.2	193.5	180.0	1.4	1.0

TABLE 7 - ADDITIONAL BIAxIAL DATA (CONT)

Material	Spec No.	Test Temp °F	Grain Direction	State of Stress	Biaxial Modulus Ex10 ⁶ psi *	Biaxial Ultimate ksi	Biaxial Yield ksi	% Elongation (1/2 in. gage) (Long Grain Direction)	% Elongation (1/2 in. gage) (Tran. Grain Direction)
5Al-2.5Sn Titanium Alloy (Annealed) (ELI) Con't	BTW5	-320		1:1	28.9	196.0	178.5	3.6	2.7
	BTW7	-320		1:1	28.2	184.2	165.0	4.7	4.7

* - Biaxial (effective) modulus was calculated as shown by techniques shown in Section IV.

APPENDIX J

COMPARATIVE PHOTOFRACTOGRAPHY ANALYSIS OF
FRACTURE MODES

This appendix presents a unique comparison of fracture mode data. These comparisons illustrate the type of fracture mechanism present in the failure zone for various program materials at the three stress states at the four test temperature conditions. In addition weldment effects are also illustrated. The objective of this part of this research was to determine the types and differences in failure modes observed in the failure zone under variable conditions already mentioned. In addition, the effect of these failure mechanisms on the performance of a material was also an objective.

In essence the following general observations were made from the detailed electron microscope analysis.

- (a) The failure modes for each program material, test temperature, and stress state illustrate that each condition has varying degrees of tension and shear present in the failure zone. This observation illustrates the relative effect of temperature and stress state on the particular alloy.
- (b) Differences in the amount of tension or shear present varied with alloy, test temperature, and stress state.
- (c) Conditions (material, temperature, stress state) that exhibit more shear than tension for the biaxial stress states conform less closely to prediction theory (ultimate and yield strength).
- (d) When an alloy exhibits more shear than tension for a biaxial stress state condition, results from uniaxial tests seem to indicate the same trend of more shear than tension.
- (e) A relationship between increased amounts of shear deformation and ductility increases seems to exist in most alloys.
- (f) The effect of weldments on failure zone conditions for each program material, test

temperatures, and stress state was generally to increase the amount of shear to tension ratio. This effect is related to lower experienced allowable values, unless a material in the unwelded state has a "preferred tendency" to shear before failure, as was observed in the titanium alloy.

The specific material observations seen in Figures 77 through 84 are discussed in the following paragraphs. These observations were formulated from electron microscope analysis of failure zones (X-Z and Y-Z planes).

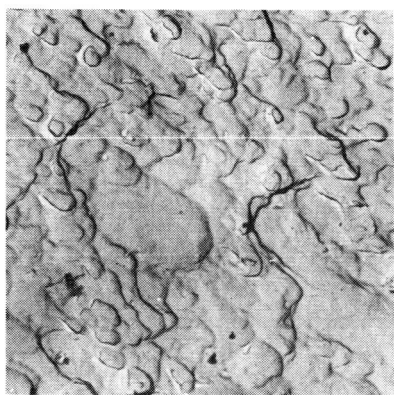
- (a) The 2219-T87 aluminum alloy exhibits nearly the same amount of shear and tension in the fracture area in the unwelded condition in both the 1:1 and 2:1 stress states at both -105°F and -320°F . This point is also reflected in the nearly uniform shape of the percent elongation versus temperature curve (Figure 5) even though the 2:1 stress state sustained a larger amount of elongation. The relative large amount of shear present in these fracture zones also correlates with the point that failure stress values higher than that predicted by theory were experienced. Weldments in this alloy exhibited, generally speaking, definite increases in the amount of shear present in the fracture area compared to the unwelded (parent) material which is related to the lower experienced allowables along with definite increases in grain size.
- (b) The 6Al-4V titanium (ELI) alloy exhibited more tension in the fracture zone than shear in the majority of the test points (stress state and temperature). At test points where the fracture zone exhibited mostly tension the ultimate strength compared closely to theory with the reverse being true where the fracture illustrated mostly shear in the fracture zone. However, the point of reduced amounts of shear also are related to the reduced amount of elongation that was experienced at -423°F (Figure 8).
- (c) The Inconel 718 alloy microphotographs also illustrated the complex relationship between the amount of shear present in the final fracture zone and the amount of elongation obtained and the correlation of the biaxial ultimate strength

to predicted theory values. For example the -423°F temperature samples illustrate reduced amounts of shear; but also reduced elongation values. In addition the 1:1 biaxial stress state tests in this alloy show less agreement with theory than the 2:1 stress state tests while the 1:1 stress state points also exhibited the greater amounts of shear in the fracture areas. Weldments in this alloy exhibited increased levels of shear in the fracture areas (also lower allowables) for the 1:0 stress states while the 1:1 stress state tended to reduce this tendency even though it is still present to a significant degree.

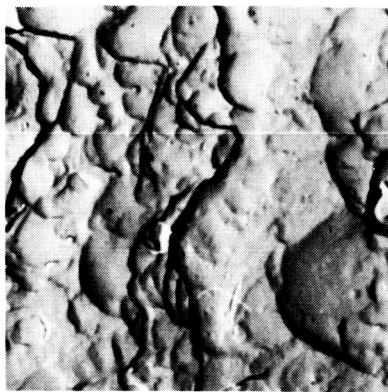
- (d) The fracture resistance effects (partial through cracks) shown in Figures 80, 81 and 82 illustrate that the Inconel 718 has more tension than shear in the 1:1 stress state tests compared to the 1:0 stress state while Figure 20 illustrates a corresponding higher fracture resistance for the 1:0 stress state than the 1:1 state. However, the opposite is true for the 5Al-2.5Sn titanium alloy, e.g. the 1:0 stress state still results in a larger amount of shear than the 1:1 stress state; but the 1:1 stress state allowed a higher fracture toughness allowable. This is undoubtedly related to the significant tendency for the titanium alloys to deform by shear deformation (preferred tendency) along the basal (111) plane. This tendency allows greater shear deformation in a uniaxially applied stress field than in a biaxial field when the load is basically perpendicular to the level plane. In the case of the 2219-T87 aluminum alloy the fracture toughness resistance for the 1:0 state increased in the -320°F to -423°F range while the reverse was true for the 1:1 stress state. These conditions are illustrated in the fracture surfaces studies where the 1:1 stress state has a large amount of shear deformation at the -423°F temperature compared to the -320°F temperature. In this alloy an increase in shear deformation in the plane strain fracture area allows early critical crack growth which results in lower fracture resistance even though significant ductibility accompanies this process. In the case of the 1:0 stress state (higher fracture resistance) a better balance of shear and tension was observed (about equal). In other words reasonable shear (ductility) with

significant resistance to crack growth due to a balance of shear and tension fracture. An additional reason for these complex conditions in the plane strain fracture toughness tests (uniaxial and 1:1 biaxial) is related to the degree of triaxial stress state present. These conditions offset the materials ability to sustain tension field stresses which is paramount in fracture toughness while also affecting the materials ability to flow under shear deformations in local fracture zones. This whole problem is, of course, influenced by the materials original crystalline structure and the applied thermal environment. Therefore these fracture zone studies do correlate well with and also indicate the reason for the rather complex relationship between fracture toughness values, stress states and temperature for three of the program materials.

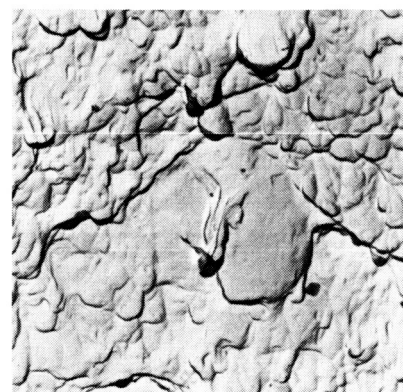
Figures 87 through 94 illustrate typically failed uniaxial, biaxial, fracture toughness and creep test specimens. These photographs include specimens of the various program alloys, stress states and test temperatures, as well as, alloys tested in both the welded and unwelded conditions. It was from failed specimens like these that the fracture mode studies were made while viewing the fracture origin areas in the fracture plane. It may be seen in these illustrations that the 1:1 biaxial specimens (basic, fracture toughness and creep) fail in the center of the specimen the location of the 1:1 stress state. The failed 2:1 specimens fractured in the second depression in one corner of the specimen, the location of the 2:1 stress state. The various failed uniaxial specimens show the location of failure, as well as, the amount of "necking" present in the failure zone at the noted test temperature.



STATE OF STRESS 1:1
TEST TEMPERATURE -105° F

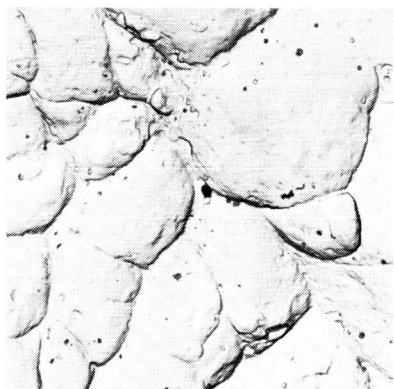


STATE OF STRESS 2:1
TEST TEMPERATURE -105° F

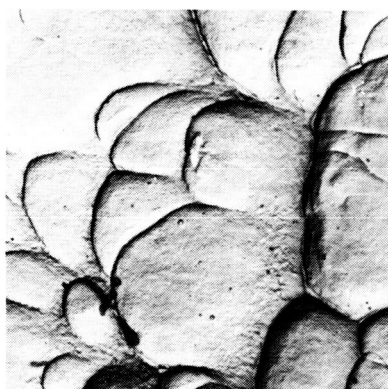


STATE OF STRESS 2:1
TEST TEMPERATURE -320° F

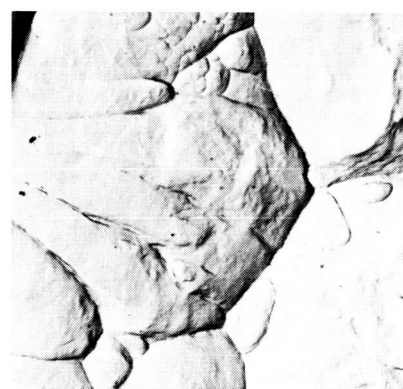
FIGURE 77 - COMPARATIVE ELECTRON MICROSCOPE MICRO-PHOTOGRAPHS OF FRACTURE ORIGINS IN (UNWELDED) 2219-T87 ALUMINUM ALLOY FOR 1:1 AND 2:1 STATES OF STRESS - 3000X



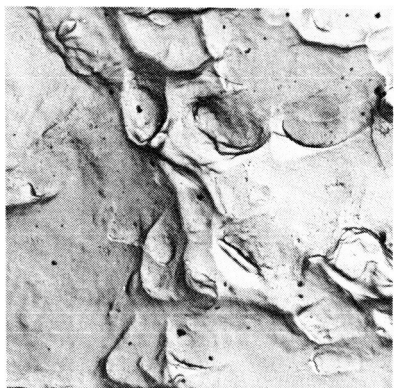
STATE OF STRESS 1:1
TEST TEMPERATURE -105° F



STATE OF STRESS 1:1
TEST TEMPERATURE -320° F



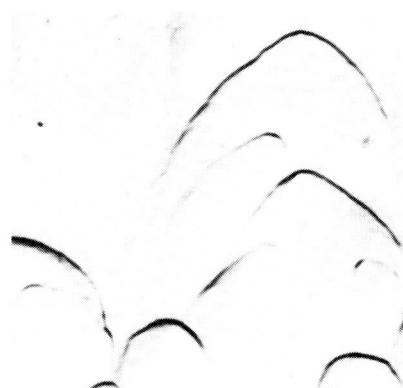
STATE OF STRESS 2:1
TEST TEMPERATURE 75° F



STATE OF STRESS 2:1
TEST TEMPERATURE -105° F

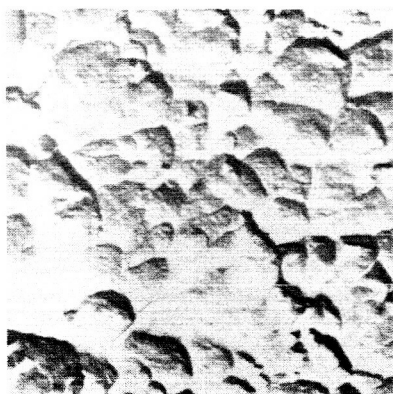


STATE OF STRESS 2:1
TEST TEMPERATURE -320° F



STATE OF STRESS 2:1
TEST TEMPERATURE -423° F

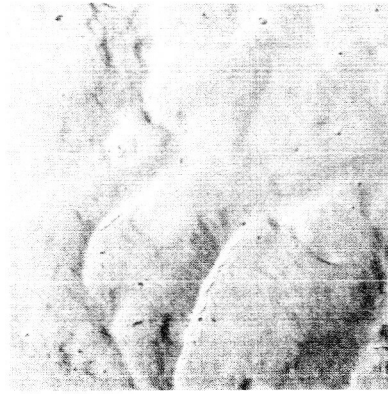
FIGURE 78 - COMPARATIVE ELECTRON MICROSCOPE MICRO-PHOTOGRAPHS OF FRACTURE ORIGINS IN (UNWELDED) 6AL-4V TITANIUM (ELI) ALLOY FOR 1:1 AND 2:1 STATES OF STRESS - 3000X



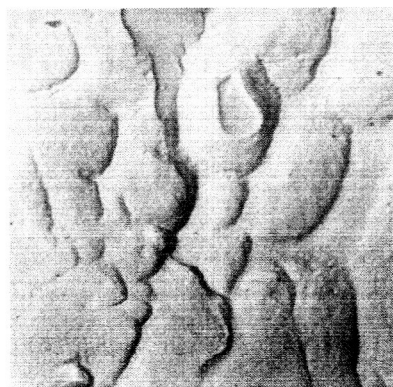
STATE OF STRESS 1:0
TEST TEMPERATURE 75° F



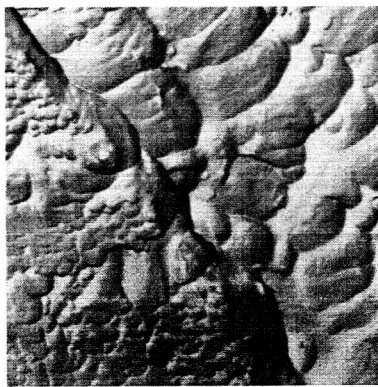
STATE OF STRESS 1:0
TEST TEMPERATURE -432° F



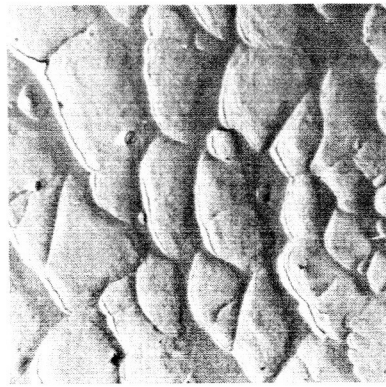
STATE OF STRESS 1:1
TEST TEMPERATURE -105° F



STATE OF STRESS 1:1
TEST TEMPERATURE -320° F



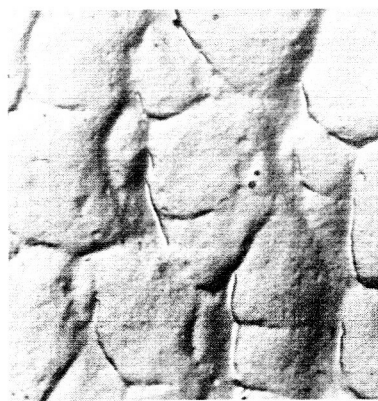
STATE OF STRESS 1:1
TEST TEMPERATURE -423° F



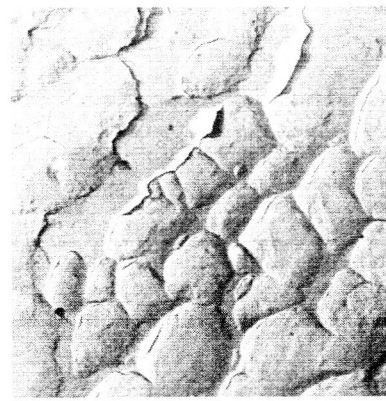
STATE OF STRESS 2:1
TEST TEMPERATURE 75° F



STATE OF STRESS 2:1
TEST TEMPERATURE -105° F

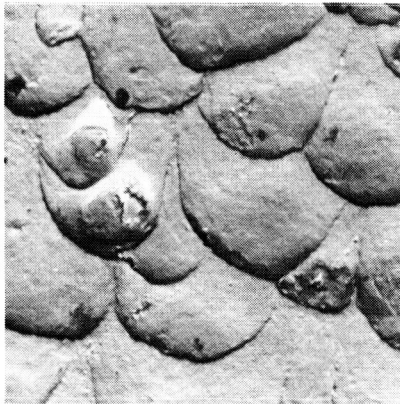


STATE OF STRESS 2:1
TEST TEMPERATURE -320° F

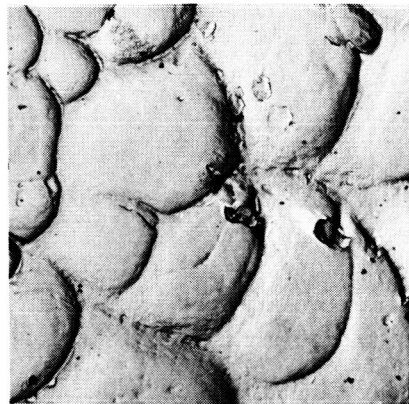


STATE OF STRESS 2:1
TEST TEMPERATURE -423° F

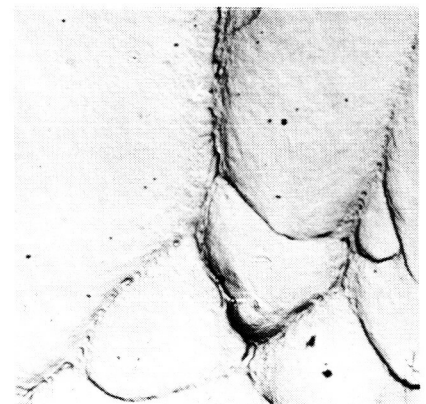
FIGURE 79 — COMPARATIVE ELECTRON MICROSCOPE MICRO-PHOTOGRAPHS OF FRACTURE ORIGINS IN (UNWELDED) INCONEL 718 ALLOY FOR 1:0, 1:1 AND 2:1 STATES OF STRESS — 3000X



STATE OF STRESS 1:0
TEST TEMPERATURE -423° F

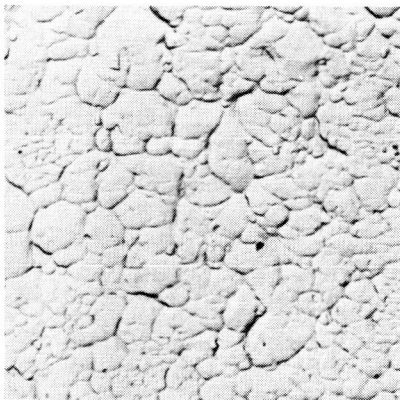


STATE OF STRESS 1:1
TEST TEMPERATURE -320° F

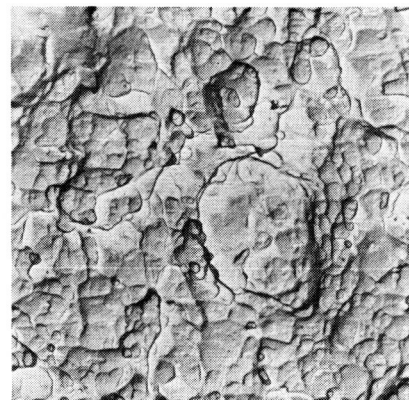


STATE OF STRESS 1:1
TEST TEMPERATURE -423° F

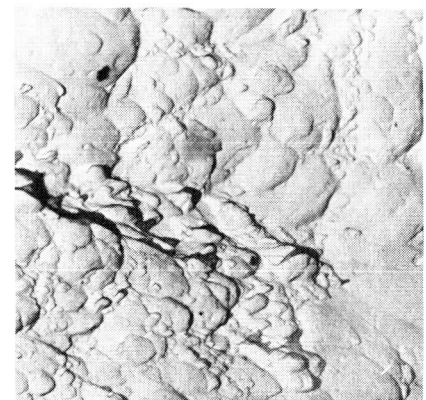
FIGURE 80 — COMPARATIVE ELECTRON MICROSCOPE MICRO-PHOTOGRAPHS OF FRACTURE ORIGINS IN (WELDED) 6 AL — 4V TITANIUM (ELI) ALLOY FOR 1:0 AND 1:1 STATES OF STRESS — 3000X



STATE OF STRESS 1:0
TEST TEMPERATURE -320° F

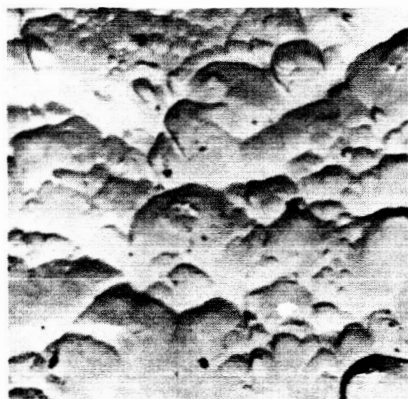


STATE OF STRESS 1:1
TEST TEMPERATURE -423° F

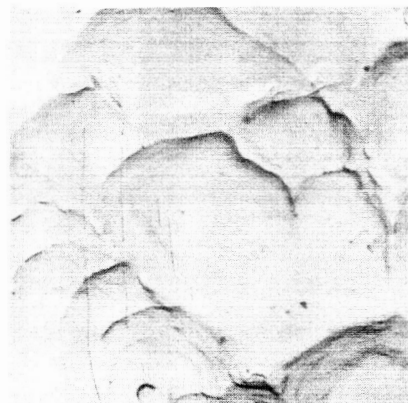


STATE OF STRESS 1:1
TEST TEMPERATURE -423° F

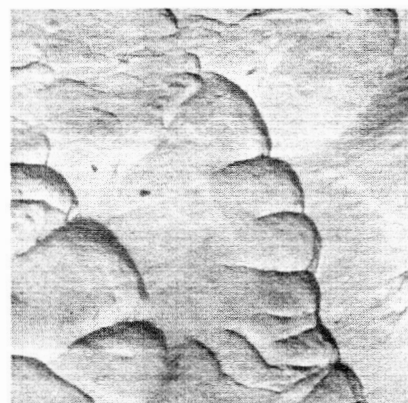
FIGURE 81 — COMPARATIVE ELECTRON MICROSCOPE MICRO-PHOTOGRAPHS OF PLANE-STRAIN FRACTURE TOUGHNESS FAILURE SURFACES IN 2219-T87 ALUMINUM ALLOY FOR 1:0 AND 1:1 STATES OF STRESS — 3000X



STATE OF STRESS 1:1
TEST TEMPERATURE -42°F



STATE OF STRESS 1:1
TEST TEMPERATURE -320°F

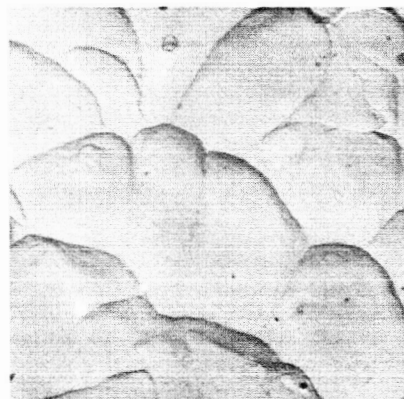


STATE OF STRESS 1:0
TEST TEMPERATURE -42°F

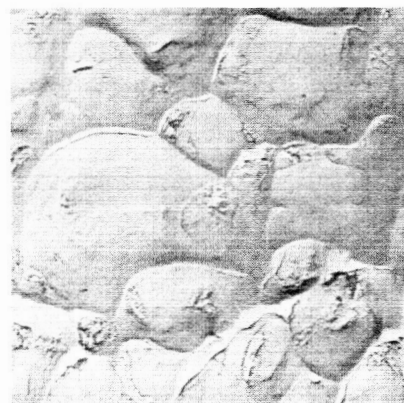


STATE OF STRESS 1:0
TEST TEMPERATURE -320°F

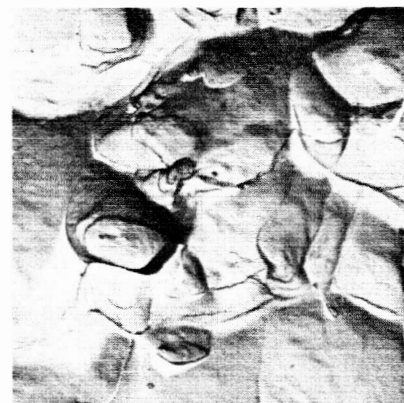
FIGURE 82 — COMPARATIVE ELECTRON MICROSCOPE PHOTOGRAPHS OF PLANE-STRAIN FRACTURE TOUGHNESS FAILURE SURFACES IN INCONEL 718 ALLOY FOR 1:0 AND 1:1 STATES OF STRESS — 3000X



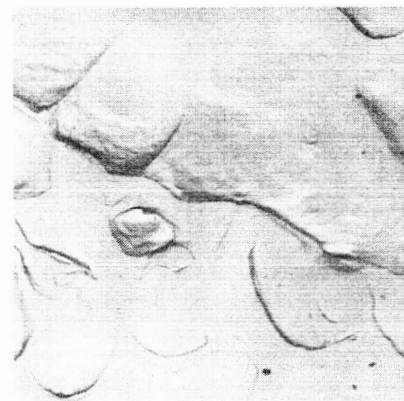
STATE OF STRESS 1:1
TEST TEMPERATURE 42°F



STATE OF STRESS 1:1
TEST TEMPERATURE -320°F

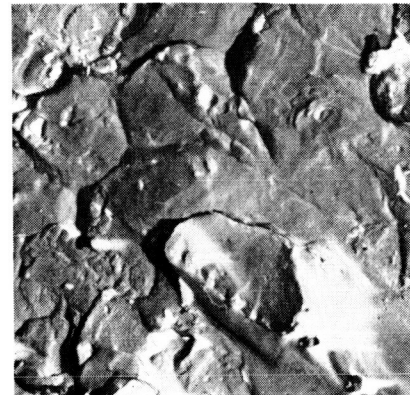


STATE OF STRESS 1:0
TEST TEMPERATURE -42°F



STATE OF STRESS 1:0
TEST TEMPERATURE -320°F

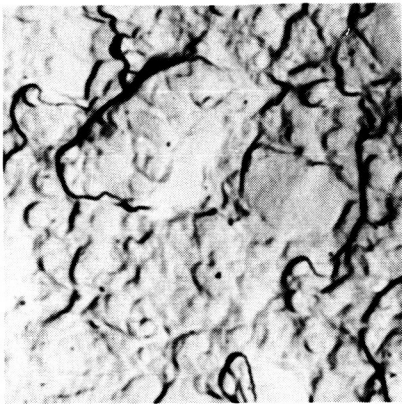
FIGURE 83 — COMPARATIVE ELECTRON MICROSCOPE PHOTOGRAPHS OF PLANE-STRAIN FRACTURE TOUGHNESS FAILURE SURFACES IN 5AL-2.5SN ALUMINUM ALLOY FOR 1:0 AND 1:1 STATES OF STRESS — 3000X



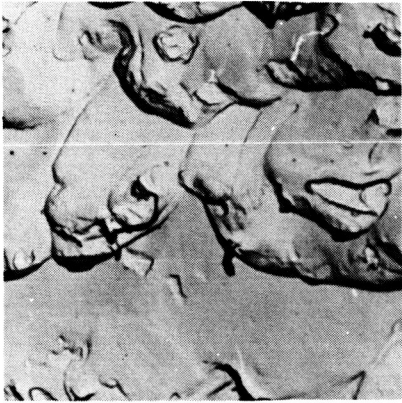
STATE OF STRESS 1:0
TEST TEMPERATURE -320° F



STATE OF STRESS 1:0
TEST TEMPERATURE -423° F

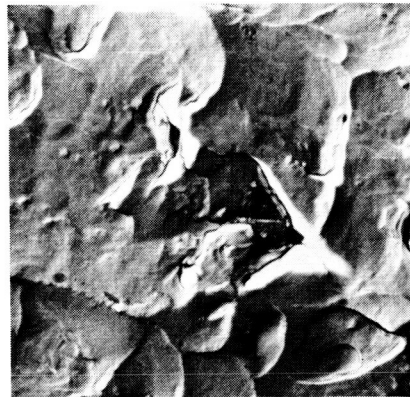


STATE OF STRESS 1:1
TEST TEMPERATURE -320° F

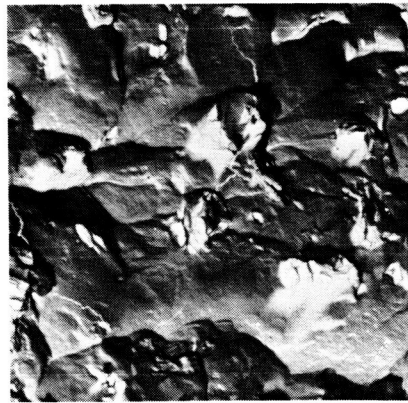


STATE OF STRESS 1:1
TEST TEMPERATURE -423° F

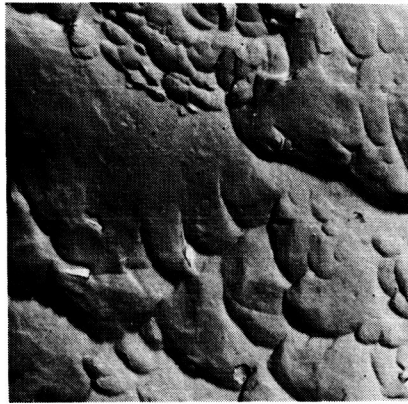
FIGURE 84 — COMPARATIVE ELECTRON MICROSCOPE PHOTOGRAPHS OF FRACTURE ORIGINS IN (WELDED) 2219-T87 ALUMINUM ALLOY FOR 1:0 AND 1:1 STATES OF STRESS — 3000X



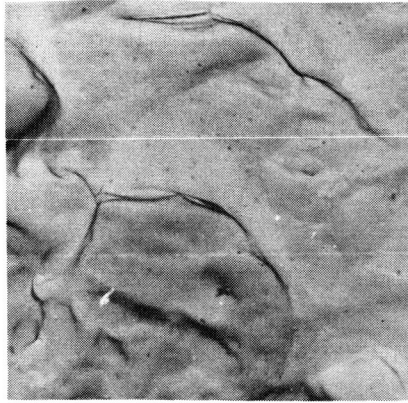
STATE OF STRESS 1:0
TEST TEMPERATURE -320° F



STATE OF STRESS 1:0
TEST TEMPERATURE -423° F



STATE OF STRESS 1:1
TEST TEMPERATURE -320° F



STATE OF STRESS 1:1
TEST TEMPERATURE -423° F

FIGURE 85 — COMPARATIVE ELECTRON MICROSCOPE PHOTOGRAPHS OF FRACTURE ORIGINS IN (WELDED) INCONEL 718 ALLOY FOR 1:0 AND 1:1 STATES OF STRESS — 3000X

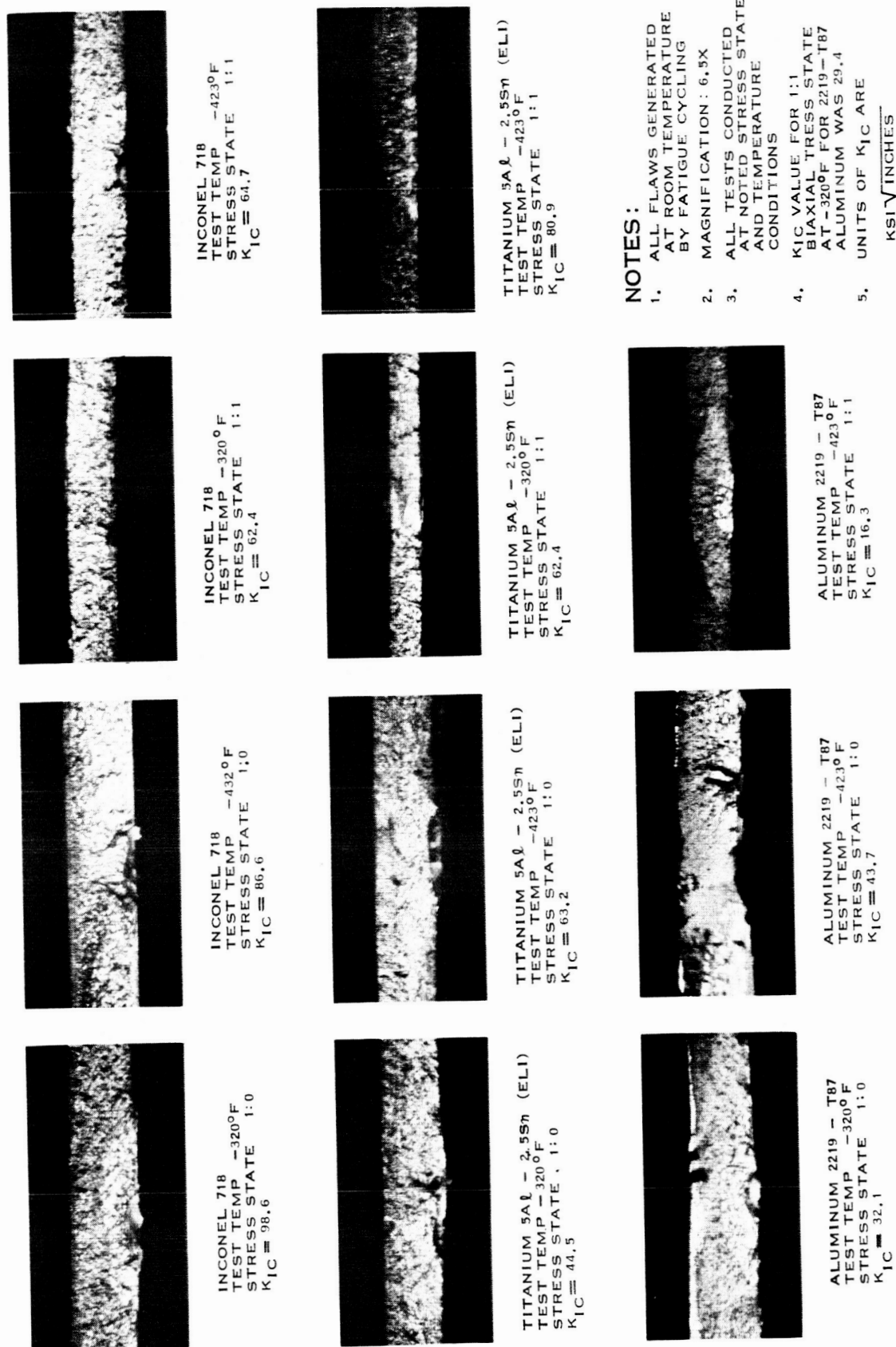


FIGURE 86 — COMPARATIVE ILLUSTRATION OF FRACTURE ORIGIN AND FLAW ZONE AREA IN TYPICAL UNIAXIAL AND BIAXIAL PARTIAL THROUGH CRACK TESTS

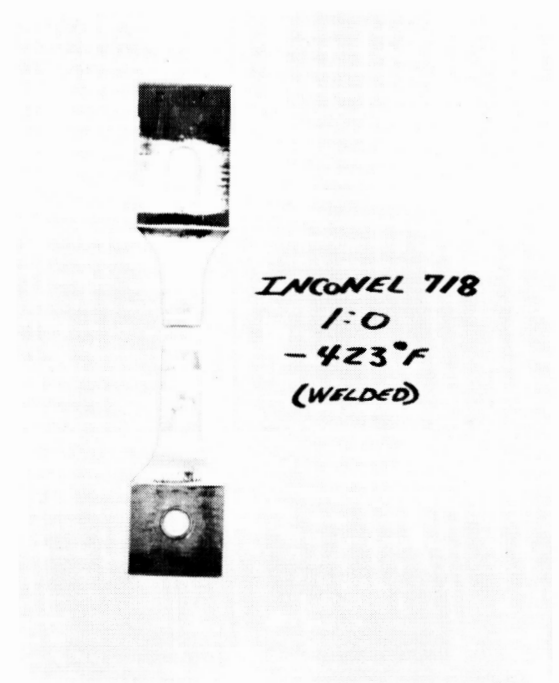
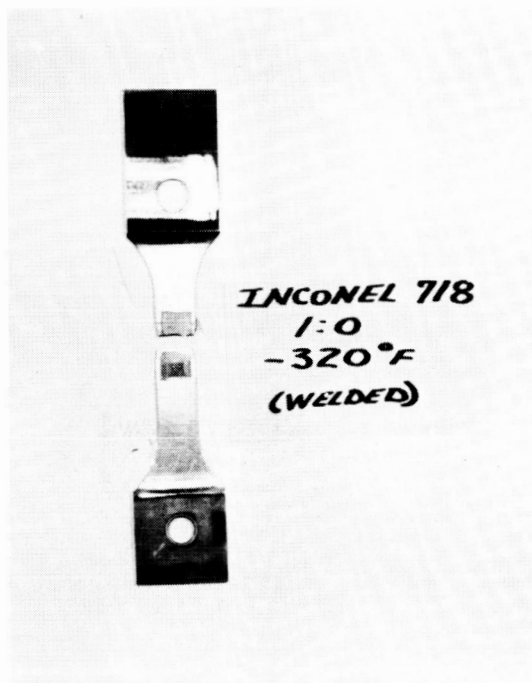
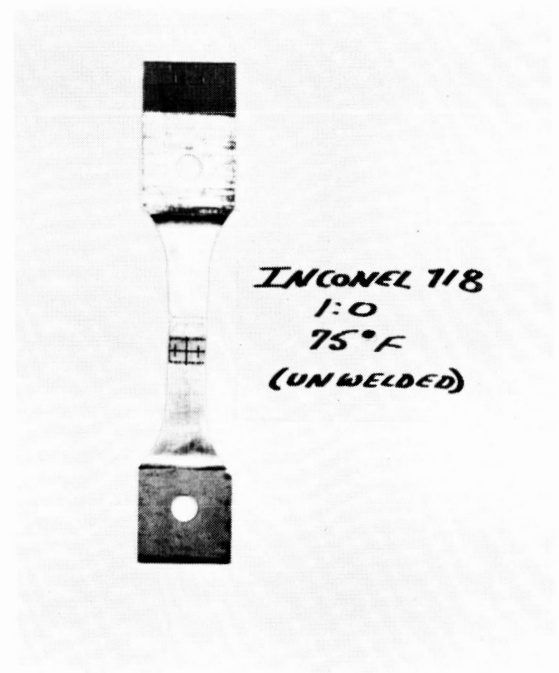


FIGURE 87 — FAILED UNIAXIAL TEST SPECIMENS

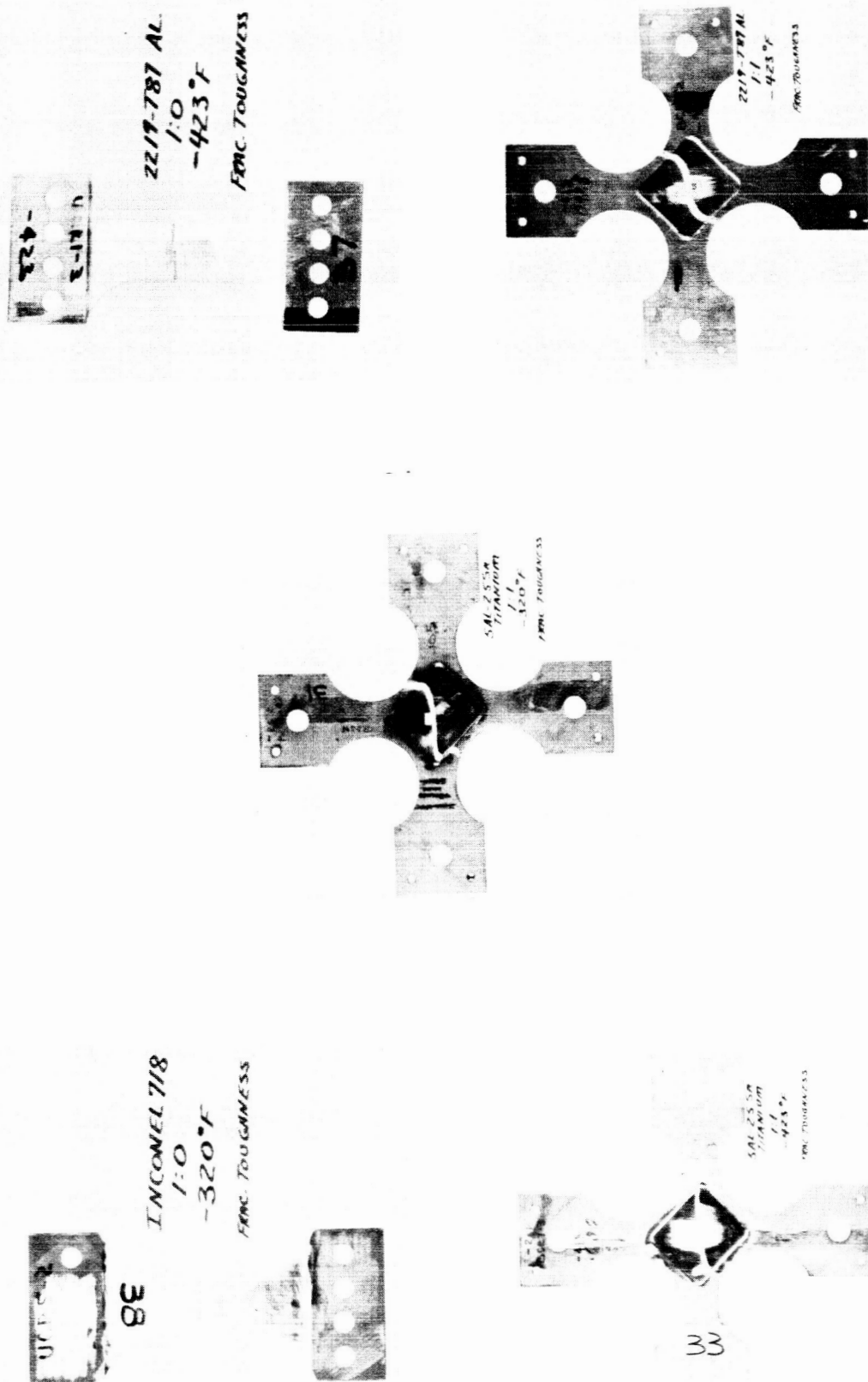


FIGURE 88 -- FAILED UNIAXIAL AND 1:1 BIAxIAL FRACTURE TOUGHNESS SPECIMENS

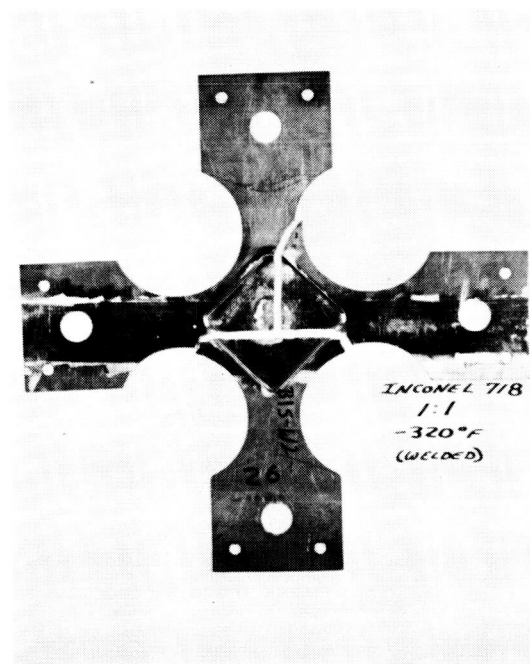
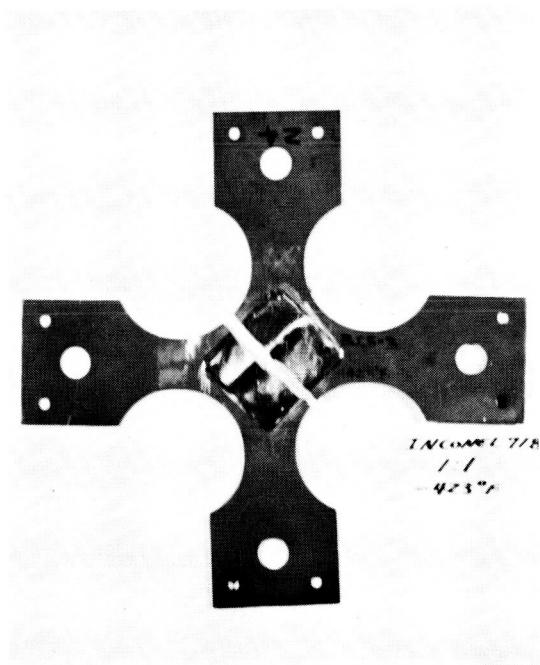
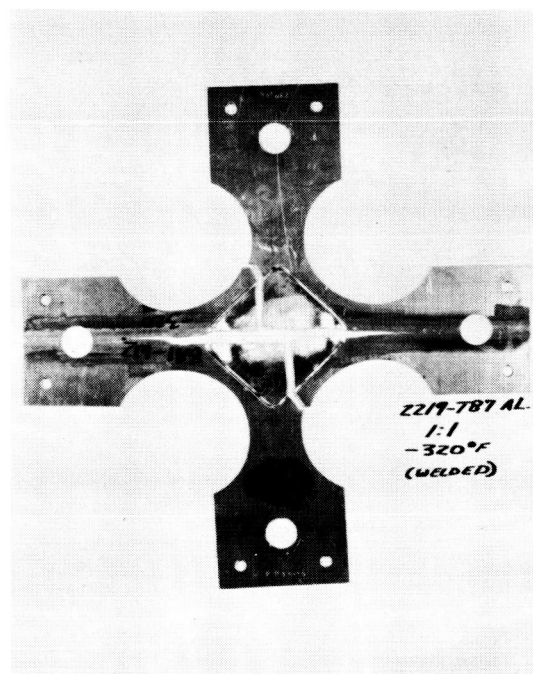
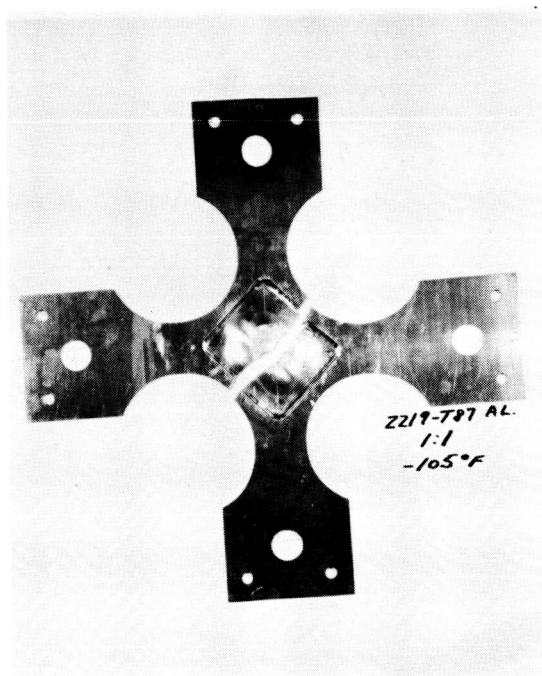


FIGURE 89 — FAILED 1:1 BIAXIAL TEST SPECIMENS (WELDED AND UNWELDED CONDITION)

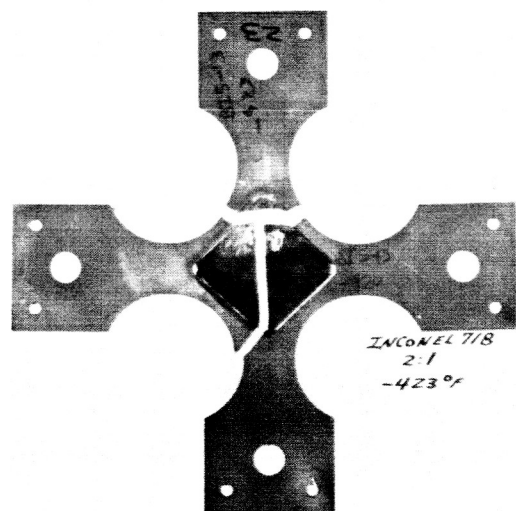
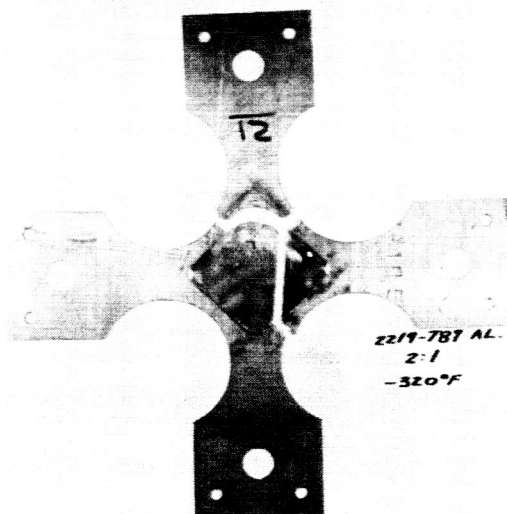
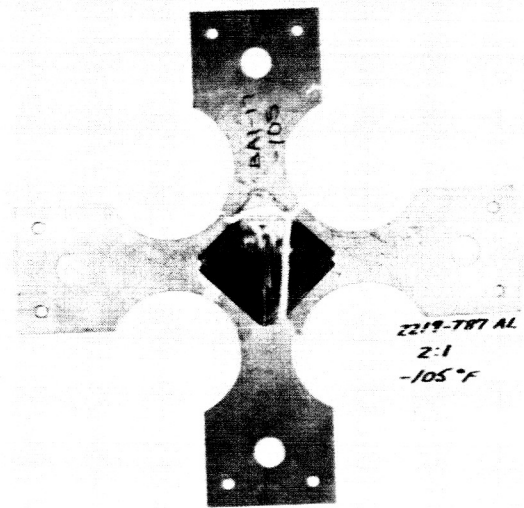
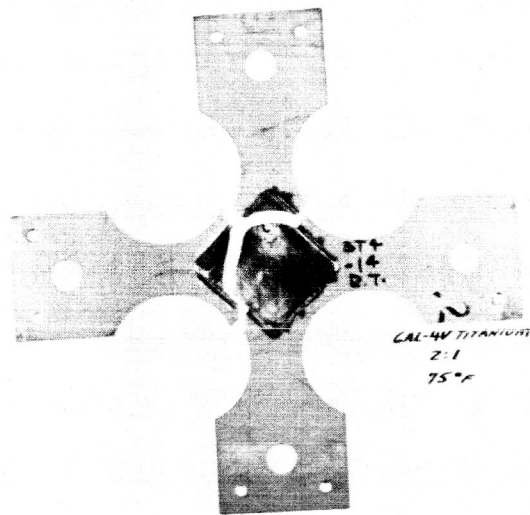


FIGURE 90 — FAILED 2:1 BIAXIAL TEST SPECIMENS (UNWELDED CONDITION)

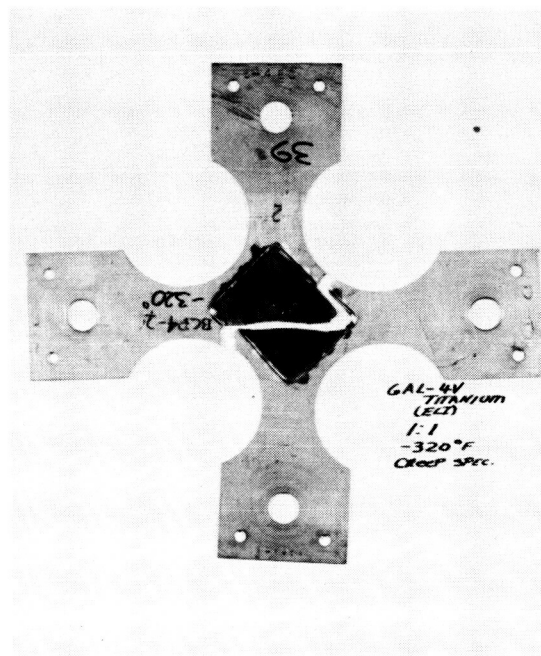


FIGURE 91 — FAILED 1:1 BIAxIAL CREEP TEST SPECIMEN (-320°F ; 90% F_{TY} STRESS LEVEL; 172 HOURS TO FAILURE)

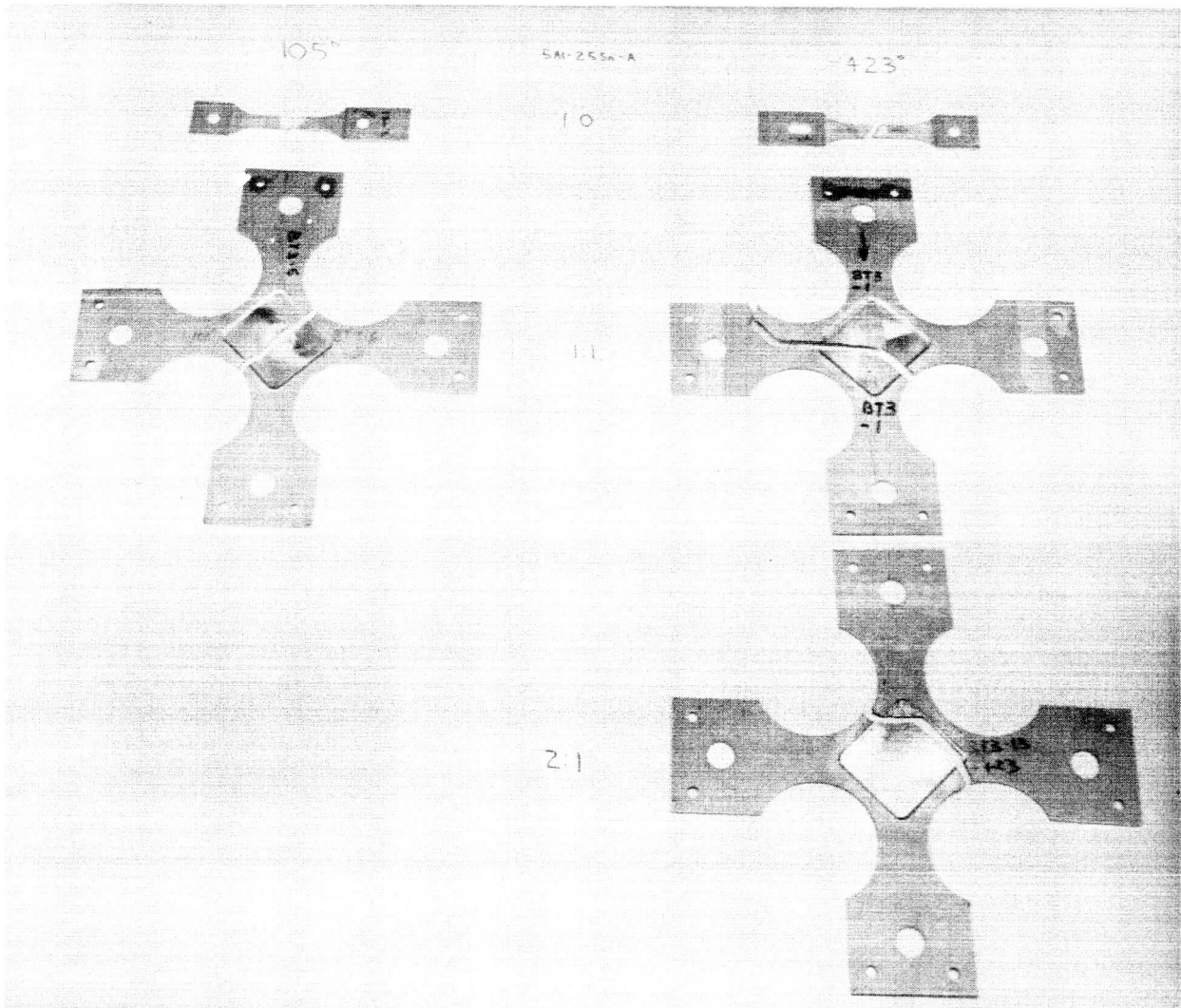
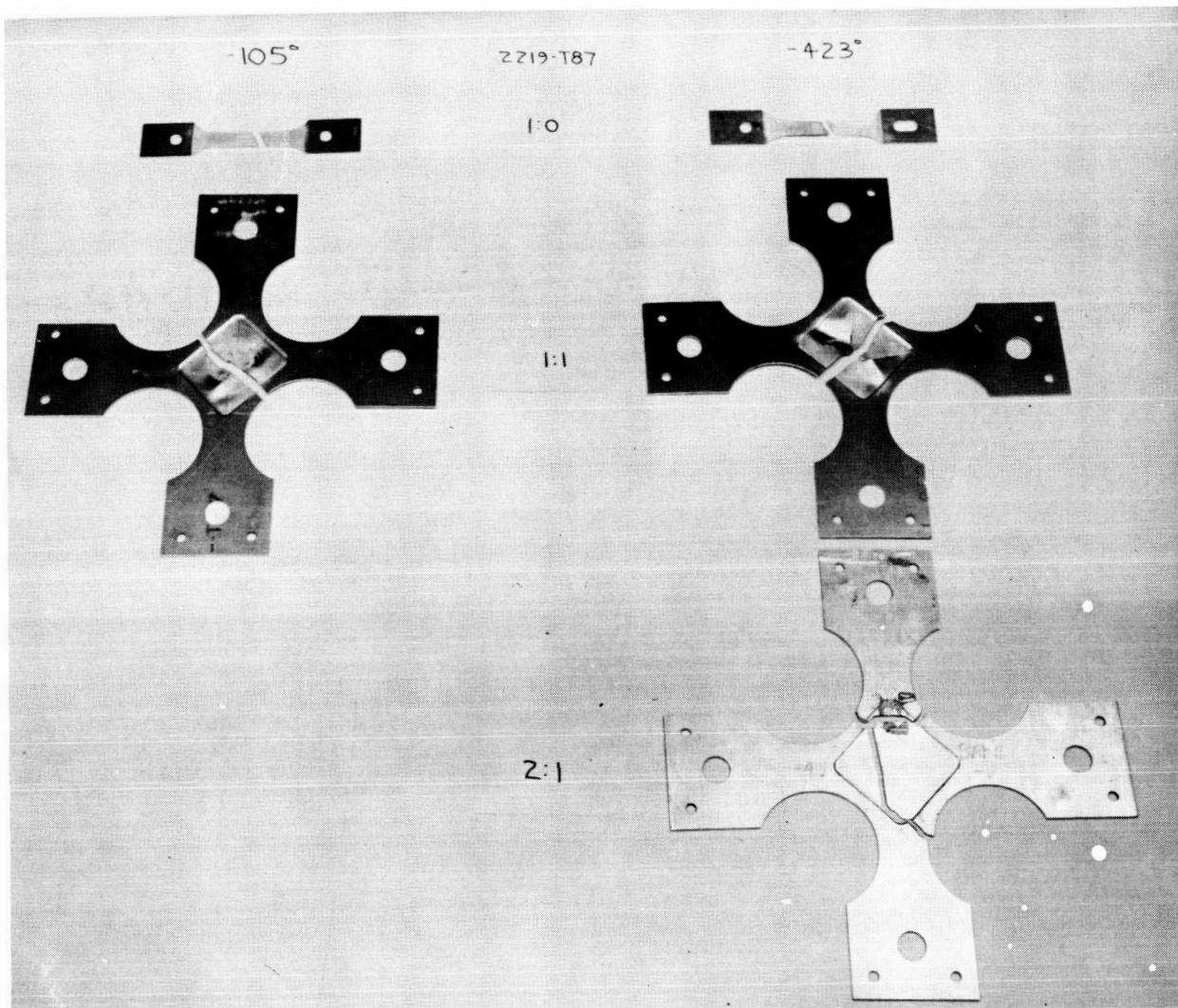


FIGURE 92 — COMBINED VIEW OF SEVERAL FAILED 5AL-2.5SN
TITANIUM ALLOY (ANNEALED) TEST SPECIMENS AT
VARIOUS STRESS STATES AND TEMPERATURES



**FIGURE 93 — COMBINED VIEW OF SEVERAL FAILED 2219 — T87
ALUMINUM ALLOY TEST SPECIMENS AT VARIOUS STRESS
STATES AND TEMPERATURES**

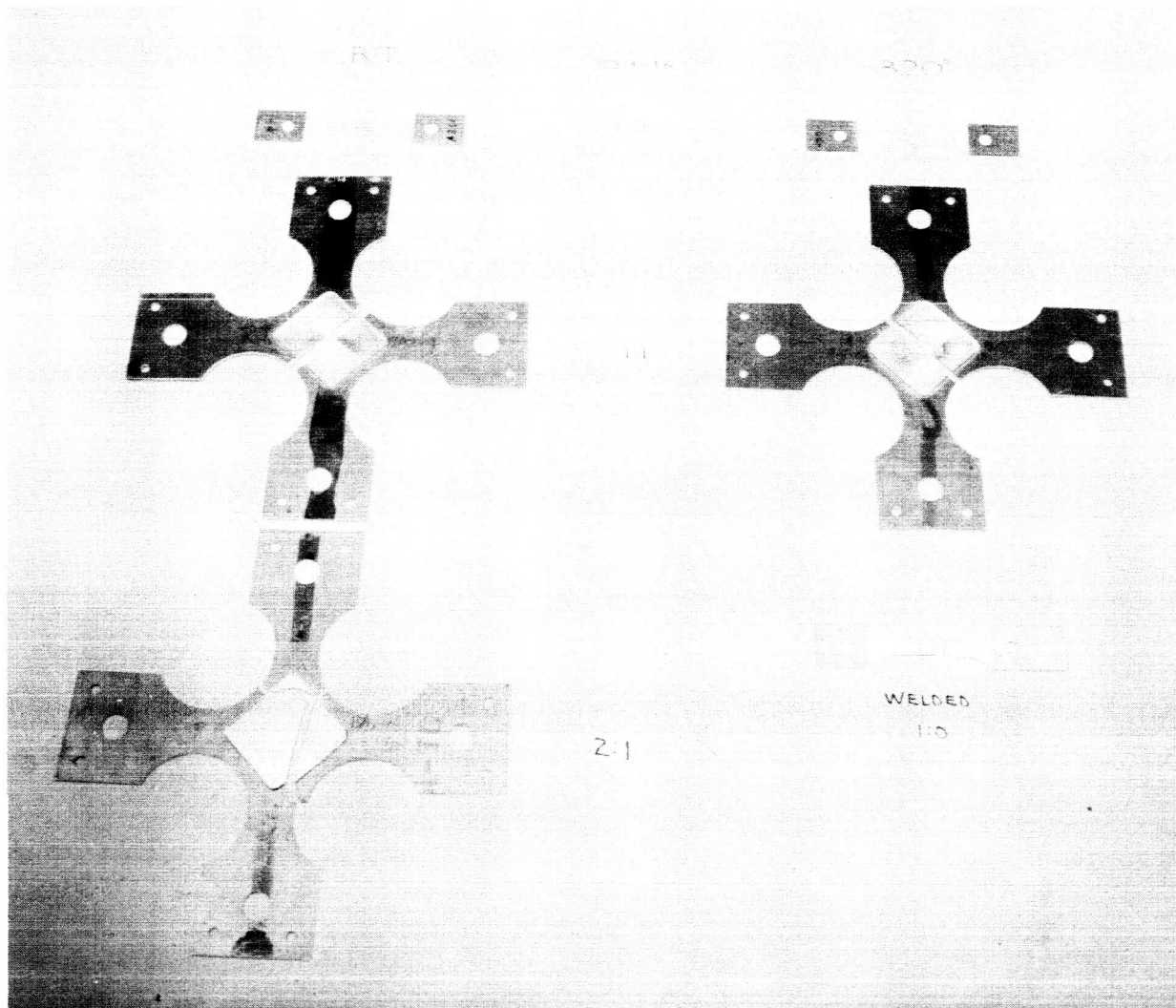


FIGURE 94 — COMBINED VIEW OF SEVERAL FAILED 2014-T6 ALUMINUM ALLOY TEST SPECIMENS AT VARIOUS STRESS STATES AND TEMPERATURES